Particulate Pollution and Stone Deterioration

Particulate Pollution and Stone Deterioration

Michaela Kendall

Submitted to Middlesex University in partial fulfilment of the requirements for the degree of Doctor of Philosophy

November 1998

Urban Pollution Research Centre
Middlesex University
London

Abstract

The soiling and damage of building surfaces may be enhanced by particulate air pollution, reducing the aesthetic value and lifetimes of historic buildings and monuments. This thesis focuses on the deposition of atmospheric particulate material to building surfaces and identifies potential sources of this material. It also identifies environmental factors influencing two deterioration effects: surface soiling and black crust growth.

Two soiling models have been compared to assess their effectiveness in predicting the soiling rates of two materials – stone and wood - in five cities in Europe. An exponential decay model was found to describe the reduction of reflectance well at two of these sites, while a square root relationship is not as effective. Different measures of weekly particulate concentration were not statistically related to soiling rate, whereas SO_2, rainfall, and temperature were statistically related to reflectance loss over time. Wind speed and solar insolation were also indicated to influence soiling rates.

Concentrations of total suspended particulate (TSP), particulate elemental carbon (PEC), total organic carbon (TOC) and thirty-nine particulate-associated hydrocarbons were measured in airborne particles at two sites in London, for one year. These hydrocarbons were also measured in black crusts from St Paul's Cathedral to relate atmospheric and deposited material, and to identify potential sources of the deposited particulate matter. Detailed scanning electron microscope-energy dispersive X-ray (SEM-EDX) analysis of black crust similarly indicated potential sources of these deposition layers. Analysis revealed the complex structure of these crusts, comprising gypsum "growth stems", calcite and large numbers of particles mainly originating from oil combustion. Hydrocarbon analysis supported the fact that oil combustion – probably at Bank power station – was the dominant source of this deposited layer. Other particle morphologies were commonly found, such as those typical of coal combustion and diesel engine exhaust. Metals analyses also indicated other possible sources such as vehicles.

Acknowledgements

Thanks go to everyone who helped with the completion of this thesis. Thanks go especially to my supervisors who guided me through the whole process, my parents and brother for always being as supportive as one could hope for, and to Smart who has always been a source of inspiration, wit and wisdom. There are many others, and I hope they all know how much they have contributed to this thesis. I am indebted.

PARTICULATE POLLUTION AND STONE DETERIORATION

Chapter 3
STONE DAMAGE AND THE ROLE OF PARTICULATE MATTER

Chapter 4
MODELLING THE SOILING PROCESS

LIST OF TERMS AND ABBREVIATIONS

AD - aerodynamic diameter.

Aerosol – defined as a suspension of fine solid or liquid particles suspended in a gas.

AUN - automated urban network; a network of automatic monitoring sites operated by the DETR.

BG - Bounds Green, North London.

Black smoke – associated with the Smoke Stain technique (BSI, 1993) developed in the 1960s.

CMB- chemical mass balance; source apportionment model used successfully for particles.

CoV - coefficient of variation, calculated as the standard deviation divided by the mean and expressed as a percentage.

CPI - carbon preference index; expressed as the summation of the odd number homologues (eg *n*-alkanes) within a specified range of carbon numbers divided by the sum of the even number homologues within the same range.

D - diameter (eg of particles).

Damage function – a function directly relating material deterioration to pollutant concentrations and other environmental factors.

DCM - dichloromethane; organic solvent used in solvent extraction of organic compounds.

DETR - Department of Environment, Transport and Regions, UK Government (formerly DoE).

Dose response – a measure of the response of materials to pollutant dose.

EAC – effective area coverage is defined as the proportion of a surface covered by particles expressed as a percentage.

EDX- energy dispersive X-ray; technique used in conjunction with the SEM for the identification of the elemental composition of a material surface, or particle.

GCMS - gas chromatography/mass spectrometry; analytical technique especially suited for the identification of organic compounds.

MMAD- mass median aerodynamic diameter (of particles).

ρ - density (eg of particles).

PAC - polynuclear aromatic compounds; group of organic compounds which includes PAHs, and their derivatives.

PAHs- polyaromatic hydrocarbons; group of organic compounds consisting of two or more fused benzene rings in linear, angular or cluster arrangements.

PEC - particulate elemental carbon

PCA - principle component analysis; statistical method of factor analysis which identifies recurring and independent modes of variation within the data set.

PCBs - polychlorinated biphenyls

PM - particulate matter, as a mass concentration.

PM_{10} - mass concentration of size selected particulate matter, with a MMAD of 10 μm or less, where particulate is passed through a size selective inlet with a 50% efficiency cut-off at 10 μm.

Porosity – is the ratio of the volume of voids to the total volume of a solid eg rock. It is a measure of the amount of water that can be stored in the pore spaces and is hence one measure of durability.

RH - relative humidity (%).

SEM- scanning electron microscope.

SIM - selected ion monitoring; method of measuring presence or quantities of specific ions, using mass spectrometry.

Smoke – describes particulate matter <15 μm MMAD which predominantly originates from fossil fuel combustion.

SOF - solvent organic fraction; fraction of particles which may be extracted during prolonged solvent extraction procedure.

SP - St. Pauls Cathedral, Central London.

SPM- suspended particulate matter; equivalent to TSP.

TEOM - tapered element oscillating microbalance.

TOC - total organic carbon .

TOMPs - toxic organic micropollutants as measured at four DETR air quality monitoring sites.

TSP- total suspended particulate; mass concentration of airborne particulate matter expressed as mass of particulate per unit volume of air.

UCM – the unresolvable complex mixture is a complex mixture of hydrocarbons which cannot be resolved using current analytical techniques, such as gas chromatography.

V_d – the deposition velocity of eg particles is described as the concentration of a pollutant deposited on a surface per unit time divided by the atmospheric concentration.

LIST OF TABLES

LIST OF FIGURES

Chapter 1

INTRODUCTION AND OVERVIEW

1.1 INTRODUCTION

This thesis details research carried out over three years at the Urban Pollution Research Centre, Middlesex University and investigates the effects of particulate deposition on building surfaces. In particular, this thesis focuses on the processes involved in building soiling and surface crust formation in an urban environment.

A review of literature on particulate composition in the UK, and soiling and black crust development on building surfaces assesses the factors governing the deposition of particulates and the consequent effects on building materials. Using soiling data from five European cities (including London), the relationship between rates of actual soiling and existing models of soiling was investigated to determine the accuracy of these soiling prediction tools under different conditions. Composition analysis of selected organic components of aerosols and black crusts at the London site over one year identified the main components involved in the crust formation process, together with the sources of these compounds.

1.2 BACKGROUND

The scientific community now recognises particulate pollution as one of the most influential factors in the degradation of culturally important monuments and buildings (Del Monte *et al*, 1981 and 1984). Deposited particles of anthropogenic origin are believed to be responsible for the soiling of buildings in urban areas, with a resultant building cleaning cost in the UK estimated at £74-80 million during 1989 (Newby *et al*, 1991). Particulates have further been implicated in other environmental impacts such as increased human mortality and morbidity, visibility reduction, climate change and public nuisance. The wide extent of the environmental

importance of particulate matter is due to the different characteristics attributable to particles found in the urban atmosphere, namely the small size distribution of particles, the organic (largely petroleum derived) content of these particles and the inorganic components which include acidic compounds.

In urban environments, continuous deposition of gases and particulate matter to surfaces occurs. Surfaces interact with this deposited matter differently depending on the specific chemical composition of the air-surface interface (ie not bulk composition), the chemical composition of the underlying material, other environmental factors such as meteorology and the interactions of all these factors over time.

Soiling is the net discoloration effect on a surface resulting from atmospheric deposition and any removal processes acting on that surface. The soiling process involves the weak chemical association between particle and surface which may be undone by cleaning. Soiling of vertical painted wood and portland stone surfaces results from slightly different processes. On smooth, painted wood surfaces, particles are associated with the surface by adhesion and chemisorption. Particles on stone surfaces deposit in a similar manner with enhanced capture and retention due to the higher surface roughness. Particles may be initially chemisorbed, but over time in the presence of moisture and acidic compounds, the particles and the stone surface may interact to form strong bridges of material between the particle and surface. The deposited particle acts as a carrier and fixation site for acidic compounds which react with the underlying stone to cause surface recession and, in some cases, surface growth. In specific conditions therefore, a soiled stone surface may produce a surface crust which further increases the surface roughness, in turn increasing particle entrapment, which in turn increases crust growth. The identification of factors affecting soiling rates will therefore identify the conditions necessary for primary crust formation.

The data included in this thesis has contributed to a report commissioned by the European Community (Contract No: ES5V-CT94-0519) to investigate the role of particulate pollution in the process of stone damage. The project was a collaboration with Imperial College, the Building Research Establishment (BRE) and Vienna (Austria) and Aveiro (Portugal) Universities. As part of this contract, my role was to compare the reflectance measurements made during the previous

contract with existing soiling models, to collect and analyse ambient particulate samples for speciated organic components and analyse particulate matter deposited onto St Paul's Cathedral (black crusts). I also carried out extensive SEM examination of the morphology and elemental components of black crusts.

1.3 AIMS OF THE RESEARCH PROGRAMME

The main aims of this research programme were to investigate the factors affecting the soiling process and to explore the interelationships between particulate matter, soiling and surface crust formation. This thesis investigates four separate, but related phenomena:

1) The rates and factors affecting reflectance change of painted wood samples over time in five different environments.

2) The rates and factors affecting reflectance change of portland stone samples over time in five different environments.

3) Relationships between ambient airborne particulate and deposited particulate matter contained in crustal material, in particular the organic components.

4) The morphology of deposited particulate matter and surface crusts.

1.4 OBJECTIVES OF THE RESEARCH PROGRAMME

Five main objectives were pursued as part of this research programme:

The first objective was to produce a detailed literature review of the characteristics of airborne particulates in the UK and the characteristics of particles associated with damage to building material in urban areas. Chapter 2 provides a comprehensive characterisation of airborne particulate matter in the UK. This review covers the different systems used to classify particles in the UK, including size fractions, shape, sources, and chemical composition of particles. Chapter 3 provides a summary of building stone characteristics and the known effects of

particulate matter on building surfaces. This chapter assesses the factors governing the deposition of atmospheric particles to stone surfaces and describes the surface deterioration effects mediated by these particles, focusing on the formation of crustal material.

The second objective was to assess the accuracy of two existing soiling models in the prediction of the soiling of two types of vertical surfaces which were exposed simultaneously in five European sites, for one year. Chapter 4 introduces the two soiling models which assume different particle characteristics influence the soiling process. The rates of soiling at these five sites were measured using reflectometry and compared with the two models. The effectiveness of the two models in soiling reflectance prediction over time have been determined. The importance of environmental parameters such as particulate concentrations and meteorological factors are also discussed. A third objective was to establish an empirical model to predict soiling of two different types of material in different environments.

The fourth objective was to investigate the organic content of current atmospheric particles and deposited particulate matter on St Paul's Cathedral. Chapter 5 details the sampling and analytical methods used to monitor particulate-associated organic compounds and samples of black crust. Concentrations of total suspended particulate (TSP), 39 solvent extractable organic compounds, particulate elemental carbon (PEC) and total organic carbon (TOC) associated with airborne particles at two sites in London are presented in Chapter 5. These data are then compared with quantitative data on organic compounds extracted from black crust material collected from St Paul's Cathedral. Quantitative analysis of sixteen polyaromatic hydrocarbons (PAHs) and the homologous series of *n*-alkanes (C_{10}-C_{34}) in TSP and black crust samples are reported together with qualitative analysis of other detectable compounds. Limited samples of black crust and stone material collected from St Paul's Cathedral and Stefansdom Cathedral (Vienna) were also subject to bulk metals analysis.

A fifth objective was to investigate the form and chemical composition of the surfaces of black crusts associated with historic buildings, and in particular with St Paul's Cathedral. Samples of black crusts were subject to detailed morphological examination in-situ, and in the laboratory using scanning electron microscopy (SEM). These results are also presented in Chapter 5.

The main results generated by this work are summarised in Chapter 6. This chapter also recommends several areas for related research work.

1.5 ASSOCIATED RESEARCH ACTIVITY

Associated research related activities have included;

i) ***Publications***

M. Kendall, R. Hamilton, I. D. Williams and D. M. Revitt. "Smoke Emissions from Petrol and Diesel Engined Vehicles in the UK". International Dedicated Conference on the Motor Vehicle and the Environment - Demands of the Nineties and Beyond, Aachen, Germany (2 November 1994).

Sitzmann, B., Kendall, M., Watt, J. and Williams, I. "Personal Exposure of Cyclists to Particulate Pollution in London". Journal of Aerosol Science, Vol 27, Supplement 1, September 1996.

ii) ***Posters***

Kendall, M. , Kunzli, P., Luxton, W. and Muncaster, G. "The Urban Pollution Research Centre", NEC, Birmingham.

Sitzmann, B., Kendall, M., Watt, J. and Williams, I. "Personal Exposure of Cyclists to Particulate Pollution in London". European Aerosol Conference, Delft, The Netherlands. 9-11 September 1996.

Kendall, M., Rickard, A. and Kendall, A. "Quantification of PM_{10}-Associated Organic Compounds in London". Health Effects of Particulate Matter (co-organised by the US EPA and WHO) Prague, Czech Republic. 10-12th April 1997.

iii) ***Conferences Attended***

NSCA and Middlesex University Air Quality Conference, Westminster University, London (4 April 1994).

Investigation of Air Pollution Standing Conference, NEC, Birmingham (8 June 1994).

International Dedicated Conference on the Motor Vehicle and the Environment - Demands of the Nineties and Beyond, Aachen, Germany (31 October - 4 November 1994)

Fifth International Symposium on Highway and Urban Pollution, Copenhagen, Denmark (22-24 May 1995).

Investigation of Air Pollution Standing Conference, CBI, London (5 December 1995).

European Aerosol Conference, Delft University, Delft, Holland (9-11 September 1996).

First Symposium on Air Pollution, University College London, London (19 September 1996).

Health Effects of Particulate Matter, Prague, Czech Republic (10-12th April 1997).

iv) ***Courses Attended***

Using the Scanning Electron Microscope and Associated Particle Analytical Techniques, Imperial College, London (November 1994).

Faculty Research Workshop Series for training in skills essential to research (November 1994 - July 1995).

Engine Emissions Measurements, Leeds University, Leeds (5 and 6 July 1995).

Middlesex University and NSCA Particulate Air Pollution Training Seminar, NEC, Birmingham (31 January 1996).

Particle Analysis Techniques, HSE, Sheffield (9 September 1996).

v) ***Seminar Presentations***

"Airborne Carbonaceous Particulate Matter in the Urban Environment", Faculty Research Day presentation.

"Impacts of Particulate Pollution in the Urban Environment", Urban Pollution Research Centre Seminar, Middlesex University, London (March 1995).

"Particulate Air Pollution in London", Middlesex University Conference on Research in Technology 1995 (MUCORT'95), Middlesex University (June 1995).

"Airborne Carbonaceous Particles in London", First Symposium on Air Pollution, UCL, London (September 1996).

vi) ***Meetings and Workshops***

Project Meeting - STEP EC contract EV5V-CT94-0519 "Air Pollution and Stone Decay", Santiago de Compostela, Spain (27 November 1994).

EC Workshop on Degradation and Conservation of Granitic Rocks in Monuments, Santiago de Compostela, Spain (28-30 November 1994).

Urban Pollution and Respiratory Health Meeting, Aerosol Society, Queen Elizabeth Hospital, Birmingham (6 October 1994).

Project Meeting - EC Contract EV5V-CT94-0519, Aveiro, Portugal (7 December 1995).

Workshop on Monitoring and Characterisation of Airborne Particulates in Urban Areas, UCL, London (24 January 1996).

Project Meeting - EC Contract: EV5V-CT94-0519, Vienna, Austria (7 June 1996).

vii) ***Related Work***

Student representative of the Bounds Green Equal Opportunity Committee; attended meetings and invited speakers.

Member of organising committee of Middlesex University Conference on Research in Technology 1995 (MUCORT'95).

Founding member of postgraduate London Air Pollution Research Forum.
(Web site: *http://doric.bart.ucl.ac.uk/web/ben/polctcts.html*).

Co-organiser and Host of First, Second and Third Symposia on Air Pollution held at The Bartlett College, UCL (19th September 1996, 10th September 1997 and 21st September, respectively).

Participated in community projects at Barnet High School, SET'94 and SET'95.

First President of Middlesex Research Society (MRS), 1996-1997. Invited speakers, organised events and helped in the administration and publicising of the group. (Web site: *http://mdx.ac.uk/research*).

viii) ***Lectures***

Two lectures on Environmental Science and Technology Course, Middlesex University (Second Semester, 1994-1995).

Series of lectures on Biology as part of the Technology Access Course, Middlesex University (Summer 1995).

Two guest lectures as part of the second year of the BTEC HNC Environmental Health Course, College of North East London (First Semester, 1995-1996).

ix) ***Supervised Projects***

Supervised three projects in the Environmental Science and Engineering School:

Particulate Air Pollution in Central London (Final Year Project 1994/5).

SEM Analysis of Vehicular Particles (Final Year Project 1995/6).

Personal Exposure of Cyclists to Particulate Matter in London (ERASMUS German Final Year Project student, 1995/6).

Chapter 2

THE NATURE OF ATMOSPHERIC PARTICLES IN THE UK

2.1 INTRODUCTION

In order to estimate the impacts of airborne particulate matter in the UK atmosphere, the properties of the particles must be determined and the particles classified as to their characteristics. This has led to the classification based on several aspects of particles, for example, source, size, composition, number or mass concentration, but no one classification system encompasses all aspects simultaneously.

The presence and proximity of different sources of particulate matter together with the action of meteorological factors such as temperature, humidity, precipitation, incident sunlight and wind conditions all affect the size, chemical composition, concentration, movement and water content of airborne particles. Particulates include both solid and wholly or partly liquid droplets. The behaviour and final impact of emitted particles are dependent on the complex interplay of particle characteristics, microphysical elements and the environment into which they are released. Spatial and temporal variations exist in the broad uniformity of these particle sizes, composition and loading in the UK atmosphere. The geographical distribution of particle sources is highly non-uniform resulting in wide variations in particle concentration and composition throughout the UK atmosphere.

This chapter describes some of the work carried out to characterise particles and evidence to describe their origin, behaviour, classification and eventual impact, particularly in the UK.

2.2.1 Definitions of Particulate Matter

Particles are classified by their characteristics. Table 2.1a summarises the particle classification systems in current usage, and lists the basis for the classification of these particles.

Table 2.1a Particle classification systems in current use.

Particle Classification System	Basis for Classification
Aerodynamic Diameter	Actual diameter, shape and density
Modal Distribution:- Mass	Mass of particles in a given size range
- Number	Number of particles in a given size range
Regional Aerosol	Size range, number, modal distribution and composition
Black Smoke	Optical properties, including size distribution
Chemical Composition	Speciation of particle components

2.2.2 Particle Size

The diameter, shape and density of the particle will influence the terminal settling velocity, likelihood of resuspension, diffusion to a surface and thus the behaviour of the particle in the atmosphere. The parameter aerodynamic diameter (AD) has been defined to classify all particles greater than 0.5 μm AD in terms of these properties. The AD of a particle is the diameter of a sphere of unit density, ρ_0 ($\rho_0 = 1 \times 10^3$ kg m^{-3}) having the same terminal settling velocity as the particle in question. For a spherical particle of diameter D_1 and density ρ_1

$$AD = D_1(\rho_1/\rho_0)^{1/2}$$

The aerodynamic diameter defines the aerodynamic properties of a particle and consequently the environmental impact of the particles, such as the availability of particles for inhalation or the rate of deposition to a surface. Particles <0.5 μm AD use the particle diffusion diameter which is the diameter of a sphere with the same diffusion coefficient as the particle in question.

2.2.3 Modal Distributions

Modal distributions indicate the size range within which a measured mass or number of particles are found. The distributions are governed by the source, chemical composition and aerosol microphysics of the aerosol. Modal distributions of different aerosol types vary, thereby providing a basis for particle classification. For example, background measurements of the mid and upper troposphere have revealed an almost monodisperse aerosol (Kleinman and Daum, 1991) centred between 0.2 and 0.5 μm AD (Leaitch and Isaac, 1991; Clarke, 1993). Three modes of particle sizes are commonly cited as describing particles at distinct stages of development; nucleation, accumulation and coarse. The size ranges and central value of these modes differ with source and time after emission.

The modal aerodynamic size distribution of aerosol mass has been described as monodisperse, bimodal and trimodal (Hidy, 1985). For the purpose of this review, approximate sizes have been selected to represent each mode. Nucleation mode particles (<0.05 μm AD) are either the product of gas phase to particulate phase chemical conversions (eg the oxidation of SO_2 to form H_2SO_4) or particles formed during the condensation of hot vapours from combustion processes. Condensation will also occur when the concentration of a volatile substance exceeds the saturation vapour pressure, whereby similar molecules combine to form a condensation nucleus or molecules condense onto existing nuclei. Particles in this mode have short atmospheric lifetimes, rapidly colliding as a result of Brownian motion and coagulating into the accumulation mode. Agglomeration causes the formation of larger droplets or long dendritic chains of particles, such as those generated by diesel engines (Van Borm, 1989). This mode may contain large numbers of particles but constitutes a small fraction of the aerosol

mass concentration in rural aerosol and a much larger proportion of urban aerosol.

Accumulation mode particles (0.05 - 2 μm AD) are coagulated nucleation mode particles or condensates from hot vapours. Lifetimes within this mode are estimated to be the longest due to the inefficiency of removal processes such as agglomeration, gravitational settling and scavenging by rainfall, which effectively remove larger particles. Lifetimes of between 7 - 30 days have been estimated, during which time transportation over large distances may occur before deposition (QUARG, 1996). A significant fraction of the background or naturally occurring aerosol mass exists in this and the coarse modes. Particles in this size range are important facilitators for long-range transport of adsorbed species and are efficient light scatterers.

Coarse mode particles (>2 μm AD) are mainly formed by mechanical attrition processes and therefore include soil, house dust, sea spray and many industrial dusts. These particles have a short atmospheric residence time due to high deposition velocities and concentrations are dependent on local conditions. Although smaller in number, these particles contribute substantially to measurements of particulate mass.

2.2.4 Chemical Composition of Particulate Matter

While aerodynamic diameter defines particles in terms of their physical properties, chemical composition also influences the behaviour and impacts of emitted particles. Composition is an important factor in the effects on health (Iwado *et al*, 1991; Gundel *et al*, 1993; Dockery *et al*, 1993; Ostro, 1993; Bates, 1995), climate change (Pratsinis *et al*, 1984; Charlson *et al*, 1992; Penner *et al*, 1994; Andreae *et al*, 1995; Pandis, 1995) and building soiling (Hamilton and Mansfield, 1989; Mansfield *et al*, 1991).

2.2.5 Regional Aerosol

Generalisations may be made by the classification of the type of aerosol being considered, eg urban, rural or marine, which contain common chemical components at relatively similar concentrations. Despite the variety of airborne particle types, it is possible to roughly classify an aerosol as to its sources and thus region of coverage. Eight tropospheric aerosol classes

have been identified by Pandis *et al* (1995), based on average modal distributions, particle numbers, mass concentration and chemical composition: marine, remote continental, nonurban continental, urban, desert, polar, biomass burning and background. Table 2.1b summarises data collated by Pandis *et al* (1995) on regional aerosol types.

Table 2.1b Modal distributions of particle number for regional aerosol types (Pandis, 1995).

Aerosol Type	Description	Mode Centres (μm AD)	Number Conc'n (particles cm^{-3})
Background	Monodisperse	0.2 - 0.5	30
Polar	Monodisperse	0.15	15 - 150
Biomass Burning	Monodisperse	0.2 - 0.4	1000
Desert	Monodisperse	>1	-
Marine	Trimodal	<0.1; 0.1 - 0.6; >0.6	100 - 300
Urban	Trimodal	Varied	$> 10^5$
Nonurban Continental	Trimodal	Varied	10^3
Remote Continental	Trimodal	0.02; 0.12; 1.8	10^4

Marine aerosol is perhaps the best characterised due to the uniformity of the aerosol at the monitoring sites (Savoie and Prospero, 1989; Fitzgerald, 1991). However, even within a particular aerosol type there may be distinctly different sources, for example industrial emissions from urbanised areas vary particulate composition substantially (AEA, 1995).

2.3 SOURCES AND EMISSIONS OF ATMOSPHERIC PARTICLES IN THE UK

Particles are generated by combustion of solid fuels, grit and dust from varied industrial processes, emissions from motor vehicle exhaust, material wear, wind lift from the ground and gaseous state to solid state chemical conversions. Proximity to a source of particulate matter will usually determine the concentration of airborne particles, together with the size, aerodynamic diameter and composition of the particles. Ball (1984) and Brimblecombe (1987) list historical sources of particulate pollution in the UK, particularly in London.

Many authors report successful identification of sources using source apportionment models, such as chemical mass balance (CMB) models. A great deal of work has been carried out in the US and other countries (Pratsinis *et al*, 1984; Simoneit, 1985; Chow *et al*, 1992; Cheng and Kamens, 1993), but extrapolation of this data to the UK may prove unreliable due to the influence of local sources and conditions. Table 2.2 shows the results of one of the few source

apportionment studies carried out in the UK; Smith and Harrison (1994) used principal component analysis (PCA) to identify the sources of particulate samples taken in Birmingham.

Table 2.2 Source apportionment of particulate matter study in Birmingham (Smith and Harrison, 1994).

Source Category	Total Suspended Particulate (%)
Road Dust/Soil	32 ± 5
Vehicles	25 ± 4
Secondary Aerosol and Fuel Oil Combustion	23 ± 4
Coal Combustion	11 ± 7
Incineration/Metals Industry	7 ± 2
Road Salt/Marine	2 ± 2

The analysis of individual particles can provide information about the particle's mechanical, chemical and environmental history. Coarse particles tend to reflect their origin more than finer particles formed during untraceable gas phase reactions. Determination of the sizes, morphology and composition of particles can contribute to the identification of sources, especially when reference source material can be directly compared with the unknown sample. Single particle analysis using the scanning electron microscope (SEM) and energy dispersive X-ray spectrometry (EDX) allows the characterisation and classification of particles by size, morphology and elemental composition of particles in the micron range (Sabbioni and Zappia, 1993; Ying Xie and Hopke, 1994). Analysis of single particles using an electron microprobe provides similar information (Van Borm *et al*, 1989). The size fraction in which a species is detected can also provide information of source (Harrison and Jones, 1995).

A basic classification of particles is that made between primary and secondary particles, and this reflects the origin of the particles.

2.3.1 Primary Particulate Matter

Primary particulate matter comprises that which is emitted directly to the atmosphere from a source and so includes natural and anthropogenic emissions. Primary particulate emissions arise from mobile sources such as petrol and diesel vehicles, and also stationary sources. Stationary sources include both legally controlled chimney stack emissions and fugitive emissions from uncontrolled activities such as bonfires, where high particulate concentrations may be released directly to the atmosphere from eg smoke filled rooms or kitchens. The impact

of fugitive emissions on the concentration of urban particulate is difficult to quantify (Goodwin, 1996). Background primary PM_{10} concentrations in the UK are estimated to be approximately 10 $\mu g\ m^{-3}$ (Steadman, 1998).

Emission inventories have proved to be a useful technique in the assessment of emissions and the relative contributions of specific sources to the overall particulate load. Most useful in estimating anthropogenic emissions of particulate material, emission inventories provide an indication of trends in emission rates and the proportional importance of activities which result in particulate release. Emissions of primary particulate matter in the UK during 1994 are presented in Figure 2.1.

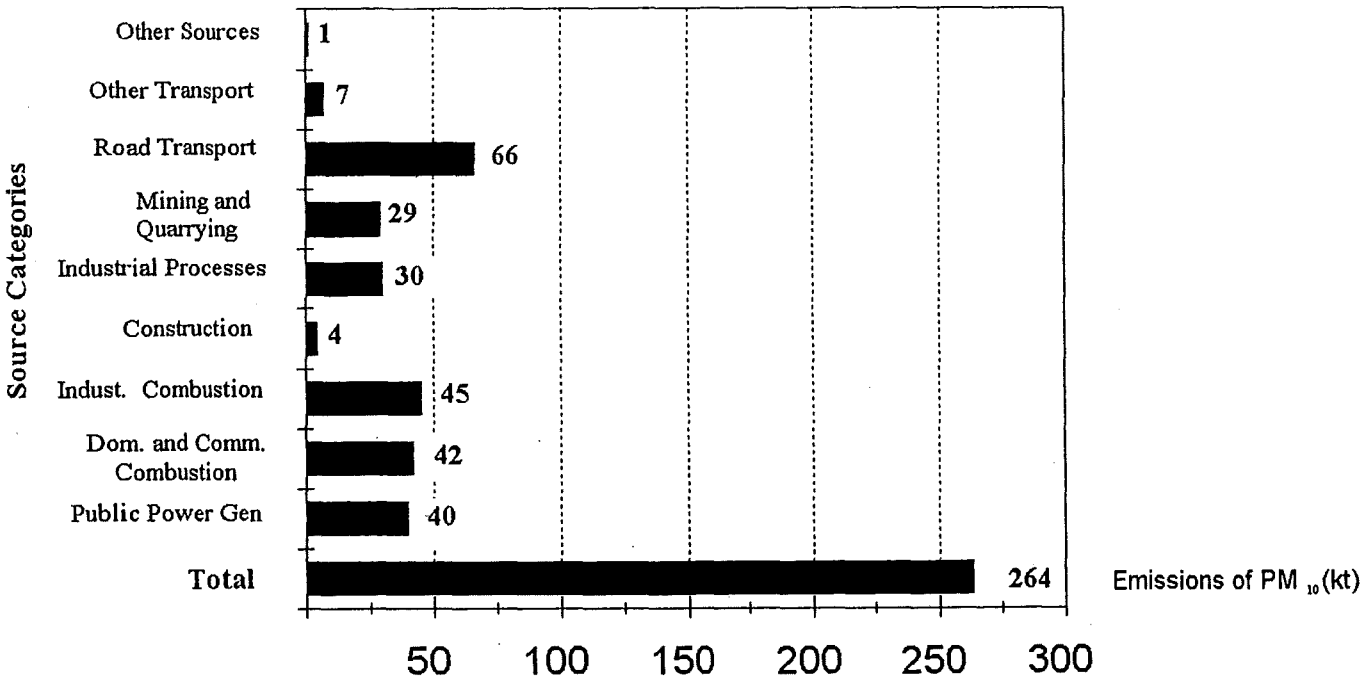

Figure 2.1 Emissions of primary particulate matter in the UK during 1994 by source (AEA, 1995).

2.3.2 Secondary Particulate Matter

Secondary particulate matter forms within the atmosphere from the condensation of vapours or by chemical reaction of gases of natural or anthropogenic origin. Secondary particulates arise from gas phase species reactions which generate a product of very low vapour pressure; this product then condenses around a pre-existing nucleus. The main source of these secondary particles is from the oxidation of sulphur dioxide (SO_2) and nitrogen dioxide (NO_2) to sulphuric acid and nitric acid respectively. These particles exist as solid particles at low humidities and as droplets at higher humidities. The sources of SO_2 and NO_2 in the UK are presented in Table 2.3.

The most abundant secondary particle constituent is estimated to be ammonium sulphate which results from the reaction of ammonia gas with sulphuric acid, itself a result of the atmospheric oxidation of sulphur dioxide (SO_2). Sulphuric acid reacts irreversibly in two stages to form either ammonium bisulphate or ammonium sulphate.

Both nitric acid and hydrochloric acid vapours react reversibly with ammonia gas to form ammonium salts. The formation of ammonium salts occurs where SO_2 and NO_2 are emitted, and ammonia is available for neutralisation. SO_2 and NO_2 are oxidised within hours of emission and particle formation is largely dependent on the meteorological conditions.

Table 2.3 Estimated emissions of sulphur dioxide and nitrogen oxides in the UK during 1993 (DoE, 1995).

Source Category	SO_2 Emissions		NO_x Emissions	
	Emissions (1000 tns)	% of Total	Emissions (1000 tns)	% of Total
Domestic	866	27	283	12
Commercial/public Sector	279	9	90	4
Industry	1,302	41	384	16
Agriculture	40	1	14	1
Road Transport	131	4	1,208	51
Other Transport	125	4	198	8
Miscellaneous	395	12	129	5
Exports	34	1	28	1
Other Emissions	16	1	13	1

Particle formation by bimolecular condensation may occur when two vapours condense to form a solid crystal in fixed stoichiometry, for example, ammonia and nitric acid condense to form ammonium nitrate in a one-to-one stoichiometry. Solid particles may also be formed from the gas phase, as in the production of radon daughters from radon.

2.4 ATMOSPHERIC LIFETIME AND TRANSPORT

The transport and atmospheric lifetimes of particles depend on their aerodynamic properties. Coarse mode particles have high deposition velocities and thus short atmospheric residencies.

Consequently, mass concentrations vary within meters of the source (eg quarry emissions) and coarse particles are important soiling agents within a short radius of the emission point. The deposition of coarse mode particles from industry and mining activities - once a common cause of soiling problems - has now been reduced by stricter legislation (COMEAP, 1995).

Fine particulate matter exhibits high spatial uniformity over large areas of the UK due to relatively long atmospheric lifetimes and the influence of meteorology. Fine particles in the 0.05-1 μm range have reported residence times averaging 7 days and may be transported over long distances before removal occurs (Jaenicke, 1988). The coagulation of fine particles, especially those containing the strongly adsorptive components such as particulate elemental carbon (PEC), may be accelerated by Brownian motion whereby agglomerates form and deposit faster (Del Monte *et al*, 1984). In the accumulation size range, particles are likely to be removed from the lower atmosphere by rain scavenging. The smallest particles (1 nm AD) agglomerate quickly with similar sized particles and thus have short residencies of around 10 minutes. Monitoring of the Chernobyl incident in 1986 provided a unique insight into the transport of persistent particles containing ^{137}Cs: primary particles were measurable for over 2 months and showed a mean residence time of approximately 10 days, reaching all parts of the northern hemisphere (QUARG, 1996).

2.5 REMOVAL MECHANISMS

2.5.1 Dry Deposition

Dry deposition is the continuous transfer of particles and gases to surfaces by impaction, sedimentation and Brownian motion. The atmospheric boundary layer extends approximately 1 km above the Earth's surface and describes the air directly affected by friction and heat exchange at the surface. Friction of the wind at the Earth's surface ensures roughly uniform particle concentrations throughout this layer, except for a millimetre or so layer immediately adjacent to the surface within which air movements are retarded. Particles deposit from the boundary layer by a combination of gravity, Brownian motion, interception and impaction. Electrophoresis, thermophoresis, diffusiophoresis, and photophoresis may also be important locally. In the thin band of stable air adjacent to surfaces, Brownian motion - the erratic movement due to the impacts of air molecules - tends to dominate. The smallest particles show the greatest response to molecular impacts, and the effects decrease with increasing particle size. This phenomenon causes the slow dispersion of particles in still air and increases

collisions of particles with each other and surfaces. The rate of dry deposition is generally expressed as the deposition velocity, V_d, where

$$V_d\ (m\ s^{-1}) = \frac{Flux\ density\ towards\ surface\ (g\ m^{-2}\ s^{-1})}{Concentration\ at\ reference\ height\ (g\ m^{-3})}$$

where the surface is taken to include any vegetation, buildings, etc.

2.5.2 Wet Deposition

Wet deposition is the transport of particles and gases to the Earth's surface in aqueous form. Due to its dependence on precipitation, wet deposition is episodic; precipitation occurs less than 10 % of the time in the UK. Particles of 0.05 to 2 μm AD are the least efficiently scavenged by wet deposition. Two mechanisms of wet deposition may be identified; rain-out or in-cloud scavenging. This is the main route for wet deposition, where particles are included in the developing droplet in the cloud; and wash-out or below cloud scavenging which is a much less efficient removal process, where particles are scavenged by precipitating droplets.

In the UK, rain formation involves an initial stage of ice crystal formation. The ice crystals are larger than the more numerous water droplets associated with the higher parts of the cloud. Falling ice crystals collect cloud droplets by impaction and interception and melt to form raindrops. Condensation nuclei are therefore efficiently scavenged within the cloud, while the entire aerosol size distribution is subject to high removal rates during rainfall (Hadi *et al*, 1995). By averaging wet and dry days in the UK together, the results imply an effective removal rate of approximately 7 % for particles of 1 μm AD and 15-30 % for particles of 3-5 μm AD and larger (QUARG, 1996).

2.6 MEASUREMENTS OF AIRBORNE PARTICULATE MATTER IN THE UK

2.6.1 Particle Mass Concentrations

A number of techniques have been used to measure particle mass concentration in the UK. The largest database - compiled over thirty years - derives from the use of the smoke shade reflectance technique which measures the soiling capacity of particulate matter and estimates the mass concentration of particles (BS1747 Pt 11, 1993). This methodology is, however, most appropriate where coal combustion is the primary source of particulate emissions as in the 1950s when the method was developed. Black smoke is measured using a black smoke sampler

which exhibits a 50% size cut-off at 4.4 μm AD, therefore predominantly collecting fine particles (McFarland *et al*, 1982). The particles are collected on a filter of measured reflectance. After 24 hours the reflectance of the filter is measured and the particulate load calculated from the reflectance change by a calibration curve produced empirically in the 1950/60s. Figure 2.2 shows the falling contribution of coal to UK smoke emissions and the increasing importance of diesel since the introduction of smoke-free zones in Clean Air Act (1956). Despite this, the black smoke measurements are still made at 225 sites in the UK (AEA, 1995) to provide a continuous dataset.

Total suspended particulate temporarily succeeded as the standard measure of particulate matter. Particles were collected on a pre-weighed glass fibre filter for gravimetric analysis using a high-volume sampler. In 1992, the UK Automated Urban Network (AUN) was established and incorporated tapered element oscillating microbalances (TEOMs) with PM_{10} size-selective inlets at the national monitoring sites. Table 2.4 shows urban PM_{10} concentrations in 1993 at ten major UK cities, as measured by TEOMs. TEOMs provide continuous PM_{10} data for 15 AUN sites and a number of local authority sites throughout the UK. TEOMs incorporate a pre-heating stage to 50°C after size selection and prior to weighing.

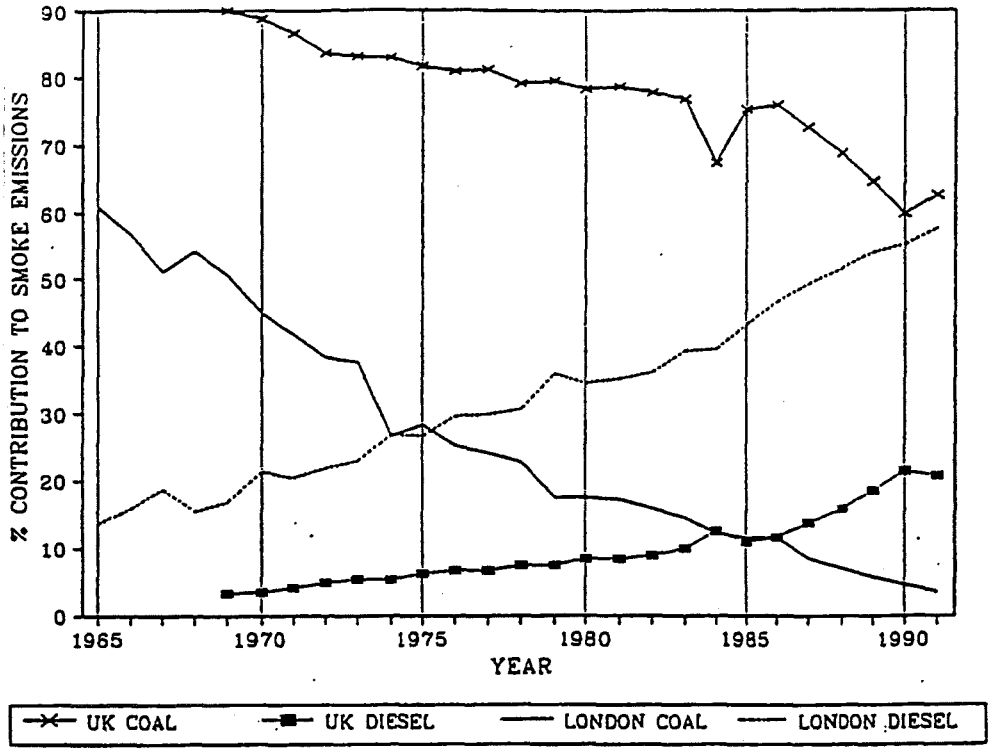

Figure 2.2 Contributions of coal and diesel fuel to smoke emissions in the UK (Kendall et al, 1994).

Table 2.4 Urban PM_{10} concentrations in ten UK city centres during 1993 (AEA, 1995).

Site	Annual Mean ($\mu g\ m^{-3}$)	50th %ile ($\mu g\ m^{-3}$)	90th %ile ($\mu g\ m^{-3}$)	98th %ile ($\mu g\ m^{-3}$)	Max Hourly ($\mu g\ m^{-3}$)	Max Daily ($\mu g\ m^{-3}$)
London (Bloomsbury)	29	24	51	81	140	100
Edinburgh	23	20	39	57	140	66
Cardiff	31	26	56	85	280	89
Belfast	32	25	58	108	445	120
Birmingham	26	21	48	76	186	102
Newcastle	29	25	55	84	236	79
Leeds	27	22	52	81	162	96
Bristol	27	22	53	82	270	81
Liverpool	29	23	56	94	331	163
Birmingham (E)	14	12	24	45	76	31

The relationship between these different measures of particle mass is complicated by the changing nature of the particulate pollution. PM_{10} mass concentrations are higher than those of black smoke at co-located AUN sites, and remain seasonally variable and highly site-specific (AEA, 1995). Measured particle mass concentrations are also dependent on the measuring technique employed. Results from different samplers operating simultaneously do not always agree despite nominally capturing the same particles (Monk, 1995; Rickard and Ashmore, 1996). Rickard and Ashmore, in a comparison between a TEOM and cascade impactor, found that the TEOM systematically underestimated the concentration of fine fraction and associated these losses with volatilisation of ammonium nitrate and chloride and hydrocarbons, a conclusion supported by the evidence of Clarke (1996). The sampler pre-heats the sample to 50°C to standardise weighing conditions, altering the concentrations of low boiling point organic species, and reducing the total mass collected. Size selectivity is not affected as heating is applied after the selective inlet.

2.6.2 Particle Number Density

The number density of particulates (the number of particles within a given volume of air) in "clean" maritime air is approximately 200 particles cm^{-3} as measured with a condensation nucleus counter. Using the same technique, number densities measured in Birmingham ranged between 1000 cm^{-3} and in excess of 100,000 cm^{-3}, the instrument limit. Jones and Harrison (1995) report average number densities of 20-25,000 cm^{-3} between midnight and 4am rising to 45-50,000 cm^{-3} between 7am and 7pm in Birmingham (Figure 2.3). The pattern of number

density approximates to that of PM_{10} mass concentrations for 24 hour average data (correlation coefficient, r = 0.64) with number density increasing earlier and peaking later in the day than PM_{10} mass concentration. This suggests that the coarse mode particles, which contribute the greatest mass to the PM_{10} mass concentration, are settling out leaving large numbers of small particles to agglomerate or be removed by wind action.

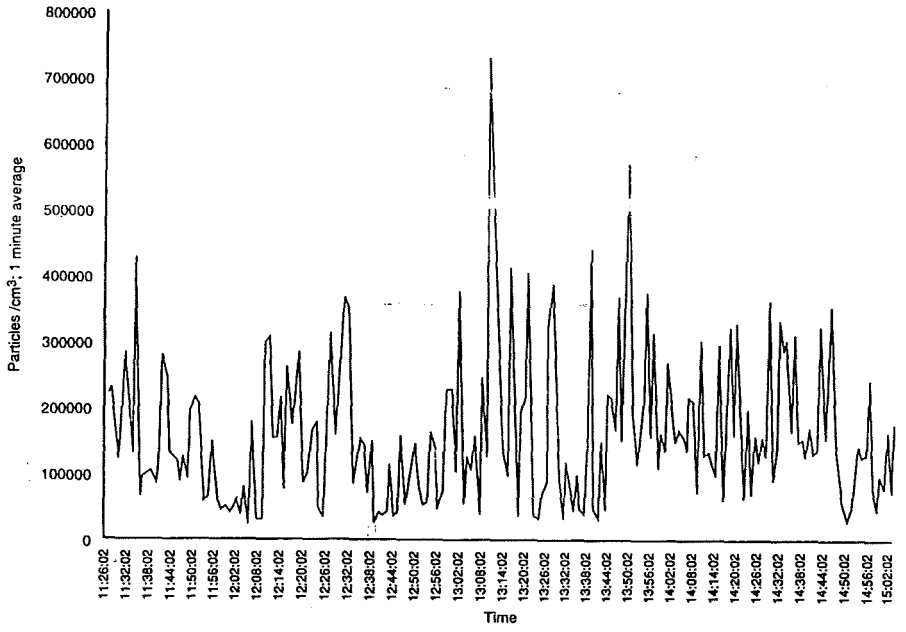

Figure 2.3 Typical particle number density as measured by a condensation nucleus counter in Birmingham 1994 (Collins and Harrison, 1994).

Measurements of particles in London (Waller, 1967) using scanning electron microscopy (SEM) indicated background levels of approximately 10,000 cm^{-3}, roadside levels of 30-50,000 cm^{-3} and upto 160,000 cm^{-3} in tunnel and urban fog samples. Table 2.5 shows the results of this study. This data must be treated with caution due to the changing sources and thus nature of urban particulates since this study was completed. However, the number concentration and median diameter, and the mass median diameter results are strikingly similar to those observed in more recent studies in the UK and USA.

Table 2.5 Results of SEM analysis of particle number density in London (Waller, 1967).*

Sample Site Type	Sample Ref.	Particle Number Concentration (1000 cm^{-3})	Number Median Diameter (μm)	Mass Median Diameter (μm)
Normal Pollution	A	7.8	0.09	0.7
	B	15.7	0.13	0.8
Street Sample	A	27.3	0.12	0.5
	B	49.7	0.10	0.4
Tunnel Sample	A	164.5	0.08	0.9
	B	120.4	0.09	0.7
Urban Fog	A	154.5	0.10	0.9
	B	144.7	0.09	0.5
	C	73.9	0.09	0.6
Light Haze	A	27.1	0.09	0.8

* Nomenclature from the original paper.

2.6.3 Particle Size and Particle Size Distributions

Particulates range in size from molecular aggregates of 0.005 μm AD to coarse particles greater than 100 μm AD. The range of sizes is limited at the lower end by the size of a cluster of approximately 5-10 molecules, which is the smallest condensed phase particle that can exist. Larger particles do exist within the aerosol but cannot be considered truly suspended except in high wind conditions. A variety of descriptions are employed to describe the distribution of particle size, depending on the method used for characterisation.

Size distributions have been measured in terms of numbers of particles with a certain diameter and as the mass of particles of a particular diameter. The mass distribution for TSP, as measured in Cricklewood, North London (Biggins, 1979), approximated to a log-normal distribution of mass with a mass median diameter of 2.8 μm and a significant proportion of particles in the coarse mode. Number size distributions of airborne particles measured in Birmingham (Collins and Harrison, 1994) provided evidence of a bimodal distribution between 0.01 and 1 μm, with two modes centred on 30 nm and 120 nm. These distributions varied with the time of day and meteorological conditions and the respective associated emission and chemical activity. Number median diameters also varied with time of day and averaged between 40-50 nm. The 1967 SEM study in London (Waller, 1967) reported mass median diameters in urban and roadside samples of between 0.4 and 0.8 μm and number median diameters of 0.09 to 0.13 μm. More recently, Rickard and Ashmore (1996) found that of a

weekly average PM_{10} concentration of 29.8 $\mu g\ m^{-3}$ in Greenwich during June/July 1995, $PM_{2.1}$ accounted for 58% and $PM_{1.1}$ accounted for 48% of the total on average. The size distribution was found to be bimodal with a mode in both the 3-5 μm and submicron range.

The humidity of the atmospheric aerosol will affect the size distribution of airborne particles. Water vapour condensing onto the particles will increase the size of particulate matter particularly that which contains hygroscopic material. Supersaturated water vapour condensing onto cloud condensation nuclei causes the particles to grow to sizes exceeding 10 μm (Loyalka and Griffin, 1993). Particles with high sulphate content also increase in size when exposed to high relative humidities (Keeler, 1988; Koutrakis *et al*, 1994). Since the UK has a typical atmospheric relative humidity of 70-80% and particles contain hygroscopic material, particles will be influenced by water accretion.

2.6.4 Particle Shape

Particle shape and morphology may give an indication of origin and may dictate aerodynamic diameter and hence behaviour, eg the deposition of asbestos fibres in the human lung. Shape will also affect the adhesion properties of the particle since the extent of contact (contact area) with a surface will be determined by shape. Classification systems for particles have been developed by several authors based on the surface characteristics and elemental composition of individual particles (Cheng *et al*, 1976; Sabbioni and Zappia, 1993; Ying Xie and Hopke, 1994). In general, diesel engine particles are reported as chain-like agglomerates of submicron particles (eg Figler *et al*, 1996), petrol engine exhaust particles as larger smooth and pitted particles, oil-fired particles as porous near-spherical particles and coal particles as perfectly smooth spherical particles (Sabbioni and Zappia, 1993).

Shape will influence the condensation rate of vapours onto particle surfaces. The accommodation coefficient α is a measure of the kinetic limitation to condensation at the particle surface, which is governed by a number of factors including the condensing species, and the composition and surface area/mass ratio of the particle (Pandis, 1995). The condensed species will in turn influence the deposition and hygroscopicity of the particle. The surface area of the particle is then extremely important in the particles eventual impact.

2.6.5 Chemical Composition of Particles in the UK

In the UK, airborne particles comprise three main categories of compounds: insoluble minerals derived from crustal material, hygroscopic inorganic salts and carbonaceous material. Background particulate concentrations are strongly dependent on the presence of primary and secondary particles. As no survey has been carried out to simultaneously assess all particulate components, conclusions must be drawn from the existing studies of specific components.

The Quality of Urban Air Review Group (QUARG, 1993 and also Harrison and Jones, 1995 and COMEAP, 1995) produce an estimate of the typical UK urban airborne particulate matter composition summarising the analytical work carried out in the UK to date. This work comprises the national monitoring surveys for metals and toxic organic compounds which investigated those trace components with implications for human health (Harrison and Williams, 1982; McInnes, 1990; Baek *et al*, 1991; Archer *et al*, 1994; DoE, 1995) together with academic research into the bulk components of particulate matter, primarily the soluble fraction (Harrison and Pio, 1983; Clarke *et al*, 1984; Colbeck and Harrison, 1984; Sturges *et al*, 1989; Harrison and Allen, 1990; Kitto and Harrison, 1992). Such a comparison of research carried out intermittently over a significant period, at different sites, using non-standardised site selection, sampling and analytical procedures makes interpretation difficult.

An approximate breakdown of particulate matter in the UK is shown in Table 2.6.

2.6.5.1 Elemental Carbon

Particulate elemental carbon (PEC) is the black component of smoke responsible for soiling of materials and the absorption of light. Light absorption by particles is almost exclusively caused by PEC (Horvath, 1993) which is the most influential factor in the measurement of smoke concentration using the black smoke reflectance method. PEC also has strong adsorptive properties due to a high porosity (and consequent large surface area) and the availability of one extra valence electron per exposed carbon atom at particle surfaces. Elemental carbon provides an effective catalytic site for atmospheric reactions such as the formation of sulphuric and nitric acids and acts as a carrier for condensed vapours. PEC measurements taken in the UK indicate levels of $\sim 6\%$ in Leeds (Clarke *et al*, 1984) and $\sim 3\%$ in Birmingham (Harrison and Jones, 1995) which represents $\sim 10\%$ of PM_{10} by mass.

Table 2.6 Concentrations of chemical components of airborne particulate matter as found by composition studies carried out in the UK (COMEAP, 1995).

Analyte	Typical Concentration	% TSP	% Fine Fraction	Reference
Soluble Ionic Species				
Sulphate (SO_4^{-2})	5-10 $\mu g\ m^{-3}$	20-25 %	~85 %	Clarke *et al*, 1984 Harrison and Pio, 1983
Nitrate (NO_3^-)	2-10 $\mu g\ m^{-3}$	10-20 %	60-70 %	Colbeck and Harrison, 1984 Harrison and Allen, 1989 Kitto and Harrison, 1992
Chloride (Cl^-)	1-3 $\mu g\ m^{-3}$	<10 %*	~10 %	
Ammonium (NH_4^+)	2-6 $\mu g\ m^{-3}$	<15 %	>95 %	Clarke *et al*, 1984 Harrison and Pio, 1983 Harrison and Allen, 1989
Strong Acid (H^+)	0.1 $\mu g\ m^{-3}$	Trace	~100 %	Kitto and Harrison, 1992 Archer *et al*, 1994
Carbonaceous				
Elemental Carbon	3 $\mu g\ m^{-3}$	10 %	~80 %	Pio *et al*, 1994
Organic Carbon	5 $\mu g\ m^{-3}$	15 %	~80 %	
Minerals				
Natural Minerals	5-15 $\mu g\ m^{-3}$	20-25 %	~5 %	Sturges *et al*, 1989
Metals				
Sodium	1 $\mu g\ m^{-3}$	2 % *	21 %	Harrison and Pio, 1983
Magnesium	0.1 $\mu g\ m^{-3}$	0.2 % *	19 %	
Calcium	0.4 $\mu g\ m^{-3}$	0.8 % *	25 %	
Potassium	0.1 $\mu g\ m^{-3}$	0.2 % *	44 %	
Lead	0.1 $\mu g\ m^{-3}$	0.2 %	90 %	McInnes, 1990
Iron	0.5 $\mu g\ m^{-3}$	1 %	35 %	Harrison and Williams, 1982
Others	5-50 $ng\ m^{-3}$	Trace	Most	McInnes, 1990
Toxic Organic Micropollutants				
Dioxins	4 $pg\ m^{-3}$	Trace	Most	Clayton, 1992
PCBs	1 $ng\ m^{-3}$	Trace	Most	Baek *et al*, 1991 QUARG, 1996
PAHs	150 $ng\ m^{-3}$	Trace	Most	

PCBs = Polychlorinated biphenyls
PAHs = Polyaromatic hydrocarbons
* indicates this compound was measured in a marine influenced aerosol

2.6.5.2 Organic Carbon

The organic component of urban particles and its influence on particle behaviour is poorly understood due to the complexity of, and relationships between, the compounds involved. The

enormous range of organic compounds detected in urban particles may be divided into two major source groups; primary condensates and oxidised hydrocarbons. Primary condensates - alkanes (C_{17}-C_{36}), alkenes, aromatics and polyaromatics - originate directly from the incomplete combustion of fossil fuels and are sorbed onto the surface of particulate matter. Oxidised hydrocarbons may either be attached to the particulate as primary condensates or may be produced during atmospheric oxidation reactions. Such compound groups include carboxylic acids, aldehydes, ketones, quinones, esters, phenols, dioxins or dibenzofurans.

Organic carbon constitutes 60-80% of the total particulate carbon. Total organic carbon concentrations in Birmingham are ~ 5 μg m^{-3} corresponding to $\sim 15\%$ of PM_{10} by mass (Harrison and Jones, 1995). Eichmann *et al* (1979; 1980) measured TOC concentrations in air at the west coast of Ireland and compared these results with identically collected samples at six other "clean air" sites. Table 2.7 shows how marine air has very low TOC concentrations while continental air parcels contain higher concentrations due to contributions from vegetation, etc.

Table 2.7 Ambient concentrations of TOC at isolated "clean" locations.

Compound	Sample Type	Concentration (μg m^{-3})	Reference
Total Organic Carbon (TOC)	Marine (Ireland)	0.57	Eichmann *et al*, 1979.
	Marine (continental influence)	1.84	
	Continental (clean)	4.49	
	Marine (Australia)	0.64	Eichmann *et al*, 1980.

Measurements are only made of those compounds with the greatest impact on human health due to the range of particle-associated compounds present in the UK urban aerosol. Difficulties also exist in identifying representative sites, sampling heights and monitoring periods, since sampling and analysis tend to be time intensive. Toxic organic micropollutants (TOMPs) are present in airborne particles and in gaseous form, depending on concentration, meteorological conditions and the availability of an adsorptive surface. The main groups for which monitoring has taken place are dioxins (polychlorinated dibenzo-*p*-dioxins), polychlorinated biphenyls (PCBs) and polynuclear aromatic compounds (PACs).

PACs occur naturally in sediments, fossil fuels and by natural combustion eg forest fires (Williams, 1995). The major sources of these compounds are anthropogenic, including petrol and diesel engines, oil and coal fired power stations, coke production, municipal refuse incineration and residential furnaces.

PAC may be subdivided into different subgroups depending on the heteroatom in the polyaromatic structure. Combustion generated groups of interest are polyaromatic hydrocarbons (PAHs), nitrogen containing PAH (PANH), sulphur containing PAH (PASH) and nitro containing PAH (NPAH). PAHs are one of the most well monitored groups of organic compounds in the UK and consist of two or more fused benzene rings in linear, angular or cluster arrangements. In the urban environment, the presence of PAH is mainly attributable to fossil fuel combustion. Analysis of these compounds is made difficult by the complexity of the mixtures, the variation in of component concentrations and phase distribution between gaseous and particulate forms. In the urban atmosphere, two and three ring PAHs are commonly found at concentrations three orders of magnitude higher than five ring PAHs (Williams *et al*, 1986).

PAHs tend to be associated with the fine particulate mode $d_p < 2.5$ μm particles (Daisey *et al*, 1986; Baek *et al*, 1991b). PAH have been shown to oxidise slowly on exposure to O_3, NO_2 and N_2O_5 to form oxygenated PAH, nitro-PAH and possibly aromatic polycarboxylic acids. Reactions of PAH with solar UV radiation or O_3 have produced polyaromatic ketones (PAKs) and polycyclic aromatic quinones (PAQ) (Van Cauwenberghe, 1983). Directly emitted PAKs are considered to be the transformation products of PAHs containing a single-bonded carbon atom (methylene PAH) which are oxidised immediately after escaping the reductive combustion zone (Van Cauwenberghe, 1983). PAKs have been identified in petrol and diesel engine emissions and biomass emissions (Ramdahl, 1983).

The main source of organic compounds in the urban atmosphere is vehicles. Needham *et al* (1989) report diesel particulates as comprising of carbon, a solvent organic fraction (SOF), a sulphate fraction and associated water, and other trace components including metals. The SOF arises from unburned components of the original fuel, lubricating oil and pyrosynthesised

compounds formed at the high temperature and pressure conditions of the engine. This fraction typically contributes 5-80% of the total particulate mass (Abbas *et al*, 1987). Lubricating oil is reported to contribute significantly to the SOF, including polyaromatic compounds (Williams *et al*, 1986). The viscosity of lubricating oil increases with vehicle use, due to the entrainment of soot particles, influencing particulate SOF emissions over time. Hilden and Mayer (1984) report that 30-50% of the SOF is attributable to lubricating oil; Cartillieri and Tritthart (1984) report lubricating oil to be responsible to 19-88% of the SOF. Abbass *et al* (1987) report lube oil contributions of 10-50% of the condensible fraction.

Kelly *et al* (1993) found particulate-associated PAHs in diesel exhaust consisted mainly of three and four ring compounds (phenanthrene, fluoranthene and pyrene). Five and six ring PAHs (benzofluoranthenes, benzopyrenes, dibenzo[a,h]anthracene and benzo[ghi]perylene) were the most prevalent PAHs in airborne particulate samples. The authors attribute this difference to the ageing of the airborne particulates and the subsequent losses of lower molecular weight PAH through volatilisation. Williams *et al* (1986) showed that the major PAH components of diesel exhaust were naphthalene, fluorene and phenanthrene and their alkylated derivatives. Williams *et al* (1995) also indicated that much of the particulate-associated PAH derived from unburned fuel, while five-ring PAH were formed in-cylinder. At low air/fuel ratios the ratio of PAH particulate emission to PAH in the fuel increased.

Simoneit (1984) found the PAH content of diesel fuel emissions to be greater than that of petrol emissions. PAH mixtures found in the aerosol of wood and coal burning areas were typically unsubstituted ring systems ranging from phenanthrene to dibenzanthracene, dominated by fluoranthene, pyrene, benzanthracene and benzofluoranthene (Simoneit, 1984).

Rogge *et al* (1993) amongst others have shown elevated winter concentrations (in California) of 16 PAH compounds during one year. Rogge *et al* showed benzo(ghi)perylene to exhibit the highest monthly concentration (up to 20 ng m^{-3}) of the PAHs measured. Total PAH concentrations (of 15 PAH) of up to 40 ng m^{-3} were found in the fine particulate fraction. The low summer concentrations were attributed to increased temperatures and atmospheric dilution, increased photochemical activity and reduced heating combustion. Baek *et al* (1992) amongst

others demonstrated that the phase distribution can be adequately described by the Langmuir equation. Table 2.8 shows seasonal phase distribution factors (ratios of particulate to gas phase concentrations) for selected PAH calculated from samples collected in London during 1987.

Table 2.8 Seasonal phase distribution factors* for selected PAH sampled during 1987 in London (Baek *et al*, 1992).

PAH	Winter Phase Distribution Factor	Summer Phase Distribution Factor
Phenanthrene	0.03	0.01
Anthracene	0.09	0.02
Fluoranthene	0.40	0.11
Pyrene	0.34	0.09
Benzo[c]phenanthrene	0.67	0.16
Cyclopenta[cd]pyrene	3.85	0.45
Benzo[a]anthracene	3.03	0.37
Chrysene	3.85	1.03
Benzo[k]fluoranthene	9.09	5.78
Benzo[e]pyrene	14.29	3.13
Benzo[a]pyrene	9.74	3.23

* Phase distribution factors are defined as the ratios of particulate to gas-phase concentration (Cautreels *et al*, 1978).

Baek *et al* (1991a, 1991b) measured the concentrations of 18 PAH over 8 six week periods 4 m from a major road in Central London, between October 1985 and December 1987. Table 2.9 shows the concentrations of individual PAH detected. The concentrations measured by Baek *et al* were probably high due to the height of the two sampling sites and monitoring periods which did not include weekends.

Table 2.9 Annual average concentration (ng m^{-3}) of selected PAH recorded at Exhibition Road, London in 1985/6 and 1987 with comparative data from a rural site (Baek *et al*, 1991a).

PAH	1985/6 Particulate Mean (Range) *(n = 23)*	1987 Particulate Mean (Range) *(n = 25)*	1987 Gaseous Mean (Range) *(n = 25)*	Rural Site Mean (Range) *(n = 2)*
Phen	0.41 (0.13-1.26)	0.11 (0.02-0.24)	5.01 (1.64-13.42)	0.02 (ND-0.03)
Anthr	0.45 (0.13-1.84)	0.18 (0.02-0.45)	2.66 (1.03-12.49)	0.03 (ND-0.05)
Fluor	1.66 (0.36-6.06)	0.81 (0.15-2.43)	2.65 (1.06-5.77)	0.21 (0.19-0.23)
Pyr	1.17 (0.06-3.95)	0.79 (0.06-2.23)	3.00 (1.10-5.59)	0.21 (0.16-0.26)
BaA	0.55 (0.05-1.80)	0.79 (0.22-2.39)	0.62 (0.03-3.27)	0.28 (0.16-0.39)
Chry	1.18 (0.21-3.87)	1.22 (0.29-4.65)	0.40 (0.19-0.60)	0.16 (0.13-0.19)
BbF	1.08 (0.25-3.10)	1.61 (0.57-3.37)	0.17 (0.03-0.61)	0.52 (0.45-0.58)
BkF	0.51 (0.12-2.92)	0.68 (0.30-1.68)	0.07 (ND-0.30)	0.21 (0.17-0.25)
BaP	0.99 (0.18-5.44)	1.44 (0.38-3.44)	0.19 (ND-0.71)	0.43 (0.41-0.45)
DahA	0.13 (0.02-0.53)	0.12 (0.04-0.37)	ND	0.05 (0.02-0.07)
BghiP	2.86 (0.71-10.01)	3.30 (1.52-6.63)	0.01 (ND-0.10)	1.16 (0.89-1.42)
I123P	0.99 (0.21-3.43)	1.57 (0.73-3.32)	ND	0.54 (0.43-0.65)

AEA Technology operate four TOMPs monitoring sites which commenced weekly averaged measurements of dioxins, PAHs and PCBs in January 1991. Other studies of urban PAH concentrations have been carried out in London (Baek *et al*, 1991a and 1992b; Brown *et al*, 1996) and Birmingham (Smith and Harrison, 1994). Table 2.10 shows total concentrations of selected PAHs (in both the gaseous and particulate phases) measured in Kensington and Westminster, London (Brown *et al*, 1996). PAH concentrations attached to different size fractions of PM_{10} (Baek *et al*, 1991a) showed that the majority of particulate-associated PAHs were found to exhibit unimodal distributions peaking between 0.4-1.1 μm.

Table 2.10 Comparison of selected total PAH concentrations measured at two sites in Central London, January 1991 - July 1992 (Brown *et al*, 1996).

PAH	Exhibition Road (ng m^{-3})	Marsham Street (ng m^{-3})
Phenanthrene	26.06	72.85
Anthracene	2.80	6.57
Fluoranthene	20.58	12.66
Pyrene	18.98	12.18
Benzo[a]anthracene	3.83	2.01
Chrysene	6.61	3.24
Benzo[b]fluoranthene	2.53	1.79
Benzo[k]fluoranthene	2.27	1.97
Benzo[a]pyrene	1.83	1.15
Ideno[1,2,3-cd]pyrene	2.93	2.45
Benzo[ghi]perylene	0.09	0.41

Similar patterns of particulate-associated PAH concentrations were found in Birmingham where PAH were sampled at a height of 15 m and a distance of 300 m from one of the busiest roads in Birmingham. 24 hour samples were collected on Nucleopore filters in series with a pre-impactor. The results of winter (January 2-February 28) and summer (July 27-August 1992) sampling campaigns are shown in Table 2.11.

Other organic compounds are less well monitored. *n*-alkanes are useful organic indicator species since characteristic distributions of a series of compounds are directly emitted from vehicles, present in biogenic detritus, particle-associated and relatively unreactive once in the atmosphere. Aerosol concentrations can therefore indicate direct emissions of primary anthropogenic and biogenic particles, using the carbon preference index (CPI).

Bray and Evans (1961) developed the carbon preference index (CPI) as an indicator of the extent of odd or even carbon number homologues within a sample. The CPI is expressed as a summation of the odd number homologues within a specified range of carbon numbers divided by a summation of the even number homologues within the same range. This inter-sample comparison is useful in identifying sources and establishing dominant sources of aerosol organic matter, as certain biologically produced *n*-alkanes show a pronounced

Table 2.11 Mean selected particulate-associated PAHs sampled at Birmingham University, 1992. (Harrison *et al*, 1996).

Compound	Winter (ng m^{-3})	Summer (ng m^{-3})
Naphthalene	0.69	0.14
Acenaphthylene	0.61	0.12
Fluorene	1.06	0.21
Acenaphthene	1.60	0.29
Phenanthrene	1.08	0.25
Anthracene	0.39	0.16
Fluoranthene	1.17	0.35
Pyrene	2.36	0.55
Benzo(a)anthracene	1.48	0.13
Chrysene	2.21	0.21
Benzo(b)fluoranthene	1.87	0.34
Benzo(k)fluoranthene	1.12	0.14
Benzo(a)pyrene	0.73	0.23
Dibenzo(a,h)anthracene	0.78	0.07
Benzo(ghi)perylene	1.91	0.76
Indeno(1,2,3-cd)pyrene	1.95	0.42
Coronene	1.03	0.27

predominance of odd carbon numbers, eg the *n*-alkane fraction of plant waxes. Hydrocarbons of abiological origin typically show no carbon number preference or tend towards low (< 1) CPI values. The calculation of CPI's requires concentration data on a range of C-numbers limited by even numbers. The CPI can be calculated on an individual sample basis, the average of individual sample CPI scores or as the CPI of the range of carbon numbers within a set of samples. The average of sample CPIs eliminates random noise within the data and the second averaging method allows the calculation of standard deviation within the samples. The type of CPI calculated depends on the analysis and the resultant CPI should be stated within its context. Separating the lower (C_{15}-C_{24}) and higher (C_{25}-C_{34}) ranges is a more sensitive method (Saiz-Jimenez, 1993).

Organic matter of recent biogenic origin shows a preference for odd carbon numbered *n*-alkanes with CPI_{odd} values of 6-9 and more (Bray and Evans, 1961; Simoneit, 1984; Simoneit

and Mazurek, 1981). Emissions from fossil fuels have a CPI_{odd} value close to 1. Hauser and Pattison (1972) compared *n*-alkane distributions in motor oil, diesel fuel, gasoline, auto exhaust, diesel soot and ambient air. The mass median carbon number in the fuels (C_{19}) increased to C_{24} in the combustion gases. The mass median *n*-alkane for motor oil was (greater than or equal to) C_{26} and this was therefore attributed to the increase in carbon number in the exhaust. The CPI therefore gives an estimation of the relative contribution of petroleum and biogenic hydrocarbons.

Eichmann *et al* (1979) measured particulate phase concentrations of C_9-C_{28} *n*-alkanes in air at the west coast of Ireland and compared these results with identically collected samples at six other "clean air" sites. The SOF concentration was found to be very uniform, accounting for approximately 10% of TSP and varying by approximately 1 $\mu g\ m^{-3}$ across all sites. *n*-alkane measurements were performed at two sites. The average concentration of *n*-alkanes (C_{10}-C_{28}) was 7 $ng\ m^{-3}$. Eichmann also compared calculated CPI values for the "clean air" sites and Table 2.12 shows the calculated CPI (C_{10}-C_{28}) of the collected samples by type.

Table 2.12 Calculated CPIs (C_{10}-C_{28}) for clean air sites representative of north Atlantic air (Eichmann *et al* 1979).

Sample Type	Range of *n*-C numbers	CPI *	CPI +
Marine air (M)	C_{10} - C_{28}	0.86	0.90
Continental air (C)	C_{10} - C_{28}	1.65	1.55
Combined (M + C)	C_{10} - C_{16}	0.85	0.79
	C_{16} - C_{28}	0.98	1.12

* CPI average from individual sample CPI's.
\+ CPI average from average distribution of carbon numbers in all samples.

Petrol engine exhaust contains only low concentrations of *n*-alkanes, which typically represent those found in lubricating oil, rather than from the original fuel itself. Simoneit (1985) reported *n*-alkanes in petrol exhaust between C_{15}-C_{27} with a maximum at C_{21} and a CPI of 0.93. Diesel exhaust on the contrary, does contain residual uncombusted fuel and all the *n*-alkanes present may be attributable to the fuel. A second group of compounds in the diesel exhaust were associated with a secondary naphthenic hump, was shown to originate from the engine lubricating oil. The absorbed hydrocarbons in diesel exhaust particulate typically have

a carbon number distribution from C_{14} to C_{40} (Black and High, 1979).

Broddin *et al* (1980) report maxima peaks from anthropogenic emissions at C_{24} and attribute odd carbon number preference in the higher *n*-alkanes (C_{27}-C_{31}) to natural emissions (ie vegetation). Vehicular emission samples were found to comprise *n*-alkanes with no carbon number predominance (from the fuel), unresolvable components (from the lubricating oil) and identifiable molecular markers (from both the fuel and lubricating oil). Gasoline exhaust showed no unresolvable hydrocarbons, while diesel exhaust samples showed variable amounts of unresolvable compounds and a slightly lower carbon number maximum at C_{20}. Simoneit (1983) took samples from selected vehicle types and found that diesel samples had on average a slightly lower carbon number maximum than gasoline vehicle samples (C_{20}, compared to C_{21}). Gasoline samples did not contain any unresolvable hydrocarbons. Lubricating oil samples exhibited a hydrocarbon hump with a boiling range average at around C_{30}.

Simoneit (1983) collected a series of one-off aerosol samples at 8 sites in the western United States, together with samples of local vegetation and vehicle exhaust (both gasoline and diesel powered vehicles) for the identification of molecular markers. Although the less remote rural samples were contaminated with petroleum residues, the relative petroleum contamination in urban areas was significantly greater. Plant wax components were also detected in urban aerosols. The urban samples contained *n*-alkane peak concentrations around C_{19}-C_{26} which agreed well with the same compound distributions in both diesel and gasoline exhaust where the maxima peaks are C_{22}-C_{23}.

Rogge *et al* (1993) identified and quantified *n*-alkanes in the fine fraction (<2.1 μm) of four urban locations and one remote site in California. The fine mass was found to comprise 20-40% carbon, one third of which was elemental. Of the bulk organic aerosol, 45-60% was extractable and elutable on the chromatographic columns. Of the elutable fraction, 23-29% of the mass was resolvable, of which 75-85% was positively identified as individual compounds. In total then, 2-4 % of the total fine particulate mass could be resolved as individual organic compounds, $\sim$75% of which was identifiable. *n*-alkanes ranging between C_{23}-C_{34} were found at all sites, with the rural site showing little seasonal variation in total *n*-alkane (C_{23}-C_{34})

concentration between summer (1.3 ng m^{-3}) and winter (1.7 ng m^{-3}). Seasonal variation at the urban sites however was much more pronounced with low monthly concentrations during the summer (20-40 ng m^{-3}) and highs during the winter (a December peak of 146 ng m^{-3}). Annual maximum peaks occurred at C_{25} and C_{31} at all urban sites.

Rogge *et al* (1993) also constructed normalised concentration profiles using elemental carbon as a tracer species to eliminate dispersion variations. This dilution-corrected data showed emissions to be higher during winter at all sites, especially in the range C_{23}-C_{30}, whereas C_{31}-C_{34} remained fairly constant throughout the seasons particularly at the least urban sites where biogenic influences were strongest. Cluster analysis revealed three sub-clusters at each site; PAH, PAK, PAQ, diterpenoid woodsmoke markers and higher *n*-alkanoic acids (*n*-C_{20} to *n*-C_{30}, probably originating from woodsmoke; elemental carbon and *n*-alkanes which indicate primary anthropogenic emissions; and finally, aliphatic and aromatic polycarboxylic acids which were likely indicators of secondary aerosol formation and transport.

2.6.5.3 Carbonate

Carbonaceous matter represents approximately 40% of particulate matter, making up ~50% of the fine fraction and ~15% of the coarse fraction. Carbonate constitutes approximately 5% of the total mass, comprises soil derived minerals, and is present mainly in the coarse mode.

2.6.5.4 Minerals

Harrison and Jones (1995) estimate that the remaining 20-25% unidentified mass of particulate matter is the insoluble mineral fraction. No UK studies have carried out quantitative analysis of compounds. A number of worldwide studies (QUARG, 1993) indicate the majority of compounds found are common to all and that composition of the coarse fraction in particular is highly dependent on local geology.

2.5.5.5 Water Content

During their atmospheric lifetime, particles are exposed to atmospheric water vapour which may be adsorbed depending on particle characteristics such as initial diameter, shape and chemical composition, and environmental factors such as humidity and temperature (Busch *et*

al, 1995). Ho *et al* (1974) estimated the aqueous fraction to contribute up to 50% of particulate weight at relative humidities of 70-80%, which are typical in the UK. Since aerodynamic diameter is influenced by water content, particle mass measurements based on aerodynamic diameter size-selection techniques will collect different particle fractions at different humidities and particle hygroscopicities.

Graedel and Crutzen (1993) estimate that an individual particle of 0.6 μm diameter of which 30 % of the total weight is water, will have a water shell of approximately 130 monolayers thick. The shell will consist of 40 monolayers when water represents 10 % of the total weight of the same particle. The water layer surrounding the core provides an ideal site for chemical reactions, particularly the dissolution of water soluble salts. Microphysical properties such as deposition velocity and agglomeration rate will also be affected. Weingarter *et al* (1995) investigated the growth and structural change of individual salt and fresh petrol and diesel engine generated particles at different relative humidities (RH). Results showed that while 78 nm sodium chloride particle diameters increased rapidly at deliquescence humidity, 108 nm agglomerated carbon particles shrink slightly between 70-90% RH, only beginning to grow at approximately 95 % RH. Weingarter *et al* (1995) attribute shrinkage to capillary forces acting on the sites of water condensation on the particles, causing the agglomerate as a whole to contract.

Gradual acidification of sorbed water may result in the dissolution of solid state constituents of the particle. The thinness of the aqueous layer and the abundance of anions and cations results in high ionic strengths within the water layer, depending on water accretion rates. The role of organics in water sorption is currently unclear. Saxena *et al* (1995) estimated that while organic compounds increased water sorption to particles in the Grand Canyon by 25 - 40 %, in Los Angeles organics were shown to reduce water sorption by 25 - 35 %. Both phenomena occurred at high RH (80 - 93 %), but neither mechanism could be identified. Evidence exists that organic components can increase or reduce hygroscopicity depending on the compounds involved.

2.6.5.6 Sulphates

Sulphate consistently accounts for ~30-35% by mass of the soluble ionic fraction and approximately 25% of the fine fraction, demonstrating good spatial uniformity (Harrison and Jones, 1995). Their likely origin as fine secondary particles of ammonium sulphate is consistent with the evidence of ionic balance studies which associate NH_4^+ as the predominant cation; this suggests sulphate is present as $(NH_4)_2SO_4$, NH_4HSO_4 or H_2SO_4 depending on the abundance and resultant neutralisation by ammonia. Radojevic and Harrison (1992) suggest the majority of sulphate is present as ammonium bisulphate or sulphuric acid. As most studies were influenced by the marine aerosol, sodium sulphate was expected to be present and was confirmed in the Lancaster 1979-81 study of Harrison and Pio, 1983.

According to Clarke *et al* (1984), sulphate is predominantly found in the fine fraction of both urban and rural particulate matter. Seasonal sulphate concentrations in Essex (Kitto and Harrison, 1992) differed substantially; concentrations between February and April 1987 were over twice those measured between August and November 1986. All four sites exhibited similar sulphate concentrations and experienced the seasonal fluctuation. Indeed, three simultaneously monitored sites in Essex (Harrison and Allen, 1990) gave concentration regression coefficients of between 0.92 and 0.96, indicating good spatial uniformity. Rickard and Ashmore (1996) found that sulphate comprised 22.8% of urban PM_{10} mass (6.8 $\mu g\ m^{-3}$) in Greenwich, London during June/July 1995, and was unimodal in distribution with a peak in the submicron range.

2.6.5.7 Ammonium Compounds

Ammonium is present as chlorides, sulphates and nitrates formed by naturally occurring ammonia and acidic gases from pollution sources. All studies (see Section 2.6.5.1) measuring sulphate also measured ammonium concentrations. The correlations (0.99) for fine NH_4^+ and fine SO_4^{2-} at both the urban and rural sites confirms the hypothesis that fine particles are largely composed of ammonium sulphate formed through reaction in the atmosphere. Ammonium accounts for ~18-25% of the soluble ionic fraction of particulate matter in all of the studies considered, with the majority in the fine fraction.

2.6.5.8 Nitrates

These compounds - predominantly ammonium nitrate and limited sodium nitrate - represent ~25% of the soluble ionic fraction in the studies considered. The bulk of nitrates are found in the fine fraction, although not exclusively. Rickard and Ashmore (1996) measured levels of NO_3^- in the Greenwich aerosol and found it to represent ~7% of PM_{10} mass (2.1 $\mu g\ m^{-3}$) with a unimodal distribution peaking in the 3-5 μm range.

2.6.5.9 Chlorides

Chloride concentrations exhibited good spatial uniformity in both the fine and coarse fractions across different aerosol types for studies across the UK. The dominant form of chloride is dependent on location with NaCl dominating in coastal areas, NH_4Cl predominating inland. The majority of chloride is present in the coarse mode (8% of coarse fraction mass) as sodium chloride and some ammonium chloride; chlorides represented 2% of the fine fraction mass mainly the result of gaseous HCl condensing to form ammonium chloride. Ammonium chloride is found at proportionally higher concentrations in the UK studies than those from the US (Sturges *et al*, 1989) possibly due to the higher concentrations of HCl resulting from the combustion of high chloride coal (Lightowlers and Cape, 1988) or the influence of the marine aerosol. Rickard and Ashmore (1996) found chloride represented 1.7% of PM_{10} mass (0.5 $\mu g\ m^{-3}$) on average with a unimodal peak between 3-5 μm.

Two distinct sources of chloride are apparent in the studies carried out by this group of authors and others. The application of road deicing salts during freezing conditions and in areas distant from coastal aerosol, road deicing salt have been found to be the sole origin of airborne sodium chloride (Sturges *et al*, 1989), almost exclusively in the coarse fraction (>2 μm AD). Table 2.13 shows autumn and winter average chloride concentrations in Essex during 1986/87.

Table 2.13 Autumn and winter measurements of chlorides at four sites in the South East of England (Kitto and Harrison, 1992).

Period	Essex Uni. ($\mu g\ m^{-3}$)	Colchester ($\mu g\ m^{-3}$)	Dedham ($\mu g\ m^{-3}$)	Walton Pier ($\mu g\ m^{-3}$)	Mean of Sites ($\mu g\ m^{-3}$)
21.8.86 - 13.11.86	0.89	1.06	1.28	1.13	1.09
24.2.87 - 16.4.87	2.27	3.06	2.31	2.39	2.51

2.6.5.10 Metals

Airborne metal-containing particles originate from natural and anthropogenic sources. Sodium and magnesium compounds occur predominantly in the soluble ionic fraction of natural particles originating from sea water. Magnesium is also associated with carbonates in areas of dolomitic geology. Heavy metals found in urban areas tend to be anthropogenic in origin, especially in and around heavily industrialised regions. Condensation of hot gases from industrial metal processing leads to the formation of fine particulate and surface layers on particles with a high surface area:mass ratio. Chemically active transition metal atoms condense on the surface of combustion particles. The resultant submicron particles are thus able to bypass emission control technologies and exhibit long atmospheric lifetimes, permitting long-range transport.

The former Warren Spring Laboratory (WSL) Multi-Element Survey (McInnes, 1990) and an AEA Technology survey of urban and rural sites (Lee *et al*, 1994) provide a longterm dataset of sites across the UK. WSL selected 20 urban sites initially which reduced to 5 sites after two years (these five sites were selected because of above-average concentrations of several monitored elements). Consequently, the sites may not represent typical urban metal concentrations, rather areas with industrial metal sources and heavy urbanisation. In central London, trace metal concentrations reduced over the monitoring period, with the most marked reduction achieved for lead, following the progressive reduction of lead in petrol and the increased use of unleaded fuel; WHO guidelines for lead (0.5 - 2 $\mu g\ m^{-3}$) were met at all sites after 1986. The WSL 'Lead in Petrol' survey (QUARG, 1993) similarly recorded falling lead levels at roadside sites, although exceedences of guideline levels continued up to 1989 in Cardiff and Manchester. The AEA Technology study of nine sites (six urban, two rural and one industrial, Lee *et al*, 1984) shows similar trends for the same and different metal

concentrations. Measured metal concentrations on average halved between the two sampling periods (1975-78 and 1986-89) at both the urban and rural sites.

2.7 SUMMARY

Airborne particles can be assessed by many methods which determine one or more characteristic, but there is no one comprehensive method of characterization. There has never been a comprehensive study of airborne particulate pollution in the UK which entirely characterises particles to monitor the number, size distribution, morphology and composition of particles. Until this has been carried out it is impossible to accurately quantify the impacts of particulate air pollution in the UK. Even background concentrations of particles and the patterns of concentration are unknown. Despite this, some generalisations may be made.

The composition of particulate matter is dependent on source, chemical transformations in the atmosphere, long-range transport effects and removal processes. Difficulties associated with the measurement of the size/composition distribution have prevented a thorough understanding of diurnal and seasonal trends. Difficulties in measuring the chemical composition of the smallest atmospheric particles eg those smaller than 50 nm have prevented actual assessment of composition. Most of the existing measurements are ground based and therefore little information is available on the vertical distribution of aerosol.

Chapter 3

STONE DAMAGE AND THE ROLE OF PARTICULATE MATTER

3.1 INTRODUCTION

Buildings and monuments are continually exposed to potentially damaging meteorological conditions such as precipitation, fluctuating temperature and wind. The damage caused by these elements has been found to be a function of stone type and condition, and related to the presence of anthropogenic air pollutants. This chapter focuses on the published literature relating to the soiling and damage of calcareous and granitic building materials by particulate matter. The extent to which the composition and concentration of particles are involved in these processes has proved difficult to quantify. Most studies focus on calcareous and granitic stone which have traditionally been used for buildings and monuments in the UK due to its availability, workability and durability, but which are susceptible to chemical corrosion.

Particulate soiling of buildings is an expensive and uncontrolled phenomenon. The effects are unsightly and reduce the value of buildings, and may be particularly damaging to those of historic importance. Removal techniques however, may be more damaging than the soiling layer, simply exposing a fresh and therefore more chemically active surface to attack.

The formation of black crusts is similarly undesirable in aesthetic terms and may cause internal stone damage beyond the building surface due to the leaching of minerals. An accurate understanding of the weathering process, the formation and composition of the black crust and the influence of air pollution is essential in establishing cleaning and conservation policies for historic buildings and monuments. Similarly, particulate emission control strategies should include the causes, effects and costs of particulate deposition onto surfaces. As black crusts may comprise hundreds of compounds, this complexity caused difficulties in establishing sensitive removal techniques which do not exacerbate stone deterioration (Amoroso and Fassina, 1983).

3.2 PHYSICAL PROPERTIES OF CALCAREOUS BUILDING STONE

3.2.1 Chemical Composition

The chemical composition of limestones varies with type and consequently source, and often the bed from it is extracted. Limestones are also inhomogeneous stones with inclusions such as fossilised shells which act as discontinuities within the stone. The average composition of limestones is presented in Table 3.1

Table 3.1 Average composition of limestone (Mason, 1966).

Compound	Percentage Composition (%)	Concentration (mg g^{-1})
SiO_2	5.19	51.9
TiO_2	0.06	0.6
Al_2O_3	0.81	8.1
Fe_2O_3	0.54	5.4
FeO	-	-
MgO	7.89	78.9
CaO	42.57	425.7
Na_2O	0.05	0.5
K_2O	0.33	3.3
H_2O	0.77	7.7
P_2O_5	0.04	0.4
CO_2	41.54	415.4
SO_3	0.05	0.5
BaO	-	-
C	-	-
MnO	-	-

The two most important constituents of limestone are calcite and dolomite, sometimes with smaller amounts of siderite (iron-bearing carbonates). Many of the commonly occurring limestones contain organic, detrital and chemically precipitated material in varying proportions. Both calcite (hexagonal $CaCO_3$) and aragonite (orthorhombic $CaCO_3$) are present in modern limestone accumulations. However, since aragonite is more easily dissolved or converted to calcite, it is absent in ancient limestones. Carbonates recrystallise easily during diagenesis, usually by compaction and cementation.

Great variation exists within the composition of limestone and the proportions of the principal constituents - silica, clay, oxides of iron, magnesium carbonate and organic matter - dictate colour and classification characteristics. Silicious limestones contain up to 50 % silica; more than 50 % silica leads to their classification as calcareous sandstones. Dolomitic limestones contain more than 20 % magnesium carbonate, argillaceous limestone contains an appreciable proportion of clay and ferruginous limestones have iron ore as a dominant constituent. The typical composition of Whitbed Portland Limestone is: 95.8% calcium carbonate ($CaCO_3$), 1.2 % magnesium carbonate ($MgCO_3$), 0.3 % aluminium and iron oxides (Al_2O_3 and Fe_2O_3), 1.3 % silica (Si_2O_3) and 1.4 % water and loss. The oolitic Portland beds are part of the Jurassic system, the quarries of which can be found on the Portland Isle. Calcarenite is a limestone composed of predominantly clastic sand-size (0.06-2mm) grains of calcite, with quartz. Organic limestones are formed when the skeletons of plants and animals precipitate in the absence of other sedimentary material.

Marble is metamorphosed limestone which is produced by recrystallisation. The hardest and most aesthetic marbles have been used as building stone for centuries due to the variety of distinctive colours and patterns which arise from their chemical and mineralogical composition (mostly calcite). Sandstones are sedimentary rocks composed of sand-size grains. These rocks have a minimum of 60 % free silica, cemented by various materials including carbonates.

3.2.2 Porosity

Porosity may be defined as the ratio of internal pore volume to the bulk volume (Tombach, 1982) and is expressed as a percentage. Typical porosity values for limestone range between 0.3-30%, much higher than those of igneous and metamorphic rocks (typically less than 5%). Stones with low porosities are much more resistant to weathering, as this prevents the water penetrating to the interior of the stone. Portland stone is used in St Paul's Cathedral and has the lowest porosity in limestones measured by Schaffer (1932).

Marble and limestone are both low porosity carbonate rocks which display relative chemical homogeneity.

3.2.3 Permeability

Permeability is defined as the capacity of a rock to allow a liquid to flow through it. The permeability of a rock is dependent on porosity and fluid viscosity. Stone types with high porosity and low permeability are particularly susceptible to destructive freeze-thaw action, where water is effectively trapped within the pores of the stone and may cause damage through expansion below temperatures of 4 °C.

3.2.4 Thermal Properties

The non-uniform application of heat to stone will create thermal gradients that may lead to thermal stress. Stresses may be introduced because of the differences in the amount of expansion and contraction of composites within the stone or because of poor heat conductivity of the material. For example, strong insolation may cause differential expansion of the rock surface and the rock core leading to exfoliation of thin sheets of stone. Differential expansion rates of adjoining materials may likewise damage stone work.

Efflorescences of gypsum may repeatedly dissolve and recrystallise in alternating periods of wetness and dryness. At high ambient temperatures, this can lead to supersaturation of solutions and a resultant increase in pressure within the intergranular space on recrystallisation. Although these are extreme conditions, Lal Gauri and Holdren (1981) report failure of sandstone as a result of repeated recrystallisation over long periods.

3.3 Weathering of Stone

Physical, chemical and biological processes contribute to the weathering of building stone. Tombach (1982) devised a classification system for the mechanisms contributing to stone decay. The five generic classifications are:

i) external abrasion

ii) volume change of stone

iii) volume change of material in capillaries and interstices

iv) dissolution of stone or change in chemical form

v) biological activity

Table 3.2 presents these decay mechanisms together with the environmental factors that influence them. These include meteorological factors such as rainfall and temperature which are the most commonly cited controlling factors. Gaseous and particulate pollutants are also cited as primary factors in initiating chemical change and secondary factors in causing physical alterations.

Del Monte and Sabbioni (1986) identified evidence of chemical, physical and biological weathering in their study of a cathedral in a relatively unpolluted environment. They concluded that while biological weathering is the most important weathering mechanism in clean environments, the sensitivity of endolithic algae and lichens to pollution dictates that their importance as weathering agents is reduced in polluted atmospheres. Indicator minerals of biological growth include oxalates (calcium oxylates hydrates formed due to oxalic acid secretion on calcite), weddellite and whewellite.

3.4 FEATURES OF DETERIORATED STONE AND THE ROLE OF PARTICULATE

The relative importance of biological, chemical and physical deterioration mechanisms have not been systematically investigated or evaluated (US EPA, 1996). While laboratory studies have been able to isolate one factor, in-situ analyses of stone deterioration have tended to focus on one or more selected pollutants or effects. The following section reviews the work carried out to assess the effects of particles on building stone deterioration. Particles have been implicated in four main effects, namely soiling, chemical alteration of the surface, surface recession and gypsum crystal growth.

Table 3.2 Classification of mechanisms relating to stone decay (Tombach, 1982). ⊗Primary factors ⊙Secondary factors

Mechanism	Rain	Fog	Humidity	Temp	Solar Insolation	Wind	Gaseous Pollutants	Particles
External Abrasion								
Erosion by wind-borne particles						⊗		⊗
Erosion by rainfall	⊗							
Erosion by surface ice	⊗	⊗		⊗				
Volume Change of stone								
Differential expansion of mineral grains				⊗			⊙	
Differential bulk expansion due to uneven heating	⊗			⊗	⊗			
Differential bulk expansion due to uneven moisture content	⊗	⊗	⊗	⊗	⊗	⊙	⊙	⊙
Differential expansion of differing materials at joints				⊗				
Volume Change of Material in Capillaries and Interstices								
Freezing of water	⊗	⊗		⊗				
Expansion of water when heated by the sun	⊗	⊗		⊗	⊗			
Trapping of water under pressure when surface freezes	⊗	⊗		⊗				
Swelling of water-imbibing minerals by osmotic pressure	⊗	⊗	⊗				⊙	⊙

Table 3.2 Classification of mechanisms relating to stone decay (continued). ⊗Primary factors ⊙Secondary factors

Mechanism	Rain	Fog	Humidity	Temp	Solar Insolation	Wind	Gaseous Pollutants	Particles
Hydration of effloresences, internal impurities and stone constituents	⊗		⊗				⊙	⊙
Crystallisation of salts			⊗	⊗	⊗	⊗	⊙	⊙
Oxidation of materials into more voluminous forms	⊗	⊗					⊙	
Dissolution of Stone or Change in Chemical Form								
Dissolution in rain water	⊗			⊗			⊗	⊗
Dissolution by acids formed on stone by atmospheric gases or particles and water	⊗	⊗	⊗	⊗			⊗	⊗
Reaction of stone with SO_2 to form water soluble material	⊗	⊗		⊗			⊗	
Reaction of stone with acidic clay aerosol materials	⊗	⊗		⊗				⊗
Biological Activity								
Chemical attack by chelating, nitrifying, sulphur reducing, or sulphur-oxidising material			⊗	⊗			⊗	
Erosion by symbiotic assemblages and higher plants that penetrate stone or produce damaging excretions	⊙	⊙	⊗	⊗ ⊗	⊗ ⊗			

3.4.1 Factors Affecting Deposition of Atmospheric Particles to Stone Surfaces

Most of the transfer of particulate matter across the air-surface interface occurs in the bottom 2 m of the atmosphere, a region described as the mass transfer boundary condition. The rate of transfer and the site of deposition is governed by the complex interaction of particle, surface and local environmental conditions. The number of particles depositing to a surface depends on the concentration of particles and the deposition velocity. The factors governing particle deposition to, and retention by, a surface are summarised in Table 3.3.

3.4.2 Soiling

Soiling may be defined as the discolouration of a material which reduces the aesthetic quality and usefulness of a surface, through the absorption and scattering of incident light. This is of particular importance when considering buildings of historic importance or technologies such as solar cells. Increased frequency of cleaning, washing or repainting becomes an economic burden and may affect the lifetime of a material. Carey (1959) found that when black particles covered 0.2 % of a white surface, the surface appeared soiled in comparison to an adjacent clean surface. This conclusion was supported by Hancock (1976), who stated that an effective area coverage (EAC) of 0.2 % resulted in soiling. Soiling rates depend on the factors noted in Table 3.3, together with the contrast between particle and surface.

Beloin and Haynie (1975) first reported the use of reflectance change of a substrate over time compared with reflectance at time zero, ie the unsoiled sample value. Soiling can be measured using such a technique employing a simple reflectometer which measures white light reflected from a surface with a 0-100% scale. The method provides a relative reflectance value to a white tile to measure the soiling rate over time. The method is quick, cheap and effective, although no authors report accuracy or reproducibility figures for the technique. Indeed, some authors have observed localised measurement variation in readings due to environmental conditions such as humidity (CE Contract No. STEP-CT90-0097) and limited data scatter could be expected to result from variable moisture content at the sample surface due to local meteorology. However long term trends have been measured by many authors using this method (Beloin and Haynie, 1975; Mansfield, 1989; Creighton *et al*, 1990; Haynie and Lemmons, 1990).

Table 3.3 Factors identified as affecting particle deposition velocity and particle retention by surfaces.

Parameter	Characteristic	Macro-Effect	Micro-Effect	Reference
Aerosol	Size distribution	Determines deposition velocity and adhesive properties	Increased deposition to a surface with increasing size; elasticity of particle - deformation of smaller particles may increase adhesion to surfaces	Corn, 1966; Schneider, 1973; Visser, 1975; Ghosh and Ryszytiwskyj, 1988; Hollander and Pohlman, 1991.
	Concentration	Deposition flux increases with increased concentration	Determines diffusion gradient to a surface	Sehmel, 1956.
	Shape	Deposition velocity; adhesive properties	Adhesion depends on amount of particle:surface contact, and is therefore dependent on shape	Sehmel, 1956; Corn, 1966; Esmen, 1996.
	Bulk composition	Deposition velocity; chemical reactivity; moisture content; adhesive properties	Density; hygroscopicity, solubility and mass gain; long term reactivity with and corrosion of deposition surface; recrystallisation of solutes; particle retention net electronic charge	Junge and McLaren, 1971; Winkler, 1988; Lammel and Novakov, 1995; Weingarter *et al*, 1995.
	Surface composition	Deposition velocity; chemical reactivity of surface layer may dominate particle retention	Hygroscopicity; surface charge; initial reactivity with deposition surface	Gill *et al*, 1983; Winkler, 1988; Albers *et al*, 1992; Andrews and Larsen, 1993; Faude and Groschnick, 1993; Hollander *et al*, 1995.
Surface	Surface roughness	Deposition velocity and particle retention	Increased surface roughness increases deposition velocity	Corn and Stein, 1965; Chamberlain, 1967; Sehmel and Hodgeson, 1978; Hahn *et al*,1985.
	Orientation	Deposition velocity influenced by wind, rainfall and insolation	Edge effects; erosion of surface; thermophoresis	Little and Wiffin, 1977; Roth and Anaya, 1980; Horvath *et al*, 1997.
	Surface layers	Particle retention	Adhesion (capillary force) and resuspension	Bowling, 1988; Nicholson, 1980.
	Composition	Particle retention by reactivity	Solubility; recrystallisation; structure	Del Monte *et al*, 1984; Mcgee *et al*, 1992.
	Thermal properties	Particle retention influenced by thermal expansion and radiation	Enhanced erosion of surfaces by freeze/thaw	Nazaroff and Cass, 1991.
Environmental	Wind conditions	Deposition velocity influenced by wind speed and direction	Surface boundary layer thickness	Sehmel, 1973;Garland, 1982; Horvath *et al*, 1997.
	Humidity	Condensation	Adhesion; dissolution of surfaces	Camuffo *et al*, 1982; Hanel, 1982.
	Rainfall	Removal of particles	Mechanical removal of particles from atmosphere/surfaces; dissolution of surface	Roth and Anaya, 1980; Cuddihy, 1988; Hamilton and Mansfield, 1992.

Alternative methods for measuring soiling include light transmission for light transparent materials such as glass, paper and filter paper which particles have been collected onto. More complex methods include the spectrophotometer or colour light meter (eg X-Rite SP68 sphere spectrophotometer), which is able to differentiate between reflected electromagnetic frequencies and record patterns of different colours across surfaces (Murray and Massey, 1996 and 1999; Murray 1998).

Cuddihy (1988) identified three distinct soiling layers at the surfaces of solar cells. Figure 3.1 shows the identified layers. A primary layer (C) of particles was found to be strongly chemisorbed to the surface, surface material dependent and removable only by vigorous scrubbing. A secondary layer (B) of particles was physically attached creating a gradation of surface energy from a high at the interface with the first layer to a low on the outer surface. This layer was found to be resistant to removal by rain, but easily removed by washing or by adhesive tape. A third surface layer (A) was susceptible to removal by rain action. All layers were not observed on the same materials at different sites or on different materials at the same site, and were therefore adjudged to be site and material dependent. Camuffo *et al* (1981) define the soiling layer as deposited dust with some chemical attachment to a surface which can be removed by washing to leave no sign of deterioration.

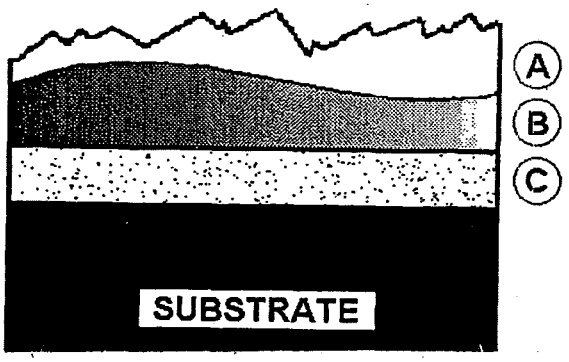

Figure 3.1 The three distinct layers identified as causing soiling of materials (Cuddihy, 1988).

The soiling of horizontal surfaces is theoretically related to the surface area of the particle and the deposition velocity (US EPA, 1982). As the surface area of particles reduces quadratically with decreasing particle size (assuming spherical particles) and deposition velocity increases

with the square of the diameter, large particles are expected to contribute more to surface soiling than an equivalent mass of smaller particles. Although second order effects enhance deposition rates of small particles, deposition of particles >10 μm is likely to be higher. However larger particles tend to be lighter colour and transported smaller distances from their source. Other factors which may influence soiling rates are mineralogical leaching from the inner stone to the surface, eg iron staining, or the growth of biological colonies such as algae, fungi, lichens, bacteria and moss (Webster *et al* 1992).

Soiling of vertical and downward-facing surfaces is predominantly due to fine particle deposition (Creighton *et al*, 1990). In urban areas in the UK, these sized particles are likely to originate from vehicles and have a high soiling potential due to their composition eg particulate elemental carbon (PEC). The rate of deposition of these particles is governed by the rate of particle migration across the thin surface boundary layer.

Newby *et al* (1991) estimated the costs of soiling in the UK to be £74-80 million per year, due to cleaning expenses associated with removing soiled layers. Webster *et al* (1992) quantified the costs of sandstone cleaning in Scotland. Freeman (1982) estimated the soiling and cleaning savings achievable by introducing air pollution control measures in 1978 in the US, to be US $3 billion. The US EPA (1982) estimated that amenity loss due to exterior household soiling ranged from $1-3.5 billion (in 1978 dollars). The 14 μg m^{-3} annual average TSP reduction between 1970-78 was estimated to provide a $14-50 million per μg m^{-3} reduction in cleaning costs. Ball and Caswell (1983) and Mansfield (1989) proposed that diesel vehicles were likely to be the greatest contributor to soiling in London and other conurbations in the UK where stationary sources of particulate had been greatly reduced through legislation.

Several authors have analysed deposited particles and their size distributions, and these data provide an indication of the nature of the particles deposited and thus the mechanism of deposition. A bimodal size distribution with a minimum at 1-5 μm was found by Haynie (1985) in an analysis of particles depositing to glass slides positioned 2 m and 20 m from the road. This study also found that surface coverage was dominated by particles >10 μm - covering 63% -deposited by gravitational settling. Even on a vertically positioned glass slide

2 m from the road particles >10 μm accounted for 32 % of surface coverage. Larger particles were therefore more frequently found away from the road with smaller particles accounting for a greater proportion of surface coverage on the roadside sample. Roadside surface coverage was double that found at 20 m from the road.

The difference in particle size distributions on horizontal and vertical soiled samples is interesting when related to TSP measurements. Haynie (1985) suggests that high volume samplers may provide a fair indication of soiling for vertically oriented surfaces and not for horizontal surfaces where gravitationally deposited dust surface coverage dominates.

Creighton *et al* (1990) exposed horizontal and vertical glossy and flat painted wood samples over thirteen weeks and analysed deposited particle size distributions using scanning electron microscopy (SEM) analysis. Particle number concentration was found to reduce rapidly with decreasing particle size on all exposed samples, with higher <1 μm particle densities on horizontal samples. Surface area coverage was estimated assuming particles were spherical and deposited in a monolayer; Table 3.4 summarises the results of this study. Sheltered horizontal samples experienced higher surface coverage (14%) than unsheltered (3.5%) due to coverage by coarse particles in the 10-60 μm range. Surface coverage of unsheltered horizontal samples was dominated by particles of 4 μm diameter. The percentage area coverage of particles <1 μm was similar for both sheltered and unsheltered surfaces, indicating the greater retention of smaller particles by surfaces. Size distributions were similar for both sample types (<6 μm), with slightly higher number concentrations of particles $>$ 6 μm accumulated on the sheltered vertical sample.

Weekly reflectance and meteorological measurements showed rain episodes to be very influential in the slowing of reflectance loss. Percentage loss of reflectance of all the samples after thirteen weeks are recorded in Table 3.4. While the unsheltered horizontal surface experienced a higher reflectance loss than the sheltered sample due to the action of rain removing particles above 10 μm, the unsheltered vertical surface experienced a higher reflectance loss than the sheltered sample. Glossy surfaces were shown to retain greater reflectivity than flat paint.

Table 3.4 Percentage surface coverage of painted wood samples by deposited atmospheric particles and the particle sizes responsible (Creighton *et al*, 1990).

Surface Orientation	Estimated Area Coverage (%)	Dominant Particle Size	Reduction in Surface Reflectance (%)
Sheltered Horizontal	14	10 - 40 μm	21
Unsheltered Horizontal	3.5	< 4 μm	15
Sheltered Vertical	3	< 10 μm	1.5
Unsheltered Vertical	2	< 6 μm	7

These findings are in good agreement with the experimental work to remove particles from surfaces carried out by Schneider (1973), where particles in the 5-10 μm range adhered most tenaciously to surfaces. This also agrees with the work of Roth and Anaya (1980) and Draft *et al* (1982) who found that soiling particles were predominantly less than 5 μm.

Rain appears to be the primary particle removal mechanism for soiled surfaces (Roth and Anaya, 1980; Cuddihy, 1988; Camuffo *et al*, 1982). All soiling studies have shown rain to be effective in the removal of coarse particles (>5 μm) from surfaces and inefficient at removing smaller particles. Removal by the resuspension action of wind may also be important for larger particles, but removal by this mechanism will reduce in the presence of condensed liquid at the building surface and is unlikely to be effective for small particles.

3.4.3 Surface Chemistry Alteration

Stone surfaces may be subject to limited chemical change on exposure to the environment, leading to the formation of a chemically changed surface layer which neither extends beyond the surface nor causes it to recede. Sengupta and de Gast (1972) found that SO_2 sorption causes physical changes in stone porosity and water retention, so that hard, non-porous layers form following the removal of $CaCO_3$. Camuffo *et al* (1982) describe surface layer alteration in white crusts which are defined as the zone of weathering to the depth at which there is no evidence of structural or chemical change within the stone. This layer is formed in areas exposed to regular wetting by direct rainfall impaction or run-off and dissolved calcite is removed from the stone surface. Lal Gauri and Holdren (1981) found that the weathering zone ranged from 0.5 mm in low porosity marble to 4 mm in higher porosity stone.

Viles (1990) found that gypsum growth was more pronounced on Portland stone than on Monk's Park stone after exposure in rain-protected positions in central London. Hutchinson *et al* (1992) found that exposure of Portland and Monk's Park limestones to gaseous or liquid acidic species caused surface darkening or staining. This was believed to be due to the relocation of iron compounds from within the stone to the stone surface. Jaynes and Cooke (1987) analysed the surface (top 1 mm) concentrations of sulphate, nitrate and chloride. Sulphate concentrations in London samples of Portland stone and Monk's Park stone were 3.43 and 2.54 times higher respectively, than rural counterparts. Exposed samples had considerably less sulphate than protected samples since deposited sulphate was likely in the form of $CaSO_4$. Chloride concentrations were also higher in London than at rural non-coastal sites, while coastal sites experienced the highest chloride concentrations.

3.4.4 Surface Recession

Surface recession is the result of dissolution of ions from the stone material in precipitation which may impinge on the stone directly or as run-off. Precipitation in equilibrium with atmospheric CO_2 has a pH of approximately 5.65 due to the dissolution of CO_2 to form weak carbonic acid (H_2CO_3). Emissions of nitrogen and sulphur oxides from power stations, domestic heating sources and vehicles have increased the acidity of precipitation. This increased acidity has led to the accelerated degradation of building materials in industrialised and urbanised regions. The transboundary nature of precipitation acidity has also led to increased degradation in remote areas. Pye and Schiavon (1989) demonstrated that the sulphur contained in building stone gypsum always came from atmospheric sources, including soils, ground and sea water, atmospheric pollution, waste ground-fill and highway de-icing salts.

The crystallisation of salts may occur on a stone surface (efflorescence) or within individual pores (cryptoflorescence). The salts formed are mainly the sulphate salts of potassium, sodium and calcium, formed by the reaction of sulphur dioxide gas or sulphates in the atmosphere with water and soluble salts. Soluble salts may originate from the leaching of building stone itself or may be the product of stone decomposition in the presence of external factors, such as jointing materials, soil and the atmosphere. Cryptoflorescence creates pressure within the pores as crystals expand and water evaporates, leading to enhanced erosion of the surface layer.

Stone surface recession can be calculated by measuring the difference between the present surface and a marking device. This type of deterioration is prevalent in carbonaceous rock due to sulphation and dissolution (Del Monte *et al*, 1981). Sharp *et al* (1982) calculated average recession rates of 0.066 and 0.081 mm yr^{-1} using lead plugs. Jaynes and Cooke (1987) found recession rates of 16 μm yr^{-1} Portland stone in Central London compared to 10.3 μm yr^{-1} at rural sites, and that recession rates increased over time. Rates measured by Honeyborne and Price (1977) between 1955-65 were 29 μm yr^{-1} in central London and 9.96 μm yr^{-1} in a rural location. Protected samples experienced 1/3 of the weight loss of exposed samples. Trudgill *et al* (1990) reported long-term (1718-1987) and short-term (1980-985) recession rates of 0.081 mm a^{-1} and 0.06 mm a^{-1}, respectively.

Baedecker *et al* (1992) measured recession rates of between 15-30 μm yr^{-1} for marble and 25-45 μm yr^{-1} for limestone at five sites in the US. Calcium ions in runoff from samples accounted for half the measured rate, suggesting grain loss from surfaces was important in the recession process. Dry deposition of SO_2 between rain events and not rainfall acidity seemed to have the greatest effect. Natural rainfall acidity accounted for 70% of erosion by dissolution alone.

Butlin *et al* (1992) found good correlations of stone damage and weight change with mean annual SO_2 concentration, rainfall volume and hydrogen ion loadings. Butlin (1995) also found that the relative importance of each term depended on the measurement location. Webb *et al* (1992) studied limestone degradation in the UK and found increased weight loss of samples was strongly associated with increased SO_2 concentration. Rainfall did not significantly affect limestone degradation. The average overall recession rate was 24 μm yr^{-1} and increased stone loss due to SO_2 was less than 1μm $yr^{-1}pbb^{-1}$. Yerrapragada *et al* (1992) found that SO_2 was more reactive with marble when more NO_2 was present. Haneef *et al* (1993) found that ozone enhanced the deposition of SO_2, NO_2 and NO deposition to limestone. Cobourn *et al* (1993) found that deposition of SO_2 to carbonaceous stone increased with increasing water on the stone surface, following epsomite formation. Schuster *et al* (1994) determined the contributions of wet and dry deposition of SO_2 to marble damage, found 10-50% of calcium in runoff was removed through the process of gypsum formation when dry and dissolution during rain. Sabbioni *et al* (1992) found particles with a high sulphur content enhanced the reactivity of the

limestone samples with SO_2. Under high wind conditions, particles may enhance the slow erosion of surfaces through impaction (Yocom and Upham, 1977).

Dose response functions have been developed from these experimental results for use in the prediction of air pollution impacts and the enforcement of air pollution control strategies. The UN/ECE materials programme developed a limstone surface recession dose response function based on results from 100 observations. Surface recession R ($\mu m\ yr^{-1}$) was found to be

$$R = 2.7[SO_2]^{0.48}\, e^{0.018T} + 0.019\ Rain\ [H^+]\ t^{0.96}$$

where SO_2 is sulphur dioxide concentration ($\mu g\ m^{-3}$), T is temperature (°C), t is time (years) and $[H^+]$ is hydrogen ion concentration in precipitation ($mg\ l^{-1}$). These dose response relationships indicate the chemical nature of recession by sulphur dioxide and rain, and other mechanical effects should also be considered (Haagenrud and Henriksen, 1997).

3.4.5 Stone Surface Crusts

3.4.5.1 Formation

Sulphation of calcitic stone to form a white crust is the most common feature of damage by air pollution to building stone. Black crusts comprise reprecipitated calcite embedded with gypsum crystals and carbonaceous particles. Crusts appear in areas that receive no direct surface wetting which would exert mechanical stress on the stone surface, but which are wetted indirectly through percolation and condensation (Del Monte, 1981). While the black layer initially provides a hydrophobic cover (Nord and Ericcson, 1993), crusts may eventually detach, damaging the surface and exposing the underlying stone (Brimblecombe, 1992).

Del Monte *et al* (1984) found that the reaction of marble calcite into gypsum was catalysed by black carbon particles produced by oil burning. The sulphur associated with such particles has been indicated as the source of sulphur for gypsum formation in the presence of rainfall (Fisher *et al*, 1978). The high surface area of such particles and the activity of PEC as a catalytic site for the oxidation of SO_2 and NO_x, supports this evidence. Gypsum crystals grown on the surface of oil-fired particles under laboratory conditions exhibit bladed gypsum crystal growth.

Rodriguez-Navarro and Sebastian (1996) grew gypsum crystals on fresh wetted limestone after

24 hours exposure to 100 ppm SO_2 at 100 % RH when a thin layer of diesel particulates was deposited on the surface of the stone. After 48 hours, massive interwoven gypsum crystals were apparent, associated with metallic or carbonaceous particles. Incipient gypsum crystal growth occurred after 48 hours when petrol exhaust particulates were deposited on a similar surface. No gypsum crystals were detected on fresh limestone devoid of particulate matter. The authors therefore postulated that black crust formation was initialised by dust deposition which fixed atmospheric SO_2. The oxidation of SO_2 was assumed to take place with metal-rich and carbonaceous particulate matter acting as oxidant and catalyst, so that

$$2SO_2 + O_2 \rightarrow 2SO_3$$

where catalytic action may be enhanced by the synergistic action of the different metals contained within the particles. Hydrolysis of SO_3 in water, produces sulphuric acid

$$SO_3 + H_2O \rightarrow H_2SO_4$$

which will attack limestone in the presence of humidity, to form gypsum. Due to the mineralogical composition of this dust and its high porosity, water retention would be high.

$$H_2SO_4 + CaCO_3 + H_2O \rightarrow CaSO_4.2H_2O + CO_2$$

The final stage of crust growth would involve dissolution and reprecipitation of bladed and tabular gypsum crystals at the surface and within the pores of the stone. Mcgee and Mosotti (1992) showed that gypsum crystals form at the pore/opening interface where evaporation is greatest and are thus stone type dependent. Crust formation is enhanced by increased porosity or an irregular surface.

Nord *et al* (1994) found a positive correlation between the occurrence of gypsum crusts on limestone, marble and calcitic sandstone, and levels of air pollution. Levels of air pollution were categorised from the sum of twenty years worth of SO_2 and NO_2 concentration data. Limestones and marbles in 40 areas around Europe were investigated and the occurrence of gypsum crusts on building surfaces were assessed and recorded as a grade corresponding to "rare" through to "very common". The degree of gypsum formation (DGF) on 378 samples of calcitic sandstones in each area was also assessed by defining DGF as

$$DGF\ (\%) = \frac{100\ (wt\%\ gypsum)}{(wt\%\ gypsum\ +\ wt\%\ calcite)}$$

Good correlations were found between these measures, and crusts were not only found to grow thicker in polluted areas (ie Poland and Germany), but also in warmer climates.

3.4.5.2 Morphology and Structure

Many different crust structures on calcareous stone have been described in the literature (eg Fassina ,1976; Leysen *et al*, 1989; Del Monte and Sabbioni, 1986; Sabbioni and Zappia, 1992; Fobe *et al*, 1995). However these may be roughly divided into four types;

1) white/grey crusts comprising calcite and gypsum;
2) thin, dense black layers comprising calcite, gypsum and black particles;
3) thin, dense brown layers comprising calcite, gypsum, iron and black particles;
4) spongy grey/black layer of variable thickness comprising calcite, gypsum and black particles.

Typically, these crusts lie above a weathering zone of variable thickness where damage to the underlying stone has been sustained.

3.4.5.3 Elemental Composition

Fassina (1976) investigated the carbon, sulphate and chloride content of black crusts at two locations in Venice and these are presented in Table 3.5, expressed as percentages.

Table 3.5 Composition of black crust samples taken at two sites in Venice (Fassina, 1976).

Sample Site	Thickness of Crust	Carbon (%)	SO_4^{2-} (%)	Cl^- (%)
Papadopoli Palace (Under guttering)	1 mm	24.5	21.7	0.2
Rialto Bridge (Under guttering)	3 mm	24.9	16.4	0.2

Sabbioni and Zappia (1992) calculated enrichment factors for selected elements in black crusts found on sandstone and calcarenite monuments in Bologna. Thin, black surface layers and an underlying, powdery layer were analysed. Figure 3.2 shows the rock and crust enrichment factors calculated for the samples collected; sulphur was clearly the dominant enriched element

in both the rock and the surface crust. Enrichment by Ca was associated with the formation of gypsum from this deposited S. Pb exhibited the second highest enrichment factor and V enrichment was encountered in all samples and linked to oil combustion.

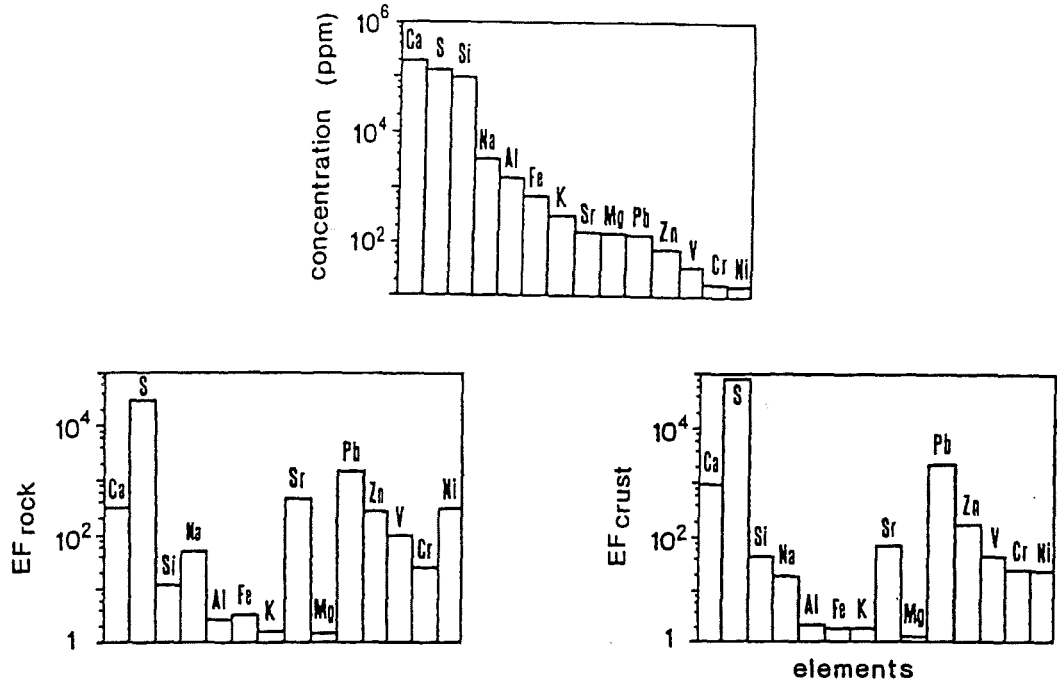

Figure 3.2 Selected enrichment factors of rock (EF_{rock}) and black crust (EF_{crust}).

Leysen *et al* (1989) found four typical elemental distributions in Belgian limestone crusts:

i) an absence of sulphur.

ii) the S/Ca ratio is 1 (indicating gypsum); Fe was concentrated in limited zones.

iii) the S/Ca ratio varied between 0-1, with some zones of high Fe concentrations.

iv) the S/Ca ratio and Fe concentration varied significantly.

Sulphate concentrations were found to be high to up to a few centimetres in depth. In black crusts, carbon particles were detected, together with Na and K. Black crusts had higher sulphate concentrations than white "weathered zone" crusts. Al, K and Fe enrichment was found in surface layers of stone and trace elements including Cu, Zn and Pb were enriched in the surface layer; Rb, Ni, Cr, V, Sr, Mg and Ti were found at extremely low concentrations. N and Cl containing salts contributed little to the overall crust composition compared to S.

Nord and Ericsson (1993) comprehensively analysed 25 samples of the thin black layers found on historic buildings and quarries in Sweden and buildings in continental Europe. Two types

of crust were identified; a hard, thin crust (0.02-0.2 mm thick) which forms on non-calcite-bearing stone surfaces and a thicker crust with a lumpen, spongy appearance. Iron and sulphur concentrations were much higher at the surface than in the underlying stone. Chlorine and phosphorous concentrations also increased toward the surface. Carbon and heavy metals were found in high concentrations in the thin black layers. Table 3.6 shows the concentrations of selected elements in black layers collected from different stone types at both urban and rural locations in Europe. This analysis showed that surface carbon and hydrocarbon concentrations are higher in urban locations, particularly in Polish urban samples. Surface iron concentrations tended to be lower in the urban samples than in the rural and quarry samples and this appeared to be a stone and time dependent phenomenon, which was possibly influenced by the presence of other pollutants. Of all the samples analysed in this study, the urban crusts had much higher proportions of iron in the stone, although lower total iron concentrations.

The urban black crust samples tended to exhibit lower surface iron concentrations and higher surface carbon concentrations and a strong inverse relationship existed between the two. Assuming that iron concentrations were initially similar in stone prior to exposure, either surface enrichment was enhanced in clean atmospheres, by for example biological activity, or surface iron was leached from the stone in urban environments, perhaps through the action of acidic runoff.

Table 3.6 Concentrations of elements in thin black crusts collected from historic buildings in different locations in Europe (Nord and Ericsson, 1993).

Sample Type	Stone Type	C	H	Pb	V	Fe
		(mg cm^{-2})				(wt %)
Urban, Sweden	*qs*	1.47	0.26	1.77	0.03	13.4
	qs	2.74	0.44	2.14	0.02	3.8
	g	1.88	0.37	2.03	0.04	9.4
	qs	2.03	0.20	1.82	0.01	12.6
Rural, Sweden	*qs*	0.22	-	-	-	21.4
	qs	0.18	-	-	-	40.7
	qs	0.26	0.02	0	0	19.6
Quarry, Sweden	*qs*	0.16	0.01	0	0.002	39.7
	qs	0.18	0.03	0	0.008	22.1
Urban, Poland	*L*	3.98	0.37	-	-	10.9
	qs	4.12	0.90	0.02	0.012	22.5
	b	4.76	1.59	1.04	0.01	11.5
	qs	5.67	1.39	0.04	0.004	4.2
Urban, Paris	*L*	2.36	0.06	-	0.01	8.6

qs = quartz-cemented sandstone, *g* = granite, *L* = limestone, *b* = brick.

Nord *et al* (1994) sampled 1400 black crusts from different facade materials from 40 countries in Europe. Increased surface concentrations of Cl and P were determined in almost all of the 627 samples analysed for these elements. Table 3.7 shows the concentrations of selected soot associated elements detected in over eighty black crusts. Higher carbon values were recorded for cities outside Sweden, and Polish samples contained the highest carbon concentrations (with a maximum of 7.66 mg cm^{-2}).

Table 3.7 Concentrations of soot associated elements in black crusts from historic monuments in Europe (Nord *et al*, 1994).(Carbon results for Swedish samples only).

Element	No. Samples	Average Rural Conc. (mg cm^{-2})	Urban Conc. Range (mg cm^{-2})
Carbon	28	0.20	0.85 - 2.74
Lead	57	<0.01	0.05 - 0.2
Vanadium	57	<0.01	0.01 - 0.03
Nickel	57	<0.01	0.01 - 0.1
Chromium	57	<0.01	0.01 -0.1

Schiavon *et al* (1995) studied black patinas from granitic building stone from Aberdeen and Dublin. Iron-rich particles, carbonaceous cenospheres (with calcium and sulphur) and < 10 μm diameter spherical particles with aluminosilicate and or calcium and iron components were the most common. Thin discontinuous layers of soiled material (0-20 μm thick) were collected from Aberdeen. These layers displayed a fairly constant composition with high concentrations of iron, phosphorous, calcium, sulphur and chlorine, and micron-size spherical particles. These particles were embedded within the gypsum matrix, in micro-fractures and trapped within the cleavage planes of mica deposits, and were relatively less common than in the Dublin gypsum-rich crusts. The iron-rich crusts found in Aberdeen were considered to be the result of the low availability of sulphate ions, possibly enhanced by the action of biological activity. Schiavon *et al* associated severe physical damage of granite surface layers with the high pressures of gypsum crystal growth created due to gypsum crystallisation energies (Winkler and Singer, 1972). Schiavon *et al* differentiated between gypsum- and iron-rich crusts identifying this characteristic as an indication of different formation processes.

Fobe *et al* (1995) studied the elemental composition of black crusts from Seville and Mechelen. The results for some elements were found to be similar in all samples: 3.5-4.8 % C, ~1.4 % H, 0.14-0.19 % N and 10-12 % S. Ash content was 76-78 % for all samples. All crusts were found to contain only 50-80 % of the Ca concentration found in the original stone and were enriched with Fe. All crusts were enriched with Ti (600 ppm) and Mn (100-200 ppm), Zn (x10 the stone concentration at 150 ppm) and Cu (70 ppm). The Spanish crusts were enriched with K, Ba and Na, but Belgium samples contained less than the parent rock. Belgium samples were enriched with Sr (1200 ppm compared to 200 ppm in stone) while Spanish samples were not.

Rodriguez-Navarro and Sebastian (1996) found that elemental concentrations of certain elements differed significantly from that of fresh limestone. Crustal material had enhanced concentrations of the calcophilic elements Pb, Zn and Cu, together with Fe, Mn, V and Ni. A linear relationship between the proportion of gypsum and the concentration of calcophilic elements in the crust was suggested by elemental and XRD analysis of the crust. In chemically unaltered dusts collected from the stone-work, similar elements were found.

3.4.5.4 Minerals

The most common mineral components of black crusts are calcite, gypsum and quartz (Del Monte and Sabbioni, 1986). Rodriguez-Navarro and Sebastian (1996) report gypsum in all crustal deposits taken from Granada Cathedral. The main difference between the mineralogy of loosely deposited dust and black crust taken from the site, were the morphology and proportion of gypsum. In the thin black crusts ~ 1 mm thick, calcite is the major phase with minor amounts of clays, quartz and gypsum, while gypsum was the major phase in the thicker crusts (0.2-2 cm thick), with calcite, quartz, clay minerals and oxallates as minor components.

3.4.5.5 Black Carbonaceous Particles

Carbonaceous particles are important in the formation of black crusts for two reasons. Firstly, they efficiently scatter and absorb light thereby changing the appearance of stone and secondly, in the supply of sulphur to stone surfaces, increasing gypsum growth (Del Monte *et al*, 1981; Lipfert, 1989; Hutchinson *et al*, 1992; Sabbioni, 1995; Ausset *et al*, 1991; Salmon, *et al*, 1995). If depositing material contains both insoluble and soluble salts, droplets of salt solution may form under conditions of high humidity. As humidity reduces, evaporation of the salt solution forms a precipitated salt bridge between the insoluble particle and the surface.

Saiz-Jimenez and Bernier (1981), Del Monte *et al* (1984), Saiz-Jimenez and Sabbioni (1993), Sabbioni (1995) and Rodriguez-Navarro and Sebastian (1996) describe similar classification systems for particles in black crusts, analysed using SEM-EDX for characterisation:

i) porous, spherical carbonaceous particles with regular pore distribution (oil)

ii) porous, spherical carbonaceous particles with irregularly shaped pores (distilled oil)

iii) smooth, spherical aluminosilicate particles (coal)

iv) agglomerations of sub-micron particles (distilled oil)

v) rare metallic particles, mainly containing iron or titanium.

Novakov *et al* (1974) established a relationship between the oxidation of atmospheric SO_2 to sulphate and the presence of carbonaceous particles. This process was accelerated by the presence of some transition and other metals (Fe, V, Cr, Ni, Pb, etc) which catalyse the oxidation and hydrolysis of the SO_2 to sulphuric acid (Urone *et al*, 1968). Del Monte *et al*

(1981 and 1984), Sabbioni (1992) and Rodriguez-Navarro and Sebastian (1996) showed that sulphation of limestone using oil-fired carbonaceous particles was possible under conditions of high humidity. Cheng *et al* (1987) similarly caused the deterioration of marble surfaces. However, this hypothesis was strongly contested by Hutchinson *et al* (1992) who believed that while coal and oil fly ashes contributed small amounts of sulphur and calcium to stone surfaces, they did not promote gypsum formation, only acted as nucleating agents. The differences between oil and coal fly ash particles are compared in Table 3.8.

Table 3.8 Physicochemical properties of carbonaceous particles derived from oil and coal (Cheng, 1983).

	Oil	Coal
Mass Median Diameter (μm)	0.38	4.9
Trace Elements		
Major	V, Fe, Si, S, Ca	Fe, Ti, Si, S, K, Ca
Minor	Mg, Al, P, Ti, Cr, Mn, Ni	Al, P, Cl, Mn, Cu
Bulk Density (g cm^{-3})	0.33	0.93
Sulphate (Soluble, % wt)	16.94	4.04
Nitrates (Soluble, % wt)	<0.01	ND
Chlorides (Soluble, % wt)	0.18	0.01
pH	2.7	3.75

Carbonaceous particles are very sorptive, exhibit high surface areas and consequently have a surface layer of adsorbed, tarry organic matter resulting from the nature of combustion. Polyaromatic hydrocarbons in particular have been found to sorb strongly to the particles due to their composition (Christwell *et al*, 1988; Saiz-Jimenez, 1993). The main sulphur compounds found in these particles are sulphates, sulphites and SO_2 adsorbed onto the surface of the particles by different mechanisms (Novakov *et al*, 1972).

Del Monte *et al* (1981) used an optical microscope to calculate the size distribution of particles found in black crusts collected in Venice. Figure 3.3 shows the particle size distributions which indicates a number median diameter close to 10 μm.

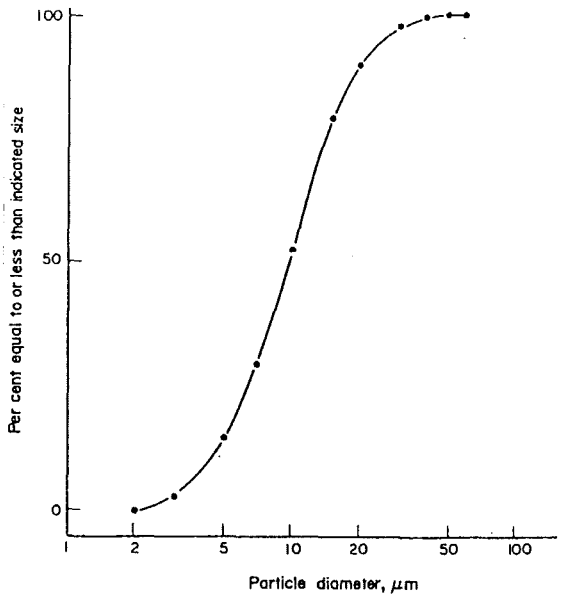

Figure 3.3 The size distribution of particles found in the black crusts by Del Monte *et al* (1981).

These particles contained carbon, silicon, sulphur, aluminium and calcium as major constituents. Table 3.9 shows the major, minor and trace elements associated with these particles. Del Monte *et al* (1984) identified these black particles as the nucleating agents of gypsum formation due to their association within the crusts.

Table 3.9 Major, minor and trace elements present in individual carbonaceous particles removed from limestone and marble deterioration layers in Northern Italy (Del Monte *et al*, 1981).

	Si	S	Al	Ca	K	V	Fe	Cu	Na	Mg	Ti	Cr	Ni	Mn	Zn
Major	*	*	*	*											
Minor					*	*	*	*							
Trace									*	*	*	*	*	*	*

Nord and Ericsson (1993) found that even in the thin black crusts found on non-calcite-bearing stone surfaces, eroded spheroidal particles rich in Ca, Al, Si, O and C and smooth spheres rich in Fe were found occasionally. The blackness of the layer was attributed to these particles and to a lesser extent dark-coloured iron compounds, usually in combination.

Fobe *et al* (1995) dissolved crusts from Seville and Mechelen in HCl and measured the

elemental composition of the residual particles. The dominant particle types were quartz dust (Si-rich), fly ash (Si and Fe-rich), organic particles (no dominant element), Ti-Cu-Zn-rich (Ti, especially in Mechelen), Ca-rich and S-rich samples.

Schiavon and Zhou (1996) measured the magnetic properties of bulk limestone crust samples collected from historic buildings in five urban and rural sites in the UK. Four types of magnetic particle types were described; 1-5 μm smooth iron-rich spherical particles ($\sim$60% of total number analysed) within which Fe was the only element or was associated with AlSi; 3-10 μm iron-rich spherical particles with surface texture (16%) which while dominated by Fe also featured Al, Si, K, Mg, Ca and Ti as minor elements; irregular iron fragments exhibiting solid, vesicular or gridded surface (19%); and finally, iron-rich crystalline particles interpreted as magnetite, pyrite and ilmenite (5%). The morphology, crystallinity and composition of these particles indicated anthropogenic sources, specifically coal fly ash. However, little variation in magnetic properties of particles occurred between sites despite the likely historic differences in local air quality conditions.

3.4.5.6 Organics

Organic compounds adsorbed at the surface of particles are deposited onto buildings by wet and dry deposition and are entrapped by the growth of gypsum crystals. The diversity of organic compounds in the crusts is dependent on the nature of the trapped aerosol. Organic species may be subject to change by weathering in the aerosol and on the building surface, resulting in a complex mixture of many different groups of compounds. The identification of the organic species in both the aerosol and the crust is important in identifying the sources of these compounds and also in understanding the weathering and deposition processes.

Nord and Ericsson (1993) found carbon to be mainly chemically bound in graphite and aliphatic hydrocarbons. 93 compounds were identified in the urban sample, while only 14 were identified in the rural sample. Predominant compounds (by weight) in the urban sample were aliphates, alkylated phenols, benzenes, phthalates, alcohols, esters, cyclohexanol and cyclohexanone, and isopropyl. Some 60 compounds were identified in a Polish sample. PAHs were identified at concentrations ranging between 0.01-0.1 $\mu g\ g^{-1}$ in both the urban and rural

samples. Vulcanised Rubber from car tyres was also identified. Nord *et al* (1994) analysed two further samples from central Krakow and Brussels, which contained a total of 60 and 69 organic compounds respectively. All urban samples were similar, comprising 0.5-10 $\mu g\ g^{-1}$ linear and branched hydrocarbons (C_{12} - C_{30}, peaking C_{20} - C_{25}), esters of fatty acids and some alkenes (C_{11} - C_{18}), $<0.1\ \mu g\ g^{-1}$ of alcohols, aldehydes, ketones and phenol derivatives and $<0.1\ \mu g\ g^{-1}$ various PAHs and PAH-Ns. Carbon concentrations ranged between 4.12 mg cm^{-2} (Krakow) and 0.26 mg cm^{-2} (background sample).

Saiz-Jimenez (1993) found the organic components of black crust collected in Seville to comprise mainly aliphatic hydrocarbons and some polycyclic aromatic compounds (PACs). The PAHs indene, naphthalene, fluorene, phenanthrene and pyrene were identified. A wall nearest a bus terminal had sustained severe damage due to black crust formation and this crust had a different composition to other samples. This sample exhibited a large unresolved hump in the range C_{20}-C_{34} together with triterpanes predominantly of the 17 alpha (H),21 beta(H)-hopane and tricyclic terpane series and steranes, identifying vehicular emissions as the origin (Simoneit, 1985). Further samples collected from Dublin, Mechelen and Seville showed that the crusts contained mainly *n*-alkanes ranging C_{13}-C_{40} and fatty acids (C_{14} -C_{34}), with trace components of diterpenoids, triterpenoids, triterpanes, steranes, PAH and dialkyl phthalates. Table 3.10 shows the ranges of hydrocarbons detected and the CPI for each crust (for CPI definition see Section 2.6). The CPIs of fatty acids in the first two samples in Table 3.11 indicated a biogenic origin for some of the organic extract.

Table 3.10 Selected series of organic compounds present in black crusts collected at three sites (Saiz-Jimenez, 1993).

Sample Site	*n*-Alkane	C_{max}	CPI	Fatty acids	C_{max}	CPI	Triterpanes
Dublin	C_{13}-C_{35}	C_{29}	1.3	C_{10}-C_{32}	C_{16}	2.9	C_{27}-C_{34}
Mechelen	C_{14}-C_{40}	C_{29}	1.7	C_{12}-C_{34}	C_{16}	5.1	C_{27}-C_{34}
Seville	C_{15}-C_{40}	C_{31}	1.0	C_{10}-C_{34}	C_{22}	1.9	C_{27}-C_{35}

Saiz-Jimenez *et al* (1994) identified 250 organic components of black crusts collected from the Custom House, Dublin. The main compound classes are summarised in Table 3.11 according

to the analytical technique used. All the classes of compounds shown in Table 3.11 have been identified in either the gas or particulate phase in the urban aerosol.

Table 3.11 Main classes of compounds identified using three different analytical techniques in the analysis of black crust collected in Dublin (Saiz-Jimenez *et al,* 1994).

Class of Compound	Solvent Extraction Range	Pyrolysis Range	Py/Methylation Range
n-Alkanes	C_{13}-C_{35}	C_5-C_{32}	C_9-C_{29}
n-Fatty Acids	C_{10}-C_{32}	-	C_6-C_{26}
n-Dicarboxylic Acids	+	-	C_7-C_{17}
(Alkyl)benzenes	+	C_6-C_{17}	C_6-C_{26}
(Alkyl)naphthalenes	C_{10}-C_{13}	C_{10}-C_{14}	C_{10}-C_{13}
(Alkyl)phenanthrenes	C_{14}-C_{16}	C_{14}-C_{17}	C_{14}-C_{16}
Diterpenoids	C_{18}-C_{20}	C_{18}	C_{18}-C_{20}
Triterpenoids	C_{27}-C_{34}	C_{27}-C_{35}	+
PAH	C_{10}-C_{22}	C_{10}-C_{24}	C_{10}-C_{18}

Fobe *et al* (1995) extracted and analysed further samples in a similar manner. *n*-alkanes (C_5-C_{40}) were detected in both samples. Spanish samples gave a CPI of 1, with a low (C_{15}-C_{24}) CPI of 0.8 and a high (C_{25}-C_{34}) CPI of 1.1; Belgium samples gave CPI's of 1.7, 1.1 and 2.1, respectively. This indicated that while the Seville samples were attributable to petroleum sources by the CPI of 1 and the broad envelope of unresolved compounds, the Mechelen samples had a biogenic signature in the bimodal distribution and the dominance of *n*-C_{29}. Of the isoprenoid species, pristane and phytane (diagenetic products of phytol not biota) which also indicated a petrol source. PAHs ranged from C_{10} (naphthalene) to C_{20} (benzopyrene) with the dominant analogues of vehicle exhaust (fluoranthene, pyrene, benzanthracene and benzofluoranthene) all present. Alkyl PAHs found in the Seville sample were believed to have originated from diesel engine exhaust. Other classes of organic compounds such as diterpenoids, tricyclic terpanes, steranes and triterpanes were also detected. Discovery of molecular markers for bacterial growth in the Seville extracts led to the discovery of *Phormidium* sp. growing at the gypsum-calcite interface.

Schiavon *et al* (1995) identified alkanes, alkenes, aromatic hydrocarbons and derivatives, aldehydes and ketones in granitic black crusts collected in Aberdeen. Similar compounds

together with polyaromatic hydrocarbons (PAHs) and nitrogen-containing organic compounds were identified in granitic crustal material from Dublin. Polyaromatic compounds from incomplete combustion were found only in the Dublin crusts and included indene, biphenyl, fluorene, naphthalene and methylated naphthalene compounds. In summary, the organic compounds identified in the black crusts from Aberdeen and Dublin were characteristic of anthropogenic origin and no definitive molecular markers for biogenic activity were observed.

Grimalt *et al* (1991) reported the similar nature of organic compounds detected in the black crusts from Barcelona and those detected in the particulate and gaseous phase of the local aerosol. The aliphatic and aromatic fractions of both crusts and particulates were found to match closely. The most abundant aliphatic compounds were the *n*-alkanes ranging from *n*-eicosane to *n*-tritriacontane, with maxima at *n*-eicosane or *n*-heneicosane and a CPI of 1 below C_{25}. Between C_{25} and C_{31}, odd carbon number homologues dominate. Regular isoprenoids (norpristane, pristane and phytane) and distributions of 17∝(H), 21ß(H)-hopanes. Similar parent polyaromatic hydrocarbons were also observed in both gypsum crusts and airborne particles, although the reactive PAH were found in particulates only.

3.5 SUMMARY

Particle deposition rates are principally governed by the size and aerodynamic properties of the particle. Other characteristics of the depositing particle, the surface and the local environment are also important in mediating the process. Soiling of building surfaces is the first stage of particle damage to stone surfaces and occurs largely in the absence of sulphur and moisture. No chemical fixation occurs between the particle and surface.

Black crusts occur on calcareous materials when atmospheric sulphur and moisture is available. Particulate matter is one source of sulphur. Particles transport acidic components to surfaces and provide a slow releasing source on stone surfaces, catalysing the conversion of SO_2 to sulphate to form sulphuric acid in the presence of moisture. Gypsum growth may be enhanced on the surface or from the particle itself, even at high relative humidities. Sulphur compounds have been repeatedly shown to be the main agent in the corrosion of calcareous stone.

While black crust formation has been recorded for centuries (Leysen *et al*, 1986; Brimblecombe, 1992), the question remains if present day pollution is increasing, exacerbating or even influencing the sulphation of building stone and the formation of black crusts. Some authors have suggested that present-day pollution is accelerating the rate of building stone decay. Whalley *et al* (1992) describe a 'memory' effect where black crusts grow in response to present and past pollutant deposition. Rodriguez-Navarro and Sebastian (1996) provide evidence to suggest that vehicle traffic is certainly contributing to stone deposited material. Certainly the compounds attached to the particle - together with particle morphology - can indicate the source of these particles.

Chapter 4

MODELLING THE SOILING PROCESS

4.1 INTRODUCTION

The relationship between air pollution and the soiling process is poorly understood. Much qualitative evidence exists that air pollutants cause material damage, but quantitative data to link specific factors of environmental exposure to material damage, are inconclusive. The assumption is that the deposition of airborne particles causes or enhances soiling and that the particulate mass concentration can be related to soiling effects.

The composition and size distribution of deposited particles on a surface will determine the optical properties - thus their soiling potential - and also the ability of the particles to adhere to a surface. Building soiling is a cumulative process, which may be reduced or enhanced by local meteorological conditions. The soiling process is therefore complex, dependent on many environmental factors and may consequently be site specific. One method of assessing the soiling process is by modelling reflectance change. While some mathematical models have tried to assess the soiling rates in terms of many environmental factors, the complexity of considering all factors, together with their inter-relationships, has proved difficult to model. The most successful models have simplified the soiling process, to consider only the particulate concentration, the characteristics of the particulates and the deposited layer. However, while other workers have developed soiling models empirically (see Section 4.2), these models are rarely tested at other locations, where particulate characteristics are likely to differ.

The modelling undertaken in this study used previously collected surface reflectance data, collected over one year at five different locations in Europe and the methodology is further described elsewhere (CE Contract No STEP-CT90-0097). It has therefore been possible to compare continuous soiling data with predictions from two established soiling models. Identical

vertical-sample carousels were exposed to the five different environments (London, Vienna, Oporto, Coimbra and Breitenfurt) and the relevant environmental factors monitored. While other authors have used multiple exposure sites before to develop soiling models (Haynie and Lemmons, 1990), sites were in the same country so that particulate pollution sources (and consequently characteristics) and other factors such as meteorological conditions are similar even if particulate concentrations are different. In this study, exposure sites were located in three different countries with probable differences in particulate characteristics and climatic conditions. Hence any soiling model which could explain significant proportions of the process using the measured variables would have global applicability.

4.2 EXISTING SOILING DAMAGE FUNCTIONS

Many authors have sought to define a soiling damage function for the soiling effects of particulate matter on building material surfaces (Beloin and Haynie, 1975; Haynie, 1986; Lanting, 1986). Essentially, a damage function mathematically quantifies the relationship between damage caused to a material and a measured level of particulate matter, which can then be theoretically related to the physical soiling process. The difficulty in quantification of material damage due to particulate matter derives from the presence of other pollutants in combustion emissions, such as sulphur and nitrogen oxides, which may result in chemical interactions with the surface.

The rate of soiling of surfaces by particulate matter, which is measured as the surface reflectance change over time, is commonly used to describe surface degradation by airborne particles. A review of the literature indicates there are two main methods of quantifying building soiling. One method assumes the exponential decay of reflectance such that it can be defined by the equation

$$R = R_o e^{-kt}$$

where, k = soiling constant (per year) R = reflectance of soiled surface (%)

R_o = initial reflectance of surface (%) t = exposure time (weeks)

The other approach assumes reflectance decrease can be empirically modelled by the equation of the form

$$R = R_o - k\sqrt{t}$$

Table 4.1 lists the studies completed to date and summarises the duration and conditions. All studies made measurements of ambient particulate load and measured reduction of reflectance using a reflectometer.

Table 4.1 Investigations carried out to quantify the amount of soiling damage attributable to airborne particulate matter.

Author	Duration	Orientation	Exposure to Rain	Materials	Measurement Interval
Beloin and Haynie (1975)	2 yrs	*V*	Unpro	paint concrete brick limestone shingle glass	3 months
Martin *et al* (1986)	2 yrs	*V* + *H*	Unpro	concrete aluminium paint glass	12 months
Mansfield and Hamilton (1989)	222 days	*V*	Pro	paint tile	7 days
Hamilton and Mansfield (1992)	110	*V*	Pro + Unpro	paint	1 day
Haynie and Lemmons (1990)	16 weeks	*V* + *H*	Pro + Unpro	flat paint gloss paint	2, 4, 8 and 16 weeks
Creighton *et al* (1990)	13 weeks	*V* + *H*	Pro + Unpro	flat paint gloss paint	1 week

V = vertical
H = horizontal
Pro = Samples are covered by a protective hood which prevents rain impaction
Unpro = Samples are unprotected

Beloin and Haynie (1975) developed the first dose-response relationships for particles on surfaces of 6 different types of material. Five sites were selected with TSP concentrations ranging between 60 and 250 $\mu g\ m^{-3}$ and monitored over a two year period. The five locations included rural, urban, industrial and mixed-use areas. Samples were exposed at five sites with a range of TSP concentrations and reflectance measured over two years with three and six monthly measurements. Coefficients of determination (r^2 values) of 0.74-0.90 were observed

by plotting reflectance loss of painted wood samples against the square root of the dose (ie the total suspended particulate concentration C_{TSP} multiplied by exposure time).

$$R = R_o - k\sqrt{Ct}\ .$$

The best results were achieved for the white exposed materials, painted surfaces and asphalt shingle. The soiling of other materials could not be accurately described using the same model. Lodge *et al* (1981) however found this a "curious and weak dependency", lacking a physical explanation.

Haynie (1986) reported a theoretical model of soiling which related the ambient mass concentration to the accumulation of particles at a surface. The average reflectance from the surface equalled the reflectance from the surface not covered by particles $[R_o(1-X)]$ plus the reflectance from the particles (R_pX), where X is the fraction of surface covered by particles. Under constant conditions, rate of change in surface coverage is proportional to the proportion of surface yet to be covered. This gives the equation

$$R = R_o e^{-kt}$$

where k is a function of particle size distribution and dynamics. Haynie assumed that reduction in reflectance was directly related to the fraction of substrate covered. The principles are the same as those employed in Lanting's first model (1986, see below), except Haynie anticipates that all deposited particles contribute to soiling, irrespective of composition. Particle size and deposition velocities were assumed to be responsible for differences in contribution to soiling, since particles smaller than the wavelength of light ($<0.5\ \mu$m) tend to cause light interference as opposed to absorption. Using the same exponential equation, k is defined as

$$k = \sum_i \frac{3C_iU_i}{4r_i\rho_i}$$

where i is an interval of the size spectrum, U is the deposition velocity r is particle radius and ρ is the specific mass of particles.

Haynie and Lemmons (1990) conducted a rural soiling study to determine the relative effects

of environmental factors on the soiling of white painted surfaces. Fine, coarse and total suspended particulates and hourly wind speed and rainfall data were collected. Gloss and flat painted surfaces were exposed in vertical and horizontal positions, either protected or unprotected from rain, for 16 weeks. SEM stubs were also collected at 2, 4, 8 and 16 weeks when reflectance measurements were also taken. Horizontally exposed samples soiled faster than vertical surfaces and gloss paint soiled faster than flat paint. Unprotected surfaces experienced initially higher rates of soiling than protected surfaces, which were later reduced by rain.

Deposition velocities were calculated using least squares regression analysis of dose versus deposited particles. Deposition velocities to horizontal and vertical surfaces were statistically similar for the fine mode, but differed by a factor of five for coarse mode particles (1.55 and 0.355 cm s^{-1}, respectively). The fine mode therefore avoided removal by rain while larger particles dissolved or washed away. The empirical equation for a vertical gloss painted surface based on the model developed by Haynie (1986) reads:

$$R = R_o e^{(-0.0003[0.0363C_f + 0.29C_c]t)}$$

and

$$R = R_o e^{(-0.0003[0.363C_f + 1.341C_c]t)}$$

for horizontal gloss painted surfaces, where C_f and C_c represent the concentration of fine and coarse mode particles, respectively. This model does not take into account the different sized particles response to rain removal and thus the coarse mode coefficient is likely to change over time.

Lanting (1986) evaluated two similar models of soiling by particulate elemental carbon (PEC) and determined that they were good predictors of building soiling by black smoke. The first model relies on the same exponential decay in reflectance of a white surface when it is covered by dust particles. If the particles are assumed to be spherical and no removal mechanisms occur

$$X' = \frac{C_{PEC}\ V_d\ 0.24}{\rho r}$$

where X' = fraction of surface area covered by particles per unit time (per yr)

ρ = specific mass of particles

C_{PEC} = concentration of particulate elemental carbon (μg m^{-3})

Therefore, while both the Haynie and Lanting models are based on the same exponential decay of reflectance, they assume different particle characteristics are responsible for soiling. Lanting's model allows the calculation of the annual effective area coverage (EAC) for any ambient PEC concentration. In urban areas in the Netherlands with an estimated annual mean concentration of 3 μg m^{-3} PEC, 5% EAC would be reached in two months. Under these conditions the calculations revealed that a 90% reduction in reflectance would be reached in 7.5 years with current levels of black smoke.

The second Lanting model assumes the specific absorptivity of PEC is responsible for soiling, eliminating the assumptions about particle size. This model assumes that the exposed surface is covered at a uniform rate and that reflectance decreases with increased light absorption by deposited particles, which is determined by the soiling layer thickness. It states:

$$k = 2AC_{PEC}V_d$$

where A is the specific absorptivity of PEC and the factor 2 is included as the light passes through deposited particles twice on a smooth surface. Specific absorptivity is assumed to be 1 x 10^4 m^2 kg^{-1}.

Van Aalst (1986) reviewed particle deposition models noting that the lack of empirical data was the singularly most important fault with many existing models. Hamilton and Mansfield (1991 and 1992) applied the models of Haynie (1986) and Haynie and Lemmons (1990) to their own data and found them to be in good agreement.

4.3 SOILING MEASUREMENTS TAKEN

4.3.1 Monitoring Sites

Five sampling sites were chosen in three countries to relate soiling measurements to

atmospheric conditions. The five sites chosen were Coimbra and Oporto (Portugal), Vienna and Breitenfurt (Austria) and London (UK) and the collaborating institutions were Aveiro University (Portugal), Vienna University, Building Research Establishment (BRE, UK) and Middlesex University (UK). These groups oversaw data collection and quality assurance procedures at the sites located in their respective countries.

Figure 4.1 shows the positions of the five sites in Europe. Coimbra is a small University town (100,000 inhabitants) situated in the steep-sided valley of the Mondego river; the sampling site was 15 m above ground level. Oporto (or Porto) is a larger city (approximately 800,000 inhabitants) situated to the north of Portugal at the mouth of the Duoro River on the Atlantic Ocean. The Oporto sampling site was at 25 m above ground level and was centrally located. Vienna is a densely populated capital city situated in central Europe, in Lower Austria, and experiences large annual temperature differentials as the European land mass heats and cools. The sample exposure site was stationed at ~30 m on St Stefansdom Cathedral in the city centre. Breitenfurt is in a semi-rural area 30 km to the west of Vienna and the samples were positioned at 3-4 m above ground level, 30 m from a quiet road. London is located in the south-east of England on the Thames and is a densely populated capital city. The London exposure site was the roof of St Paul's Cathedral to the east of central London at a height of approximately 35 m above ground level. The heights of the sampling sites may influence soiling rates since particulate mass concentrations decrease with increasing height (Monn *et al*, 1997).

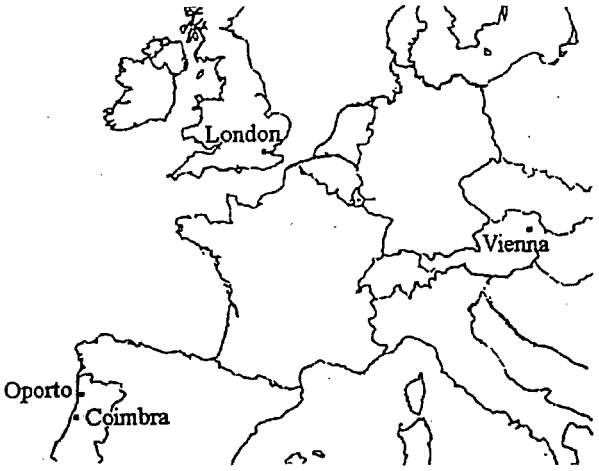

Figure 4.1 The exposure site locations used in this study.

Using the data generated by this project, it was possible to generate and assess the relationships between the soiling rates experienced at the five different sites and the models which have been generated by previous studies of the soiling phenomenon. The objective of this work was to establish a mathematical model to predict soiling of two different materials in the same environment under entirely different, but monitored, conditions of exposure.

4.3.2 Data Collection

Samples of wood and stone were exposed over a similar period at five different locations in Europe, using a standardised exposure protocol described by the UK Building Research Establishment (CE Contract No STEP-CT90-0097, 1995). Operators in each country made single reflectance measurements approximately each week (see Appendix 1). Two different types of tablets were used for these soiling measurements; white painted wood and Portland stone. These tablets are surrogates for building surfaces and, while they may vary in characteristics such as surface roughness, composition and scale, they are assumed for the purpose of the experiment to represent the building surface. No measurements of surface roughness were made. Identical stands (shown in Figure 4.2) were erected at each site, consisting of a mast with a metallic hood. A set of four tablets of each material were placed vertically in a square formation, one set in a protected position below the hood (protected samples) and the other in an exposed position above the hood (unprotected samples). Therefore, on each stand, one tablet of each material faced north, south, east or west in both protected and unprotected positions. At the London site, the samples were placed in north-west, south-west, south-east and north-east positions. The protected samples were therefore exposed to wind and, as a result, to horizontally transported rain during periods of high wind.

Each tablet was removed from the exposure stand weekly and its reflectance measured on site with an EEL Reflectometer. The samples were then replaced and exposed for a further week. The first measurement recorded was used as the representation of original reflectance (R_o). Measurements of air pollution parameters were taken on a weekly basis at Coimbra, Oporto and London, and daily at Vienna and Breitenfurt. All sites measured daily black smoke and sulphur dioxide (SO_2) concentrations which were averaged over the week to coincide with reflectance measurements. At each site, reflectance measurements were taken on either a daily or weekly basis from all tablets. All measurements were analysed with weekly averaging periods leading to some loss in sensitivity, since short term effects and causes are obscured. Missing data represents periods of equipment or sampling failure.

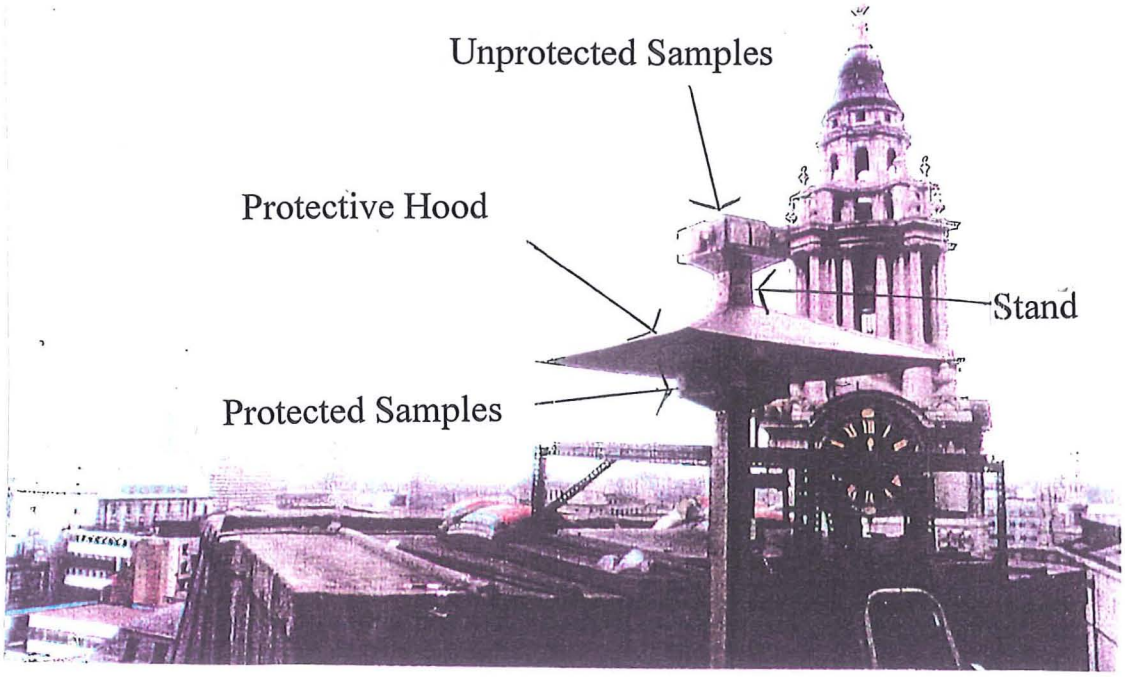

Figure 4.2 One of the sample stands used in the material exposure programme.

Selected meteorological variables were also monitored and weekly means recorded.

4.3.3 Sampling Duration

Table 4.2 shows the dates between which the sampling took place. The table also shows the total numbers of weeks for which data was collected and the total number of weekly samples obtained from each site. Other variables were measured over a similar period.

Table 4.2 Longevity of sampling and total number of reflectance measurements recorded at each site.

Site	Sampling Began	Sampling Ended	Total No. Weeks	Total No. Measurements
London	3/2/93	4/11/93	29	464
Vienna	29/12/92	3/2/94	56	656
Oporto	1/10/92	23/5/94	74	1184
Coimbra	14/10/92	10/1/94	57	912
Breitenfurt	1/12/92	12/12/93	53	848

4.4 THE MODELS TESTED

Several models have been proposed as being capable of predicting soiling rates of smooth white surfaces, of which two models have been tested. Both models have been used to relate the soiling of surfaces to the local particulate concentration and characteristics. Both assume that soiling is due to the deposition of particulate matter from the atmosphere and both models are restricted in their consideration of "the environment" as a whole, considering particulate concentration only. Neither the effects of resuspension or optical changes associated with damage to the material caused by acid deposition are considered within these models. These two models were used to determine k, the soiling rate constant per year. This soiling constant has then been used to predict the projected rate of soiling and for intersite comparisons of soiling rates.

Model 1 (described in pages 73-76) predicts that the reflectance of an exposed surface reduces exponentially with time, producing the soiling constant k_1.

$$R = R_o e^{k_1 t}$$

Model 2 (described in pages 74-75) assumes reflectance loss is related to the square root of time, producing the soiling constant k_2.

$$R = R_o - k_2 \sqrt{t}$$

It is important to note that to date, both of these soiling models have been compared against relatively short term data. The ability of either model to predict long term soiling trends (greater than 18 months) remains untested. One limitation of Model 2 is that, as an empirical model, extrapolation of the model past the period over which it was derived is unsafe. Consequently, the model cannot be used over long exposure times.

4.5 RESULTS

4.5.1 Derivation of Soiling Constants

Values of k_1 and k_2 were initially derived graphically and these graphs are located in Appendix 2. The value of k_1 was determined by plotting lnR/R_o against time (t), where k_1 is the gradient of the regression line emanating from the origin (see Appendix 6). To summarise Appendix 6, trendlines are forced through the origin because when $t = 0$, $lnR/R_o = 0$. The value of k_2 was determined by plotting $ln(R_o - R)$ against $1/2\ ln\ t$, where the point at which the line of best fit intersects the y axis is equal to $ln\ k_2$. The log plot was selected for Model 2 graphs for better visual comparisons with Model 1 plots and in the absence of any consensus on how these data should be presented or analysed. It should be noted that the trendlines represent the fit of the model to the data, including outliers. Figure 4.3 shows example plots of data for which Models 1 and 2 gave the best and worst fit of all the samples; (a) and (c) represent the best fits for Models 1 and 2, (b) and (d) show the worst fits for Models 1 and 2, respectively.

The coefficients of determination (r^2) and p values for similar exposure periods ($\sim$270 days) at each site were computed using the statistical package SPSS (V6.1.3). r^2 values were used to measure the applicability of the model to the data, and values are presented in Table 4.3. Tabulated k_1, k_2, r^2 and p values for all samples are located in Appendix 3. (The p value is calculated by the test of the null hypothesis that the multiple correlation is zero; $p < 0.05$ indicates that the operator can be $>95\%$ confident that the r^2 value is not zero). While other statistical relationships between the data exist, no other method could be used to measure the fit of the model to the data. In cases where data is missing, where there is low variation in reflectance values measured (eg NE face of protected stone sample in London) or where $ln(R_o - R) = 1$ (giving a natural log of zero), the model does not fit the measured data representatively. However in such cases, the r^2 values for such cases are low indicating a poor fit for the model. A discussion of the limitations of both models is included in Appendix 6.

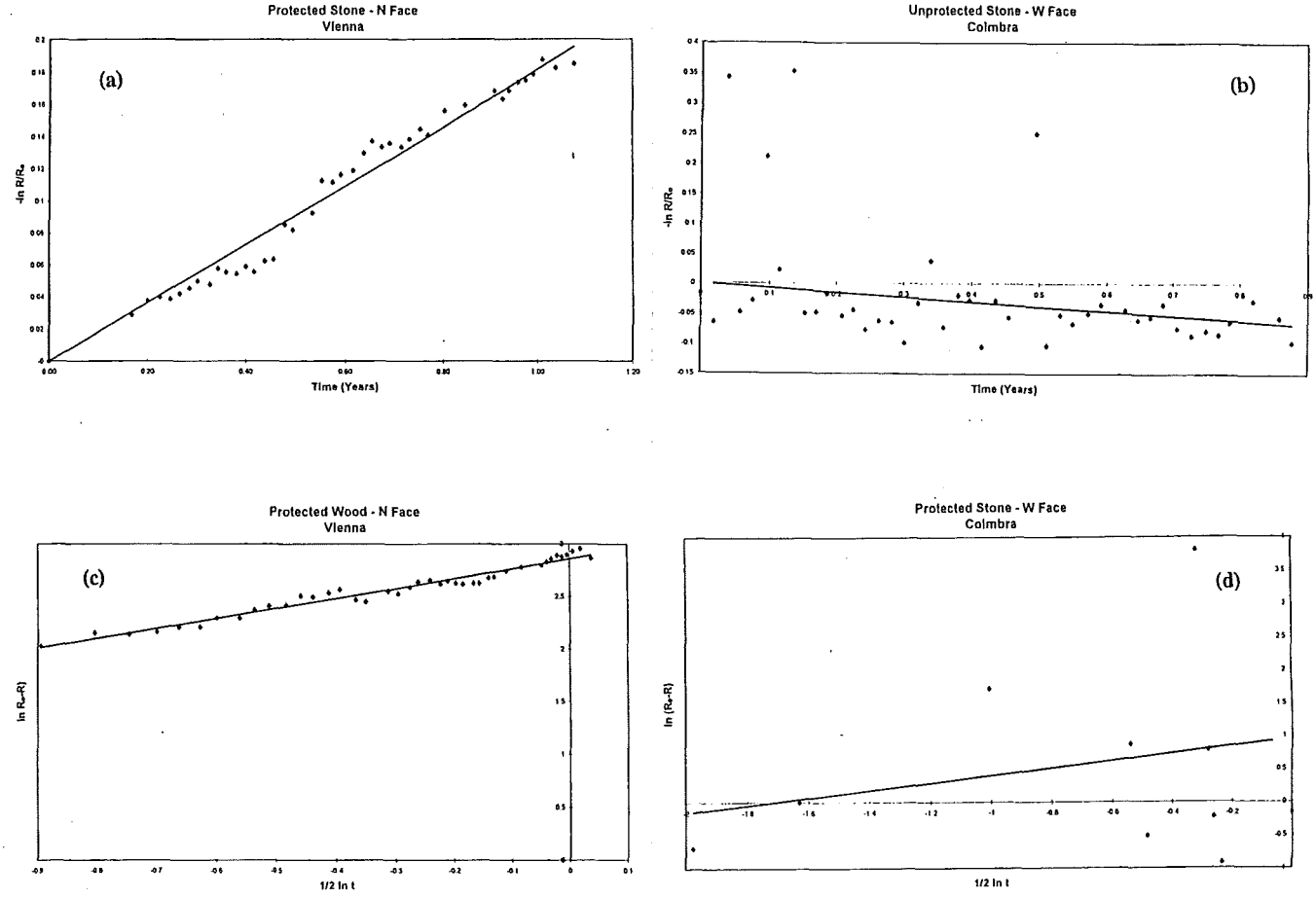

Figure 4.3 Examples of data plots for Models 1 and 2.

The r^2 value given indicates the strength of the relationship between the best-fit line defining the soiling constant k and the original data, however the value must be treated with caution and only be considered in conjunction with the graphed data and the associated significance value (p value). A confidence interval limit of 95% was adopted unless otherwise stated. Average k_1 and k_2 values of each sample type together with their corresponding r^2 values can be found in Table 4.3. r^2 values of 0.80 or higher indicate good correlations between the line of best fit and the measured data and are shown in bold for easier identification. P values indicate the quality of the relationship between the r^2 values and the measured data, with values of 0.05 or less indicating that r^2 values are significant at the 5% level or less.

Table 4.3 A comparison of the ability of two models to predict soiling rates at five sites in Europe, using the coefficient of determination r^2 to indicate the best predictive model.

Site	Sample Description		Model 1		Model 2	
	Material	Position	k_1	r^2	k_2	r^2
London	Stone	Unprotected	0.18	*0.66*	5.08	0.11
		Protected	0.15	*0.74*	5.38	*0.42*
	Wood	Unprotected	0.30	***0.95***	17.79	***0.92***
		Protected	0.22	***0.95***	13.63	***0.80***
Vienna	Stone	Unprotected	0.17	*0.73*	9.55	*0.30*
		Protected	0.12	***0.97***	10.32	***0.83***
	Wood	Unprotected	0.26	***0.97***	20.22	***0.91***
		Protected	0.22	***0.95***	17.44	***0.93***
Breitenfurt	Stone	Unprotected	-0.04	*0.63*	2.54	0.10
		Protected	-0.06	***0.87***	-	-
	Wood	Unprotected	0.14	***0.98***	10.55	*0.78*
		Protected	0.09	***0.83***	5.00	0.03
Oporto	Stone	Unprotected	0.03	0.08	10.66	*0.49*
		Protected	0.26	***0.80***	4.81	0.21
	Wood	Unprotected	0.23	***0.90***	16.00	*0.75*
		Protected	0.12	***0.82***	7.48	*0.49*
Coimbra	Stone	Unprotected	-0.02	0.03	2.98	0.15
		Protected	-0.11	*0.31*	1.14	0.06
	Wood	Unprotected	0.15	***0.84***	8.25	*0.38*
		Protected	0.10	*0.67*	6.87	*0.34*

Italics indicate r^2 values with p values <0.05
Bold indicates r^2 values over 0.80

It is apparent from Table 4.3 that trends in soiling are best predicted by the exponential model, Model 1. The average r^2 value for Model 1 from all data sets is 0.73, whereas Model 2 yields an average r^2 value of 0.45. Model 1 is therefore a better model of reflectance change occurring on both protected and unprotected wood sample surfaces (with an average r^2 value of 0.89 at all sites) and protected stone sample surfaces (yielding an average r^2 of 0.74 at all sites). Model 2 yields the best r^2 for some sample types and conditions, but is generally a less useful predictive tool over the time period modelled.

4.5.2 Consequences of Calculated Soiling Constants

It has been estimated that when surface reflectance decreases by approximately 30%, cleaning

may be triggered (Mansfield, 1989). Using the calculated k_1 soiling rate constants derived from observed data, it is possible to estimate the exposure period which may be expected to give rise to cleaning. Predicted exposure periods are presented in Table 4.4. These values represent exposure periods for each material assuming the material is exposed, since most building materials would not be protected from rainfall. According to the results of this analysis, unprotected samples represent the worst case scenario.

Table 4.4 Predicted exposure periods (in years) of unprotected wood and stone surfaces resulting in a specified reduction in reflectance.

		Percentage Reduction in Reflectance			
Site	Material	30%	40%	50%	60%
London	Stone	1.98	2.84	3.85	5.09
	Wood	1.19	1.70	2.31	3.05
Vienna	Stone	2.10	3.00	4.08	5.39
	Wood	1.37	1.96	2.67	3.52
Breitenfurt	Stone	-	-	-	-
	Wood	2.55	3.65	4.95	6.54
Oporto	Stone	1.37	1.96	2.67	3.52
	Wood	1.55	2.22	3.01	3.98
Coimbra	Stone	-	-	-	-
	Wood	2.38	3.41	4.62	6.11

It is clear that according to these predictions, a 30% reduction in reflectance for a unprotected painted wood surface would be achieved within 1.2 years in London, 1.4 years in Vienna, 1.6 years in Oporto and 2.4 years in Coimbra. A 30% reduction in the reflectance of unprotected stone surfaces would take longer to achieve according to the calculated k_1 values at the London and Vienna sites. A 30% reduction in reflectance would take approximately 2 years to occur in both London and Vienna, and approximately 1.4 years in Oporto. The generation of k values and the prediction of repainting or cleaning cycles will therefore lead to better estimates of building soiling costs.

4.5.3 Comparison of Model Performance Under Different Conditions

4.5.3.1 Variations Between Sites

In order to conduct a thorough analysis, the *k* and corresponding r^2 values at each site have

been studied in conjunction with the graphed data (in Appendix 2) to determine any intra- or inter-site trends. The following interpretation also refers to the results in Table 4.3.

At the London site, Model 1 provides the best fit for the data, particularly for the protected wood, unprotected wood and protected stone samples. Model 2 provides two distinct trends, which appear consistently throughout the sample types and exposure positions. The r^2 values for Model 2 stone samples are low (correlations are within the 95% confidence limits) probably due to the inclusion of outlying data points. The removal of outliers yields a greater r^2 value, however due to the potential importance of outliers in the soiling process, outliers were not removed. The NW sample of both materials in protected and unprotected positions exhibit the highest k_1 value, and hence the highest soiling rate. Since these sample faces are leeward or 'wind facing', one explanation of the different soiling rates at different direction orientations may be the effect of meteorological conditions. The relationship between sample orientation and meteorology, and in particular wind direction, is further discussed in Section 4.5.3.5.

At the Vienna site, clear trends in reflectance change emerge. All the plots show a two stage relationship between time and reflectance change with a distinct shift in reflectance change at approximately six months (which agrees with the work of Hamilton and Mansfield, 1991). The rate of reduction or blackening reduces after approximately six months, particularly on the west face. This effect was also observed by Pio (in CE Contract No STEP-CT90-0097, 1995) who - using the same data - reported soiling proceeding in 2 steps, an initial period of high soiling rates lasting 100-200 days followed by lower soiling rates. Model 1 provides the best model of soiling at this site, with high r^2 values. r^2 values for Model 2 are also high - particularly for three faces of the protected stone sample and the unprotected and protected wood samples. In contrast, the reflectance measurements taken from the protected stone samples are in good agreement with Model 1. The north and west faces of the stone samples exhibit a significantly different soiling pattern to that of the other faces, and again this is related to wind direction in Section 4.5.3.5.1.

Breitenfurt was the only semi-rural site included in the study and experienced the lowest soiling rates of all the sites. Wood sample soiling rates were the lowest of all the sites, marginally lower than those calculated for Coimbra. Results for the stone samples were difficult to interpret since they were cleaner at the end of the trial than at the beginning, producing

negative k_1 values. These samples still exhibited higher soiling rates for unprotected samples samples than protected samples of both materials, a feature of all the samples that is examined further in Section 4.4.3.4).

Neither model was particularly effective at modelling the soiling rates for the Portuguese stone samples where reflectance values for some samples actually increased over the sampling period, particularly those in protected positions. At the Oporto site, reflectance values commonly increase above the original reflectance value obscuring the overall trend, which was therefore difficult to interpret. The overall trend emerges as a steady soiling rate for 4-5 months at which point the soiling rate is reduced and reflectance fluctuates periodically, possibly due to rainfall. In Oporto, Model 2 provides high r^2 values for the wood samples (average r^2 value for Oporto wood samples is 0.62). This is in good agreement with the work of Pio *et al* (1997). Soiling constants were not derived for many of the stone sample faces as too few points could be plotted due to the exceedence of the R_o reflectance values. Model 1 also produces a very low k_1 value for the unprotected stone sample for the same reason. Pio (in CE STEP-CT90-0097, 1995) cites the corrosion of calcareous material by acidic compounds and the formation of gypsum (a white material) at the surface, as being responsible for reflectance *increase* over the sampling period. This would explain why the reflectance of unsheltered samples exceeded R_o since these samples are regularly subject to acidic deposition followed by precipitation impaction, which effectively cleans the stone of particles, leaving a fresh surface.

At the Coimbra site, the reflectance measurements again regularly increase above the original reflectance value. As at Oporto, soiling constants were not derived for much of the stone data as reflectance remained higher than R_o for most of the sampling period. r^2 values for both models were lowest at this site, with the data producing a similar trend to that at the Oporto site. The stone samples were found to get cleaner at this site, resulting in a negative k_1 value for both protected and unprotected stone samples indicating a cleaning effect. The south faces of both material types exhibited the lowest soiling rates. k_1 values for wood samples were only marginally higher than those found at Breitenfurt. Again, similarly to Breitenfurt despite negative soiling constants, the protected sample was more negative indicating that the unprotected samples were more soiled than the protected samples at the end of the monitoring

period, which is in agreement with all other samples at all other sites.

4.5.3.2 Effect of Ambient Particulate Matter and Sulphur Dioxide Concentrations

Daily total suspended particulate (TSP), black smoke, PM_{10}, particulate elemental carbon (PEC) and SO_2 measurements were taken at the five sites during this study (CE Contract No CT90-0097, 1995) and a subsequent study conducted during 1995/96 (Watt and Kendall, 1997). Samplers were co-located with the stone tablets where practical. Table 4.5 shows the mean daily concentrations recorded.

At individual sites, a complex relationship exists between these particulate matter measurements, which is not consistent at all sites. This may be a function of the different sources of data for particulate matter or may reflect the complexity of aerosol composition or the measurement of aerosols. Soiling rates at different sites may therefore vary due to the optical properties of the particles or particulate matter concentration plus the effect of other unmeasured variables may influence soiling rate, such as chemical composition or particle size distribution. Mean concentrations of other variables measured during the 1995/6 monitoring campaign are also given in Table 4.5, and further details are presented in Chapter 5.

Table 4.5 Mean daily concentrations of particulate matter and sulphur dioxide measured at the five sites.

Pollutant	London	Vienna	Oporto	Coimbra°	Breitenfurt
TSP ($\mu g\ m^{-3}$)	43.5^{+}	40.3^{+}	63.4^{+}	52.1	30.6^{+}
Black Smoke ($\mu g\ m^{-3}$)	18.8^{+}	77.1^{+}	36.8^{+}	23.7	37.2^{+}
PM_{10} ($\mu g\ m^{-3}$)	29.0$^{\#}$	-	34.9^{+}	29.6	-
PEC ($\mu g\ m^{-3}$)	2.3^{+}	3.4^{+}	5.1°	3.4	-
SO_2 ($\mu g\ m^{-3}$)	10.8^{+}	10.1^{+}	18.3^{+}	7.1	5.3^{+}
TOC ($\mu g\ m^{-3}$)	7.6*	12.1*	10.2*	-	11.2*
PEC ($\mu g\ m^{-3}$)	2.5*	3.4*	3.9*	-	2.5*
PAH ($ng\ m^{-3}$)	7.2*	22.7*	43.8*	-	-
n-Alkanes ($ng\ m^{-3}$)	247.6*	311.1*	260.5*	-	-

$^{\#}$ Mean taken from the London Bloomsbury site; $^{+}$ Measurements taken during the study period; ° From Harrison *et al* (1997); * Weekly measurements averaged over a one year sampling period in 1995/6.

One feature of this data which is relevant to modelling the soiling of surfaces at the five

locations is that it highlights the improbability of soiling being due to the mass concentration of total suspended particulate matter alone. As each site exhibits varying concentrations of different classes of particulate matter and yet experiences very different surface soiling rates, it is likely that other factors are important in the soiling process. This aspect may be investigated further by regressing environmental factors against soiling rates to gauge the relative importance of each parameter.

The mean values for each pollutant in Table 4.5 were regressed individually against the mean k_1 values for each sample type, ie protected wood, unprotected wood, protected stone and unprotected stone. Only the four urban sites were considered. For example, the k_1 values for each site were regressed against the TSP concentrations measured at each site. The r^2 values, the regression coefficients (B) and the associated p value for each variable are presented in Table 4.6. The r^2 value indicates the amount of variance of k_1 which can be explained by each independent variable, the regression coefficient (B) indicates the influence of each independent variable upon the dependent variable according to the equation for a straight line

$$Y = A + BX$$

where A is the intercept, Y is the dependent variable and X independent variable. The p value represents the statistical significance of the r^2 and B value and if below 0.05 the null hypothesis that $r^2 = 0$ can be rejected. The p value indicates whether the r^2 value is significantly different from zero. If $p < 0.10$, it is concluded that the observed r^2 value (and associated B value) is significant at the 0.10 level. In otherwords, one may be reasonably confident that r^2 value is not zero, and the null hypothesis can be rejected.

Table 4.6 Coefficients of determination (r^2), regression coefficients (B) and p values for the linear regression of mean k_1 value for each sample type and environmental factors.

Independent Variable		Pro Wood (n=4)	Unpro Wood (n=4)	Pro Stone (n=4)	Unpro Stone (n=4)
TSP	r^2	0.68	0.21	0.06	0.59
	B	-0.01	-<0.01	-<0.01	+0.23
	p	0.18	0.53	0.75	-0.01
Black smoke	r^2	0.17	0.04	0.04	0.15
	B	-<0.01	-<0.01	+<0.01	+<0.01
	p	0.59	0.81	0.79	0.62
PM_{10}	r^2	0.78	0.40	0.01	0.71
	B	-<0.01	-<0.01	+<0.01	-0.01
	p	0.31	0.57	0.94	0.36
PEC	r^2	0.38	0.13	0.16	0.33
	B	-0.03	-0.02	+0.05	-0.05
	p	0.38	0.64	0.60	0.42
SO_2	r^2	0.02	0.08	0.77	<0.01
	B	-0.01	+<0.01	+0.03	-<0.01
	p	0.85	0.71	0.12	0.93
TOC	r^2	0.01	0.41	0.01	0.02
	B	-<0.01	-<0.01	-<0.01	-<0.01
	p	0.94	0.56	0.93	0.91
PAH	r^2	0.82	0.97	0.64	0.87
	B	-<0.01	-<0.01	+<0.01	-<0.01
	p	0.28	0.11	0.41	0.24
n-Alkanes	r^2	0.11	0.07	0.26	0.07
	B	+<0.01	-<0.01	-<0.01	+<0.01
	p	0.79	0.82	0.66	0.83

Pro = Protected

Unpro = Unprotected

- means p could not be calculated (too few values)

Highest r^2 were found for PAH and PM_{10} concentrations, although these factors were associated with a reduction in soiling rate (ie B is negative) and no relationships produced p values below 0.11 (ie no relationships were significant at the 0.10 level).

The mean values for each pollutant in Table 4.5 were regressed individually against the mean k_2 values for each sample type, ie protected wood, unprotected wood, protected stone and unprotected stone. The results of these regressions are presented in Table 4.7. These relationships should be viewed as tentative in view of the limited number of data points.

Table 4.7 Coefficients of determination (r^2), regression coefficients (B) and p values for the linear regression of mean k_2 value for each sample type and environmental factors.

Independent Variable		Pro Wood (n=4)	Unpro Wood (n=4)	Pro Stone (n=4)	Unpro Stone (n=4)
TSP	r^2	0.74	0.19	0.30	0.06
	B	-0.42	-0.22	-0.20	0.09
	p	0.14	0.57	0.45	0.75
Black smoke	r^2	0.43	0.35	0.72	0.43
	B	+0.13	+0.12	+0.12	+0.09
	p	0.35	0.41	0.15	0.34
PM_{10}	r^2	0.84	0.13	0.10	0.30
	B	-0.20	-0.11	-0.04	-0.12
	p	0.26	0.76	0.80	0.63
PEC	r^2	0.27	0.01	0.01	0.43
	B	-2.27	-0.43	+0.25	-2.07
	p	0.48	0.90	0.92	0.34
SO_2	r^2	0.60	0.05	0.13	0.02
	B	0.59	-0.25	+0.40	+0.12
	p	0.22	0.77	0.63	0.85
TOC	r^2	0.09	0.25	0.58	0.66
	B	+0.66	+0.47	+1.02	+1.06
	p	0.81	0.67	0.45	0.40
PAH	r^2	0.46	0.25	0.03	0.83
	B	-0.19	-0.06	-0.03	+0.15
	p	0.52	0.67	0.88	0.27
n-Alkanes	r^2	0.43	0.65	0.92	0.25
	B	+0.10	+0.05	+0.09	+0.04
	p	0.54	0.40	0.18	0.66

Pro = Protected

Unpro = Unprotected

- means p could not be calculated (too few values)

No parameters were associated with inter-site k_2 value trends at the 0.10 significance level. However, some variables were correlated with k_2 values for some sample types, such as *n*-alkanes, PAH, black smoke and PM_{10}.

4.5.3.3 Effect of Sample Material

Table 4.8 gives the average r^2 values for both protected and unprotected stone and wood samples at the five sites showing that coefficients of determination for Model 1 and soiling rates over time, are consistently higher for painted wood samples. The results in Table 4.3 also show that Model 1 consistently predicts the soiling of unprotected wood samples best at all sites, with the next best predictions for protected wood samples. Unprotected stone samples in Vienna and London did not conform to the models, and although a trend was apparent it did not coincide with the predictions of either model.

The effect of acidic deposition and subsequent rainfall exposure clearly may influence the ability of the model to predict soiling rates effectively. This surface removal effect during rainfall may be responsible for the reduced success of Model 1 in predicting soiling rates for stone samples, causing scatter and reducing r^2 values.

Table 4.8 Mean coefficients of determination (r^2) for Model 1 and all sample types at the five sites.

	London	Vienna	Oporto	Coimbra	Breitenfurt
Stone	0.70	0.85	0.44	0.17	0.75
Wood	0.95	0.96	0.86	0.76	0.91

Soiling constants for stone surfaces are lower at all sites. This may be due to the fact that although more material may be deposited on these surfaces due to higher surface roughnesses than the painted wood samples, the particles may deposit in the indents of the surface. Such particles will not influence the reflectance properties of the surface as they are not part of the true surface of the sample.

4.5.3.4 Effect of Sample Position and Orientation

The soiling rates of the same materials in protected and unprotected positions were compared. At each site, the ratio of the averaged four faces of each material sample under unprotected and protected conditions was calculated and these are presented in Table 4.9. At all sites the ratio of unprotected to protected k_1 values exceeded 1. This contradicts earlier work which clearly states that higher soiling rates are experienced on protected samples where samples are protected from removal mechanisms such as rain (Beloin and Haynie, 1975; Haynie and Lemmons, 1990), but agrees with the analysis of Pio (in CE Contract No STEP-CT90-0097, 1995) and the work of Creighton *et al* (1990).

Table 4.9 Ratios of k_1 values for all unprotected and protected samples of each material at each site.

	London	Vienna	Oporto	Coimbra	Breitenfurt
Stone	1.17	1.39	5.50	-	1.50
Wood	1.38	1.16	1.53	1.88	1.60

One possible explanation of these results is that the wetting of the surface by rainfall aids particle deposition onto a surface, particularly of submicron particles. These particles are not removed easily by rainfall (Creighton *et al*, 1990) unless via the dissolution of the sample surface itself which may occur with the stone samples. This may explain the lower soiling constants exhibited by the stone samples. This hypothesis agrees with the findings of Pio analysing the same Portuguese data, who determined that while the stone samples were cleaned by rainfall periods, no cleaning effect was evident for painted wood samples, indeed unprotected samples became more soiled after rain. Another possibility is that the protective hood which was positioned over the protected samples afforded some protection from wind which may be a factor in soiling (see Section 4.5.3.5.1). Another possibility is the growth of mildew which has been reported by other workers (eg Beloin and Haynie, 1975), although no SEM examination was carried out on the samples.

BRE exposed samples in protected and unprotected positions at four of the same sites over a 2 year period between 1992 and 1994 (CE Contract No STEP-CT90-0097, 1995). This study found that exposed samples lost weight over the exposure period which was attributed to the loss of surface material through the deposition of and consequent erosion by sulphurous material. Table 4.10 shows the weight change of exposed stone tablets at the four sites. It was assumed that protected samples gained weight probably through the incremental particulate deposition in the absence of removal mechanisms.

Table 4.10 Weight change of exposed stone tablets at the four sampling sites in Portugal, UK and Austria for a two year period (percentage of dry weight per year).

	White Mansfield Stone		Portland Stone	
Site	Unsheltered	Sheltered	Unsheltered	Sheltered
Oporto	-0.51	+0.13	-0.48	+0.16
Coimbra	-0.16	+0.02	-0.15	+0.04
London (St Paul's)	-0.34	+0.03	-0.34	+0.11
Vienna (Stephansdom)	-0.16	+0.04	-0.12	+0.06

- Indicates weight loss. + Indicates weight gain

If the results of this study regarding the reducing reflectance of stone samples at the London and Vienna sites are considered together with those of BRE and NMEP (allowing for the fact that reflectance data from Coimbra and Oporto may be treated with caution), one may conclude that the soiling of stone process is a complicated one which includes three main processes: continuous leaching of *internal* material to the surface producing a darkening effect, atmospheric deposition of material and the removal of stone material from the surface. Mildew formation at the surface may also be involved in the darkening of surfaces and may enhance leaching of materials to the surface (Webster *et al*, 1992). There are several possible hypotheses which may be proposed in the light of these results:

i) dissolution of the soluble $CaCO_3$ results in the exposure of darker insoluble materials such as silica which acts as an effective particle trap because of its surface characteristics and by protruding through the boundary layer;

ii) the dissolution and chemical reaction of the surface components results in the formation of

of a darker more chemically resistant surface layer (ie gypsum) which exhibits less light reflectance properties due to the particles trapped in it;

iii) the gypsum growth on the sheltered samples results in heavier samples by fixing atmospheric sulphur dioxide, despite continuous leaching of material from the interior of the stone;

iv) the transportation of small particles to the lower layers of the stone and the inclusion of large particles at the stone surface, ensures surface darkness increases despite the continual removal of the larger surface particles; and,

v) the deposited material on the sheltered samples is paler than the sample surface and that blacker particles are trapped on the unprotected surface due to preferential adhesion.

Rainfall, wind speed and the direction of prevailing wind were also recorded at each site. Table 4.11 shows the weekly means of these parameters experienced at the five sites during the sampling period. Since all of the sites were located in different positions at different cities, each was exposed to different conditions. Parameters were monitored on-site, except at the London site where rainfall measurements from a UK Meteorological Office mast monitor positioned at a similar height within one kilometre were used. Mean wind direction as measured by the UK Meteorological Office at four of the sites monitored are also presented.

Table 4.11 Weekly means of meteorological parameters measured.

	London	Vienna	Oporto	Coimbra	Breitenfurt
Mean Rainfall (mm)	1.48	1.35	3.10	2.44	2.32
Mean Wind Speed ($m\ s^{-1}$)	3.7	1.0	5.0	2.3	0.9
Met Office Mean Wind Direction	E	S/SE	E/SE	S/SE	-

Haynie (1986) showed that increasing wind speed increases the deposition of larger sized particles to vertical surfaces. Larger particles have an important role in the soiling process (Creighton *et al*, 1990).

No seasonal differences were detected in the time series data, indicating that seasonal variations in other meteorological factors, which were not measured, were not directly

influential over soiling rates. To investigate this, the UK Meteorological Office prepared summaries of hourly recordings of relative humidity, wind speed and wind direction for each site over the respective measurement periods. Weather measurements were binned into banded categories for each parameter and sites were compared on this basis.

The mean value of each meteorological variable considered was regressed individually against the mean k_1 value for each sample type (see Section 4.5.3.2). The r^2, B and p values are presented in Table 4.12. These relationships should be viewed as tentative in view of the limited number of data points.

Table 4.12 Coefficients of determination (r^2), regression coefficients (B) and p values for the linear regression of mean k_1 value for each sample type and meteorological factors.

Independent Variable		Pro Wood	Unpro Wood	Pro Stone	Unpro Stone
Wind Speed	r^2	0.74	0.26	0.01	0.66
	B	+0.03	+0.02	-0.01	+0.05
	p	0.14	0.49	0.89	0.19
Temperature	r^2	0.94	0.64	0.12	0.91
	B	-0.05	-0.04	-0.04	-0.07
	p	0.30	0.20	0.65	0.04
Relative Humidity	r^2	0.89	0.50	<0.01	0.84
	B	-0.01	-0.01	+ <0.01	-0.02
	p	0.06	0.29	0.98	0.08
Rainfall Weekly Average	r^2	0.87	0.43	<0.01	0.81
	B	-<0.01	-<0.01	+ <0.01	-0.01
	p	0.07	0.34	0.98	0.10

Pro = Protected
Unpro = Unprotected

The mean value of each meteorological variable considered was regressed individually against the mean k_2 value for each sample type (see Section 4.5.3.2). The r^2, B and p values are presented in Table 4.13.

Table 4.13 Coefficients of determination (r^2), regression coefficients (B) and p values for the linear regression of mean k_2 value for each sample type and meteorological factors.

Independent Variable		Pro Wood	Unpro Wood	Pro Stone	Unpro Stone
Wind Speed	r^2	0.88	0.33	0.51	<0.01
	B	+2.67	+1.66	+1.52	-0.07
	p	0.06	0.43	0.28	0.96
Temperature	r^2	0.99	0.78	0.83	0.91
	B	-3.88	-3.49	-2.63	-0.074
	p	0.01	0.12	0.09	0.04
Relative Humidity	r^2	0.80	0.37	0.37	0.84
	B	-0.77	-0.53	-0.39	-0.016
	p	0.10	0.39	0.39	0.08
Rainfall Weekly Average	r^2	0.85	0.37	0.42	0.01
	B	-0.24	-0.16	-0.13	+0.02
	p	0.08	0.40	0.35	0.89

Pro = Protected
Unpro = Unprotected

Three variables were shown to be individually associated with k_1 soiling rates at the 0.10 significance level. Weekly mean rainfall and mean relative humidity were both significantly associated with a reduction in soiling rate (k_1) of protected wood and unprotected stone samples, although of course they are physically related factors. Clearly rainfall would be intuitively associated with soiling rate reduction. Increasing temperature was associated with a reduction in soiling rate, and was most strongly associated (the 0.05 significance level) with the unprotected stone samples. This may be important when insolation effects are considered (see Section 4.5.3.5.4 and Table 4.12). Wind speed was the only meteorological variable (or environmental variable, see Section 4.5.3.2) considered where variable increases were associated with a increased soiling rate on most sample types, although not within the 0.10 significance level.

Temperature was the most closely related variable to k_2 soiling rates at all the sites, with significance of high r^2 values between 0.01 and 0.12. Temperature was consistently found to be closely related to a decrease in the soiling rate k_2. RH was also found to be related to k_2 soiling rates for protected wood and unprotected stone samples, at the 0.10 significance level. Rainfall weekly average was also found to relate closely with k_2 values of protected wood

samples at all sites.

4.5.3.5 Effect of Meteorological Conditions

4.5.3.5.1 Wind Speed and Direction

Soiling of vertical surfaces by particles is dependent on local meteorological conditions. While rain impaction was controlled in this experiment, local wind systems appear to have influenced the soiling behaviour of the four directional faces of the same sample at the same site. Table 4.14 shows the average k_1 values for the four directional faces of the wood and stone samples together with the dominant wind direction at that site.

Table 4.14 Average k_1 values for each directional face of all samples at each site.

Sample Face	London*	Vienna	Oporto	Coimbra	Breitenfurt
North	0.26	0.20	0.21	0.14	0.14
South	0.21	0.19	0.12	0.08	0.09
East	0.16	0.19	0.14	0.14	0.10
West	0.22	0.20	0.16	0.15	0.13
Prevailing Wind Direction	E	S/SE	E/SE	S/SE	-

* For London site read NW, SW, NE and SE for N, S, E and W.

At all sites, the north and west samples experienced the most soiling. These samples represent the leeward faces at each site. A break-down of the UK Met Office wind speed data is presented in Table 4.15.

Table 4.15 A breakdown of wind speed data for each site.

Wind Speed (Knots)	Percentage Distribution of Wind Speeds			
	London (%)	Vienna (%)	Oporto (%)	Coimbra (%)
< 3	13.8	21.1	36.5	51.9
3 - 10	72.8	48.1	49.1	42.0
10 - 21	12.6	28.5	14.0	5.8
21 - 33	0.8	2.7	0.5	0.4
Mean Wind Speed ($m\ s^{-1}$)	3.7	4.3	2.9	2.2

Vienna and London experience the highest wind speeds and for longer periods. This is important since higher wind speeds lead to a suppression of the surface boundary layer,

retarding particle movement and increasing particle deposition. The mean wind speeds are very different to those recorded at the four sampling locations. The Meteorological Office data was used in preference to the on-site data for greater comparability.

4.5.3.5.2 Rainfall

Rainfall has been found to be an important factor in the soiling of building surfaces, increasing surface reflectance by removing deposited particles (Camuffo *et al*, 1981; Creighton *et al*, 1990; Hamilton and Mansfield, 1991). This leads to lower soiling rates for unprotected samples.

Table 4.8 shows the effect of protection of the sample by a hood which effectively reduces direct rain impaction and runoff. Unprotected samples consistently experienced higher soiling rates than protected samples at the same site contradicting the work of other authors (eg Creighton *et al*, 1990). However, as the trend is absolutely consistent for each material and at each site, this appears to be a genuine phenomenon.

In general, cleaning effects by periods of rainfall are notable on the stone samples, a finding which is agreement with Pio (in CE Contract No STEP-CT90-0097, 1995) and Hamilton and Mansfield (1993). However, due to the high variability of rainfall occurrence, intensity and duration, quantitative relationship is difficult to establish and may co-depend on other factors eg wind speed, temperature of the surface, etc. Difficulties also arise from weekly or daily measurements when the effects of 1 hour of rainfall may be obscured when averaged to a week or even a day. However the increase in reflectance directly after rainfall may be attributable to particle washing of the sample surface, which leads to a wetted surface and the chemical reactivity of the surface to form a covering monolayer which is more effective at reducing light reflectance.

4.5.3.5.3 Relative Humidity

UK Meteorological Office measurements of relative humidity (RH) were used to assess RH levels at all sites. These measurements were made over the monitoring period and banded into 5% bands. RH influences the size distribution of the ambient particulate matter concentrations

and hence deposition velocities, and may result in surfacial moisture layers which may also influence deposition and surface retention of particles. The results showed that RH was approximately 10% higher at the two Portuguese sites.

At the London site, relative humidity (RH) was between 66% and 90% for more than half of the sampling period. The 75-80% RH category contained the largest proportion of measurements and RH was 96-100% for only 1% of the time. Mean RH was 69%. RH in Vienna was most frequently in the 71-75% band and was between 96-100% for 6% of the time. Mean RH was 70%.

RH was significantly higher at the two Portuguese sites, probably due to the proximity to the sea. RH was between 81-100% for half of both sampling periods. At Porto, RH was between 96-100% for 20% of the time (the most frequently occurring band). At Coimbra, RH was 90-95% for 16% of the time, making that category the most common. Mean RH in Oporto and Coimbra were 81 and 78%, respectively.

4.5.3.5.4 Insolation

The results in Table 4.12 show that all of the south-facing samples at all sites exhibited the lowest soiling rates, except the London site which did not have a true south-facing sample. This is certainly the only intersite agreement observable.

Soiling patterns of some features at St Paul's Cathedral show similar patterns of soiling. The south-facing sections of the dome roof and the dome drum beneath the supporting pillars of the dome roof are less soiled than the other sections. Figure 4.4 shows the south-facing sections of the dome drum (shown on the left of the photograph) which are clearly less soiled than the other sections (on the right).

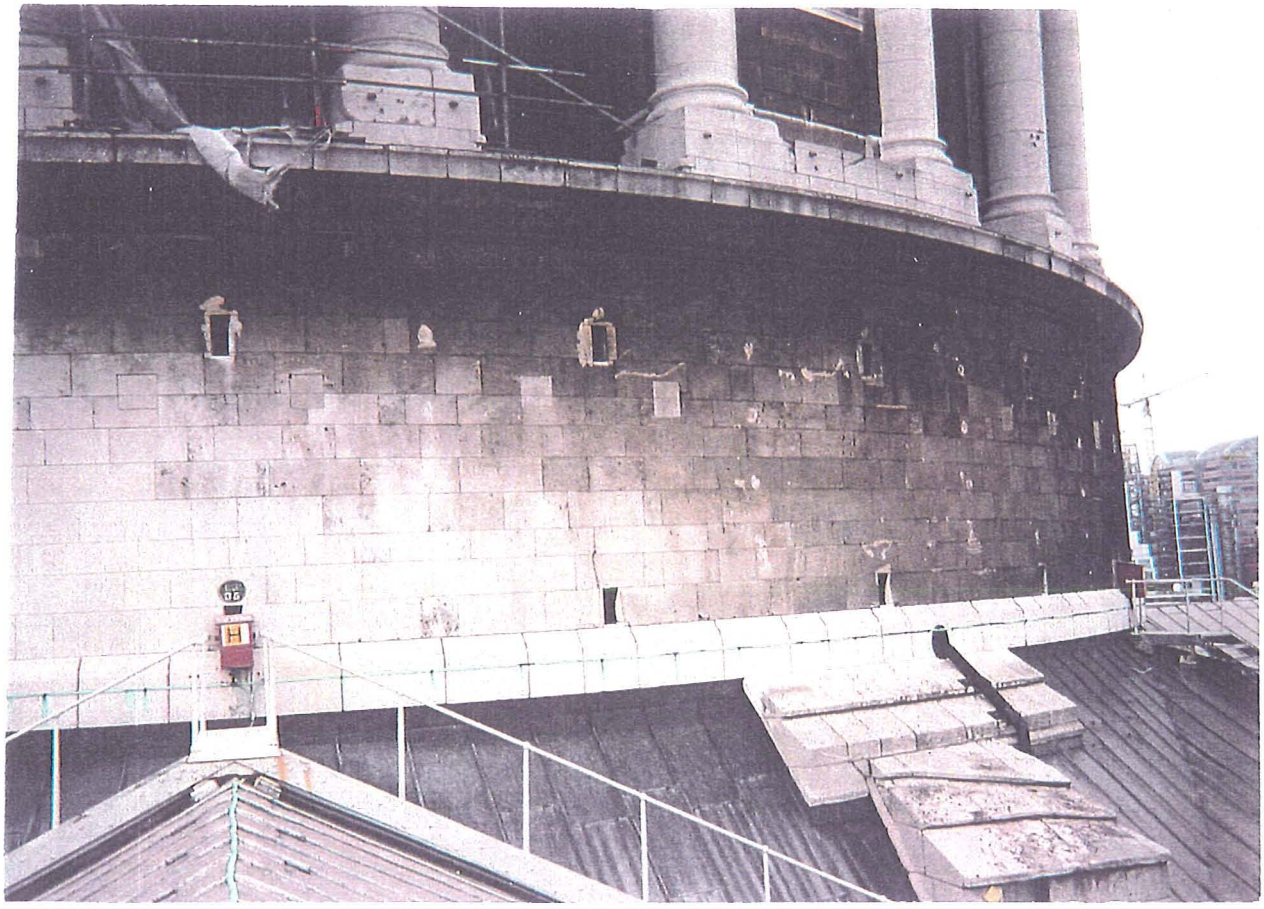

Figure 4.4 The south-facing sections of the dome drum (on the left of the photograph) are clearly less soiled than the other sections (on the right).

4.5.4 Comparisons with other Results and Models

Using the particulate data presented in Table 4.4, rates of soiling experienced at the five monitored sites have been compared with predictions made by different models which approximate *k* values from ambient TSP and PEC concentrations. Table 4.11 provides the *k* values calculated using three proposed models. Haynie's model assumes that soiling is due to surface coverage by TSP, while Lanting's models considers PEC to be the most important factor in soiling. Lanting's equation (A) in Table 4.16 assumes soiling is due to surface coverage by PEC and equation (B) considers that the soiling layer thickness is responsible for measurable soiling. All three models have been developed for and performed best when predicting the soiling behaviour of smooth white surfaces and therefore may not be appropriate for use in the prediction of stone surface soiling.

Table 4.16 Predicted k_1 values using soiling models proposed by different authors for smooth, white surfaces.

Author and Proposed Model	London	Vienna	Oporto	Coimbra	Breitenfurt
Haynie (1986) $R = R_o e^{-kt}$ where $k = 0.0085 C_{TSP}$	0.37	0.34	0.53	0.44	0.26
Lanting A (1986) $R/R_o = (1-x) + R_p/R_o.x$ Approximates to $k = 0.095 C_{PEC}$	0.22	0.32	0.48	0.32	-
Lanting B (1986) $R = R_o e^{-kt}$ where $k = 0.13 C_{PEC}$	0.30	0.44	0.66	0.44	-
This Study - Protected Wood Samples	0.22	0.22	0.12	0.10	0.09
Unprotected Wood Samples	0.30	0.26	0.23	0.15	0.14

Comparison of Tables 4.16 and 4.3 shows that Haynie's model tends to over predict soiling rates in London and Vienna by a very small margin (approximately 0.01), whereas Lanting (A) accurately predicts the soiling rate of protected wood in London and Lanting (B) predicts the exact rate of unprotected wood soiling in London. Lanting (A) is also effective in predicting soiling of painted wood samples in Vienna to within an accuracy of 0.1. It is clear from the results that all three models massively over predict the soiling rates measured at Oporto, and particularly at Coimbra and Breitenfurt. This is likely to be a function of the difference in particle characteristics or meteorological conditions at these sites. The skewed size distribution in the urban aerosol towards submicron particles and the differences in optical properties of these smaller particles is likely to have produced this difference. The tendency of the models to over-predict may also be due to their empirical derivation over short exposure periods.

4.6 SOILING MODELS USING MULTIPLE REGRESSION

4.6.1 Weekly Mean Data

In order to assess the relative importance of all the measured factors at all sites and to identify any complex multivariate relationships, multiple regression was carried out using SPSS. Weekly mean values of all available parameters were regressed against weekly reflectance values. Dummy variables were used to create interactive variables which assessed the effect of each measured variable at each of the sites separately and then all sites together. In essence,

the effect of each variable and any interactive effects with other measured variables could be detected using this method, according to the equation

$$Y = A + B_1 X_1 + B_2 X_2 + B_3 X_3 \ldots$$

where X_1, X_2, etc, represent independent variables and B_1, B_2, etc represent partial regression coefficients. Dummy variables assume arbitrary metric values of 0 and 1 as in Table 4.17.

Table 4.17 Scores for each dummy variable.

	Name of Dummy Variable		
Types of Cases	D_1	D_2	D_3
Smoke	1	0	0
Rainfall	0	1	0
Wind speed	0	0	0
SO_2	0	0	0

In the regression equation,

$$Y = A + B_1 D_1 + B_2 D_2 + B_3 D_3$$

the predicted Y score for SO_2 would be

$$Y = A$$

since all D_i would equal 0 for these cases. For smoke, the predicted Y score would be

$$Y = A + B_1$$

since all other terms would be zero and D_1 is equal to one.

The variables were introduced into the regression model backwards so that for the first solution of the regression equation, all of the variables were entered and the variables were gradually removed from the model so that the final solution contained only the most important variable(s). The significance of the p value result indicated the importance of each of the factors prior to their removal and the difference in the r^2 value for the model before and after the removal of each factor indicated the importance of each factor in the regression model.

A total of four measured variables at four sites were included in the model. Breitenfurt data was rejected on the basis of insufficient reflectance and independent variable data. The

dependent variable was weekly reflectance change; positive values indicate increased soiling, negative values indicate a cleaning effect. Weekly mean values for independent variables were regressed against this dependent variable.

The results from the intersite multiple regression model indicate that relationships are very weak between the independent variables and the dependent variable. Table 4.18 summarises the results of the analysis. Significance levels were set at 0.10.

Table 4.18 Summary table of the results from the multiple regression of all variables at all sites.

Sample	r^2	Partial Regression Coefficients (B) for Each Independent Variable			
		Smoke	Rainfall	Wind Speed	SO_2
UWN	0.08				
UWS	0.06				
UWE	0.18	+ 0.010			- 0.034
UWW	0.13	+ 0.008		+ 0.271	
PWN	0.02				
PWS	0.03				
PWE	0.10		- 0.015		
PWW	0.01				
USN	0.09			+ 0.610	
USS	0.07			+ 0.512	
USE	0.06			+ 0.648	
USW	0.08			+ 0.580	
PSN	0.13		+ 0.037		
PSS	0.08		+ 0.016		
PSE	0.09				- 0.023
PSW	0.10		+ 0.031	+ 0.398	

U = Unprotected, P = Protected, W = Wood, S = Stone and the final letter of each sample name represents the four directional faces of the sample of north, south, east and west.
+ values indicate this variable is associated with reflectance loss
- values indicate this variable is associated with reflectance increase

The r^2 value represents the amount of variation in reflectance change (the dependent variable) which is accountable by the independent variables included in the regression analysis (ie smoke, rainfall, wind speed and sulphur dioxide). The partial regression coefficient values

found in the table represent the amount of change in reflectance - either positive or negative -which may be expected per unit of each of the independent variables. Only those that are significant at the 0.90 level have been included in Table 4.16. It is clear from the low r^2 values that the models do not include all of the factors in the soiling process. Only one model (that for the east face of the unprotected wood sample, UWE) is significant at the 0.05 level. This lack of a clear relationship may be due to the monitoring method which allowed only for weekly sampling periods, hence obscuring large reflectance changes due to short term environmental events such as high smoke concentrations.

In terms of the independent variables, none can be demonstrated to be consistently influential at a 0.10 significance level for all of the materials, at all of the exposure sites. Wind speed emerges as the most consistently influential factor in the reflectance change experienced by the different surfaces, particularly for unprotected stone. This may be explained since the stone surfaces exhibit the highest surface roughness and increasing wind speed will therefore increase the near-surface turbulence and therefore particle deposition. Smoke concentration is apparently most influential for the east and west faces of the unprotected wood samples (at the 90% confidence level). Rainfall apparently increases the soiling of the protected stone samples, but again model fits are poor. Sulphur dioxide was observed to reduce soiling on two of the surface types.

The development of similar models at individual sites provided better model fits for some sample types. Analysis of the results from the individual sites reveals that different factors are important at different sites. At the London site, regression model fits are reasonably good, particularly for the wood samples, with r^2 values up to 0.62. However, smoke concentration has a small negative effect on the soiling rate of wood samples ie smoke is associated with a reflectance increase. Rainfall is associated with an increase in reflectance of the wood samples as would be expected, but is associated with a decrease in the reflectance of the stone samples (at the 90% confidence levels). Wind speed and sulphur dioxide have a minor impact on reflectance, increasing reflectance slightly on four of the sixteen samples at the London site.

At the Vienna site, smoke concentration was the most consistently influential factor on the

At the Vienna site, smoke concentration was the most consistently influential factor on the soiling rate, particularly on the unprotected samples. Smoke concentrations increased the soiling rates of the unprotected wood samples (at the 0.05 significance level) while sulphur dioxide decreased soiling rates of these samples (at the 0.10 significance level). Regression models exhibited higher coefficients of determination than the "all-site" models, particularly for the unprotected samples. Highest r^2 values occurred for the unprotected wood samples. The r^2 values for the unprotected north and east faces of both sample materials were significant at the 0.05 level.

Neither of the Portuguese sites exhibited any significant (at 0.10 level) correlations between soiling rates of samples and independent variables. Coefficients of determination for all of the regression models were very low; the highest value was 0.1. This was due to the lack of soiling at these sites.

4.6.2 Long Term Mean Data

While weekly mean data is useful in determining short terms effects, summary data over aa longer period eg annual mean statistics are more useful for developing policy tools.

Annual means for each available parameter were regressed against k_1 and k_2 values to determine the most influential factors in the soiling process. Table 4.19 provides the mean values for the dependent variables (k_1 and k_2) and independent variables (environmental factors).

Table 4.19 Summary table of all variables included in multiple regression analysis, as long term means.

Site	Type	k_1	k_2	TSP (μgm^{-3})	Black Smoke (μgm^{-3})	PM_{10} (μgm^{-3})	PEC (μgm^{-3})	SO_2 (μgm^{-3})	TOC (μgm^{-3})	PAH (ngm^{-3})	*n*-Alkanes ($ng\ m^{-3}$)	Wind Speed ($m\ s^{-1}$)	Temp (°C)	RH (%)	Mean Weekly Rain (mm)
London	Pro Wd	0.22	13.6	43.5	18.8	29.0	2.3	10.8	7.6	7.2	248	3.7		69	1.5
	Unpro Wd	0.30	17.8												
	Pro St	0.15	5.4												
	Unpro St	0.18	5.1												
Vienna	Pro Wd	0.22	17.4	40.3	77.1	-	3.4	10.1	12.1	22.7	311	4.3		70	1.4
	Unpro Wd	0.26	20.2												
	Pro St	0.12	10.3												
	Unpro St	0.17	9.6												
Oporto	Pro Wd	0.12	7.5	63.4	36.8	34.9	5.1	18.3	10.2	43.8	261	2.9		81	3.1
	Unpro Wd	0.23	16.0												
	Pro St	0.26	4.8												
	Unpro St	0.03	10.7												
Coimbra	Pro Wd	0.10	6.9	52.1	23.7	29.6	3.4	7.1	-	-	-	2.2		78	2.4
	Unpro Wd	0.15	8.3												
	Pro St	-.11	1.1												
	Unpro St	-.02	3.0												

The best predictive multiple regression models for each sample type are presented in Table 4.20. Models were developed using the information generated by the single linear regression of individual parameters (see Tables 4.6, 4.7, 4.12 and 4.13).

Table 4.20 Results of multiple regression models using k_1 and k_2 as dependent variables and environmental variables as independent variables.

	Sample Type	Regression Model	r^2	p
k_1	Pro Wood	$0.927 - 7.87 \times 10^{-4}(BS) - 0.058(T)$	1.00	0.01
	Unpro Wood	$0.320 - 0.004(RF) + 0.011(SO_2)$	0.94	0.25
	Pro Stone	$-0.062 - 0.004(RF) + 0.038(SO_2)$	1.00	0.03
	Unpro Stone	$0.327 - 0.006(RF) + 0.038(SO_2)$	1.00	0.06
k_2	Pro Wood	$60.505 - 3.878(T)$	0.99	0.01
	Unpro Wood	$56.81 - 3.733(T) + 0.525(SO_2)$	1.00	0.02
	Pro Stone	$41.60 - 3.277(T) + 1.506(PEC)$	1.00	0.09
	Unpro Stone	$-2.988 + 0.087(BS) + 0.576(SO_2)$	1.00	0.05

BS = Black smoke RF = Average weekly rainfall
T = Temperature PEC = Particulate elemental carbon

The r^2 values are very high and reflect the fact that there are only four site values for each sample type. In most cases one variable accounted for a large proportion of the variation in the dependent variable (see Tables 4.6, 4.7, 4.12 and 4.13). Sulphur dioxide, temperature and rainfall were repeatedly occur in the best-fitting regression models, but it is notable that no one model is applicable for all sample types. The most common combination of factors is sulphur dioxide and average weekly rainfall in association with k_1 values. This finding which is consistent with what is known about the soiling process with SO_2 causing an increase in soiling, and rainfall associated with a decrease in soiling; these two factors are most strongly associated with the stone sample k_1 values. Again, different measures of particulate concentrations are only sporadically associated with soiling rates, although they do tend to increase soiling rates. It is striking that temperature is consistently associated with a decrease in k_2 values.

4.7 SUMMARY

Relating the results from field exposure studies directly to real buildings - particularly cultural heritage – is inherently difficult. Dose-response relationships determined from field exposure

studies are dependent on the samples, locations and exposure periods being representative. Extrapolation of the dose-response relationships developed here, to the UK building stock, would therefore be inadvisable. The dose response relationships developed in this thesis indicate the most important environmental factors involved in the soiling process and the relative importance of these factors at different sites in four countries.

Model 1 provides a reasonable predicting tool at all sites and for all materials, except the stone samples at Coimbra where stone samples did not soil and consequently could not be modelled effectively. Model 1 is consistently the more successful at modelling soiling of stone samples at all sites. This is consistent with other work, since the exponential model was developed for the soiling of painted wood samples. Stone sample surfaces may experience chemical change on environmental exposure, which is not accounted for in the model. Model 2 proves a less effective predicting tool of the soiling process. However, for painted wood samples in London and Vienna, Model 2 performed well yielding $r^2 > 0.80$.

Both models produce consistently lower soiling constants for the protected samples than the unprotected samples. This is surprising as protection from rain (the main particle removal mechanism) has been found to increase soiling rates in other studies. However, Creighton *et al* (1990) noted a similar effect on one unprotected sample and attributed it to staining of the surface through the dissolution of water soluble particulate components in rain. This is a consistent intersite relationship, indicating that particle deposition to a vertical surface is not the governing factor in soiling. Exposure of a sample to rain is therefore important.

The soiling rates of samples were clearly different at each site and this difference is assumed to be a result of exposure in different environments. The different heights of samplers means that size distributions of particulate matter may have been different at the five sites, leading to different soiling rates. Particulate matter concentration is higher at ground level and the proportion of the smaller size fractions increases with increasing height (Monn *et al*, 1997). Smaller particles, particularly those below 10 μm MMAD, may not decrease significantly with height, as opposed to measures of PM_{10} and TSP which do. Clearly then, the particle size distribution at the sites will influence the rate of soiling, despite particulate mass concentration measurements being similar. Similarly, the optical properties of particles will be different. The

evidence suggests that soiling can not be predicted on the basis of particle mass concentration alone which agrees with the conclusion of the NMEP study (Murray and Massey, 1999).

The very small effect of some variables on soiling rates indicated by the multiple regression analysis may be the result of taking the means over a one week period. This would suggest that the extreme values for variables, which have been obscured by the one week averaging period adopted by the monitoring technique, may be important in the prediction of soiling. Also, it appears that the measured variables cannot fully account for intersite and inter-sample variability. Humidity for example, which was not measured continuously, may influence the particle size distribution and deposition. Additionally, on a soluble surface, the fixing of particles to a surface may be influenced. Different particle sizes have different magnitudes of adhesion forces which change according to humidity and surface morphology (Corn, 1961). Inclusion of this parameter in future exposure protocols is recommended.

The elevated soiling levels on unprotected surfaces is unexpected. This may potentially be due to a series of individual or combined effects:

- Solar radiation causing thermophoresis and/or electrophoretic effects;
- wetting and drying of surface encourages crystalline growth, enhancing particle capture;
- repeated wetting redistributing particles to the surface fissures where wet removal is less likely leading to gradual surface covering by immovable particles; and,
- surface wetness increases particle deposition velocities through increased adhesive forces or partial particle dissolution, enhancing particle capture and increasing soiling rates.

Perhaps the increased k values at the start of the exposure period as observed by this study and by Pio (CE Contract No STEP-CT90-0097, 1995), is a result of smaller particles depositing and not being removed. Discolouration of the surface may be caused by the entrapment of black particles during the formation of a mineral layer. Particle adhesion builds crusts upwards and produces the fractal shapes observed in the stone surface crusts (see Chapter 5). These structures may effectively enhance soiling through the branching structure which reduce light penetration to the surface and hence reflectance.

A compelling hypothesis of a soiling mechanism for stone involves the dissolution of the

surface which exposes resistant discontinuities such as fossilised shells, which appear more resistant to chemical and physical weathering. These surfaces act as "build up" sites for depositing particles. Hence the more resistant discontinuities present in the stone such as fossils, the more susceptible the stone surface will be to soiling, and potentially crust formation. This effect will therefore be sample specific and may account for slight inter-site differences occurring between stone sample soiling rates. This hypothesis is clearly supported by the photographic evidence of crust morphology provided in Chapter 5. The higher the PEC concentration in the surface layer, the darker the crusts will appear. Also an increase of the surface's contact with moisture through indirect mechanisms such as humidity, condensation and indirect rainfall as surface flow or splash, will increase the ability of impacting particles to adhere to the stone surface. Physico-chemical connections may form between the particle surface and the underlying building surface.

While the main parameters were measured continuously at each site, there are some important parameters which were not measured continuously and must be either estimated or ignored. These include humidity and particle size distribution which may be important factors in the soiling process (Camuffo *et al*, 1982; Haynie and Lemmons, 1990; Creighton *et al*, 1990).

Development of a new regression model using the data generated by this work is restricted by the limited number of sites for comparison. However several meteorological and environmental parameters which may be important in the soiling process have been identified. Local temperature, wind speed, rainfall, black smoke and SO_2 were all found to correlate with k_1 and k_2 values at each site. While no measure of airborne particulate was consistently correlated with soiling rates, PM_{10} and black smoke were associated with the k values of some samples.

Chapter 5

AIRBORNE AND DEPOSITED PARTICULATE MATTER IN LONDON

5.1 INTRODUCTION

Samples of airborne and deposited particulate matter were collected to assess the level of airborne particulate organic material deposited on St Paul's Cathedral. Thirty-nine combustion-associated organic compounds were monitored in airborne particulate matter and samples of black crusts analysed using gas chromatography/mass spectrometry (GCMS).

Total suspended particulate (TSP) samples were collected for one year at two sites in London. Two parallel sampling lines were situated at each of the London sites to provide one sample per week for analysis of individual particulate-associated organic carbon compounds (16 PAH compounds and 23 *n*-alkanes) and another for total organic carbon (TOC) and particulate elemental carbon (PEC) analysis. Details of TOC and PEC measurement techniques can be found in Watt and Kendall (1997).

Samples of black crust were collected from St Paul's Cathedral and Stefansdom Cathedral (Vienna) and analysed for the same 39 organic compounds. Scanning electron microscopy and energy dispersive X-ray (SEM/EDX) was used to study the detailed morphology of the black crust samples and the surface elemental composition.

PM_{10} measurements made locally to the sites were used to infer information about particle size distribution, size-association of organic compounds and the relationship between TSP:PM_{10}. Two sampling periods were used to establish the size distribution of PM_{10} at the St Paul's Cathedral site (Anderson, 1996). The size distribution of PM_{10}-associated organics at a central London site, approximately one mile from St Pauls Cathedral, was assessed for a one month period (Kendall *et al*, 1997). Weekly average PM_{10} measurements from the Advanced Urban Network TEOM site (HMSO, 1997) were used to relate TSP and PM_{10}.

5.2 SAMPLING AND ANALYTICAL METHODOLOGY

5.2.1 Sampling Sites

Two sites were monitored in London (Figure 5.1). The first site was located on the roof of the Middlesex University building at Bounds Green in North London. The site is approximately twenty metres from the intersection of the A406 North Circular and Bounds Green Roads. The sampler was positioned at a height of approximately 35 ft (11 m). The second sampling site was positioned on the roof of St Paul's Cathedral, situated approximately 11.5 km south/south-east of Bounds Green in Central London at a height of approximately 110 ft (35 m). This site was chosen because of the importance of St Paul's as a historic monument and the fact that the building exhibited black deposits on the stone surface which provided a source of black crust samples.

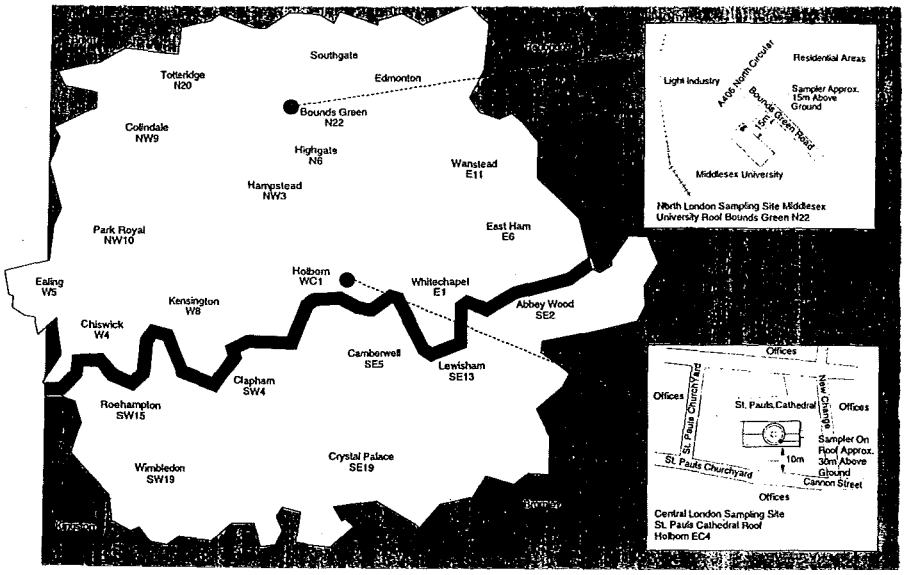

Figure 5.1 The two carbonaceous aerosol monitoring sites in London, UK.

TSP sampling began on a weekly basis at Bounds Green (BG) on 27/6/95 and on 18/7/95 at St Paul's Cathedral (SP). Sampling continued for over one year at both sites and finished at both sites on 7/11/96. Meteorological data for central London (Holborn) was also obtained

from the Meteorological Office to determine average temperature, wind speed and direction, humidity and rainfall during each sampling period.

5.2.2 Sampling Procedure

TSP was collected in London using two low volume sampling lines operating at approximately 4.5 l min^{-1} (0.27 m^3 hr^{-1}), running in parallel. Each line contained a 4.9 l min^{-1} flow limiting orifice, dry gas flow meter and timer. Sampled air was drawn through a filter, supported in the aerosol monitor case. The sampler operated in open mode with the filter facing downwards to protect it from direct rainfall and gravitational impingement of particles. A further protective, downturned funnel covered in opaque, reflective aluminium tape shielded the filter casings from both rain and direct sunlight.

New 37 mm diameter 0.6 μm glass fibre filters (Whatman QM-A quartz filters Cat. No. 1851 037) were annealed at 500°C for 8 hours and stored in a glove-box maintained at constant humidity and temperature. Relative humidity in the chamber was reduced to less than 0.01 % using silica gel and temperature fluctuated by <2 °C during mass measurements. Filters were weighed accurately to five decimal places (dp) of one gram in these conditions. Weighed filters were then sealed in a Millipore aerosol monitor cassette (Cat. No. MAWP 037 AO) and covered in foil ready for transportation.

Samples were collected over one week and the gas flow meter and timer readings were recorded before the filter cassette was removed, sealed and wrapped in aluminium foil. A clean filter and cassette were then attached to the sampling line before the timer was reset and the pump restarted. Flow rates were measured at the face of the filters at the start and end of every sampling period for three months to ensure no irregularities of flow occurred.

The soiled filters and cassettes were placed in the temperature/humidity controlled chamber, where the cassettes were opened and left loosely covered in aluminium foil for 24 hours to condition the filters prior to weighing. The filters were then removed from the cassettes with clean stainless steel tweezers, reweighed and replaced in the sealed cassette. These cassettes were then covered in foil and stored in a freezer at -15°C. One filter from each week was

solvent extracted to measure trace organic components and one filter was analysed for elemental and organic carbon.

PM_{10} samples were collected from a site approximately 1 mile from St Paul's to estimate the distribution of PAH and *n*-alkanes across four fractions of size segregated PM_{10} (Kendall *et al*, 1997). Weekly samples of total PM_{10} were collected during November and December 1996 using an Anderson 1 ACFM cascade impactor (operating at 28 l min^{-1}) which collected particulate matter on Whatman quartz fibre filters. The particles were collected in 10 fractions and combined to give four fractions of particles separated on the basis of mass median aerodynamic diameter (MMAD), namely <1.1, 1.1-3.3, 3.3-5.8 and 5.8-10 μm. Typically each fraction contained 1-5 mg of particulate and these samples underwent solvent extraction as described in Section 5.2.3. Table 5.1 gives a summary of the data collated in this study.

Table 5.1 Summary of the sampling durations of this study.

	Bounds Green (Weeks)	St Paul's (Weeks)	Euston Road* (Weeks)	Bloomsbury+ (Weeks)	Source
TSP	52	52			This study
TOC	35	34			Duarte *et al* in Watt and Kendall, 1997
PEC	35	34			Duarte *et al* in Watt and Kendall, 1997
16 PAH	48	48	4		This study
23 *n*-alkanes	47	47	4		This study
PM_{10}	5#	15#	4	52	Anderson, 1996 HMSO, 1997 Kendall *et al*, 1997

* Camden Council monitoring site (cascade impactor)

\+ Department of Environment Advanced Urban Network site (hourly TEOM measurements)

\# Hourly measurements using a cascade impactor

5.2.3 Sample Solvent Extraction

Table 5.2 gives a summary of the solvents used for the extraction of organic material from the samples collected. Toluene and methanol were chosen as the sequential extraction solvents based on extraction efficiency tests carried out in Portugal (Watt and Kendall, 1997). Extracts were redissolved in dichloromethane (DCM) prior to injection.

Table 5.2 Solvents used in the extraction procedure.

Solvent	Formula	Alternative Name	Molecular Weight
Toluene	$C_6H_5CH_3$	Methyl benzene	92.14
Methanol	CH_3OH	Methyl alcohol	32.04
Dichloromethane (DCM)	CH_2Cl_2	Methylene chloride	84.93

The filter was placed in a 200 ml round bottomed flask. Twenty-five millilitres of toluene was added to the flask which was agitated in a ultrasonic bath for 1 hour at 50°C. After sonification, the toluene was decanted to another round bottomed flask and 25 ml of methanol was added to the filter. An extraction was performed in similar conditions to the toluene extraction. The methanol was decanted and both extractions were repeated.

The toluene extracts of each filter were mixed, filtered through a 0.06 μm QM-A quartz fibre filter (previously conditioned for 500°C for 8 hours) and evaporated to 1-2 ml in a rotary evaporator at 55°C. The samples were allowed to evaporate to dryness in the fume cupboard and redissolved in 15 ml of dichloromethane (DCM).

The methanol extracts of each filter were similarly mixed together with a 10 ml aliquot of the flask containing the filter. This mixture was then filtered and evaporated to 1-2 ml in a rotary evaporator (at 45°C). The samples were evaporated to dryness in the fume cupboard and redissolved in 15 ml of DCM.

The DCM extracts of each filter were mixed and reduced to 1-2 ml in a rotary evaporator at 35°C. This solution was then transferred by pouring to a previously weighed small glass sample tube with subsequent DCM rinsing aliquots (10 ml of DCM in total). The sample tubes were then placed in the fume cupboard to produce a final dry extract. The dry extracts were accurately weighed and stored in a freezer at -15°C until analysis.

5.2.4 Calibration Standards for Organics Analysis

Calibration standards were prepared for 16 PAHs (Supelco PAH Calibration Mix, Catalogue No. 4-7940 - Table 5.3) and 23 *n*-alkanes (C_{10}-C_{34}, Supelco - Table 5.3). Four standards representing concentrations around the expected sample concentration were prepared in DCM

to construct a calibration curve. r^2 values were greater than 0.90 for all *n*-alkanes and $r^2 > 0.81$ for all PAH compounds except dibenzo(a,h)anthracene ($r^2 > 0.49$). r^2 values for the calibrations tended to decrease with increasing molecular weight.

Table 5.3 The sixteen polyaromatic hydrocarbon and twenty-three *n*-alkane compounds analysed for using GCMS.

PAH Compound	Abbreviation
Naphthalene	Naph
Acenaphthylene	Aceny
Acenaphthene	Acen
Fluorene	Fl
Phenanthrene	Phen
Anthracene	Anthr
Pyrene	Pyr
Fluoranthene	Fluor
Chrysene	Chrys
Benzo(a)anthracene	BaA
Benzo(b)fluoranthene	BbF
Benzo(k)fluoranthene	BkF
Benzo(a)pyrene	BaP
Indeno(1,2,3-cd)pyrene	I123P
Benzo(ghi)perylene	BghiP
Dibenzo(a,h)anthracene	DahA

n-Alkane Compound	Formula
Decane	$C_{10}H_{22}$
Undecane	$C_{11}H_{24}$
Dodecane	$C_{12}H_{26}$
Tridecane	$C_{13}H_{28}$
Tetradecane	$C_{14}H_{30}$
Pentadecane	$C_{15}H_{32}$
Hexadecane	$C_{16}H_{34}$
Heptadecane	$C_{17}H_{36}$
Octadecane	$C_{18}H_{38}$
Nonadecane	$C_{19}H_{40}$
Eicosane	$C_{20}H_{42}$
Heneicosane	$C_{21}H_{44}$
Docosane	$C_{22}H_{46}$
Tricosane	$C_{23}H_{48}$
Tetracosane	$C_{24}H_{50}$
Pentacosane	$C_{25}H_{52}$
Hexacosane	$C_{26}H_{54}$
Heptacosane	$C_{27}H_{56}$
Octacosane	$C_{28}H_{58}$
Nonacosane	$C_{29}H_{60}$
Triacontane	$C_{30}H_{62}$
Dotriacontane	$C_{32}H_{66}$
Tetratriacontane	$C_{34}H_{70}$

5.2.5 Quality Assurance

The following quality assurance (QA) procedures were performed. Filters were annealed to reduce the carbon blank associated with new filters. Relative humidity and temperature were strictly controlled during the weighing of filters and extracts, and filters were weighed three times or to a constant weight. Filters were sealed in aerosol cassettes before and after use. Filters were frozen between collection and analysis, and storage time was minimised.

Glassware was cleaned using ultrasonic agitation at 50°C for one hour, followed by soaking in 10% nitric acid and finally rinsing with 10% clean nitric acid and double-distilled water.

Glass-distilled solvents were used for all extractions and standard dilutions. Initially, different solvent blanks were analysed using GCMS for contaminants prior to use and solvents supplied by Rathburn Chemicals, Walkerburn, produced the lowest levels of contamination. These

solvents were adopted for the particulate extractions. Solvent blanks (comprising reduced 75 ml toluene, 75 ml methanol and 45 ml DCM) were analysed to assess background contamination. One procedural blank, consisting of a 37 mm glass fibre filter stored in similar conditions to the filters, was extracted every second extraction to monitor possible contamination. This latter value never exceeded 10% of the sample concentration and was subtracted from parallel and subsequent sample concentrations. Solvent and *n*-alkanes blanks generally produced zero readings; if a response was produced by the blank, the column was reconditioned and an injection introduced. No second injection produced a response.

Lower analytical detection limits were assessed through the analysis of progressively more dilute standards. For compounds which exhibited no zero, even in the blank, lower detection limits were taken to be three times the blank. Table 5.4 shows the detection limits defined by this series of tests which are directly comparable with airborne concentrations.

Table 5.4 Detection limits determined for the sampling and analysis of PAH and *n*-alkane compounds using the sampling protocol. The values are expressed as an airborne concentration (ie detection limits were divided by 45 m^3, the typical weekly total air volume sampled).

PAH Compound	Detection Limit ($pg\ m^{-3}$)
Naphthalene	0.8
Acenaphthylene	3.6
Acenaphthene	0.8
Fluorene	2.9
Phenanthrene	1.1
Anthracene	1.9
Pyrene	1.3
Fluoranthene	0.6
Chrysene	8.7
Benzo(a)anthracene	8.4
Benzo(b)fluoranthene	1.9
Benzo(k)fluoranthene	7.1
Benzo(a)pyrene	3.8
Indeno(1,2,3-cd)pyrene	0.9
Benzo(ghi)perylene	7.5
Dibenzo(a,h)anthracene	0.1

n-Alkane Compound	Detection Limit ($pg\ m^{-3}$)
Decane	<2.2
Undecane	<2.2
Dodecane	<2.2
Tridecane	<2.2
Tetradecane	<0.9
Pentadecane	<0.9
Hexadecane	<0.9
Heptadecane	<0.9
Octadecane	<0.9
Nonadecane	<0.9
Eicosane	<0.9
Heneicosane	<0.9
Docosane	<0.9
Tricosane	<0.9
Tetracosane	<0.9
Pentacosane	<0.9
Hexacosane	<2.2
Heptacosane	<2.2
Octacosane	<2.2
Nonacosane	<2.2
Triacontane	<2.2
Dotriacontane	<2.2
Tetratriacontane	<2.2

Replicate analyses were undertaken over a period of 5 weeks by analysing both filters from the parallel samplers to assess the total error associated with this sampling protocol. The total error may be broken down into sampling, extraction and analytical errors. The values of the second filters were compared to the results of the routine weekly analysis and the ratio calculated. This was carried out over five weeks. Table 5.5 shows the results of these tests and the calculated ratios. Clearly the ratios are high, as would be expected with so many sources of error involved in concentration determination of such small quantities, despite the sensitivity of the analytical technique. However, the samples from each week do agree well to within +/- 20% of the mean concentration.

Table 5.5 Results of PAH analysis of two parallel filters collected from the two sampling sites on randomly chosen weeks.

	ΣPAH Concentration in Filter 1 (ng m^{-3})	ΣPAH Concentration in Filter 2 (ng m^{-3})	Ratio (Filter 1/Filter 2)
Week 1 (BG118/119)	5.11	8.42	1.65
Week 2 (BG120/121)	4.49	6.16	1.37
Week 3 (BG122/123)	5.96	5.69	0.95
Week 4 (SP118/119)	20.11	26.89	1.34
Week 5 (SP122/123)	15.68	22.33	1.42

A standard reference material of urban particulate (SRM149, Laboratory of the Government Chemist) was extracted to assess the extraction efficiency of selected PAHs. Table 5.6 shows the results of these tests. Extraction efficiencies were poorest for the low molecular weight compounds, probably due to the elevated temperatures involved in the solvent extraction technique, as reported in Smith and Harrison (1996). The measured values are all within the 95% confidence levels of the certified values, except fluoranthene, and show that the extraction and analytical procedures were effective in the quantifying of PAH concentrations when large quantities of sample were available.

Table 5.6 Extraction efficiencies of the five certified compounds in standard reference material (SRM) 149 (Laboratory of the Government Chemist).

Certified Compound	Certified Concentration in SRM149 (mg kg^{-1})		Measured Concentration (mg kg^{-1})	Extraction Efficiency (%)
	Mean	95% Confidence Range		
BaA	2.6	2.3 - 2.9	2.4	92.3
BaP	2.9	2.4 - 3.4	3.0	103.4
BghiP	4.5	3.4 - 5.6	4.7	104.4
Fluor	7.1	6.6 - 7.6	6.5	91.5
I123cdP	3.3	2.8 - 3.8	3.7	112.1

Two randomly selected routine samples were analysed five times to assess the reproducibility of analysis for small quantities of ΣPAH. This was carried out because the airborne particulate sample concentrations tended to be low and in some cases close to detection limits. The results show that the analytical accuracy is reduced by the small sample concentration compared to the higher sample mass available for the extraction efficiency tests. The results in Table 5.7 present the coefficient of variation (CoV, calculated as the standard deviation divided by the mean and expressed as a percentage) for the analysis of each compound. CoVs for low concentrations tend to be highest and this reduction in accuracy is associated with the increased standard error with low concentrations.

Table 5.7 PAH concentrations and coefficients of variation (CoV) for two samples.

	Sample 1		Sample 2	
	Concentration (ng m^{-3})	CoV (%)	Concentration (ng m^{-3})	CoV (%)
Naph	0.02	13	0.03	6
Aceny	0.11	21	0.16	30
Acen	0.05	23	0.05	37
Fl	0.20	11	0.23	1
Phen	0.14	6	0.35	2
Anthr	0.15	11	0.21	6
Py	0.28	12	0.61	6
Fluor	0.11	51	0.22	6
Chrys	1.90	15	2.26	17
BaA	1.82	10	2.64	17
BbF	1.25	18	1.50	25
BkF	1.46	18	1.99	17
BaP	1.52	14	1.07	25
I123P	1.55	11	1.59	31
BghiP	5.08	12	0.49	34
DahA	0.03	21	0.03	34
ΣPAH	**15.68**	**15**	**20.11**	**19**

Similar tests were carried out for *n*-alkanes. Table 5.8 shows the results of these tests and

similarly shows that the CoV increases with decreasing concentration.

Table 5.8 Total and individual *n*-alkane concentrations and coefficients of variation (CoV) for multiple analysis of two samples.

	Sample 1		Sample 2	
	Concentration (ng m^{-3})	CoV (%)	Concentration (ng m^{-3})	CoV (%)
C_{10}	0.11	29	0.52	14
C_{11}	0.10	26	0.62	14
C_{12}	0.25	25	0.65	14
C_{13}	0.12	18	0.25	20
C_{14}	0.14	14	0.35	14
C_{15}	0.33	16	0.41	13
C_{16}	0.75	12	0.87	9
C_{17}	2.85	12	1.32	6
C_{18}	4.93	9	1.82	4
C_{19}	5.65	4	1.63	7
C_{20}	11.13	4	10.46	4
C_{21}	13.19	5	11.40	5
C_{22}	12.96	5	15.18	5
C_{23}	16.83	4	15.60	4
C_{24}	22.78	4	19.66	4
C_{25}	29.26	5	37.63	2
C_{26}	34.70	4	19.73	4
C_{27}	24.78	5	13.78	5
C_{28}	21.31	6	11.41	4
C_{29}	16.01	5	10.71	5
C_{30}	12.71	5	7.26	8
C_{32}	3.56	18	1.29	9
C_{34}	0.95	14	0.02	99
Σn-alkane	235.36	1	182.58	1
n-C_{peak}	26	26	25	25
CPI (C_{19}-C_{30})	0.91	4	1.08	1
CPI (C_{23}-C_{30})	0.95	5	1.34	1

5.3 ANALYSIS BY GAS CHROMATOGRAPHY-MASS SPECTROMETRY (GCMS)

5.3.1 GCMS Type and Settings

The GC used was the Fisons GC 8060. A 25 m SGE (Type BPX5) GC capillary column, with an internal diameter of 0.22 mm and a 0.25 μm film was fitted. The MS (Fisons MD 800) was fitted with a Fisons Instruments Organic Analysis MS Data System.

The MS was used in selected ion monitoring (SIM) mode for the analysis of ten molecular weights corresponding to 16 PAHs (Table 5.4 and Appendix 4). Identical GCMS programme conditions were used for analysis of standards and samples to allow quantification of individual

PAH compounds in particulate samples; typical scans of the two standards used can be seen in Figure 5.2.

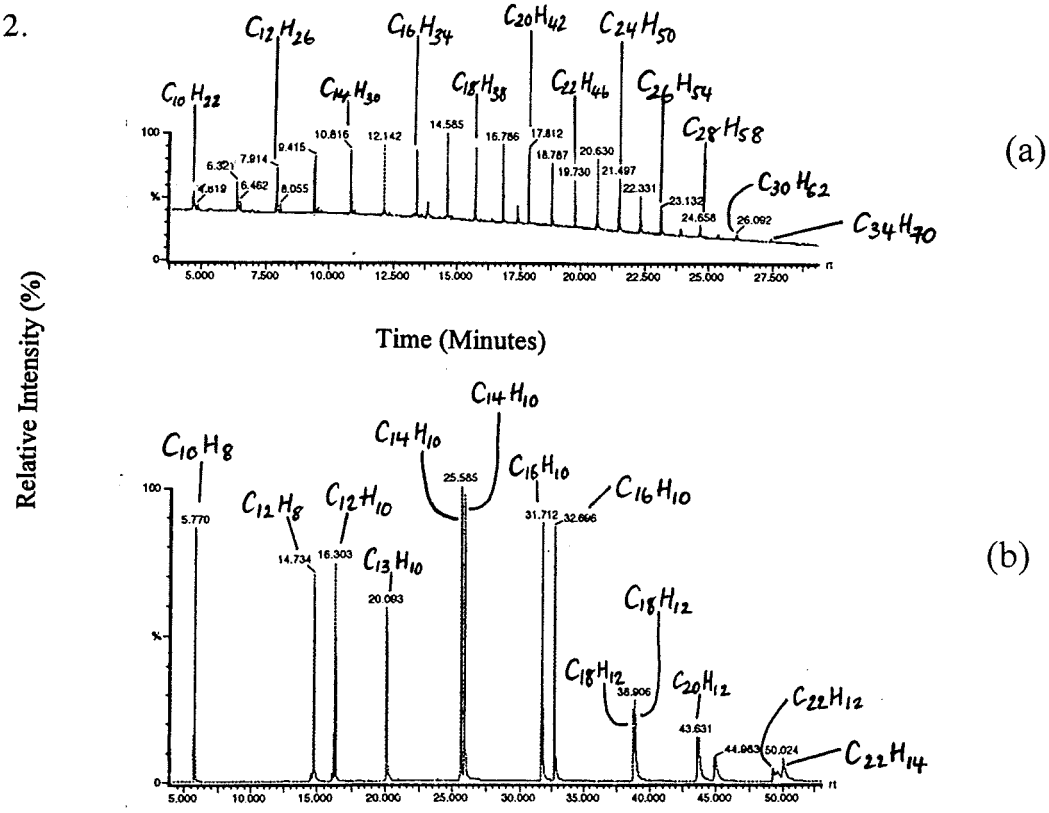

Figure 5.2 Chromatograms of the two standard mixtures used to calibrate the GCMS for the identification of the thirty-nine individual compounds listed in Table 5.3, by retention time and mass/charge ratio; (a) 23 *n*-alkanes (C_{10}-C_{34}, Supelco) and (b) Supelco PAH Calibration Mix (Catalogue No. 4-7940).

All samples were subsequently analysed in scan mode to assess the concentrations of 23 *n*-alkanes (Table 5.3). Concentrations were measured using the mass/ion ratio channel 57, which corresponds to the butyl fragment. The total ion current trace of the GCMS is approximately equivalent to the gas chromatogram. Peaks represent resolvable compounds, while unresolvable compounds contribute to the unresolvable complex hump. Individual ions are located by plotting key fragment ions over their respective GC elution range (ie mass chromatograms), and identified by comparison with a calibration standard. The peaks in the mass chromatograms represent the mass spectrum scans in the area where the various compounds elute. The fragment ion 57 was found to most accurately represent *n*-alkane concentration.

The temperature programmes used can be seen in Table 5.9. The injector was maintained at 270°C to allow flash vaporisation of the injected sample. A final temperature stage of 6 mins at 325°C was introduced to prevent any carry over of samples and standards.

Table 5.9 The GC settings and temperature programmes used for analysis.

	Ramp Time (mins)	Temperature Ramp (°C min^{-1})	Temperature Stage (°C)
n-alkanes	2	-	50
	25	10	300
	1	25	325
PAH	2	-	50
	2	25	100
	50	4	300
	1	25	325

5.3.2 Sample Preparation for GCMS

A clean 100 μl Hamilton syringe was used to add 200 μl of DCM to the dry sample, making sure all of the microbubbles were expelled. The sample vial was then slowly rotated so that all the dry residue was dissolved, while the solution was prevented from leaving a residue anywhere in the bottle or cap. A 5 μl syringe was scrupulously cleaned with DCM. This syringe was then used to take 2 μl of the sample for immediate injection into the GC, which was operating in split mode (split closed for 30 seconds).

5.4 RESULTS OF PARTICULATE MONITORING IN LONDON

Annual average results of 42 monitored airborne concentrations and four weather parameters have been compared. The 52 week sampling year was also broken down into four periods approximating winter 1995/6 (November, December and January), spring 1996 (February, March and April), summer 1996 (May, June and July) and autumn (August, September and October). The average seasonal concentrations and an analysis of the variations exhibited can be found in the following sections.

5.4.1 Particulate Matter Concentrations

The results of TSP measurements can be found in Figure 5.3. Annual mean TSP concentrations at the two sites were very similar at 43 and 46 $\mu g\ m^{-3}$ at Bounds Green and St

Paul's, respectively. This is in broad agreement with other work in other cities such as Birmingham (Smith and Harrison, 1996). Particulate loads at the two London sites can be seen to closely follow each other, with consistently higher concentrations registered at the St Paul's site, except for the Bonfire Night week sample 1995 (Week 1) when particulate levels at the suburban Bounds Green far exceeded those at the heavily urbanised St Paul's site. The data is in good agreement with a national trend described by the UK DoE (HMSO, 1997) where concentrations of TSP and PM_{10} were reported to rise steadily on Bonfire Night at urban areas throughout the country. PM_{10} reached a peak concentration of 222 $\mu g\ m^{-3}$ at the London Bloomsbury site on Bonfire Night 1995. This peak in TSP and PM_{10} (which corresponded with elevated ΣPAH and *n*-alkane concentrations) did not occur the following year, almost certainly indicating the importance of weather conditions in the dispersion of airborne pollutants.

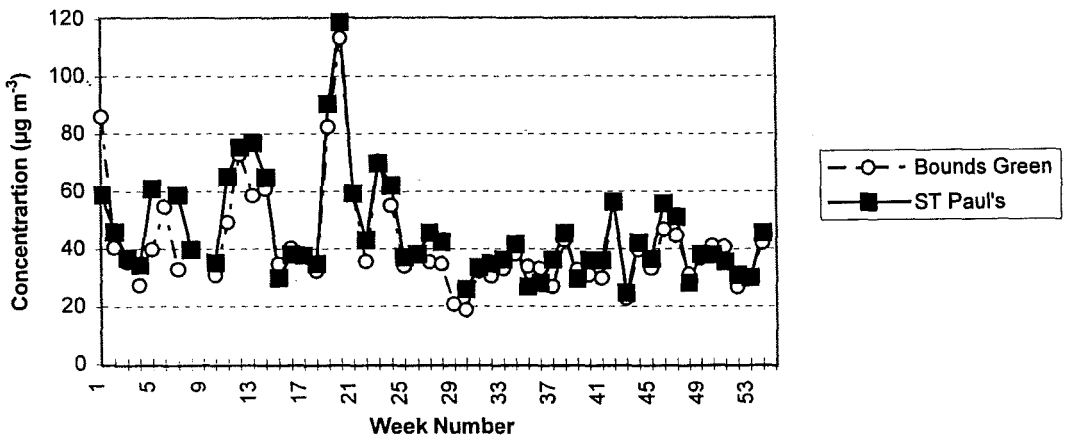

Figure 5.3 Total suspended particulate (TSP) concentrations at two sites in London.

Particulate matter concentrations at both sites correlate well on a weekly basis ($r^2 = 0.81$), with highest average seasonal concentrations in spring, followed by winter, autumn and summer in that order. Table 5.10 shows the seasonal means calculated for winter 1995/6 (November, December and January), spring 1996 (February, March and April), summer 1996 (May, June and July) and autumn (August, September and October).

Table 5.10 Measured TSP concentrations by seasonal and annual mean at both London sites.

	Annual	Winter	Spring	Summer	Autumn	
No of samples	50	11	13	13	13	BG
	50	11	13	13	13	SP
Mean TSP	43	48	53	32	37	BG
($\mu g\ m^{-3}$)	46	54	56	36	39	SP
Min TSP	19	27	32	19	23	BG
($\mu g\ m^{-3}$)	25	35	30	26	25	SP
Max TSP	113	86	113	43	57	BG
($\mu g\ m^{-3}$)	119	77	119	46	56	SP

The size distribution of PM_{10} at both sites was also investigated by Anderson (1996). Samples of PM_{10} were taken with a cascade impactor (PC 1EH, California Instruments) for one week on the roof of St Paul's Cathedral (at 35 m) and a day at the Bounds Green sampling site (15 m). PM_{10} concentrations were measured three times during the day at 11:00, 13:30 and 15:30. A comparison of the samples taken at Bounds Green and St Paul's revealed that the particle size distribution was different at the two sites, with a greater proportion of PM_{10} at Bounds Green comprising larger particles (0.8 μm MMAD particles contributed 25% of PM_{10} mass at Bounds Green). In contrast, during the sampling period at St Paul's Cathedral, approximately 80% (ranging between 78.4 - 92.5%) of PM_{10} consistently comprised particles between 0.1-0.4 μm MMAD. This size range is likely to contribute significantly to the mass of TSP, especially at the St Paul's site, and corresponds with the size distribution generated by vehicles.

Anderson's measurements of PM_{10} at St Paul's were compared with the nearest PM_{10} TEOM from the AUN which is situated at ground level in Bloomsbury Square, 30 m from the roadside. PM_{10} at St Paul's was generally lower than that measured at Bloomsbury for the first four days. However, PM_{10} at 13:30 and 15:30 on the final day of sampling at St Paul's exceeded the Bloomsbury concentrations. This may suggest that the concentrations of particulate-associated organics found at elevated heights may be less than those found at ground level since concentrations of particulate fall with distance from source (Clarke *et al*, 1984). At ground level, concentrations of PM_{10} are typically higher than at elevated heights (Monn *et al*, 1997).

5.4.2 Total Organic Carbon (TOC) and Particulate Elemental Carbon (PEC)

Table 5.11 gives a summary of the total organic carbon (TOC) and particulate elemental carbon (PEC) results collected from the two London Sites and analysed by Professor Duarte *et al* at Aveiro University, Portugal (in Watt and Kendall, 1997). PEC is a good indicator of emissions since it is unaffected directly by volatilisation losses due to temperature fluctuations. TOC is an indicator of particulate-associated organic emissions from both biogenic and anthropogenic sources. The concentrations of both TOC and PEC at the St Paul's site are clearly higher than at the Bounds Green site, in line with TSP concentrations. The minimum TOC and PEC concentrations are similar at both sites perhaps suggesting that there is a constant ambient background concentration to which local sources are additional.

Table 5.11 Total organic (TOC) and particulate elemental carbon (PEC) in TSP in samples collected from the London aerosol (Watt and Kendall, 1997).

	St Paul's		Bounds Green	
	TOC ($\mu g\ m^{-3}$)	PEC ($\mu g\ m^{-3}$)	TOC ($\mu g\ m^{-3}$)	PEC ($\mu g\ m^{-3}$)
No. of Samples	34	34	35	34
Average	8.1	2.7	6.6	2.1
Std Dev	3.7	1.1	2.4	0.7
Max	22.7	7.4	12.2	4.2
Min	2.8	0.5	2.4	0.7
As a % of TSP	17.2	5.9	17.5	5.4

PEC as a percentage of TSP is slightly lower at Bounds Green (range = 1-13%) than at St Paul's (range = 3-11%). TOC however represents a slightly higher proportion of TSP at Bounds Green (range = 7-45%) than at St Paul's (range = 10-29%), perhaps as a result of the lower height of the Bounds Green sampling site or alternatively due to biogenic sources, which would contribute to TOC but not to PEC concentrations. TOC concentrations as a proportion of TSP are certainly more variable at Bounds Green. The seasonal variation indicates that both TOC and PEC peak during winter/spring and are lowest in summer/autumn. Although absolute concentrations of TOC decrease in summer and autumn, the TOC proportion of TSP increases at both sites during this period. The ratio of winter/spring:summer/autumn TOC at Bounds Green is higher than that at St Paul's (0.66 and 0.57, respectively), possibly indicating either an additional source of TOC in winter/spring at St Paul's or an additional source of TOC in summer/autumn at Bounds Green. Proportionally, the reduction in PEC concentrations in summer/autumn from winter/spring is less than the

reduction in TOC concentrations at both sites, indicating a possible volatilisation effect of particulate-associated organics. Concentrations at both sites exhibit similar trends. However, correlation coefficents are low between both sites; regression of TOC at both sites yields an r^2 value of 0.25, while $r^2 = 0.15$ for PEC concentrations over the year at both sites. TOC concentrations may be compared with the work of Lee *et al* (1974) where means of 12.00 μg m^{-3} were reported for London. Mean TOC concentrations of approximately 0.5 μg m^{-3} are typical of remote locations (Simoneit, 1981).

Table 5.12 shows the ratios of PEC to TOC at each site during the four seasonal periods. The ratio is at its highest in summer at St Paul's and in autumn at Bounds Green. The value is lowest in winter at both sites. This apparent seasonal disparity may be due to different sources being important at different times of the year, such as coal burning in winter and biogenic sources in autumn, or may indicate a volatilisation effect caused by increased temperatures during summer/autumn.

Table 5.12 Ratios of PEC:TOC during the four quarterly periods.

	Winter	Spring	Summer	Autumn
Bounds Green	0.28	0.34	0.29	0.36
St Paul's	0.29	0.35	0.37	0.34

These results approximate to previous estimates of PEC and TOC concentrations in urban locations in the UK by COMEAP (1995, and Pio *et al*, 1994). PEC represents a much lower fraction of TSP than reported in COMEAP (2.4-5.4% as opposed to the 10% COMEAP estimate) and TOC represents a close, but higher proportion (17.2-17.5% as opposed to the 15% COMEAP estimate). Estimates of actual concentrations of PEC are close to the levels measured in this study (actual average concentrations of 2.7 and 2.1 μg m^{-3} compared to an estimate of 3 μg m^{-3}), while measured TOC is consistent with the COMEAP estimate of 5 μg m^{-3}, at 8.1 and 6.6 μg m^{-3} at the two sites. The differences in sampling sites must be appreciated when considering this data together with the location of both sites in densely populated London. Rogge *et al* (1993) found similar PEC concentrations in $PM_{2.1}$ at four urban locations in California.

Table 5.13 shows the seasonal mean concentrations of TOC and PEC. The difference in

concentrations between winter and spring, and summer and autumn were small, although taken as two six monthly means the difference was large, with the winter/spring: summer/autumn ratio of TSP, TOC and PEC at Bounds Green all between 66-69%. A similar pattern emerged at St Paul's with an even larger reduction of TOC (down to 55%) during summer/autumn. While different concentrations of TOC were recorded at both sites during winter/spring, identical mean concentrations of TOC (5.5 $\mu g\ m^{-3}$) were recorded for the summer/autumn period. This corresponded to a seasonal difference in climatic conditions, in particular temperature, which was higher by a factor of two during summer/autumn. This indicated that while during cold weather, regional emissions determine TOC concentrations, during summer TOC concentration was more influenced by local temperature. It would also seem to indicate that while some organic species volatilised at increased temperatures, a large proportion of organic material remains incorporated in the particulate material, probably strongly bound to the elemental carbon core.

Table 5.13 Seasonal concentrations of weekly mean TOC and PEC in TSP at the two monitored sites.

	Winter (n=8) ($\mu g\ m^{-3}$)	Spring (n=13) ($\mu g\ m^{-3}$)	Summer (n=11) ($\mu g\ m^{-3}$)	Autumn (n=2) ($\mu g\ m^{-3}$)	
TOC	8.8	7.7	5.6	5.3	BG
	11.3	8.1	6.3	4.7	SP
PEC	2.5	2.6	1.6	1.9	BG
	3.3	2.8	2.3	1.6	SP

5.4.3 Polyaromatic Hydrocarbons (PAH) Concentrations

All sixteen PAHs were identified in all of the filter samples with the exception of the most volatile compounds which are subject to rapid degradation. PAH concentrations were found to be lower than those reported in the literature (Baek *et al*, 1991a and 1991b; Smith *et al*, 1996). There may be a number of reasons for this. Firstly, the heights of the sampling sites used in this study are above average as most PAH studies provide PAH concentrations to assess health implications and are thus closer to ground level. Samples of PM_{10} taken with a cascade impactor show that the peak particle mass concentration is below $PM_{2.5}$ and it is this size range that contributes most to the mass of PM_{10} collected. As reported in Section 5.3.4.1, approximately 80% of PM_{10} mass concentration is attributable to particles between 0.1 and 0.4 μm aerodynamic diameter particles. While these particles are reported to have a high

concentration of PAH attached (Baek *et al*, 1991b), the PM_{10} monitoring showed that the PM_{10} mass concentrations at these heights is lower than ground level concentrations, reducing the particulate-associated organics concentration. Also long-term sampling, even at low flow rates, will result in evaporative losses, particularly at elevated temperatures.

The annual means of the sixteen PAH compounds and the sum of PAH (ΣPAH) for both sites can be seen in Table 5.14. The annual means of the majority of individual PAH compounds and ΣPAH was higher at the St Paul's site (7.24 ng m^{-3}) than Bounds Green (4.27 ng m^{-3}), despite the elevated height at St Paul's. Weekly ΣPAH at both sites is presented in Figure 5.4. Both sites showed the same seasonal pattern of lowest concentration in summer and the highest average concentration during autumn (Table 5.14), but intersite correlations of ΣPAH were poor ($r^2 < 0.10$ at both sites) which does not agree with work carried out at two sites in Birmingham (Smith and Harrison, 1996) where higher correlations ($r^2 = 0.42$) of daily ΣPAH were reported. Since the highest concentrations appear in autumn and winter which have slightly different weather characteristics, emissions associated with these two seasons may be more influential than volatilisation in determining concentration.

Table 5.14 Annual mean concentrations of 16 monitored PAH compounds in TSP at two sites in London during the period November 1995 to October 1996. Bold ratio figures indicate compounds which are at higher concentrations at Bounds Green than St Paul's.

Compound	Bounds Green (n=48) (ng m^{-3})	St Paul's (n=48) (ng m^{-3})	SP/BG Ratio of Annual Averages
Naph	0.03	0.04	1.30
Aceny	0.08	0.13	1.65
Acen	0.05	0.07	1.34
Fl	0.16	0.13	**0.83**
Phen	0.15	0.22	1.44
Anthr	0.09	0.12	1.31
Pyr	0.18	0.26	1.45
Fluor	0.06	0.09	1.49
Chrys	0.65	0.97	1.48
BaA	0.73	1.16	1.60
BbF	0.33	0.63	1.91
BkF	0.36	0.59	1.63
BaP	0.27	0.55	2.07
I123cdP	0.20	0.44	2.28
BghiP	0.93	1.78	1.91
DahA	0.01	0.03	3.23
Σ PAH	4.27	7.24	1.70

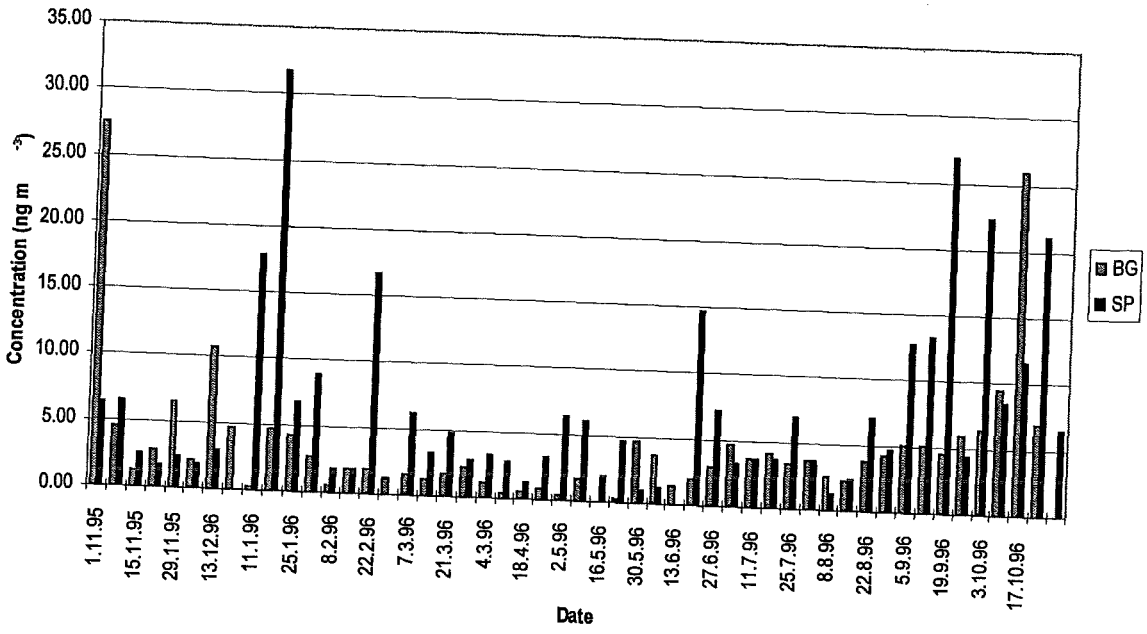

Figure 5.4 Weekly ΣPAH concentrations of sixteen PAH compounds at the two London sites.

At Bounds Green in particular, weekly mean PAH compounds do exhibit slight correlations at the 5% significance level with weekly mean Σ*n*-alkane concentration; at the St Paul's site correlations are much lower. Table 5.15 shows the coefficients of determination for individual PAH compounds and other measured variables at both sites. All of the PAH compounds (excluding naphthalene) are positively correlated with Σ*n*-alkane concentrations at both sites. The majority of PAH compounds are positively correlated with TOC and PEC although r^2 values are low. Again relationships are strongest at the Bounds Green site and slightly higher between individual compounds and PEC. The only PAH compounds associated with PEC at St Pauls were phenanthrene (r^2=0.23), pyrene (r^2=0.21) and fluoranthene (r^2=0.25). Overall then, phenanthrene, fluoranthene and pyrene are the most strongly correlated compounds with other variables measured and while these relationships are weak, they are statistically significant.

Table 5.15 Coefficients of determination (r^2) for individual PAH compounds and other measured variables at 5% significance level. Bold indicates r^2 values >0.20. + indicates a positive correlation and an r^2 <0.10, and - indicates a negative correlation and an r^2 <0.10. r^2 <0.10 are outside the 0.10 significance limits.

PAH Compound	Σ*n*-alkane	TOC	PEC	Site
Naph	-	+	+	SP
	0.28	-	+	BG
Aceny	+	+	+	SP
	+	-	+	BG
Acen	-	-	+	SP
	+	-	+	BG
Fl	-	0.16-	-0.13	SP
	+	-	-	BG
Phen	+	**0.22**	**0.23**	SP
	0.26	0.11	+	BG
Anthr	-	-	-	SP
	+	-	-	BG
Pyr	0.18	0.15	**0.24**	SP
	0.32	+	+	BG
Fluor	**0.23**	0.17	**0.25**	SP
	0.35	-	+	BG
Chrys	0.12	+	0.11	SP
	0.42	0.10-	-	BG
BaA	**0.19**	0.11	0.14	SP
	0.49	+	+	BG
BbF	0.14	+	+	SP
	0.61	-	+	BG
BkF	+	+	+	SP
	0.28	0.10-	-	BG
BaP	0.12	+	+	SP
	0.31	-	-	BG
I123P	0.10	+	+	SP
	0.25	-	-	BG
BghiP	0.13	+	+	SP
	0.42	-	+	BG
DahA	0.10	+	+	SP
	0.49	+	+	BG

Benzo(ghi)perylene was the most abundant PAH at both London sites, followed by benzo(a)anthracene and chrysene, and these three PAH dominate during all four seasons. The highest concentrations of these compounds were measured on the sampling week containing Bonfire Night at Bounds Green and during January at St Paul's. Concentrations of these three compounds contributed over 50% of the ΣPAH. Fluorene was the only PAH more abundant at Bounds Green than St Paul's, possibly because minor temperature differences at the Bounds Green site favoured particulate phase condensation, or higher local emissions. This is comparable with the work of Rocha and Duarte (1997) who used identical methods to assess PAH concentrations in Oporto and found fluorene to have the highest annual mean of all the PAHs measured. The authors put this down to the forest fires prevalent during the sampling

period and this is supported by the work of Simoneit (1981) who identified fluorene as coming from high temperature bush fires.

Rogge *et al* (1993) amongst others have shown similarly elevated winter concentrations of the same 16 PAH compounds over one year in California. Rogge *et al* also showed benzo(ghi)perylene to exhibit the highest monthly concentration (up to 20 ng m^{-3}) of the PAHs measured. Seasonal variation of PAH concentrations at both of the London sites are clear, but not as great as other authors have reported (Aceves and Grimalt,1993, report ΣPAH in urban air as being fourteen times as high in winter than in summer). In London, the winter ΣPAH concentrations are only approximately twice the summer concentrations, possibly reflecting the small number of PAH sources in London, with vehicles dominating PAH production.

The size distribution of PM_{10}-associated organics was also investigated in this study to establish to which particulate size fraction PAH and *n*-alkane compounds were associated (Kendall *et al*, 1997). Figure 5.5 shows the concentrations and distributions of the PAH compounds in four fractions of PM_{10} over a four week sampling programme.

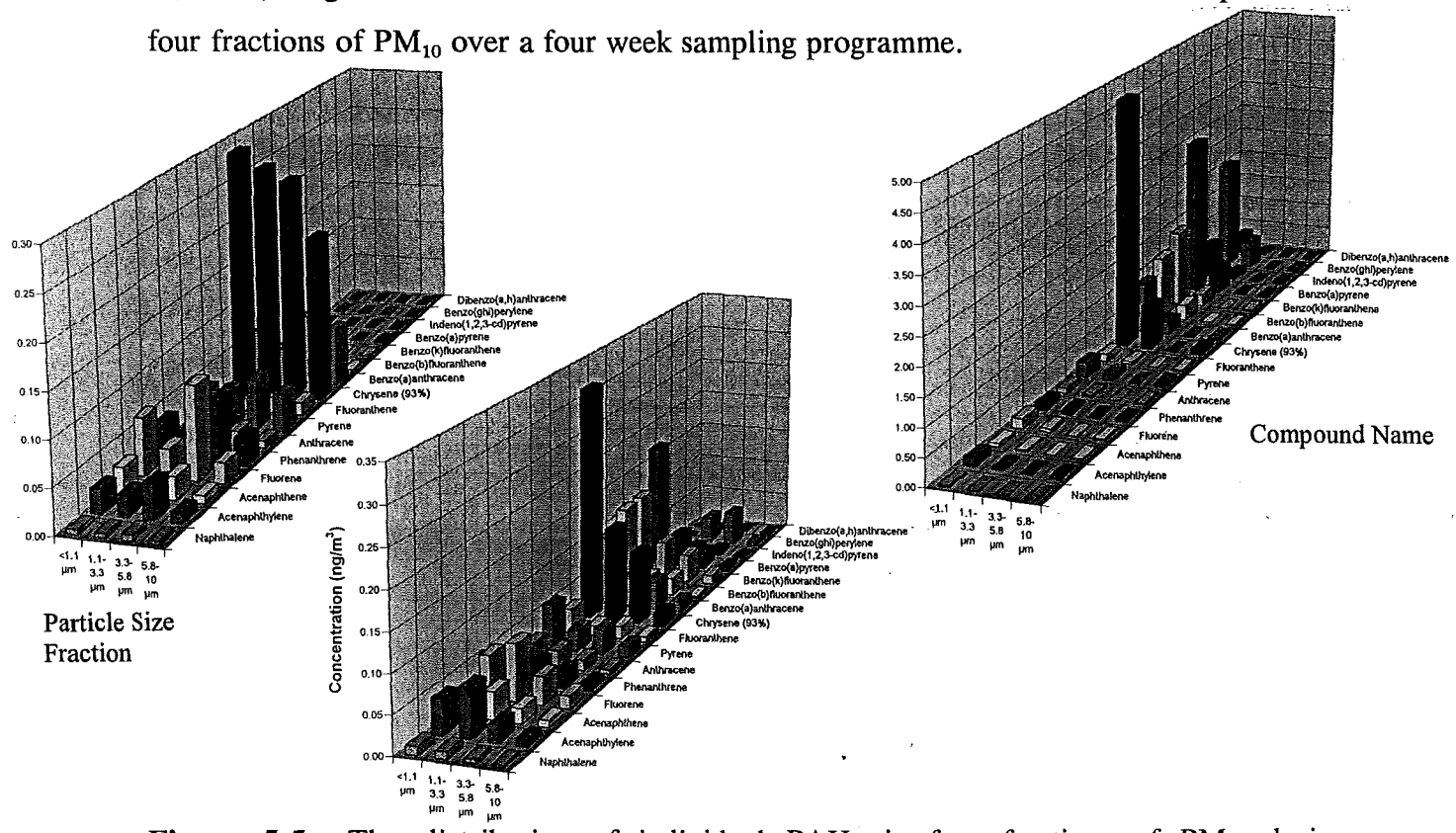

Figure 5.5 The distribution of individual PAHs in four fractions of PM_{10} during November/December 1996 (Kendall *et al*, 1997).

Chrysene is consistently the predominant PAH compound measured in PM_{10}, with benzo(a)pyrene, benzo(ghi)perylene, benzo(b)fluoranthene and benzo(k)fluoranthene all at high concentrations. Benzo(b)fluoranthene was particularly highly correlated with chrysene and represented an average of 28% of the chrysene concentration.

The particulate mass concentration, total particulate mass and extract mass all increased over the four weeks. The extractable proportion (%) of the particulate mass decreased over the four week sampling period, despite decreasing temperatures. The extractable proportion (%) increased with increasing particulate size, although less particulate mass was collected in these fractions and therefore the relative errors associated with analysis increased. The extractable proportion of < 1.1 μm particles remained constant at 40-48% throughout the four monitored weeks. Table 5.16 shows the ΣPAH concentrations during the four weeks.

Table 5.16 ΣPAH concentrations in four particulate fractions of PM_{10} during November/December 1996 (Kendall *et al*, 1997).

	ΣPAH Concentrations Associated With Each Fraction (ng g^{-1})				
	< 1.1 μm	1.1-3.3 μm	3.3-5.8 μm	5.8-10 μm	**Total PM_{10}**
Week 1*	-	-	-	-	-
Week 2	0.21	0.27	0.34	0.11	**0.23**
Week 3	1.63	0.84	-	0.16	**0.81**
Week 4	0.26	1.01	0.55	0.92	**0.60**
Average	**0.70**	**0.70**	**0.45**	**0.40**	**0.55**

* ΣPAH could not be calculated for this week since the high molecular weight PAHs were poorly resolved and therefore not quantified.

5.4.4 *n*-Alkane Concentrations

n-alkanes are useful organic indicator species since they are directly emitted from vehicles, are present in biogenic litter and are relatively unreactive once in the atmosphere. The distribution of these compounds also tends to be characteristic for each source. Seasonal patterns of aerosol concentrations therefore indicate direct emissions of primary anthropogenic and biogenic particles. Table 5.17 shows the annual mean *n*-alkane concentrations of 23 compounds (C_{10}-C_{34}) and Figure 5.6 shows the weekly Σ*n*-alkane concentration at the two monitored sites. The annual mean Σ*n*-alkane concentration is higher at the St Paul's site at 247.6 ng m^{-3} compared to 190.0 ng m^{-3} at Bounds Green, with an intersite ratio (SP/BG) of 1.28, which is lower than that for the annual mean ΣPAH concentration intersite ratio, which is 1.67.

Table 5.17 Annual mean concentrations of 23 monitored *n*-alkane compounds and calculated CPI values for two sites in London during the period November 1995 to October 1996. Bold figures indicate compounds which are at higher concentrations at Bounds Green than St Paul's.

	Bounds Green (n=49) (ng m^{-3})	St Paul's (n=47) (ng m^{-3})	SP/BG Ratio of Annual Average
C_{10}	0.74	0.29	**0.39**
C_{11}	1.78	0.31	**0.17**
C_{12}	0.87	0.54	**0.62**
C_{13}	0.86	0.38	**0.45**
C_{14}	1.26	0.71	**0.56**
C_{15}	1.53	0.98	**0.65**
C_{16}	2.76	1.43	**0.52**
C_{17}	7.82	3.75	**0.48**
C_{18}	5.36	4.70	**0.88**
C_{19}	5.93	6.96	1.17
C_{20}	8.40	12.29	1.46
C_{21}	15.23	15.44	1.01
C_{22}	14.30	17.80	1.24
C_{23}	24.07	18.62	**0.77**
C_{24}	18.54	23.50	1.27
C_{25}	22.84	27.71	1.21
C_{26}	16.21	27.20	1.68
C_{27}	12.06	21.54	1.79
C_{28}	8.04	23.12	2.88
C_{29}	10.26	23.03	2.24
C_{30}	5.59	10.70	1.92
C_{32}	4.74	5.31	1.12
C_{34}	0.85	1.27	1.49
Σn-alkane	190.03	247.57	1.30
n-C_{peak}	25	29	-
CPI (C_{19}-C_{30})	1.28	1.04	**0.81**
CPI (C_{23}-C_{30})	1.46	1.13	**0.78**

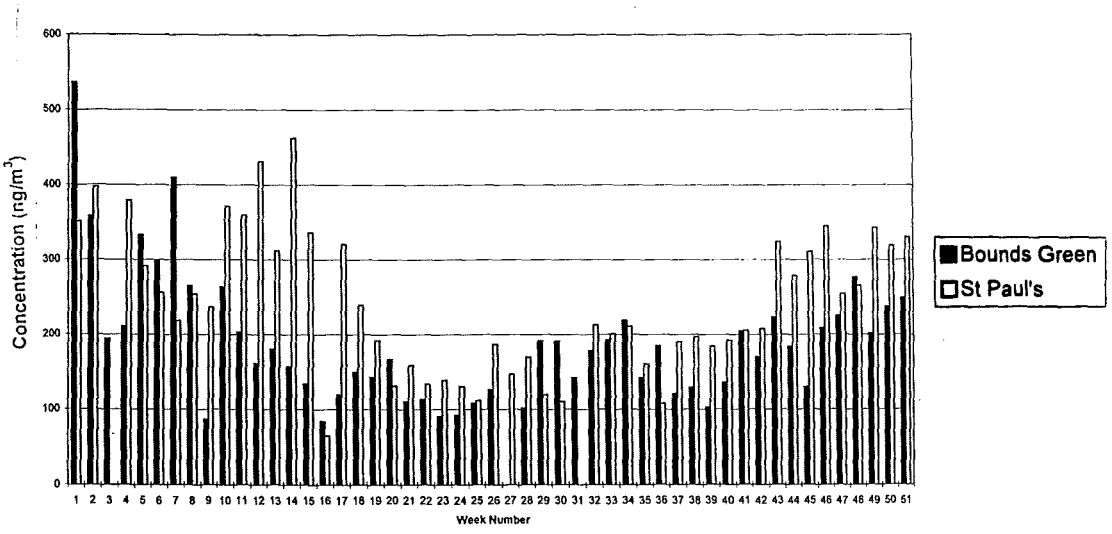

Figure 5.6 Weekly Σn-alkane concentrations of twenty-three compounds at the two London sites.

Table 5.18 shows the seasonal mean concentrations of *n*-alkanes at both sites. Weekly concentrations of *n*-alkanes at St Paul's are generally lowest during summer and highest during winter and spring. In contrast, at the Bounds Green site, odd carbon homologues are lowest during spring with peak seasonal means of n-C_{27}, *n*-C_{28} and *n*-C_{30} occurring in summer. A dominant C_{29} peak in conjunction with low concentrations of adjacent C_{even} alkanes indicates a plant wax signature typical of grass and tree litter (Simoneit, 1984; Saiz-Jimenez, 1993; Fobe *et al*, 1995). The highest seasonal mean concentrations for *n*-C_{29} at Bounds Green occur in spring and summer, and the highest CPI occurs in Autumn. The highest seasonal concentration of a single compound is that for *n*-C_{23} at Bounds Green in winter at 45.3 ng m^{-3}, followed by *n*-C_{26} at St Paul's during winter (38.6 ng m^{-3}).

n-alkanes C_{10}-C_{16} were found in extremely low concentrations. Peak mean concentrations of these compounds consistently occurred in the winter period, probably as a result of lower temperatures and possibly increased emissions, and concentrations of *n*-C_{10}-C_{18} are higher at the Bounds Green site than at St Paul's. Since the difference in concentration is only slightly - but consistently - lower, the difference may be attributable to minor differences in site conditions (eg ambient temperature), sampling conditions (eg flow rates) or local sources. Concentrations of *n*-C_{19}-C_{34} however are all higher at the St Paul's site - except *n*-C_{23} - with *n*-C_{29} at over twice the concentration at St Paul's.

Correlations of individual *n*-alkanes and particulate concentrations showed that at Bounds Green, *n*-C_{11} and *n*-C_{27} exhibited correlations with ΣPAH giving r^2 values of between 0.09 and 0.38. Different correlations were observed at the St Paul's site, with peak r^2 values for *n*-C_{11} (0.26) and *n*-C_{28} (0.15). Correlations were apparent however between individual *n*-alkanes and PEC - *n*-C_{23} to *n*-C_{28} exhibited r^2 values of 0.12-0.20, possibly indicating a diesel source. Similarly correlations exist between *n*-C_{20} to *n*-C_{28} and TOC with r^2 values of between 0.10 and 0.26. (All quoted values above 0.11 are significant at the 5% level).

The distribution of *n*-alkanes in Figure 5.7 shows that the *n*-alkane series is similar at both sites until *n*-C_{25}, where the annual mean concentrations of compounds $>$ *n*-C_{25} reduce with increasing carbon number at Bounds Green. The concentrations at St Paul's remained high,

peaking at n-C_{25} and n-C_{26}, before falling below mean concentrations of 20 $\mu g\ m^{-3}$ at n-C_{30}. The n-C_{peak} at Bounds Green was found to be n-C_{23} and n-C_{25} at St Paul's. The mode of C_{peak} across the year showed n-C_{25} to be the most common C_{peak} at Bounds Green and n-C_{29} to be the dominant peak at St Paul's.

Table 5.18 Seasonal mean concentrations of 23 monitored n-alkane compounds and calculated CPI values for two sites in London during the period November 1995 to October 1996. Bold figures indicate compounds which are at higher concentrations at Bounds Green than St Paul's.

	Winter ($ng\ m^{-3}$)	Spring ($ng\ m^{-3}$)	Summer ($ng\ m^{-3}$)	Autumn ($ng\ m^{-3}$)	
C_{10}	**1.92**	**0.11**	0.30	**0.63**	BG
	0.30	0.10	0.39	0.37	SP
C_{11}	**5.90**	**0.22**	**0.40**	**0.61**	BG
	0.28	0.17	0.36	0.43	SP
C_{12}	**1.99**	0.19	**0.43**	0.87	BG
	0.34	0.26	0.25	1.31	SP
C_{13}	**2.35**	0.16	**0.31**	**0.62**	BG
	0.45	0.27	0.30	0.51	SP
C_{14}	**3.25**	0.18	**0.51**	**1.08**	BG
	1.91	0.26	0.25	0.39	SP
C_{15}	2.35	**0.29**	**0.96**	**2.51**	BG
	2.45	0.23	0.48	0.78	SP
C_{16}	**4.61**	**0.66**	**1.60**	**4.15**	BG
	2.62	0.49	0.84	1.78	SP
C_{17}	**11.49**	**2.46**	**6.85**	**10.49**	BG
	4.74	1.93	2.07	6.26	SP
C_{18}	**8.39**	2.28	5.26	5.49	BG
	7.22	3.90	2.15	5.51	SP
C_{19}	**12.07**	2.10	**4.93**	4.65	BG
	7.86	7.10	2.68	10.20	SP
C_{20}	12.97	8.49	**7.40**	4.73	BG
	15.13	16.99	6.65	10.39	SP
C_{21}	**29.14**	8.58	**10.31**	12.91	BG
	17.50	19.19	7.53	17.55	SP
C_{22}	**27.70**	10.07	**7.76**	11.68	BG
	19.37	19.67	6.96	25.19	SP
C_{23}	**45.26**	10.79	15.55	24.66	BG
	22.08	22.31	9.79	20.30	SP
C_{24}	**31.45**	13.47	12.52	16.73	BG
	27.90	26.01	12.73	27.37	SP
C_{25}	27.73	15.68	20.54	27.43	BG
	32.60	30.77	18.20	29.26	SP
C_{26}	21.58	12.20	15.64	15.43	BG
	38.62	27.33	16.40	26.45	SP
C_{27}	11.31	10.05	13.66	13.20	BG
	30.27	20.24	15.62	20.02	SP
C_{28}	8.29	7.02	9.87	6.98	BG
	35.93	18.44	16.39	21.72	SP
C_{29}	6.08	12.84	12.54	9.57	BG
	24.42	20.66	23.72	23.31	SP
C_{30}	4.88	5.88	6.47	5.11	BG
	18.20	8.51	9.08	7.01	SP
C_{32}	**5.29**	**4.00**	3.62	5.85	BG
	4.61	3.22	6.57	6.83	SP
C_{34}	1.03	0.43	0.65	**1.29**	BG
	2.95	0.62	1.08	0.42	SP
Σn-alkane	287.00	128.35	158.09	186.67	BG
	317.75	248.67	160.50	263.36	SP
n-C_{peak}	23	25	25	25	BG
	26	25	29	24	SP
CPI (C_{19}-C_{30})	1.23	1.05	1.31	1.53	BG
	0.88	1.07	1.15	1.05	SP

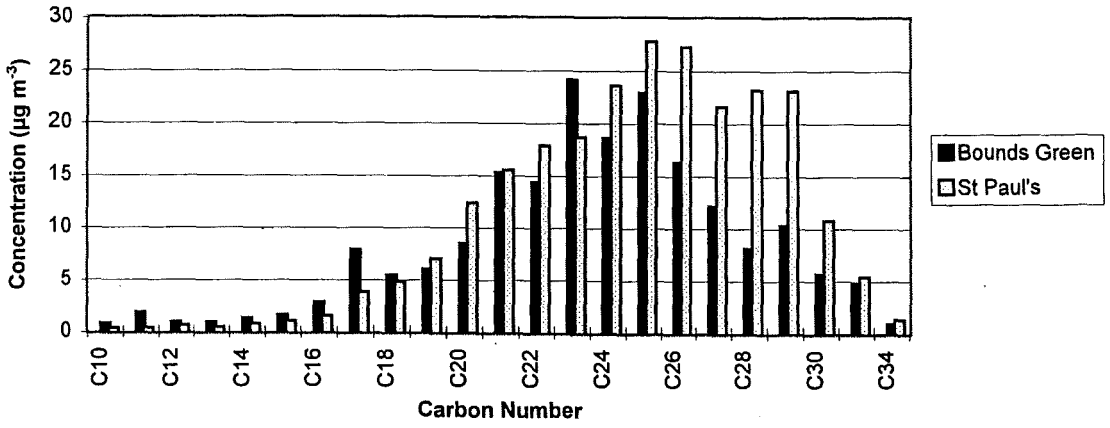

Figure 5.7 The annual average distribution of *n*-alkanes at both sites.

In a comparison of petrol and diesel emissions, Simoneit (1984) detected ten times the amount of *n*-alkanes in diesel exhaust than in petrol exhaust, and this value was increased to fifty times during cold start. The cold start diesel emission sample also exhibited a unresolvable complex mixture (UCM, or napthenic hump) C_{max} of C_{30}. The heavy diesel traffic around St Paul's may therefore account for the elevated concentrations of *n*-alkanes C_{25}-C_{30} at this site. UCMs were much larger at the St Paul's site, especially during winter. UCMs are only apparent in samples contaminated with petrogenic compounds and are not present in the analysis of biogenic aerosol (Simoneit, 1981).

Hauser and Pattison (1972) similarly showed that C_{25}, C_{27} and C_{29} were slightly predominant in urban aerosols. They also showed that the mass median carbon number of $<C_{19}$ in petrol and diesel fuel increased to C_{24} in petrol and diesel exhaust. Simoneit reports a slightly higher C_{peak} for petrol vehicles at C_{22}-C_{23} than for diesel at C_{20}-C_{21}. The mass median *n*-alkane for motor oil was found to be >26 and the overall increase in C number in vehicle emissions was attributed to partial combustion of lubricating oil, the C_{max} of which may vary with source and viscosity. This may therefore account for the difference in quantities of *n*-alkanes $>C_{23}$ at the two sites.

CPIs calculated from the ratio of n-C_{odd} to n-C_{even} of n-C_{19} to n-C_{30} gave values of 1.03 for the St Paul's site and 1.28 for Bounds Green indicating a greater anthropogenic influence at the St Paul's site and a biogenic influence at Bounds Green. Vehicle emissions exhibit a CPI of unity. When CPIs were calculated for n-C_{23} to n-C_{30} to avoid inclusion of a sampling artifact these values were increased to 1.13 and 1.46 for St Paul's and Bounds Green, respectively, which reinforced the evidence for a stronger biogenic influence at Bounds Green than at St Paul's. Using comparisons of these CPI values with those of "clean air" sites (Eichmann *et al*, 1979), it is clear that the CPI values calculated for the Bounds Green site were closer to clean continental air. This is possibly because the Bounds Green site is on a tree lined street and surrounded by small areas of vegetation, whereas the St Paul's site is a central urban location. However there is still an apparent biogenic input to the St Paul's samples indicated by the C_{29} peak and CPI greater than 1.

Seasonal CPIs of n-C_{19} to n-C_{30} showed highest CPIs occurring in summer at St Paul's (1.15) and during autumn at Bounds Green (1.53). Lowest CPIs occurred during winter at St Paul's (0.88) and in spring at Bounds Green (1.05), indicating anthropogenic sources to be more important sources of particulate during winter. This coincides with higher particulate organic and elemental carbon concentrations.

n-alkane concentrations in the size segregated particle samples collected at the Camden Council site on Euston Road, London (Kendall *et al*, 1997) can be seen in Figure 5.8. The low molecular weight compounds ($<n$-C_{16}) are at low concentrations due to higher vapour pressures and have therefore not been presented. Higher concentrations of all the compounds are associated with the lower size fraction which has the highest particulate mass concentration. Peak concentrations of all compounds were again found during the third week of sampling. CPI values (n-C_{19} to n-C_{30}) calculated for each week showed weeks 1 and 4 to have the lowest CPI values (1.01 and 1.02, respectively) and weeks 2 and 3 to have higher CPI's with values of 1.10 and 1.05, respectively. These values are very low (lower than the TSP CPI values) and indicate a petroleum source. In terms of particulate size fractions, CPI values vary about unity, with values of 1.07, 1.14, 1.03 and 0.97 for the respective increasing size fractions. The number of samples is small however and conclusions are difficult to draw.

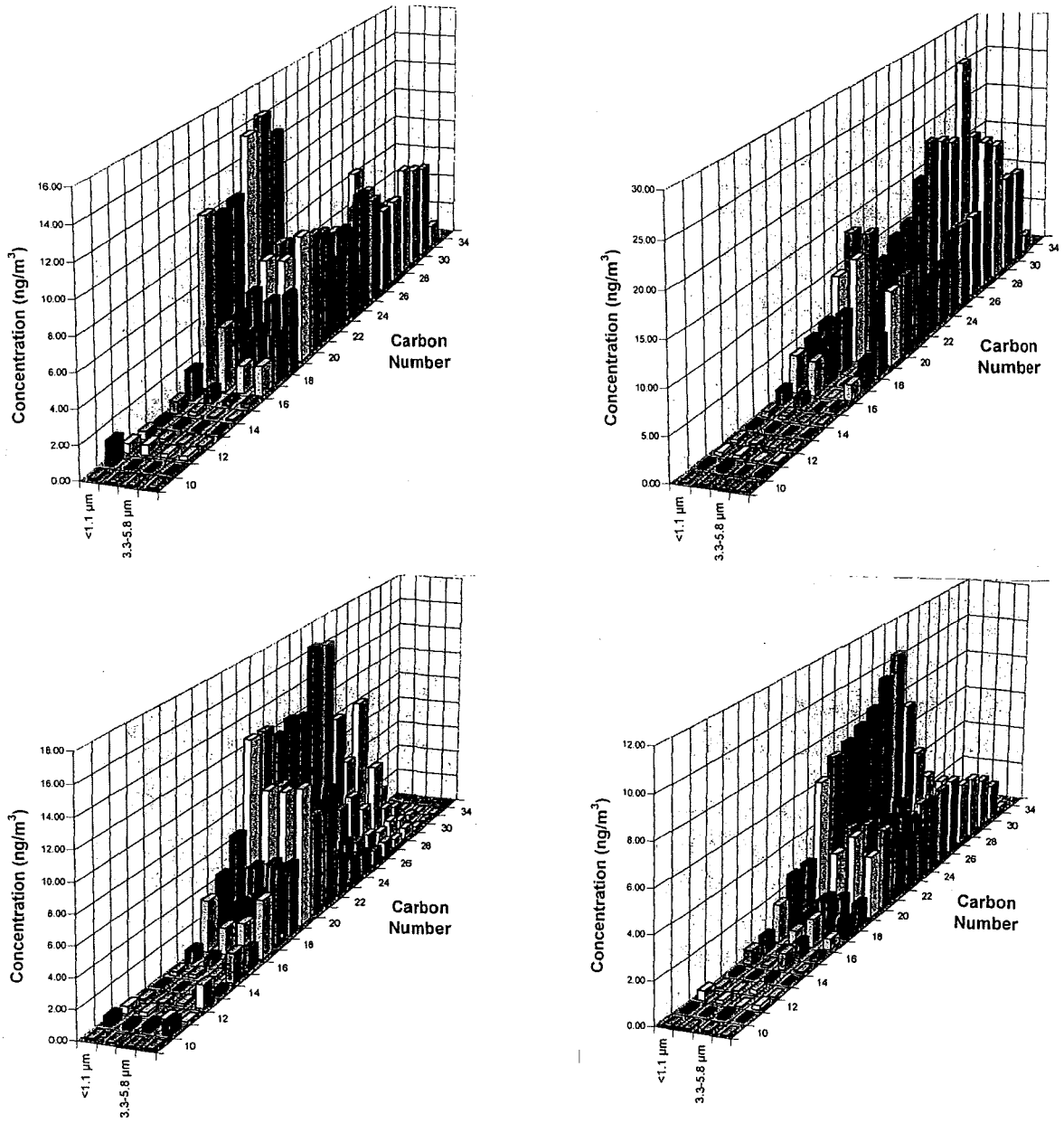

Figure 5.8 *n*-alkane concentrations in size segregated particle samples collected at Euston Road, London (Kendall *et al*, 1997).

Table 5.19 shows the Σn-alkane concentrations in the four fractions of PM_{10}. On average, the highest concentrations are found in the 5.8-10 μm fraction and the lowest in the <1.1 μm fraction. This trend becomes more apparent over the four week sampling period, with Σn-alkane concentrations increasing in the larger sized fractions and decreasing in the lower sized fractions over this period. The average Σn-alkane concentration in these samples of PM_{10} was 116 ng m^{-3}. The concentration of *n*-alkanes per unit mass of PM_{10} (nanograms of *n*-alkanes per gram of particulate matter) was relatively constant over the sampling period ranging between 21.4 ng g^{-1} in week 4 to 32.4 ng g^{-1} in week 2 (Table 5.18). There was however no consistency in the amount or carbon number of *n*-alkanes associated with individual size fractions, which

is comparable to the work of Aceves and Grimalt (1993).

Table 5.19 Concentrations of *n*-alkanes in four size fractions and total PM_{10} per unit mass of particulate matter (Kendall *et al*, 1997).

	Σ*n*-Alkane Concentration						
	< 1.1 μm (ng m^{-3})	1.1-3.3 μm (ng m^{-3})	3.3-5.8 μm (ng m^{-3})	5.8-10 μm (ng m^{-3})	**Total Conc'n (ng m^{-3})**	*n*-Alkanes per PM_{10} Mass (ng g^{-1} PM_{10})	CPI #
Week 1	34.1	21.1	28.9	28.1	**112.1**	28.8	1.0
Week 2	27.5	33.2	37.5	48.5	**146.7**	32.4	1.1
Week 3	12.2	60.1	-	63.3	**135.6***	-	1.1
Week 4	12.4	9.3	27.3	41.7	**90.6**	21.4	1.0
Average	**21.6**	**30.9**	**31.2**	**45.4**	**116.0+**	27.5	-
Average CPI#	1.07	1.14	1.03	0.97	1.05	-	-

* Sum of three fractions only

\+ Average of weeks 1, 2 and 4 only

CPI value is calculated for *n*-C_{19} to *n*-C_{30}

Figure 5.9 shows the distribution of *n*-alkanes in PM_{10} during the four different weeks. The distribution is typical of that for an urban aerosol with peak concentrations at *n*-C_{20}-C_{22}. In week 3 there is an increase in the higher molecular weight *n*-alkanes and C_{peaks} at *n*-C_{28}-C_{29}. There is a very large C_{peak} at *n*-C_{29} in the 1.1-3.3 μm and 5.8-10 μm fractions. This coincides with a peak weekly ΣPAH concentration and possibly indicates a different source contribution. CPI values in Table 5.18 show how the C_{odd} to C_{even} ratio is close to unity indicating an anthropogenic source with perhaps some biogenic influence in the 1.1-3.3 μm fraction of PM_{10}. Twelve of the total sixteen fractions analysed had C_{peaks} at C_{20}-C_{22}.

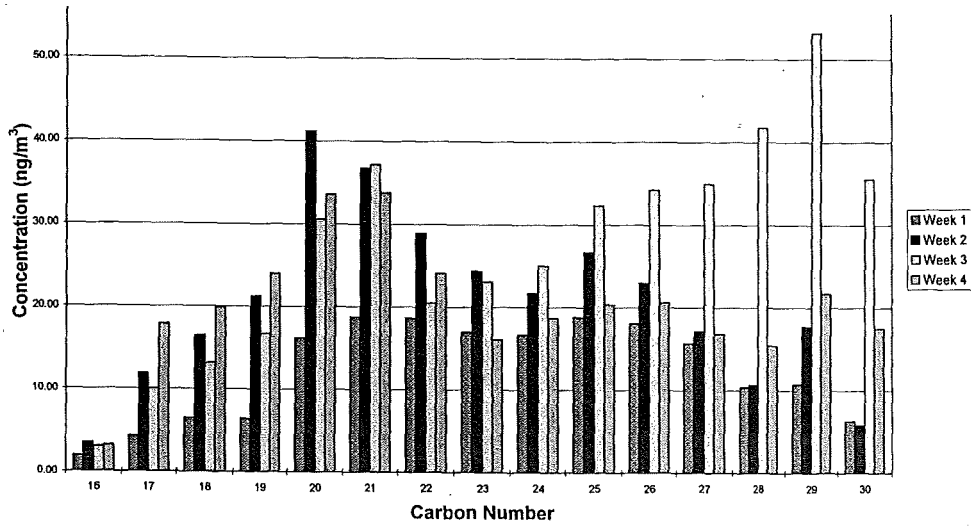

Figure 5.9 The distribution of *n*-alkanes in PM_{10} during the four different weeks (Kendall *et al*, 1997).

The UCM associated with each fraction increased with reducing particle size. The two smallest fractions of PM_{10} had the largest UCM and the UCM: resolved *n*-alkanes ratio was very large, particularly in samples taken in week 3. This is a strong indication of a lubricating oil source (Simoneit, 1981 and 1984). The UCM associated with the St Paul's site sample was always higher than the Bounds Green site sample, and the UCM at both sites increased with increasing *n*-alkane concentration.

5.4.5 Discussion of Airborne Particulate Matter Results

The low molecular weight compounds tend to be at low concentrations in this study. This may be due to the sampling technique used and resultant blow-off at elevated temperatures. However, five and six ring PAH compounds and *n*-alkanes $> n\text{-}C_{20}$ will remain unaffected by temperature variations and therefore may be considered to be accurate representations of ambient concentrations.

The heavier molecular weight PAH compounds tend to be found on the smaller particle sizes since the particles are formed through gas to particle conversion after emission (Stephanou and Stratigakis, 1993). The *n*-alkane compounds were evenly spread across the four size fractions analysed. This lack of association with finer particles may be a reflection of the bi- or trimodal distribution of particulate matter and a function of the size categories analysed and the long averaging period. Higher molecular weight compounds tend to remain in the gas phase before being adsorbed onto existing particles on cooling. Of these compounds, diesel engines contribute more than equivalent petrol vehicles since they emit more particles which contain partially combusted fuel and lubricating oil. Hence diesel vehicles are a primary source of PAH, *n*-alkane and PEC.

The concentrations of *n*-alkanes measured in this study were much higher than concentrations of *n*-alkanes (C_{10}-C_{28}) measured by Eichmann *et al* (1979) at remote locations. Eichmann *et al* reported the mean remote concentration as 7 ng m^{-3}, indicating major contamination by anthropogenic *n*-alkanes at both the sites monitored in this study. They are comparable with studies that monitored urban areas (Aceves and Grimalt, 1993; Stephanou and Stratigakis, 1993; Rogge *et al*, 1993; Rocha and Duarte, 1997), except for the work of Broddin *et al*

(1980), who reported much lower concentrations of *n*-alkanes in a residential area (Ghent). It has been shown that even in a polluted urban atmosphere, the plant wax component may lead to a slight predominance of $C_{25/27/29}$, which has been demonstrated in Los Angeles where samples had peaks at C_{23} and C_{29} (Simoneit, 1984).

Other compounds were also detected qualitatively, but not quantitatively in the particles collected. Phthalates, pristane, phytane, triterpenoidal compounds, and some methyl-PAH were all detected using the MS in single ion monitoring mode. Phthalates are now ubiquitous in the urban environment and often in remote air and water samples. Pristane, phytane and the triterpenoidal compound series are often used as molecular markers for the identification of petroleum emissions (Simoneit, 1984).

Table 5.20 gives a summary of the relationships between monitored variables and the strength of correlations between variables at both sites during the year-long monitoring period.

Table 5.20 A summary of the strength of relationships (r^2 values) between measured variables at each site (BG and SP) and between the two sites. Bold figures indicate $r^2 > 0.40$ and figures in italics indicate that 5% significance levels have been exceeded.

	Relationship Between Sites (BG and SP)	TOC	PEC	Σ*n*-alkanes	ΣPAH	Site
TSP	**0.81**	**0.65**	**0.51**	*0.04*	*0.02*	SP
		0.11	*0.10*	*0.02*	*0.02*	BG
TOC	0.25		**0.68**	0.20	*0.07*	SP
			0.55	*0.01*	*0.01*	BG
PEC	0.15			0.12	*0.11*	SP
				0.01	*0*	BG
Σ*n*-alkanes	0.22				0.14	SP
					0.45	BG
ΣPAH	*0.02*					SP
						BG

Correlations between variables tend to be low and this may be explained by the complexity of the inter-relationships, together with the errors associated with the sampling and analytical techniques. The relationships between sites show that TSP is well correlated at both sites ($r^2 = 0.81$). Other variables are less well correlated; TOC and Σ*n*-alkanes at both sites exhibit low correlations ($r^2 = 0.25$ and 0.22, respectively), at less than 5% significance levels; PEC shows a slightly lower ($r^2 = 0.15$), but similarly significant correlation at the two sites and

ΣPAH shows no inter-site correlation. TOC and PEC were clearly related, and are more closely related at St Paul's. This suggests that there were different sources of TSP at Bounds Green, despite an good overall correlation for TSP concentration at both sites. The latter suggests that it is regional influences such as weather conditions and long range transport which govern particulate mass concentration, but it is local source differences which control the organic composition of particulate matter.

Correlations between variables tend to be better at St Paul's, except for ΣPAH and Σ*n*-alkanes. Correlations between the monitored variables at each site show that TOC and PEC correlate with TSP at St Paul's (r^2 = 0.65 and 0.51, respectively), but not at Bounds Green. TOC and PEC are correlated at both sites (r^2 = 0.68 at St Paul's and 0.55 at Bounds Green). Σ*n*-alkane and ΣPAH concentrations are poorly correlated with other variables. The only statistically significant relationships exist between TOC and PEC and Σ*n*-alkanes at St Paul's (r^2 = 0.20 and 0.12 respectively, at 5% significance levels) and between Σ*n*-alkanes and ΣPAH at Bounds Green (r^2 = 0.45, at 5% significance levels). The relationship that exists between Σ*n*-alkanes and TOC/PEC at St Paul's suggests that either the source of Σ*n*-alkanes and TOC is the same or that weather conditions governing one variable (eg temperature) is also influential over the other variable. The stronger relationship between Σ*n*-alkanes and ΣPAH at Bounds Green than at St Paul's, together with the stronger relationship between PEC and *n*-alkanes, suggests that there are different sources of PAH at St Paul's, which are not associated with *n*-alkane emissions.

Table 5.21 displays the correlations between monitored variables and weather conditions which were measured approximately one mile from the St Paul's site (approximately 5 miles from the Bounds Green site). The strongest inverse relationships exist at St Pauls between PEC and temperature (r^2>0.45), followed by TOC (r^2 >0.38), Σ*n*-alkanes (r^2 = 0.21 and 0.29 for average weekly temperature and maximum temperature, respectively) and TSP (r^2 = 0.22 for average weekly temperature). Positive correlations exist between PEC, TOC and Σ*n*-alkanes and humidity (r^2=0.16, 0.26 and 0.36, respectively at St Paul's and r^2 = 0.10, 0.13 and 0.14, respectively at Bounds Green). Bounds Green values are consistently lower which may be due to the meteorological measurements reflecting the conditions at St Paul's more accurately as

this site is much closer to the meteorological monitoring station. These correlations may not be causal, but may be a result of the increased emissions during periods of cold weather which coincide with high humidities. However, while humidity is unlikely to influence PEC concentrations, it may be postulated that humidity affects adsorption of organics to particles, especially *n*-alkanes. Rainfall also has a very low positive correlation with *n*-alkanes at both sites, and a negative correlation with TSP, PM_{10} and PEC as may be expected. due to wash-out effects. Windspeed has a minor, but a consistently positive correlation with most of the monitored variables.

Table 5.21 Summary of the correlations between measured variables and weather conditions; + indicates a positive correlation and an r^2 value <0.10, - indicates a negative correlation and an r^2 value <0.10. Bold figures indicate $r^2>0.40$. Italic figures indicate that 5% significance levels have been exceeded.

	TSP	PM_{10}	TOC	PEC	Σ*n*-alkanes	ΣPAH	Site
Humidity	+	+	0.26+	0.16+	0.36+	+	SP
	+	+	*0.10*+	0.13+	0.14+	+	BG
Rainfall (mm)	-	-	-	+	+	-	SP
	-	-	-	+	+	+	BG
Rainfall (hrs)	-	-	+	+	+	-	SP
	-	-	+	+	+	+	BG
Average Weekly Temperature	0.22-	-	**0.40-**	**0.47-**	0.21-	-	SP
	0.19-	-	0.32-	0.32-	-	+	BG
Max Temp	0.17-	-	0.38-	**0.45-**	0.29-	-	SP
	0.15-	-	0.37-	0.31-	-	+	BG
Min Temp	0.21-	-	**0.40-**	**0.49-**	0.12-	+	SP
	0.18-	-	0.27-	0.32-	-	+	BG
Windspeed	+	+	+	+	0.12+	+	SP
	+	+	+	+	-	-	BG

Previous authors have consistently tried to associate PAH compounds with particular sources. Hering *et al* (1984) identified benzo(ghi)perylene, indeno(123-cd)perylene, and dibenzo(ah)anthracene as originating from spark ignition engines and benzofluoranthenes as originating from diesel engines. Li and Kamens (1993) found that benzo(a)anthracene was a good indicator of wood smoke, benzo(b)fluoranthene was a good indicator of diesel emissions and benzo(a)pyrene and benzo(ghi)perylene were good indicators of gasoline emissions. However, much variability exists in the concentration of any given PAH from a particular source emission. PAH ratios within a given source are much more stable (Li and Kamens,

1993). The ratios of fluoranthene:fluoranthene plus pyrene and indeno(123-cd)pyrene/indeno(123-cd)pyrene plus benzo(ghi)peylene are therefore used as more accurate indicators. Calculated ratios of the latter compounds indicated a dominant spark ignition vehicular source at both sites, with values ranging between 0.08 in summer at Bounds Green to 0.25 in winter at St Pauls. Ratios were always higher at St Paul's indicating a greater contribution of diesel exhaust PAH. Definitive ratios are 0.18 for petrol fuelled vehicles, 0.33 for diesel exhaust and 0.56 for coal emissions (Sicre *et al*, 1987).

Factor analysis has been used in order to reduce the complexity of the hydrocarbon data set and assist interpretation. Principal components analysis (PCA) was used to reduce the dimensionality of the hydrocarbon data matrices and, through the reduction of data, to identify the recurring and independent modes of variation within the data. These statistically independent modes of variation were sorted into a hierarchy, which explained successively less and less of the variation. The main question relating to the usefulness of such techniques is whether a transformed or derived set of reduced co-ordinates provides a true representation of the underlying relationships between variables allowing reliable interpretation. Many studies have achieved this and PCA has been successfully used in the analysis of air pollution components (eg Thurston and Spengler, 1985, and Smith and Harrison, 1997) and crust analysis (Moropoulou, 1998).

PCA reduces the dimensionality of large data sets by grouping recurring variations numerically into a small number of factors or principal components. Each principal component (PC) has an abstract eigenvalue explaining the importance of each PC in the dataset, a value for the percent of total variation accounted for by the PC and a set of abstract eigenvectors which represent the importance of each variable to each PC. The eigenvalue is the proportion of the variation within the data matrix which is accounted for by each PC. The percentage of the total variation represents the sum of the variance for each standardised variable explained by each PC. The factor loadings or eigenvectors represent both the regression and correlation coefficients between variables and each PC.

PCA was used to analyse the airborne hydrocarbon data matrices. The large datasets generated

in this study are typical of those necessary for PCA (typically more than 50 samples are required). The accuracy of variation source identification using PCA may be reduced in this case however, since the organic source tracers used may not be statistically independent. This may lead to poor discrimination between related sources, such as combustion sources. It was found that the unrotated loading matrix was readily interpretable and the application of varimax rotation did not contribute significantly to the original PCA interpretation.

Four PCs with eigenvalues in excess of 2 were extracted from the Bounds Green dataset. These PCs collectively accounted for 76.4% of the total variation within the dataset and are presented in Table 5.22. The first PC accounted for 42.9% of the variation and contained high eigenvectors (>0.60) for PAHs with four rings or more (ie with molecular weights greater than pyrene) plus naphthalene and phenanthrene. PC1 also contained high factor loadings (>0.60) for the majority of *n*-alkanes <*n*-C_{26} (with the exception of C_{10} and C_{20}). The higher *n*-alkanes were jointly associated with PCs 2,3 and 4, with lower factor loadings for each variable. The PAHs were therefore closely related to each other and to the majority of *n*-alkanes. The close association of phenanthrene despite its lower molecular weight and the co-dominance of chrysene, benzo(a)anthracene and benzo(b)fluoranthene indicated a vehicular source, but differentiation of vehicle fuel types was difficult. The highest *n*-alkane eigenvector associated with this factor was *n*-C_{23} which was in broad agreement with peak *n*-alkane compound emissions from petrol vehicles. A band of *n*-alkanes between *n*-C_{21} to *n*-C_{26} exhibited the highest *n*-alkane eigenvalues (>0.70), together with *n*-C_{11} *n*-C_{16} and *n*-C_{19}.

Five PCs with eigenvalues >2 were extracted from the St Paul's dataset using PCA. The eigenvalues, percent variation accounted for by each PC and the eigenvalue matrix is presented in Table 5.23. Collectively these PCs accounted for 78.1% of the total variation within the dataset. PC1 accounted for 31.4% of the total variation exhibited by the variables. PC1 contained high factor loadings for the higher molecular weight compounds and phenanthrene. *n*-alkanes associated with PC1 (with factor loadings >0.60) were *n*-C_{22}, *n*-C_{24} and *n*-C_{25}. The second PC accounted for 18.9% of the total variation and was negatively associated with all of the PAH compounds, and *n*-C_{10} and *n*-C_{11} , and *n*-alkane compounds >*n*-C_{28} . This separation of *n*-alkanes and PAH compounds into two PCs is difficult to explain, but has been

observed in the work of Rocha and Duarte (1997). These findings may indicate that either the compounds are generated under different conditions or from different sources, or that the compounds originate from the same source but are retained on the particulate surface at different efficiencies.

Table 5.22 The eigenvalues and PCA eigenvector matrix of the four retained principal components extracted from the Bounds Green organics dataset.

	PC 1	PC 2	PC 3	PC 4
Eigenvalue	16.7	5.6	4.2	3.3
Percent of Variation Explained	42.9	14.4	10.7	8.4
Naph	0.63	0.13	-0.16	0.36
Aceny	0.34	0.42	-0.57	0.18
Acen	0.44	0.59	-0.45	-0.12
Fl	0.33	0.44	-0.69	0.20
Phen	0.68	0.21	-0.24	-0.20
Anthr	0.38	0.44	-0.68	0.20
Pyr	0.72	0.17	-0.07	-0.41
Fluor	0.81	0.37	-0.01	-0.07
Chrys	0.86	0.29	0.08	-0.14
BaA	0.89	0.17	0.03	-0.28
BbF	0.93	0.13	0.10	-0.19
BkF	0.78	0.44	-0.12	-0.20
BaP	0.83	0.37	-0.03	-0.25
I123P	0.77	0.43	-0.11	-0.29
BghiP	0.86	0.29	0.04	-0.31
DahA	0.80	0.02	0.22	-0.17
C_{10}	0.20	-0.55	-0.16	0.32
C_{11}	0.75	-0.39	0.27	-0.14
C_{12}	0.63	-0.55	-0.14	0.36
C_{13}	0.62	-0.53	0.03	0.25
C_{14}	0.66	-0.38	-0.03	0.31
C_{15}	0.63	-0.13	-0.39	0.35
C_{16}	0.77	-0.15	0.30	0.37
C_{17}	0.50	0.25	-0.37	0.46
C_{18}	0.61	-0.36	-0.24	0.33
C_{19}	0.72	-0.41	0.11	0.12
C_{20}	0.51	-0.47	0.30	-0.23
C_{21}	0.74	-0.45	0.13	-0.20
C_{22}	0.73	-0.52	0.13	-0.22
C_{23}	0.83	0.40	0.06	-0.14
C_{24}	0.82	-0.39	0.18	-0.16
C_{25}	0.73	0.05	0.11	0.10
C_{26}	0.73	<0.01	0.44	0.13
C_{27}	0.46	0.40	0.50	0.32
C_{28}	0.28	0.33	0.63	0.21
C_{29}	-0.04	0.60	0.62	0.33
C_{30}	0.19	0.53	0.61	0.41
C_{32}	0.38	0.41	0.36	0.49
C_{34}	0.44	0.27	0.27	0.60

Table 5.23 The eigenvalues and PCA eigenvector matrix of the five retained principal components extracted from the St Paul's dataset.

	PC 1	PC 2	PC 3	PC 4	PC5
Eigenvalue	12.3	7.4	4.6	3.5	2.8
Percent of Variation Explained	31.4	18.9	11.9	8.9	7.1
Naph	-0.01	-0.32	0.04	0.61	0.53
Aceny	-0.06	-0.25	0.01	0.54	0.70
Acen	-0.02	-0.21	0.01	0.60	0.72
Fl	0.15	-0.14	0.49	-0.07	0.51
Phen	0.65	-0.30	<0.01	0.25	-0.26
Anthr	0.41	-0.23	0.55	-0.17	0.38
Pyr	0.83	-0.34	-0.05	0.06	-0.14
Fluor	0.86	-0.33	-0.14	<0.01	-0.11
Chrys	0.80	-0.23	0.21	-0.26	0.11
BaA	0.90	-0.32	0.03	-0.05	-0.07
BbF	0.88	-0.37	0.11	-0.05	-0.14
BkF	0.83	-0.29	0.26	-0.25	0.13
BaP	0.85	-0.28	0.20	-0.24	0.06
I123P	0.79	-0.24	0.27	-0.28	0.12
BghiP	0.85	-0.31	0.09	-0.18	0.02
DahA	0.72	-0.39	-0.08	0.18	-0.37
C_{10}	0.52	-0.12	0.43	0.17	-0.11
C_{11}	0.57	-0.23	0.37	0.01	0.03
C_{12}	0.40	0.25	0.31	-0.17	0.34
C_{13}	0.35	0.65	0.57	0.22	<0.01
C_{14}	0.09	0.64	0.45	0.47	-0.28
C_{15}	0.09	0.64	0.49	0.46	-0.27
C_{16}	0.17	0.68	0.55	0.37	-0.18
C_{17}	0.47	0.67	0.51	0.02	0.05
C_{18}	0.39	0.82	0.28	0.21	-0.10
C_{19}	0.38	0.79	<0.01	-0.11	0.10
C_{20}	0.33	0.67	-0.39	-0.04	0.04
C_{21}	0.43	0.67	-0.36	-0.14	0.14
C_{22}	0.61	0.57	-0.26	-0.29	0.25
C_{23}	0.57	0.56	-0.39	-0.19	0.20
C_{24}	0.64	0.53	-0.39	-0.24	0.19
C_{25}	0.64	0.40	-0.56	-0.10	0.07
C_{26}	0.53	0.26	-0.59	0.21	0.01
C_{27}	0.52	0.09	-0.56	0.47	0.14
C_{28}	0.56	-0.06	-0.36	0.58	0.02
C_{29}	0.31	-0.31	-0.15	0.24	0.01
C_{30}	0.46	-0.15	-0.43	0.53	-0.24
C_{32}	-0.07	-.025	0.14	0.18	-0.09
C_{34}	0.54	-0.39	<0.01	0.31	0.41

The concentrations of PAHs in contemporary urban air are much lower than that previously reported (Commins and Hampton, 1976). Particulate concentrations and associated compounds have steadily decreased since the enactment of the Clean Air Acts of 1956 and 1968 (Smith and Harrison, 1996 and McInnes, 1992). Table 5.24 compares the particulate-phase concentration of two compounds monitored sporadically in central London since 1962/3. The

St Bart's Hospital site was a roof top sampler and very close to the St Paul's site used in this study. These results suggest that 1960's concentrations were in excess of ten times present day concentrations. Several events have combined to reduce PAH levels, most importantly the aforementioned Clean Air Acts, the introduction of catalytic converters for vehicle exhaust systems and the trend towards gas central heating and electricity generation.

Table 5.24 Concentrations of two PAH compounds measured sporadically at three central London sites; St Bart's Hospital (Commins and Hampton, 1976), Imperial College (Baek *et al*, 1992) and St Paul's Cathedral (this study).

PAH	St Bart's Hospital 1962/63 (ng m^{-3})	St Bart's Hospital 1972/73 (ng m^{-3})	Imperial College 1985/86 (ng m^{-3})	St Paul's Cathedral 1995/96 (ng m^{-3})
BaP	16	5	1.0	1.16
BghiP	17	7	2.9	1.78

5.5 SAMPLING AND ANALYSIS OF BLACK CRUSTS

5.5.1 Sample Selection, Preparation and Storage

Sampling of black crust material in London was carried out at St Paul's Cathedral at a height of approximately 35 m, although thin layers of deposited particles can be found lower on the building and at the Bounds Green site. Samples were also taken from Vienna's Stefansdom cathedral. Three types of crust were clearly visible; black, branched coral-like structures, projecting from moderately protected vertical stone surfaces; dark grey/black growth with an irregularly pitted surface found attached to protected vertical and inverted horizontal surfaces; and finally, grey precipitate from repeated water flowing over the surface. Black particles were also preferentially deposited onto the surface of fossilised shells projecting from otherwise clean building stone.

Black crust deposits were collected by scraping approximately 5-10 g of gypsum and particulate crustal material (1-2 cm in depth) into sealable glass sample bottles with stainless steel tweezers. While all care was taken to collect only the surface black crust, deterioration of the underlying stone surface caused some unblackened stone to mix with the sample collected. Samples were then covered in foil to prevent photo-degradation and stored at -15 °C. Over thirty representative samples were collected for hydrocarbon analysis. These deposits

were taken from under the balustrade of the roof of St Paul's; the specific sites of collection were recorded. Five samples of black crust were sampled from Stefansdom Cathedral, Vienna. One sample was collected from semi-rural Breitenfurt, Austria.

Fifteen representative samples were also collected for scanning electron microscope (SEM) and energy dispersive X-ray (EDX) analysis. These samples were collected using tweezers to break off small black crust samples which were secured on sellotape in sample boxes to prevent movement or damage during transportation. Due to the nature of the analysis, smaller (2-3 mm) samples were taken together with samples of 1-2 cm depth. Sample boxes were covered with aluminium foil and stored at -15°C. For analysis, samples were attached to aluminium stubs with carbon cement and gold coated.

5.5.2 Organics Analysis

5.5.2.1 Sample Solvent Extraction and GCMS Analysis

Identical extraction and analytical procedures were followed for hydrocarbon speciation analysis of black crusts as for filter samples (see Sections 5.2.3 and 5.2.4).

5.5.2.2 Polyaromatic Hydrocarbons (PAHs) Results

The samples collected were grouped into seven types (figures in brackets give the number of samples in each group): Vienna (4), Balustrade (11), Vertical Wall (3), Fine Crusts (3), Shell (2), Roadside Limestone (2) and Moss (2). The balustrade crust samples were the most commonly found crust type at St Paul's and the other crust types were collected to investigate whether organic components varied with sample position and form. Roadside and shell types were samples of stone and shell respectively, where there was clear evidence of surface blackening. The roadside stone was the only crust type to be sampled at ground level. These samples were collected to identify whether the blackening was due to particle deposition or some other mechanism. The Vienna samples were collected for comparison purposes. Table 5.25 provides a summary of the average concentrations of the organics measured in the various sample type groups.

Table 5.25 Summary of PAH measured in different crustal and blackened stone sample types.

		London Crust Types					
	Vienna	Balustrade	Vertical Wall	Fine Crusts	Roadside Stone	Shells	Moss
	(n=4)	(n=11)	(n=3)	(n=3)	(n=2)	(n=2)	(n=2)
ΣPAH ($\mu g\ g^{-1}$)	24.98	13.29	9.52	9.84	1.72	0.52	8.26
Standard Deviation	24.81	7.47	2.11	2.72	0.22	0.10	7.77
Standard Error	12.40	2.25	1.22	1.46	0.15	0.07	5.49
Dominant PAH	Chrys	Chrys	Chrys	BaA	BaA	BaA	BaP

The Vienna crusts have the highest mean concentration of ΣPAH at 24.98 $\mu g\ g^{-1}$, while the balustrade crusts from London contain less than the Vienna crusts (the mean concentration is 13.29 $\mu g\ g^{-1}$), but more than the means of other London crust types. The mean value of the two moss samples contain PAH concentrations comparable to the means of the fine, vertical and balustrade crusts. The roadside and shell crusts exhibited low total PAH concentrations due to their nature (ie thin black surfacial layers of deposited particles on shell and stone fragments which were inevitably included in the sample weight collected). However, the distribution of PAH in these samples still gave an indication of source and some comparability with the other crust types. Figure 5.10 shows the mean PAH concentration distribution in the different crust and stone types.

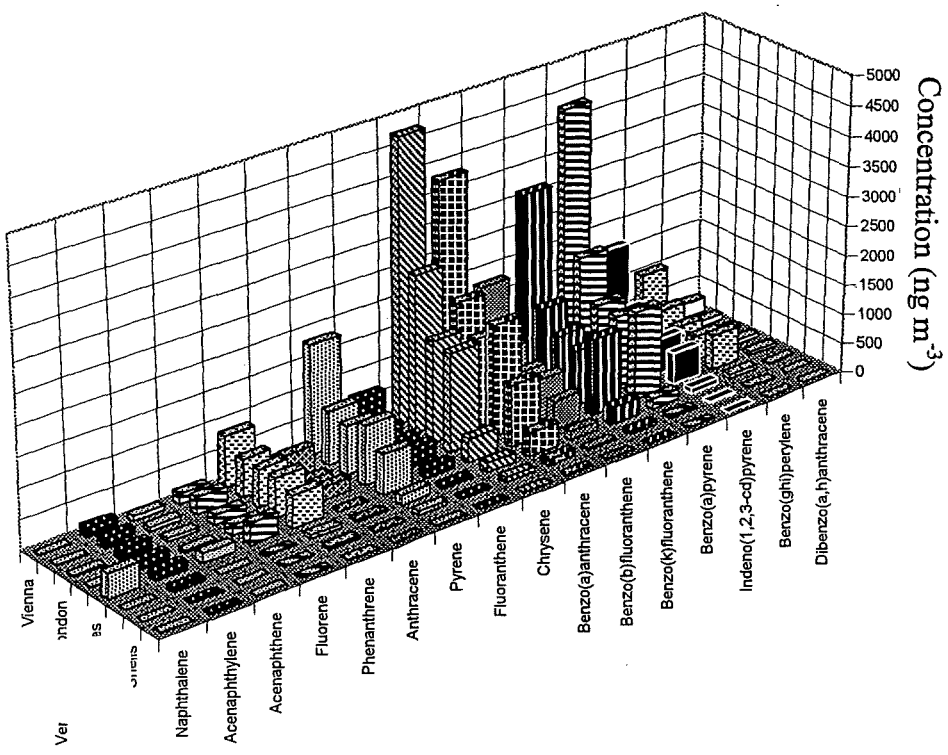

Figure 5.10 The mean PAH distribution in the different crust types.

Chrysene, benzo(a)anthracene, benzo(a)pyrene and benzo(k)fluoranthene dominate the Vienna, balustrade, vertical and fine crusts. Of the total PAH concentration in the crusts, these four compounds contribute between 56-62%, with chrysene the dominant PAH in the Vienna, balustrade and vertical crusts. Pyrene was another large contributor (~10%) to the total PAH in all of the crust types, in particular the shell crusts. Benzo(a)anthracene was the dominant PAH in the fine crusts which was similar to the case of the roadside and shell crusts. In these latter crust types, benzo(a)anthracene was the highest PAH compound, followed by chrysene (14%), pyrene (13%) and benzo(k)fluoranthene (11%) in the shell crusts and benzo(k)fluoranthene (16%), benzo(a)pyrene (10%) and pyrene (10%) in the roadside stone. The mosses contained higher concentrations of the lower molecular weight PAH such as naphthalene (14% of ΣPAH), fluorene (9%) and phenanthrene (12%). Benzo(ghi)perylene which is a major contributor to total PAH in airborne particulate matter only represented a minor fraction (3-4%) of ΣPAH in the crusts analysed and this proportion was consistent throughout all crust types. This is a clear indication that the crusts were certainly not composed of current particulate matter alone and that other historical sources of particulate matter are more important. This might have been expected as these crusts have developed over an indefinite period which probably extends to the earlier part of this century when particulate matter originated from different sources. Low molecular weight PAH compounds were largely absent since they degrade on exposure to sunlight and were largely associated with the vapour phase which exhibit low deposition velocities.

Li and Kamens (1993) identified benzo(a)anthracene as an indicator of diesel emissions and benzo(a)pyrene and benzo(ghi)perylene as indicators of petrol emissions. Benzofluoranthenes have been indicate as diesel exhaust markers (Hering *et al*, 1984; Li and Kamens, 1993). Chrysene was found to be the dominant PAH in the PM_{10} samples analysed, particularly in the finest fraction (Kendall *et al*, 1997). Ratios of indeno(123-cd)pyrene: indeno(123-cd)pyrene plus benzo(ghi)perylene indicate a coal or heating oil source, with values in all crusts ranging between 0.48 for mosses to 0.62 for the Vienna crusts. The source of these particles is likely to have been local combustion sources such as the Bankside oil-fired power station on the south bank of the Thames which operated between 1963 and 1981. Also the previous heating systems employed by the Cathedral itself probably emitted coal and oil generated particles from

chimneys situated on the main roof of the building. This would explain the extensive soiling of the roof balustrade and the Cathedral dome. This practice has now been eliminated. These particles are also likely to originate from neighbouring buildings with similar heating systems, most of which were restricted by the Clean Air Acts.

The correlation matrix in Table 5.26 shows the r^2 describing the relationships between the individual PAH compounds in crusts.

Table 5.26 Coeffients of determination (r^2) for individual PAH compounds in the crusts collected.
Bold figures indicate r^2 values >0.90. Italics indicate r^2 values with $<5\%$ significance level.

	Naph	Aceny	Acen	Fl	Phen	Anthr	Pyr	Fluor	Chrys	BaA	BbF	BkF	BaP	I123P	BghiP	DahA
Naph		*<0.01*	*0.18*	*0.05*	*<0.01*	*0.01*	*0.01*	*0.01*	*0.02*	*0.03*	*0.02*	*0.02*	*0.01*	*0.01*	*0.01*	*0.02*
Aceny			0.17	0.32	0.69	0.16	0.51	0.46	0.47	0.46	0.37	0.41	0.36	0.36	0.42	0.36
Acen				0.18	0.33	0	0.23	0.18	0.07	0.08	0.02	0.06	0.02	0.01	0.04	0.01
Fl					0.11	*0.01*	*0.04*	*0.04*	0.11	*0.07*	*0.04*	*0.03*	*0.07*	*0.03*	*0.04*	*0.03*
Phen						*0.02*	0.81	**0.94**	0.36	0.40	0.20	0.32	0.18	0.38	0.22	0.20
Anthr							*0.02*	*<0.01*	*0.02*	*0.01*	*0.01*	*0.01*	*0.01*	*0.01*	*<0.01*	*0.01*
Pyr								**0.94**	0.51	0.69	0.41	0.61	0.38	0.38	0.41	0.42
Fluor									0.72	0.79	0.54	*0.70*	0.51	0.51	0.53	0.56
Chrys										**0.94**	0.89	0.87	0.85	0.86	0.83	0.89
BaA											0.89	**0.94**	0.85	0.85	0.86	0.87
BbF												**0.93**	**0.98**	**0.99**	**0.96**	**0.99**
BkF													**0.92**	**0.92**	**0.94**	**0.93**
BaP														**0.99**	**0.97**	**0.98**
I123P															**0.97**	**0.99**
BghiP																**0.95**

There are few studies of PAH deposition. Sheu *et al* (1996) studied the dry deposition of all of the PAH measured in this study to horizontal surfaces at an urban and petrochemical industry (PCI) site and concluded that the dry deposition flux was strongly determined by pollutant concentration and that the dry deposition of particles $>10\mu m$ contributed most to deposited PAH due to higher deposition velocities. Dry deposition velocity was found to roughly increase with increasing molecular weight. The higher deposition velocities at the PCI site were attributed to higher windspeed and a higher particulate-PAH MMAD. PAHs with molecular weights greater than acenaphthylene, had more than 94.5% of their dry deposition flux resulting from the particulate phase. This is due to the association of low molecular weight PAHs with the gas phase which deposit by diffusion, not gravity which is a much faster process. Sheu's work indicates that the majority of PAH species are depositing to surfaces through the action of gravity on larger particles, which is in line with the SEM work.

5.5.2.3 *n*-Alkanes

Table 5.27 gives a summary of Σn-alkane concentrations and calculated CPI values for the different crust types.

Table 5.27 Σn-alkanes concentrations and calculated CPI values for the different crust types.

		London Crust Types					
	Vienna	Balustrade	Vertical Wall	Fine Crusts	Roadside Stone	Shells	Moss
	(n=4)	(n=11)	(n=3)	(n=3)	(n=2)	(n=2)	(n=2)
Σn-Alkanes ($\mu g\ g^{-1}$)	21.44	43.74	55.60	72.88	8.02	17.59	129.62
Standard Deviation	17.78	16.34	24.24	45.07	0.69	6.21	57.23
Standard Error	8.89	4.93	14.00	26.02	0.49	4.39	40.47
C_{peak}	28/29	28/29	29	20/29	21	29	29
CPI (n-C_{19}-C_{30})	1.06	1.03	1.36	1.22	1.32	1.39	1.40
CPI (n-C_{19}-C_{30})	1.11	1.08	1.51	1.45	1.48	1.52	1.45

Figure 5.11 shows the distribution of *n*-alkanes measured in the crusts.

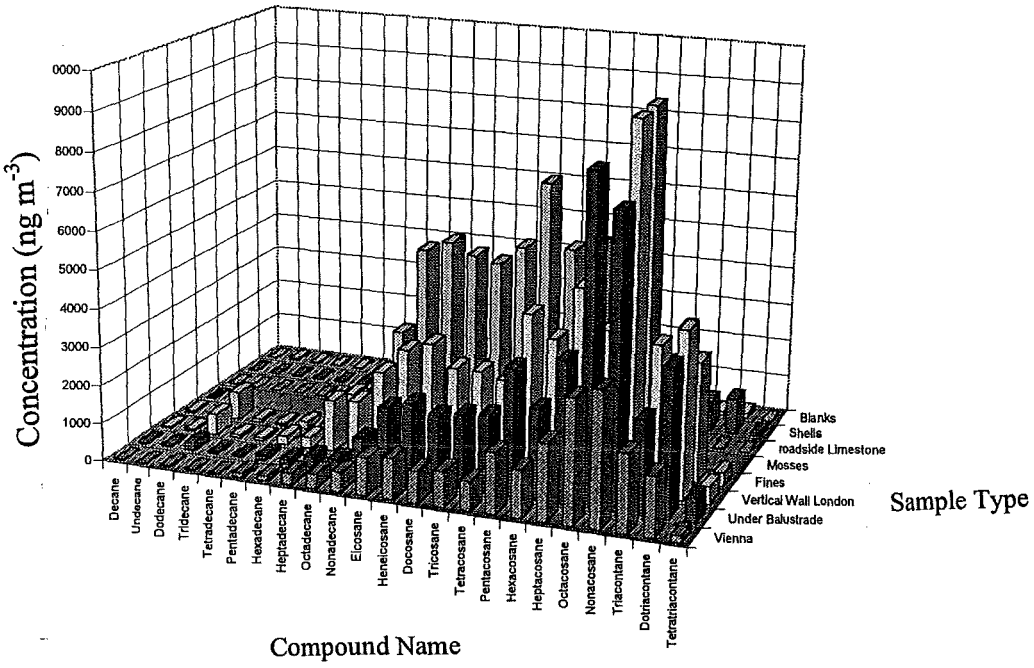

Figure 5.11 The distribution of *n*-alkanes for the mean concentrations of each crust type.

n-alkanes measured in the crusts show the distribution pattern characteristic of a vehicular source, with C_{max} at *n*-C_{21} (typical of vehicular exhaust, Simoneit 1984) and *n*-C_{29} (indicating a biogenic source, Simoneit 1984). The total ion current (TIC) trace of the GCMS showed the distinctive pattern described by Simoneit (1985) and Cox *et al* (1982), and observed in the TSP and PM_{10} samples, especially the < 1.1 μm size fraction. A bimodal distribution of *n*-alkanes is apparent together with a large unresolved complex hump typical of naphthenic (cyclic) hydrocarbons ranging from C_{12}-C_{35} which exhibit retention time maxima around C_{22} and C_{26}. Plant waxes do not exhibit this hump (Simoneit, 1985) and the source is certainly anthropogenic. High concentrations of *n*-C_{25} are also apparent in all crust types and may indicate the secondary C_{peak} due to the lubricating oil component of vehicular emissions or a biogenic contribution. This corresponds with the C_{peaks} determined in the airborne particulate matter at the St Paul's site.

The UK crust total ion current traces showed massive UCMs and high UCM: resolved compound ratios. The crusts are clearly very complex in composition and this has been explored qualitatively by others (Saiz-Jimenez, 1993). Pristane, phytane, phthalates and triterpanes were all detected using the MS SIM mode. These compounds are important indicators of petroleum sources and confirm the presence of vehicle exhaust particles. Methylated PAHs were also detected in the UK balustrade crusts.

The calculated average CPIs indicate a biogenic influence, particularly for the less common crust types such as the vertical, fine, roadside and shell crusts. Average CPI values were calculated by averaging individual *n*-alkane concentrations for each crust type and then dividing the $n\text{-}C_{odd}$ by $n\text{-}C_{even}$ within a specified range. The calculated CPI ($n\text{-}C_{23}$ to $n\text{-}C_{30}$) for the Vienna and Balustrade samples are close to unity and are of similar magnitude (1.11 and 1.08, respectively), indicating a vehicular source. The other sample types share similar CPI values which are significantly different from the Vienna and Balustrade crusts, ranging between 1.45 and 1.52. The most likely explanation of this difference in CPI value is the presence of biological particles or growth within the crusts exhibiting higher CPI values, especially since the average moss CPI value closely matches that of the group. Similar CPI values (for $n\text{-}C_{13}$ to C_{35}) were reported by Saiz-Jimenez (1993) for crusts originating in Dublin (CPI = 1.3). The C_{max} ($n\text{-}C_{29}$) for crusts from Dublin and Mechelen in the Saiz-Jimenez study likewise agreed with the findings of this study. Other crusts from Seville which were close to a heavily trafficked bus station exhibited a $n\text{-}C_{max}$ at $n\text{-}C_{21}$ which agrees well with the two samples of road-side crusts which were collected at ground-level. This C_{max} is close to that of diesel ($n\text{-}C_{21}$) and petrol ($n\text{-}C_{22}$) as determined by Simoneit (1985) and indicates that these lower crusts may be more heavily influenced by traffic emissions. The fine crusts also exhibit a large $n\text{-}C_{20}$ peak, and the *n*-alkane component may similarly be attributable to vehicular pollution.

The crust C_{peaks} at $n\text{-}C_{29}$ also correspond with that of the mosses collected from similar sampling areas. Although no evidence of biological growth on the crusts was detected either on site or using the SEM, it is clearly likely that the mosses are contributing to the $n\text{-}C_{29}$ content of the black crusts, through either spore release followed by entrapment in the crust,

or growth below the surface. The hypothesis of spore release would also provide an explanation in part to the n-C_{29} peak in the airborne particulate matter collected at St Paul's. In higher plants, elongation of palmitic acid C_{16} by the addition of C_2 units produces long-chained fatty acids. Decarboxylation of the fatty acids leads to the formation of odd numbered n-alkanes in the range C_{23}-C_{33} (Eglington *et al*, 1962) which are dominant in rural and some urban samples (Hauser and Pattison, 1972; Simoneit and Mazurek, 1983). n-C_{29} and n-C_{31} are the dominant homologues and may contribute upto 90% of all paraffins found in plant epicuticular waxes (Kolattukudy, 1970). These compounds are found in leaf surface blooms and may be dislodged during high wind conditions. Clearly there is an additional source of n-C_{24}-C_{30} in the aerosol at the St Paul's site as opposed to Bounds Green and considering the site, this is unlikely to be due to a biogenic input. It is more likely that there is a greater anthropogenic input of these compounds at this site, possibly due to the greater number of diesel vehicles at the St Paul's site.

In terms of mass concentrations, the roadside and shell crusts exhibit the lowest concentrations of total n-alkanes at 8.02 and 17.59 $\mu g\ g^{-1}$, respectively. This is to be expected since the majority of the sample comprised stone with only a thin blackened surface layer. The mosses have the highest concentrations of total n-alkanes as anticipated, followed by the fine, vertical and balustrade crusts. The Vienna crusts have relatively low n-alkane concentrations in comparison to the PAH concentrations, as do the balustrade crusts. This indicates - together with the different CPI values and n-C_{peaks} - that the sources of the particulate matter associated with these types of crusts is significantly different in organic content to that contained in the other crust types, and either originated from a different source or has experienced significantly more weathering. The ratios of I123P: I123P plus BghiP indicate a definite coal source for all crust types. As explained in the previous section, this source is likely to be a historical source dating from before the Clean Air Acts.

5.5.3 Metals Analysis

5.5.3.1 Sample Digestion and Analysis by ICP-AES and GFAAS

Six 0.5-1 g samples of black crust collected at St Paul's Cathedral were ground carefully and passed through a 125 μm sieve. One sample of moss was collected from a vertical surface of

the Cathedral for comparison; no preparation of this sample was carried out and concentrations represent metal concentrations in the moss as collected. These samples were accurately weighed (to 4 dp) and digested in 25 ml nitric acid before overnight evaporation to dryness on a sandbath. The residue was then redissolved in 100 ml of 1% nitric acid and filtered through annealed 0.6 μm glass fibre filters. Samples were transferred to plastic bottles and stored in the dark at 4 °C before analysis.

Crust samples were analysed in triplicate for 10 metals using inductively coupled plasma-atomic emission spectrometry (ICP-AES; Perkin Elmer Model Plasm 40 Instrument) for all of the metals. On the basis of these initial analyses which revealed low, but detectable levels of platinum, a further set of digestions were carried out using Aqua Regia (1% hydrochloric acid/99% nitric acid) to extract and analyse specifically for platinum. 9 crust samples and 1 blank stone sample - all prepared as above - were analysed using graphite furnace atomic absorbtion spectrometry (GFAAS; Perkin Elmer, Zeeman AAS Model 4110 ZL) to determine crust and stone background concentrations, in order to estimate crust platinum enrichment. This method follows the recommendations of Barefoot (1997) who reviewed possible methods of platinum extraction and analysis. The blank stone sample was taken from the centre of an original stone structure at a depth of >3 cm to represent the platinum concentration of the original limestone used in the construction of the cathedral.

Calibration of the ICP-AES was achieved using a 1 ppm standard for all nine metals and three appropriate platinum standards (25, 75 and 150 μl/l) for the GFAAS. The ICP-AES instrument parameters used and detection limits may be found elsewhere (Vincent, 1993). GFAAS instrument parameters can be found in Table 5.28. Sample concentrations were well above instrument detection limits.

Table 5.28 Graphite furnace settings and detection limits for platinum analysis.

Metal	Wavelength (nm)	Detection Limit ($\mu g\ l^{-1}$)	Pretreatment Temperature (°C)	Atomisation Temperature (°C)
Pt	265.9	0.5	1300	2200

5.5.3.2 Results of Metals Analysis

Table 5.29 shows the results of metal analysis by ICP and Table 5.31 shows the results of platinum analysis. Two procedural blanks showed that no contamination occurred during the extraction, and detected metals in these blanks were below the respective detection limits.

Table 5.29 Metal concentrations in single black crust samples from London and Vienna. One moss sample was collected in London and analysed for comparison purposes.

Crust		London Crusts				
Metal	Vienna Crusts	Balustrade	Balustrade	Vertical Wall	Balustrade	Moss
		Concentration ($\mu g\ g^{-1}$)				
Aluminium	1193	1742	582	497	972	5582
Magnesium	670	2214	347	175	277	3872
Iron	5477	4075	2748	341	4551	12763
Cadmium	9	5	6	14	10	8
Zinc	214	171	86	59	70	1718
Lead	468	144	233	324	380	3564
Nickel	104	46	27	27	77	45
Copper	200	38	108	138	106	851
Calcium	258	167	209	650	520	553

There is significant variation in the stone metal concentration even in samples taken from the same area which may reflect a sampling artifact where underlying stone was collected together with the black crust material. However there are strong relationships between the relative concentrations of metals in the crusts. The vertical crust was distinctly different from the other crusts. Correlation matrices comparing the composition of the different crust samples showed that while metal concentrations in all other crusts were well correlated ($r^2 > 0.74$), those in the vertical crust were poorly correlated ($r^2 < 0.14$) with all other crust types. Correlations of individual metals showed strong relationships between platinum, cadmium and calcium ($r^2 > 0.76$), lead and copper ($r^2 = 0.79$) and nickel and iron ($r^2 = 0.69$) and aluminium and magnesium ($r^2 = 0.81$). All quoted r^2 values are within 90% confidence limits.

Iron concentrations were consistently found to be highest in the L(h) and the V(v) samples -not in L(v) - at between 2.7-5.4 mg g^{-1} of crustal material. Aluminium and magnesium were the next highest metals ranging between 0.6-1.7 mg g^{-1} and 0.2-2.2 mg g^{-1} respectively. This was true for all crusts except in the vertical crust from London, where calcium dominated. This

may have been due to a sampling artifact such as stone contamination despite steps to prevent this. Fe, Mg and Al concentrations in this sample were considerably lower than those found in the other crust types. Concentrations of Al, Mg, Fe, Zn, Cu and Pb were considerably higher in the moss sample than in the crustal material, in the case of Pb and Zn by an order of magnitude.

There are two likely sources of these metals; deposition of airborne metals to the stone surface and leaching of metal-rich minerals to the stone surface. According to Inkpen (1997), heavy metal concentrations are below noise levels of AAS analysis in Whit Bed Portland stone. Table 5.30 shows the concentrations of 6 metals of interest in London during 1983/84 and 1991. Fe is clearly the metal with the highest concentration, followed by Pb and Zn. Both Pb and Cd have been used as indicators of traffic pollution since their main source in urban areas is vehicles.

Table 5.30 Average airborne concentrations of selected metals in London.

Year and Reference	Fe ($ng\ m^{-3}$)	Pb ($ng\ m^{-3}$)	Zn ($ng\ m^{-3}$)	Cu ($ng\ m^{-3}$)	Ni ($ng\ m^{-3}$)	Cd ($ng\ m^{-3}$)
1983/84 Carroll and Innes (1988)	800	414	94	22	8.6	<2.4
1991 DoE (1993)	1687	120	139	28	9	1.3

Table 5.31 shows the mean Pt concentrations determined in the ten samples analysed in triplicate using GFAAS. The first sample represents a sample of original uncontaminated stone which was extracted, and was found to be below detectable levels. Blank samples were injected between all samples to avoid contamination. In contrast, the concentrations found in the crust extracts ranged between 1.9-12.7 $\mu g\ g^{-1}$, with CoDs below 8%. Samples 2-8 were bulbous black crust taken from the same sampling area, below the balustrade ledge on the roof. Samples 2-4 (which were identically prepared fractions of the same black crust sample) exhibit Pt concentration variations of less than 1 $\mu g\ g^{-1}$, as do identical samples 5 and 6. The range of Pt concentrations in these samples is 1.9-4.0 $\mu g\ g^{-1}$. However, samples 9 and 10, which were samples of the "fine" black crust, show higher concentrations of Pt, over twice that of the other "bulbous" crust type. If it is accepted that the source of the Pt is airborne particulate matter, this increased concentration may be due to the higher surface area to volume ratio of

these fine crusts, which would result in higher deposition to these crusts relative to overall mass. Alternatively this may be due to the fact that the fine crusts are more recent and the bulk of the bulbous crusts will have little Pt since vehicular Pt emissions are relatively recent.

Table 5.31 Platinum concentrations in 9 samples of London black crust taken from vertical (v) and horizontal (h) surfaces and 1 sample of uncontaminated portland limestone.

Sample	Concentration ($\mu g\ g^{-1}$)	Crust Source Type
1 (Blank)	*ND	Uncontaminated stone
2 (h)	4.0	Balustrade
3 (h)	4.0	Balustrade
4 (h)	3.2	Balustrade
5 (h)	2.8	Balustrade
6 (h)	1.9	Balustrade
7 (h)	2.0	Balustrade
8 (h)	2.4	Balustrade
9 (v)	9.9	Fine Crusts
10 (v)	12.7	Fine Crusts

*ND Not detected

According to Farago *et al* (1995) the main urban source of airborne Pt is from vehicle emissions which pass through catalytic converters, which were effectively made compulsory on new vehicles in the UK at the beginning of 1993. Platinum is believed to be emitted due to the abrasion of the catalytic surface. Road dust samples collected in dry weather from Richmond (London) in 1994/5 and analysed with ICP-MS, contained 0.42-29.8 ng g^{-1} Pt. Pt concentrations in topsoil collected from nearby sites ranged between <0.30-7.99 ng g^{-1}. Concentrations in Richmond shale and Richmond conglomerate were between 0.6-0.7 ng g^{-1} (Simpson *et al*, 1990). This compares to 0.7 $\mu g\ g^{-1}$ in road dusts in San Diego and on plant surfaces in California (Hodge and Stallard, 1986) where catalytic convertors have been used since 1975. Emission rates from engine tests utilising catalytic converters have been estimated at 2-40 ng km^{-1} (Konig *et al*, 1992) and up to 4.7-9.7 μg per km (Helmers *et al*, 1994). Additional sources of Pt include medical wastes 30 kg per annum and coal emissions (1.5-210 ng g^{-1}).

Konig *et al* (1992) estimated that urban ambient air concentrations of Pt were between 0.005-9 ng g^{-1} near and on roads at varying traffic and wind conditions. High concentrations of Pt are associated with high traffic density. Pt tends to be associated with particles >5 μm MMAD (Konig *et al*, 1992) and 0.58-8 μm particles (Alt *et al*, 1993), which is a fraction associated

with Pb emissions from vehicles. Wei and Morrison (1994) used sequential extractions of Pt in road surface sediment in Sweden, and found that 10% was associated with carbonate, 32% with Fe/Mn, 26% with organics, 26% with residue and 15% was exchangeable between fractions. Pt tended to be associated with the smaller particulate fraction (<63 μm).

Strong evidence therefore indicates a major source of Pt in an urban environment is vehicles equipped with catalytic converters. The concentrations detected in surface crusts from St Paul's Cathedral are high in comparison to the deposited Pt results of other authors (although no author measured Pt on permanently exposed and uncleaned surfaces). However, the airborne and deposited lead values show that relatively low airborne concentrations may give rise to high concentrations of deposited lead, albeit over a much longer period of time. Another possible explanation is that the Pt is enriched in ferromanganese minerals when Pt(II) is oxidised to Pt(IV) and Pt is transported to the surface during the leaching of these minerals (Farago *et al*, 1995). The high concentrations of Fe and other metals at the surface support the leaching of metals to the surface hypothesis. However, the undetectable levels of Pt in uncontaminated stone suggests that Pt concentrations in the stone are not great enough to produce the detected concentrations at the surface.

5.5.4 Scanning Electron Microscope (SEM) Analysis

Black crustal material is clearly visible in most areas on the roof of St Paul's Cathedral while being largely absent on the walls of lower levels, presumably due to cleaning activities. Cleaning of the roof black crusts had taken place 10-13 years previously (Head Stone Mason, Pers. Comm.) by brushing with water. Care was taken to select representative samples. Scanning electron microscopy (SEM) analysis was used to identify the structure of the black crusts and particle types found within the crusts from St Paul's Cathedral, Stefansdom (Vienna) and Breitenfurt (semi-rural Austria). SEM analysis allows detailed observation of surfaces and particles >0.5 μm. Energy dispersive X-ray spectrometry (EDX) was also used in the analysis of individual particles located within the structures. Semi-quantitative elemental composition using EDX is accurate to within approximately 10 % and penetrates 4-5 μm into a surface allowing detailed surface analysis. Four or more examples of each crust type were analysed, and additionally random samples were analysed for light elements including carbon.

The three most abundant types of crusts were examined separately. The first type, shown in Figure 5.12, was the most common (by mass) at St Paul's. This crust comprised a spongy appearance which was black/grey tinged with pale brown/orange at the surface. The surface tended to be crumbly and the underlying layers were solid black gypsum strongly attached to the stone surface. This crust type was clearly influenced by local wind systems, particularly at pillar corners where local wind direction could be seen from the shape of the crust. Exfoliation of the stone surface usually accompanied crust removal, revealing damaged layers of orange/brown stone beneath. An yellowish-orange stain was apparent on the vertical walls beneath many of these crusts, indicating iron leaching. Indeed, new balustrade pillars replaced 10 years previously below areas of black crust, displayed an orange tint together with grey and green staining (from crusts/particle deposition and copper, respectively).

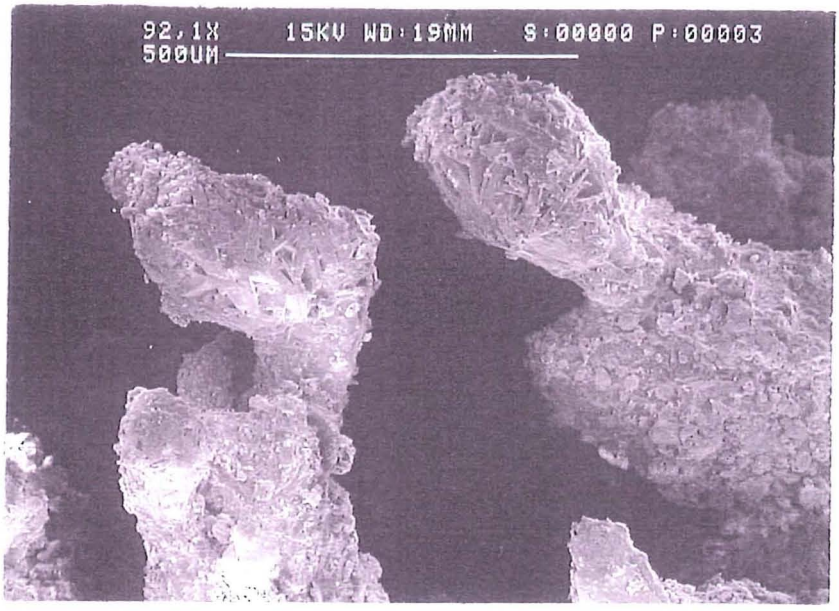

Figure 5.12 Crust type 1 which was typically distributed under the roof balustrade at St Paul's cathedral.

The second crust type was a very fine branching crust, forming a black coral-like structure (Figure 5.13). This type was found on vertical surfaces close to, but independent from, other crusts. The fine stemmed base was usually rooted to a blackened grain or fossilised shell protruding from the stone surface and ranged in size from barely visible to 5 mm in length. Individual stems of such crusts could extend 2-3 mm from the surface to cover a much wider area than the original stem, while branched crusts could extend up to approximately 5 mm

from the surface. The crusts were very fragile since attachment to a surface was usually very small (< 1 mm in diameter). These crusts were also apparent on surfaces which had been cleaned within the last 13 years.

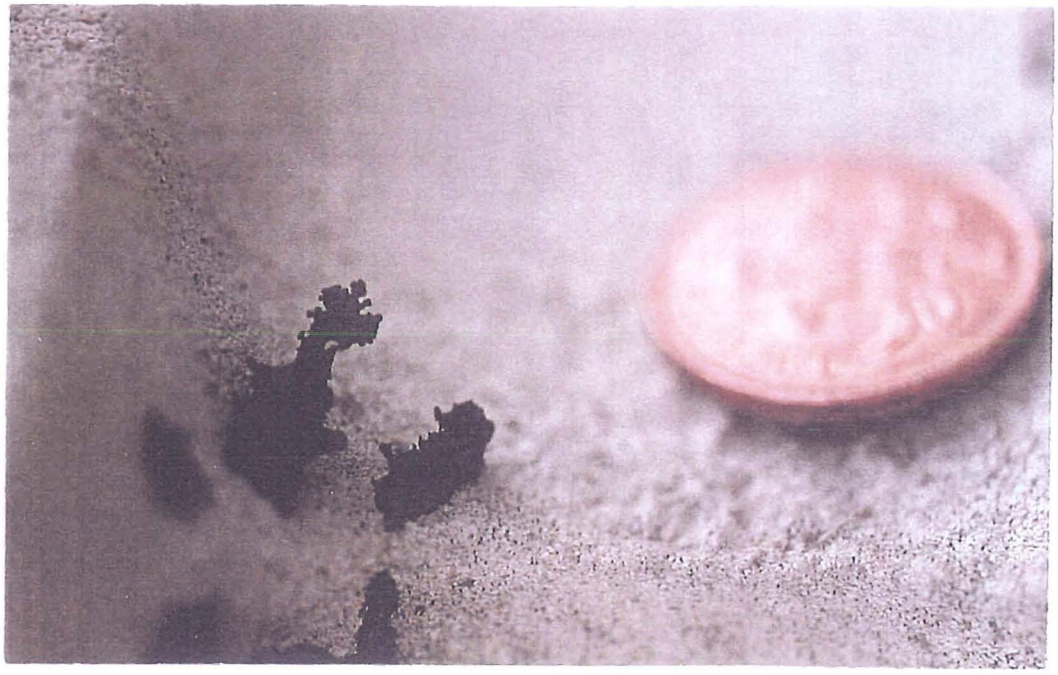

Figure 5.13 Examples of crust type 2; fine crust growth on stone surfaces.

The third type of crust was paler - grey - than the other two and exhibited a smooth surface. It appeared in areas exposed to rainfall and, to a lesser extent, where cleaning had taken place within the past 13 years. This crust was more difficult to remove than the other crust types due to its hardness. Attachment to the underlying stone was very strong and samples were difficult to collect. Under SEM examination, this type of crust was smoother than the other crust types and did not exhibit their characteristic branching stems. The surface was similar to that found in the Vienna sample.

Crust types one and two were interpreted as different stages of crust development. The detailed structure, common to both crust types, revealed black carbonaceous particles (mainly spherical and porous) interwoven in an irregular gypsum frame as noted in many previous publications (eg Del Monte *et al*, 1984). This agrees well with the identification through the PAH results

of coal and oil as the main sources. The surface of all samples was similar in structure, comprising an irregular surface with projecting stems of bladed gypsum crystals, culminating in nodules of prismatic gypsum crystals. Figure 5.14 shows one such stem projecting from the crust surface.

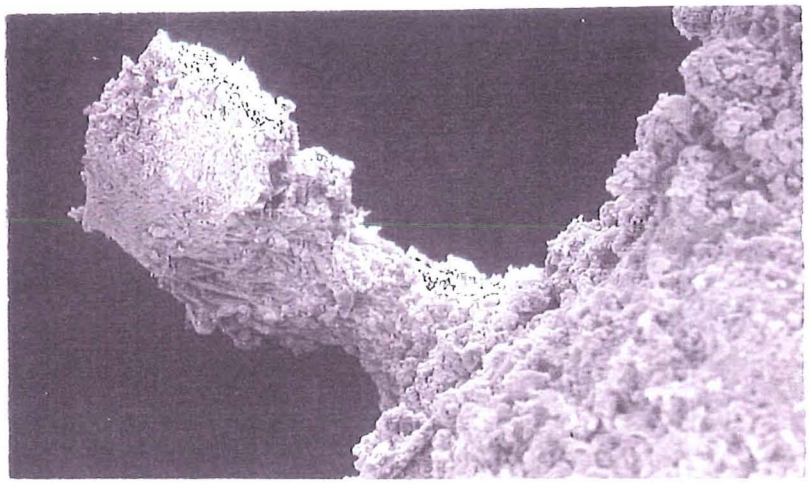

Figure 5.14 A protruding stem typical of those observed on the St Paul's black crust.

Such stems have an approximate length of 200-500 μm and diameter of 100-200 μm, appearing singly, in groups or as branched populations (Figure 5.15) on a surface. Composition (excluding carbon) is dominated by Ca and S, with some Fe, Si and Al. Smaller particles ($<$ 20 μm) are attached to all the surfaces of these stems (Figure 5.13), trapped within the bladed crystal structure and apparently adhering to the smoother prismatic crystals. Smooth spherical particles tended to have Ca or Al and Si as dominant elements, with lower concentrations of S, Si, Fe, Al and traces of Mg, Cl and K. Porous particles tended to have Ca as the major component with lesser concentrations of S, Fe, Si, Cl, Al, Ti and K. Particles often appeared "cemented" into place by crystalline growth. When analysed this crystalline material was richer in Fe and Si than the original particle.

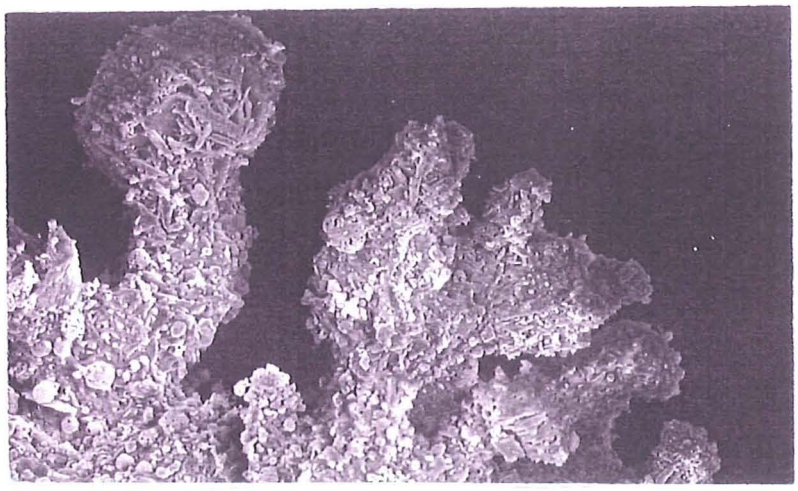

Figure 5.15 Apparent growth stems reducing the interspace to create a more solid crust structure.

It is proposed that particles initially adhere to the surface of protruding fossilised shells, probably due to the interruption of the surface boundary layer and possibly through adhesive properties of the particle and fossil surface. These surfaces gradually protrude due to the dissolution of the surrounding calcareous stone, while the relatively inert silica shells and their particle coatings, are not affected by the process. Figure 5.16 shows how the surface exposed fossilised shells are blackened compared to the surrounding stone. A fine crust gradually builds up through the formation of gypsum crystals at the fossil surface, which further disrupts the air movements around the fossil and may increase deposition.

Figure 5.16 Blackened shells and fine crust growth on shells protruding from the stone surface.

The apparent common factor in the location of these growth sites is the presence of large

numbers of porous, combustion-generated particles, such as those in Figure 5.16. Over time, stems appear to grow together and potentially merge to produce the characteristically solid crust with a uneven, spongy surface layer. More recently attached particles can be seen on all surfaces, which provide a constant source of sulphur for the further sulphation of the building stone. Del Monte *et al* (1984) analysed black crust deposits and found that gypsum crystals were associated with oil-fired carbonaceous particles which acted as carriers of adsorbed species, such as acids, and as gypsum nucleating agents. Gypsum crystals grown on the surface of such particles under laboratory conditions exhibit bladed gypsum crystal growth typical of those found at St Paul's Cathedral. Such acicular monocline gypsum crystals obscured the particle from view, producing radial crystals $\sim 200\ \mu m$ in length, emanating from the particle.

It was noted that fossilised shells appear preferentially blackened in comparison to the stone surface from which they protrude. Figure 5.17 shows how exposed sheets of calcite provide ideal deposition sites for particles, where they become trapped. Numerous particles are also found on the shell surface.

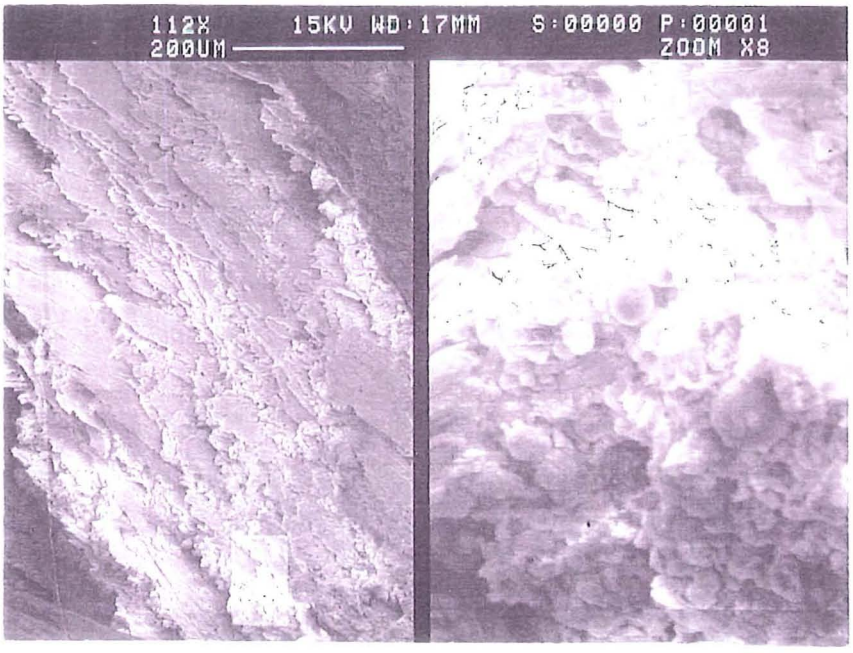

Figure 5.17 Particles trapped between the fragmented layers of fossilised shell.

Blackened and "clean" surfaces of selected shells were analysed using EDX and the results compared. Blackened surfaces tended to have high concentrations of Fe, O and C with Ca, S and Si as minor components and traces of Al, Ti, K and V. Approximately equal concentrations of S and Ca suggest gypsum formation. Analysis of "clean" surfaces (typically a fracture site on the fossil) gave Fe concentrations that were comparably low and Si dominated, with minor concentrations of O, Ca, Al and Mg. Surprisingly few particles could be detected suggesting that the blackness was due to either the high concentration of metal at the fossil surface, the presence of particles too small for SEM detection, which deposit in a process of agglomeration of very small particles (probably carbon) onto a continuous surface, complete inclusion of particles into a thin gypsum layer or a combination of these factors. The few particles found tended to be smooth spherical particles below 2 μm.

Figure 5.18 shows the typical particles observed within the black crust structure found at St Paul's. Porous particles ($\sim$20 μm diameter), such as the magnified particle, were the most common on the crust surface; smooth spherical particles were also common. Both types of particles contained sulphur and trace metal species. Smaller particles were more difficult to group due to their size which inhibited size and chemical description. However, particle agglomerates were detected on the crust (Figure 5.18c) and were suspected to be diesel particles (Sitzmann *et al*, 1996). Smooth spherical particles <5 μm were difficult to analyse using EDX, but were commonly found at the head of the growth stems. SEM analysis of Portland limestone samples exposed in an 8 year materials exposure programme showed these particles to be the most common. Particles typical of diesel emissions were also found on the crust surfaces, but were difficult to distinguish from the crust background. It is also interesting to note that while biological growth was obvious and relatively common on the surface of the exposure programme samples, no signs of biological growth was detected in any of the black crust samples collected. Schiavon (1996) similarly found an inverse relationship between the extent of black crust and biological colonisation.

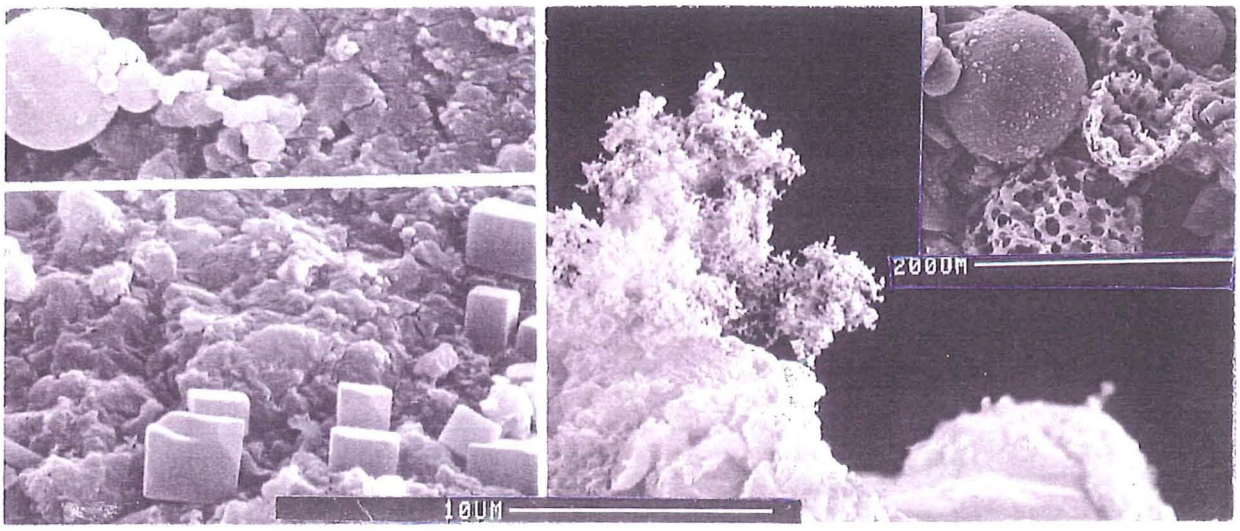

Figure 5.18 The most common types of particles observed on the surface of the St Paul's black crust: a) porous spherical particles from oil and coal combustion, b) smooth spherical particles from coal combustion sources and c) spongy diesel agglomerate.

Two Vienna crust type samples were also analysed using SEM. The structure of the crust was very different to those commonly found in the UK and similar to crust type three identified in this work and those described by Schiavon (1994). The surface was very smooth, smoother than the original stone with few visible particles at the crust surface. The only visible particles were porous spherical particles probably attributable to coal combustion.

5.5.5 Discussion of Black Crust Analysis Results

UK crust samples were grouped into 2 types according to the characteristics of the organic components; those high in PAH with low *n*-alkanes and with a low CPI (n-C_{19} to n-C_{30}) of 1.06-1.03 and those with lower concentrations of PAH, higher *n*-alkanes concentrations with a higher CPI (n-C_{19} to n-C_{30}) 1.22-1.40. Crust morphology within these groups differed enormously, although sub-groups could be identified, aided by metals analysis and Pt analysis in particular. Biological growth may be responsible for the higher CPI in the second group, but extensive SEM examination found little evidence of biological growth, although biological debris did contribute to the crust structure. The higher *n*-alkane homologues n-C_{24} to n-C_{29} dominated the St Paul's aerosol rather more than in Bounds Green, but this may be an

indicator of vehicular pollution rather than biogenic inputs, in particular of diesel vehicles which make up a large proportion of the traffic at St Paul's. The large UCMs, high ratio of UCM: resolved compounds, n-C_{peaks} of around n-C_{23} and the high concentrations of n-alkanes all indicate a vehicular - and specifically diesel - source.

PCA was applied to the organics component compounds identified in the crusts using the same techniques as those employed in the analysis of atmospheric compounds. PCA analysis identified four factors with eigenvalues greater than 2. These factors explained 92.9% of the variation associated with the 39 compound variables. The results of PCA are shown in Table 5.32.

Factor one, which explained 38.9% of the variation, contained high factor loadings for the n-alkanes and 4 PAHs. This factor appeared to be related to vehicle emissions since the main source of most n-alkanes in the atmosphere is vehicles, and three of the PAHs, phenanthrene, pyrene and fluoranthene, were indicative of diesel engine emissions (Smith and Harrison, 1996). Acenaphthylene, phenanthrene, pyrene and fluoranthene all exhibited factor loadings greater than 0.46, and phenanthrene is most strongly associated with this factor with a factor loading of 0.73. Most of the n-alkanes exhibited factor loadings of >0.80, with seven exceptions. Of these exceptions, only two compounds - n-C_{28} and n-C_{34} - exhibited factor loadings below 0.56.

Factor two explained 29.1% of the variation and contained high factor loadings for all of the PAHs except anthracene. Particularly high factor loadings were associated with the high molecular weight compounds, which would be expected on a weathered crust since low molecular weight compounds would degrade or volatilise from the surface more quickly than the higher molecular weight compounds. n-alkane factor loadings were negative or very low, with the n-C_{34} factor loading being the highest at 0.18. Since this factor was certainly combustion related and yet not associated with petrogenic n-alkane compounds, PC2 was considered to represent either deposited coal, wood or oil combustion particles. The weak association with n-C_{34} indicates a possible biogenic input.

The remaining factors cannot be identified satisfactorily, due to complex distributions of eigenvector loadings the cause of which could not be identified. Factor 3 contains high factor loadings for the lowest molecular weight species and may possibly be attributed to variations in compound concentrations due to losses by thermal and photo decomposition. The association with C_{30-34} also supports this conclusion, if the variation were taken to represent a seasonal variation in ambient concentration of these higher molecular weight compounds. Factor 4 was tentatively identified, as leaf litter or wood smoke, since there was a weak relationship between C_{17}, C_{27}, C_{29}, C_{32} and C_{34}, and anthracene. Factor 5 (with an eigenvalue <2) contains the highest factor loading for anthracene (0.69) and, although the possible source is unclear, this factor indicates that anthracene has an independent source or is emitted at variable concentrations compared with the other compounds.

Table 5.32 The eigenvalues and PCA eigenvector matrix of the four retained principal components from UK crust PCA.

	Factor 1	Factor 2	Factor 3	Factor 4
Eigenvalue	15.18	11.36	2.97	2.30
Percent of Variation Explained	38.9	29.1	7.6	5.9
Naph	0.25	0.49	0.30	-0.45
Aceny	0.55	0.70	0.06	0.09
Acen	0.27	0.67	0.23	-0.48
Fl	0.12	0.57	-0.03	-0.15
Phen	0.73	0.59	0.10	-0.06
Anthr	0.12	0.17	0.32	0.26
Pyr	0.59	0.71	-0.04	-0.17
Fluor	0.46	0.77	-0.16	-0.21
Chrys	0.19	0.97	-0.07	-0.05
BaA	0.28	0.90	-0.22	-0.09
BbF	0.26	0.94	-0.12	0.07
BkF	0.26	0.94	-0.12	0.07
BaP	0.21	0.95	-0.02	0.12
I123P	0.26	0.92	-0.10	0.17
BghiP	0.29	0.92	-0.09	0.14
DahA	0.25	0.94	-0.13	0.12
C_{10}	0.52	-0.04	0.40	0.12
C_{11}	0.58	0.05	0.58	0.16
C_{12}	0.68	-0.26	0.37	-0.48
C_{13}	0.81	-0.28	0.20	-0.03
C_{14}	0.87	-0.14	0.16	-0.09
C_{15}	0.84	-0.09	0.32	-0.18
C_{16}	0.85	-0.19	-0.32	0.05
C_{17}	0.57	-0.24	-0.68	0.22
C_{18}	0.59	-0.28	0.66	0.17
C_{19}	0.81	-0.31	-0.43	<0.01
C_{20}	0.89	-0.28	-0.17	-0.12
C_{21}	0.85	-0.34	-0.28	-0.01
C_{22}	0.86	-0.35	-0.18	-0.08
C_{23}	0.88	-0.37	-0.05	-0.14
C_{24}	0.81	-0.34	0.12	-0.29
C_{25}	0.88	-0.31	0.09	-0.13
C_{26}	0.85	-0.36	0.05	0.17
C_{27}	0.91	-0.26	0.07	0.19
C_{28}	0.13	<0.01	0.05	-0.27
C_{29}	0.84	-0.16	0.13	0.41
C_{30}	0.84	-0.20	0.34	0.25
C_{32}	0.56	-0.07	0.33	0.56
C_{34}	0.37	0.18	0.39	0.61

Different PAHs behave differently once deposited and this has been observed in PAH concentrations in soils. Lower molecular weight compounds have been reducing steadily since the 1960s, while high molecular weight compounds such as benzo(a)pyrene are accumulating in soil (Wild and Jones, 1995). This may be because resistance to degradation increases with increasing numbers of benzene rings. PAHs are certainly strongly adsorbed to soil organic matter, rendering the majority unavailable for plant uptake (Wild and Jones, 1995). The high

concentrations of PAHs and other toxic compounds may have prevented biocolonisation at the stone surfaces sampled. The high concentrations of organics in the crusts are striking when considering that the bulk of these crusts may have developed tens of years ago. The high concentrations suggest that either the degradation process associated with the organics attached to these particles is very slow or that the surface concentrations are being replenished by continual particle deposition. If it is assumed that such high concentrations must have been deposited over many years, the former is likely to be true, particularly for PAHs. Two explanations may be that the organics may be so strongly adsorbed to the particle surfaces that degradation is retarded or the structure of the crust and the growth of gypsum layers over the particles may act to protect the organic compounds from degradating mechanisms.

Table 5.33 allows a comparison of the concentrations of organic compounds measured in the black crusts with those detected in the atmosphere at the St Paul's site. This comparison indicates that the concentrations of organic compounds currently detected in the atmosphere could well contribute to the concentrations of organic compounds in the black crusts. The table shows that current atmospheric particle concentrations of ΣPAH are at most one order of magnitude greater than the concentration of crust ΣPAH concentrations. Atmospheric concentrations of Σ*n*-alkanes are one or two orders of magnitude greater than those in the crusts.

The concentration of ΣPAH is higher than Σ*n*-alkanes in only the Vienna crust; in all of the other crust types, the Σ*n*-alkane concentration is higher by a factor ranging between 3-34. The ratios of alkanes:PAH are much higher in the atmospheric samples. The range in concentrations in comparable samples is relatively small. In the UK crusts, ΣPAH concentrations range between 8-13 μg per g crust and Σ*n*-alkane concentrations range between 44-130 μg per g crust. In general, the concentration of ΣPAH decreases down the list of samples while the concentration of Σ*n*-alkanes increase down the list of samples. However, the mosses and particularly the shell crust samples are significantly higher than the other crust types. Since the concentrations in mosses may be an indicator of the composition of currently depositing particles, the shell crusts may be observed to have a much higher ratio of *n*-alkanes, which is in keeping with the ratios found in contemporary atmospheric samples. The roadside

and shell crust concentrations of ΣPAH and Σ*n*-alkane should be interpreted cautiously since the underlying uncontaminated stone was also unavoidably sampled with the crust, obscuring actual concentrations in the surface layer.

Table 5.33 The mean concentrations of ΣPAHs and Σ*n*-alkanes in different crust types (Σcompound type measured per gram of black crust) and the concentrations of ΣPAHs and Σ*n*-alkanes per unit mass of total suspended particulate matter (Σcompound type measured per gram of particulate matter).

Crust Type	ΣPAH ($\mu g\ g^{-1}$)	Σ*n*-Alkanes ($\mu g\ g^{-1}$)	Ratio Alkanes/PAHs
Vienna Crust	25	21	0.9
Under Balustrade Crusts	13	44	3
Vertical Wall Crusts	10	56	6
Fine Crusts	10	73	7
Mosses	8	130	16
Roadside Limestone	2	8	5
Shell Crusts	1	18	34
Season	ΣPAH ($\mu g\ g^{-1}$)	Σ*n*-Alkanes ($\mu g\ g^{-1}$)	
Winter	133	5,978	45
Spring	24	2,407	100
Summer	87	4,973	57
Autumn	179	5,048	28

The low level of bio-colonisation (especially lichens) on the building surfaces examined may be due to the higher concentrations of SO_2 typical of urban areas (Schiavon in Vicente *et al*, 1996). However, Schiavon (1993) did report biological activity in some areas of gypsum occurrence on sandstone and calcareous lithologies and Lewin and Charola (1981) found both Ca^{2+} and SO_4^{2-} ions in lichen thalli. The ability of bacteria, fungi and lichens to concentrate and precipitate Fe and P compounds has been reported by Nagy *et al* (1991). Dark metal pigment stains were reported on rock surfaces in a manner similar to the stains observed below the black crusts at St Paul's. However, these appear to be wash-out stains caused by the action of rain as opposed to being a biologically mediated phenomenon. The high concentrations of PAHs and other toxic compounds may well have prevented bio-colonisation at St Paul's. Interestingly, biological growth appeared to increase on St Paul's roof during the sampling period and has been observed to have increased during the last few years. However, no biological activity was observed around the crusts themselves, and no biological growth, such as lichens and mosses, was detected.

Sabbioni and Zappia (1992) reported comparable concentrations of metals in black crusts

collected in Italy. Many of the metals present may be attributable to metal leaching towards the stone surface. The presence in the crust of Na, Al, Si, Mg and, in part, Fe was attributable to this leaching process. Particulate Fe is certainly directly on deposited to the surface however, as indicated by the numerous iron-rich particles detected by SEM-EDX. Cheng (1976) identified Fe as a major element in both oil and coal derived particles. Pb, V, Zn and Cu all exhibited higher concentrations in the crust than the original stone and were therefore associated with atmospheric deposition of particles emitted by petrol engined vehicles, diesel engined vehicles, incinerators and a combination of anthropogenic sources, respectively. The concentrations of metals detected in this study almost certainly indicated accumulation by a combination of leaching and deposition. The Fe concentrations measured in black crusts cannot have occurred through deposition alone and the Pt concentrations cannot have been elevated through leaching. Some combination of the two processes has therefore probably occurred.

At St Paul's Cathedral, black crusts tended to be present in locations sheltered from direct rainfall and rainfall run-off. Close observation also indicates that areas which experience direct sunlight are generally less affected than shaded areas. This may be related to the reduction of surface moisture due to heating which reduces the "stickiness" of a surface, or may reduce the impact of thermophoretic mechanisms. The similarity of the shape of the crust seen at high magnification using close-up photography and SEM at different magnifications suggest the crusts may be a fractal phenomenon. This is supported by the work of Massey *et al* (in Watt and Kendall, 1997) who proposed two models of particulate agglomeration on a surface analogous to crust formation by particle deposition. One model assumed that the particle-surface interaction contained a sticky component and therefore stuck at the first point of contact. This model produced structures resebled to the crust structures observed although no account of crystal growth was included in this model. The system dynamics may therefore be described as a rough surface comprising spiky crystals which trap particle, which themselves have a high sorptive capacity due to their surface features and high organic content. Surface moisture may also be important in supplying both the initial surface "stickiness" and the more permanent cementation of crystalline $CaSO_4$ solution.

5.6 SUMMARY

Total suspended particulate was monitored at two sites in central and north London. Monitoring of TSP and subsequent analysis of the particulate matter for total organic carbon, particulate elemental carbon, sixteen PAH compounds and 23 *n*-alkanes revealed higher concentrations of all of these compounds at the central London location. Good intersite relationships existed between the two sites for TSP, TOC and PEC. Other organic components are poorly correlated between sites. The most common compounds identified were from both petrogenic and biological sources.

Weather factors were found to be influential over some organic species concentrations. Seasonal differences in compounds concentrations were identified at both sites, with higher concentrations of combustion related compounds occurring in winter and autumn. Peak concentrations are due to increased fuel combustion during these periods and also due to evaporative differences at different temperatures, amount of fuel used for heating and the poor performance of cold start engines.

The dominant PAH compounds were found to be the higher molecular weight compounds, namely BghiP, BaA and Chrys. In fractionated samples of PM_{10} Chrys was the dominant PAH and was found mostly in the finest fraction of particles ($< 1\mu m$). Although PAHs could not have be solely used to identify specific sources, ratios of PAHs indicated a dominant petroleum source at both sites, with a greater diesel component at the central London site. *n*-alkane compound distributions between C_{10} to C_{34} showed that the highest concentrations of compounds were between C_{21}-C_{29}. CPI values were around unity indicating a vehicular source. In a series of fractionated samples, 12 of 16 fractions of PM_{10} collected over four weeks had C_{peaks} in the C_{20}-C_{22} range. The CPIs of the PM_{10} fractions were low, around unity.

PCA analysis of the organic compounds indicated that the sources of variation within the two datasets were only slightly related at the two sites, and that much of the variation within the two compound groups was not related. This means that either the compounds are generated by different sources, or that despite originating from the same source the compounds are

generated in disproportionate amounts by different vehicles, hence obscuring any direct source of variation.

Most relationships between individual weekly PAH compounds and *n*-alkanes were weak, but strongest at the Bounds Green site. Three PAH compounds exhibited weak - but significant at the the 5% level - correlations with PEC and TOC, and these relationships were strongest at St Pauls. These three compounds are strongly associated with diesel engine and coal fire emissions. This indicates that there is an additional PAH source at St Pauls which is rich in these three compounds, and is associated with PEC and TOC emissions, although not *n*-alkanes. This is supported by the intersite ratios of PAH and *n*-alkanes at both sites. The SP/BG PAH ratio is higher than the SP/BG *n*-alkane ratio.

The concentrations of the compounds measured at the heights monitored in this study are lower than in previous studies where monitoring sites were positioned closer to ground level. Comparison with the results of previous studies carried out over the past three decades show that PAH concentrations in the atmosphere are reducing. Low molecular weight compounds were noticeably higher at the Bounds Green site, especially fluorene and the low molecular weight *n*-alkanes. These inter-site differences may be due to different sources.

Sample integrity is a major problem in the determination of organic components of urban particulates. High-volume collection techniques expose collected particles to high losses of low molecular weight organic compounds due to their high volatility in ambient air. Artifacts may also be formed during particle collection (Baek *et al*, 1991). Ambient temperature, sunlight hours together with ozone, sulphur dioxide and nitrogen dioxide concentrations all significantly affect organic compound concentration. Simoneit (1983) reported that hydrocarbon concentrations sampled by short period high volume filtration will not be accurate for compounds $< C_{20}$, but qualitative comparisons may be made. The loss of unresolvable petroleum residues (derived from lubricating oil) will be minimal as the major concentration of the compounds is $> C_{18}$ and will remain unaffected unless the ambient temperature rises above 35°C. The question remains, however, to what degree volatiles attached to collected particles were affected by evaporation or condensation after their collection on filters.

Under laboratory conditions, Broddin *et al* (1980) measured the blow-off artifact of a filter by passing clean nitrogen through an aerosol sample at the hi-vol flow rate at which it was collected. Under these conditions, blow off was shown to be significant up to C_{23} and more important for lower homologues. During actual sampling this effect may be reduced due to the presence of lower aliphatic compounds in ambient air. The gas phase contribution to the lower *n*-alkanes C_{16}-C_{19} to total airborne concentration is strongly temperature dependent and greater than the particulate phase. Gas phase contribution became negligible (nondetectable) for C_{22}-C_{23} and higher homologues in winter, and for C_{24}-C_{25} and higher homologues in summer. Of the PAHs, the benzofluoranthenes, benzopyrenes and higher molecular weight compounds experienced no significant losses. A comparison of the results of this study with those of the London TOMPs site (operated by AEA Technology) shows that indeed, this study measured lower concentrations of PAHs than AEA. However, the monitoring periods were not absolutely coincidental and reasonable agreement can be demonstrated (AEA, 1997).
The process of particle deposition is complex. SEM examination of different crusts from London's St Paul's cathedral revealed large numbers of particles of anthropogenic origin, probably emitted from oil and coal combustion sources. Different stages of crust development or structure were tentatively identified, including apparent growth stems which protrude from the crust surface. SEM analysis of the crusts identified apparently different crust types, which was supported by both the organics and metals analysis.

Large concentrations of metals were found in the surfacial crust. High concentrations of iron, aluminium and magnesium in particular indicated deposition of metals from atmospheric particles. Metals analysis also identified species indicative of petrol vehicle emissions such as lead, cadmium and platinum. Other identified metals indicated the possibility of some metal leaching from the original stone to the surface, causing the black/brown discoloration of the gypsum crust.

Very high concentrations of PAH and high concentrations of *n*-alkanes have been quantified in the crusts. A large unresolvable complex mixture (UCM) indicative of vehicle emissions was also apparent in the crust samples. A large C_{29} peak in many of the crusts indicates a significant biological input, probably from higher plant waxes in leaf litter. A secondary peak

at n-C_{21} indicates a vehicular source, and this was the C_{peak} for the roadside crusts. However, calculated CPIs for the crusts indicate an anthropogenic origin for the balustrade crusts and the Vienna. Ratios of PAH compounds indicate a large coal combustion particle contribution to all of the crusts and particularly to the balustrade and Vienna crust types.

PCA analysis of the organic compounds in the crusts indicated that the PAH compounds and the n-alkane compounds may originate from different sources. The n-alkanes are only slightly associated with most PAH compounds, and especially with the three PAHs phenanthrene, pyrene and fluoranthene. This is similar to the airborne concentrations PCA which showed that the variations of the compound concentrations were not related.

Chapter 6

CONCLUSIONS AND RECOMMENDATIONS FOR FURTHER WORK

6.1 INTRODUCTION

This thesis details work carried out over a three year period between 1994 and 1997. The main conclusions of this work are detailed in Sections 6.2, 6.3 and 6.4. Recommendations for further work are detailed in Section 6.5.

6.2 SOILING OF BUILDING SURFACES

Empirical models developed for the prediction of the rate of surface blackening (soiling) of two types of material have been compared with measurements of soiling at five sites in three countries. Measurement of selected environmental conditions were made simultaneously to enable a study of the potential factors influencing particle deposition and their relative importance.

The comparison of annual soiling rates showed that different rates of soiling were observable at all sites. This may be expected due to the differences in prevailing environmental conditions at the different sites. The progressive soiling of a surface could be effectively described by an exponential decay model at all of the sites and less successfully by the square root model at two of the sites (Vienna and London). The soiling of painted wood samples (which provided a flat, smooth surface for particle deposition) was described better than the stone samples. At the Portuguese sites, stone samples experienced an appreciable cleaning effect over the monitoring period which was not observable on the wood sample surfaces nor at the other sites.

Differences were also observed in the soiling of the two material types (wood and stone) and the two types of exposure conditions (protected and unprotected). Wood samples soiled faster than stone samples at all sites, indicating differences in the soiling processes affecting the two

than stone samples at all sites, indicating differences in the soiling processes affecting the two surface types. All unprotected samples - irrespective of material - at all sites soiled faster than the protected samples, again indicating different deposition processes or at least lower deposition rates of particles to protected surfaces.

Multiple regression was used to identify the most important variables governing the annual soiling rate identified by the exponential model. No factor could be accurately identified as causing the variance observed in soiling rates in the five countries monitored. However, the results indicated that rainfall, sulphur dioxide concentrations, wind speed and temperature were significantly related to soiling rates. Solar radiation was also indicated to have influenced soiling rates, possibly by thermophoresis. Surprisingly, no measure of particulate pollution could be significantly related to soiling rates. This may result from the fact that there was not a wide variation in particulate matter concentrations at all of the sites, or that the weekly measurements taken reduced the sensitivity of the measurement campaign to detect any cause-effect relationship between particulate matter and surface soiling.

6.3 ATMOSPHERIC PARTICLE ANALYSIS

Total suspended particulates (TSP) were monitored at two sites in central and north London. Monitoring of TSP and subsequent analysis of the particulate matter for total organic carbon, particulate elemental carbon, sixteen PAH compounds and 23 *n*-alkanes revealed higher concentrations of all of these compounds at the central London location. Good intersite relationships existed between the two sites for TSP, TOC and PEC. Other organic components were poorly correlated between sites. The most common compounds identified were from both petroleum combustion and biological sources.

Weather factors were found to be influential over some organic species concentrations. Seasonal differences in compound concentrations were identified at both sites, with higher concentrations of combustion-related compounds occurring in winter and autumn. Peak concentrations were probably due to increased vehicular and domestic fuel combustion during these periods, variations in evaporative emissions differences and phasedistributions of organic

compound at different (seasonal) temperatures and the reduced performance of engines during cold start.

The dominant PAH compounds were found to be the higher molecular weight compounds, namely BghiP, BaA and Chrys. Although PAHs could not have been solely used to identify specific sources, ratios of PAHs indicated a dominant petroleum source at both sites, with a probable greater diesel component at the central London site. *n*-alkane compound distributions between C_{10} to C_{34} showed that the highest concentrations of compounds were between C_{21}-C_{29}. CPI values at both sites were around unity indicating an anthropogenic (vehicular) source. In a series of fractionated samples, 12 of 16 fractions of PM_{10} collected over four weeks had C_{peaks} in the C_{20}-C_{22} range. The CPIs of the PM_{10} fractions were low, around unity.

PCA analysis of the organic compounds indicated that the sources of variation within the two data-sets were only slightly related, and that much of the variation within the two compound groups was not related. This may mean that the compounds are generated by different sources, or that despite originating from the same source (vehicles), the compounds are generated in disproportionate amounts by different vehicles, hence obscuring any direct source of variation.

Most relationships between individual weekly concentrations of PAH compounds and *n*-alkanes were weak, but strongest at the Bounds Green site. Three PAH compounds exhibited weak - but significant at the 5% level - correlations with PEC and TOC, and these relationships were strongest at St Paul's. These three compounds are strongly associated with diesel engine and coal fire emissions. This indicates that there is an additional PAH source at St Paul's which is rich in these three compounds, and is associated with PEC and TOC emissions, although not *n*-alkanes. This is supported by the intersite ratios of PAH and *n*-alkanes at both sites. The SP/BG PAH ratio is higher than the SP/BG *n*-alkane ratio.

6.4 DEPOSITED PARTICULATE ANALYSIS

The processes of particle deposition to stone surfaces and surface retention of particles are complex. SEM examination of different crusts from London's St Paul's Cathedral revealed

large numbers of particles of anthropogenic origin, probably emitted from historically important oil and coal combustion sources, such as Bankside power station. Different stages of crust development or structure were tentatively identified, including apparent growth stems which protrude from the crust surface. SEM analysis of the crusts identified apparently different crust types, which was supported by both the organics and metals analysis. Many different particle types were identified in the crust after morphological and elemental analysis. The dominant particle type was oil combustion particles.

Large concentrations of metals were found in the surface crust. High concentrations of iron, aluminium and magnesium in particular, indicated deposition of metals from atmospheric particles. Metals analysis also identified species indicative of petrol vehicle emissions such as lead, cadmium and platinum, indicating that the deposition of vehicular particulate matter occurs. Other identified metals indicated the possibility of some metal leaching from the original stone to the surface, causing the black/brown discoloration of the gypsum crust.

Very high concentrations of PAH and high concentrations of *n*-alkanes have been quantified in the crusts when compared with the aerosol samples. A large unresolvable complex mixture (UCM) indicative of vehicle emissions was also apparent in the crust samples. A large C_{29} peak in many of the crusts indicates a significant biological input, probably from higher plant waxes in leaf litter since no traces of biological activity were found in the black crusts. A secondary peak at *n*-C_{21} indicates a vehicular source, and this was the C_{peak} for the roadside crusts. Calculated CPIs for the crusts indicate an anthropogenic origin for the London balustrade crusts and the Vienna crust types. Ratios of PAH compounds indicate a large oil/coal combustion particle contribution to all of the crusts and particularly to the London balustrade and Vienna crust types. Oil combustion particles are likely to originate from the oil-fired Bank Side power station, operated in central London between 1963-81. Coal combustion particles may well have originated from domestic hearths and large combustion plants such as Battersea Power Station.

PCA analysis of the organic compounds in the crusts indicated that the PAH compounds and the *n*-alkane compounds may originate from different sources. The *n*-alkanes are only slightly

associated with most PAH compounds, and especially with the three PAHs, phenanthrene, pyrene and fluoranthene. This is similar to the airborne concentrations, and PCA showed that the variations of the compound concentrations were not closely related. These three PAH compounds are associated with diesel and petrol engined vehicles and this is likely to be the reason for the association with the *n*-alkanes present. Therefore these results - together with the identification of vehicle-related metals in the crusts - indicate that vehicular particulate matter is depositing to these surfaces.

6.5 RECOMMENDATIONS FOR FURTHER WORK

There are several recommendations for further work which result from the investigations undertaken as part of this thesis. This further work may be summarised as the following points:

i) investigate the *n*-alkane distributions and CPI of coal-fired particulate emissions to quantify the contribution to soiling layers on monuments;

ii) investigate the adhesion properties of the particles generated by different combustion sources (ie particles of different compositions) onto surfaces held under different conditions (ie temperature, solar radiation, humidity, wind speeds, etc), using atomic force microscopy (AFM);

iii) investigate the organic compounds contained in - and structure of - particles from different size-segregated particulate samples;

iv) investigate the surface chemistry of particulates of different aerosols;

v) investigate the effects of humidity on organic particulate behaviour, for example the effects of organic films on water accretion - the adsorption of hydrophillic molecules such as surfactants at the hydrogen surface will increase water adsorption;

vi) investigate the effect of thermophoresis and humidity on particulate deposition to surfaces;

vii) investigate the importance of resistant discontinuities such as fossilised crustacea in limestones, in enhancing particle deposition;

viii) investigate soiling rates of surfaces using short (hourly, twelve hourly or daily) averaging periods; and,

ix) investigate soiling rates at different heights with simultaneous measurement of particle mass concentration and size distribution.

REFERENCES

AEA Technology: NETCEN. "Air Pollution in the UK: 1993/4". Report of the UK Air Pollution Monitoring Networks, AEA Technology, Abingdon, Oxfordshire, 1995.

AEA Technology. "Air Pollution in the UK: 1995". Ninth Report of the UK DoE Air Pollution Monitoring Networks, NETCEN, AEA Technology, Abingdon, Oxfordshire. 1997.

Abbass, M. K., Andrews, G. E., Bartle, K. D. and Williams, P. T. "Condensable Unburned Hydrocarbon Emissions from a DI Diesel Engine" Fourteenth International Symposium of the ICHMT, Heat and Mass Transfer in Gasoline and Diesel Engines, September 1987.

Aceves, M. and Grimalt, J. O. "Large and Small Particle Size Screening of Organic Compounds in Urban Air". *Atmospheric Environment*, Vol **27B**, No 2: 251-263. 1993.

Alt, F., Banbauer, A., Hoppstock, K., Mergler, B. and Tolg, G. "Platinum Traces in Airborne Particulate Matter: Determination of Whole Content, Particle Size Distribution and Soluble Platinum". *Fresenius Journal of Analytical Chemistry*, **346**: 693-696. 1993.

Albers, P., Freund, B. Seifold, K. and Wolff, S. "Charakterisierung von Russoberflachen durch kombinierten Einsatz von XPS- und SIMS-Messungen". *Kautschuk and Gummi, Kunstoff*, **45**: 449-456. 1992.

Amoroso and Fassina "Stone Decay and Conservation". Elsevier Science Publishers, Amsterdam. 1983.

Anderson, P. "An Investigation into the Size Distribution of Particulate Matter at St Paul's Cathedral". Final Year Project, Middlesex University, London. 1996.

Andreae, M. O. "World Survey of Climatology". Henderson-Sellers, American Edition, Vol. **XX**. Elsevier, Amsterdam, 1995.

Andrews, E. and Larson, S. M. "Effect of Surfactant Layers on the Size Changes of Aerosol Particles as a Function of Relative Humidity", *Environmental Science and Technology*, Vol **27**, No 5: 857-865. 1993.

Anspaugh, L. R., Shinn, J. H., Phelps, P. L. and Kennedy, N. C. "Resuspension and Redistribution of Plutonium in Soils". *Hlth. Phys.*, **29**:571-582. 1975.

Archer, G., Harrison, R. M., Ayres, J. G. and Walters, S. Unpublished data, 1994.

Ausset, P., Lefevre, R. and Philippon, J. "Atmospheric Aluminosilicate Microspherules inside the Black Crust of Altered Limestone at Fontevraud Abbey". In *Science, Technology and European Cultural Heritage* (edited by Baer, N., Sabbioni, C. and Sors, A.): 452-455.

Butterworth-Heinemann, Oxford. 1991.

Baek, S. O., Goldstone, M. E., Kirk, P. W. W., Lester, J. N. and Perry, R. "Methodological Aspects of Measuring Polycyclic Aromatic Hydrocarbons in the Urban Atmosphere". *Environmental Technology*, **12**: 107-129. 1991a.

Baek, S. O., Goldstone, M. E. , Kirk, P. W. W., Lester, J. N. and Perry, R. "Phase Distribution and Particle Size Dependency of Polycyclic Aromatic Hydrocarbons in the Urban Atmosphere". *Chemosphere*, Vol **22**, Nos. 5-6:503-520. 1991b.

Baek, S. O., Goldstone, M. E., Kirk, P. W. W., Lester, J. N. and Perry, R. "Concentrations of Particulate and Gaseous PAH in London Air Following a Reduction in the Lead Content of Petrol in the United Kingdom". *The Science of the Total Environment*, **111**: 169-199. 1992.

Baedecker, P. A., Reddy, M. M., Reimann, K. J. and Sciammarella, C. A. "Effects of Acidic Deposition on the Erosion of Carbonate Stone - Experimental Results from the US National Acid Precipitation Program (NAPAP)". *Atmospheric Environment*, Part B, **26**: 147-158. 1992.

Ball, D. J. "Smoke from Diesel-Engined Road Vehicles: An Investigation into the Basis of British and European Emission Standards". *Atmospheric Environment*, **17**: 169-181. 1983.

Ball, D. J. " Environmental Implications of Increasing Particulate Emissions Resulting from Diesel Engine Penetration of the European Automotive Market". *Science of the Total Environment*, **33**,: 15-30. 1984.

Barefoot, R. R. "Determination of Platinum at Trace Levels in Environmental and Biological Materials". *Environmental Science and Technology*, **31**, 2: 309-314. 1997

Bates, D. V. "Summary of the Colloquium (on Particulate Air Pollution and Human Mortality and Morbidity". *Inhalation Toxicology*, **7**, No. 1: ix - xiii. 1995.

Beloin, N. J. and Haynie, F. H. " Soiling of Building Materials". *Journal of Air Pollution Control Association*, **25**, No. 4: 399-403. 1975.

BERG (Building Effects Research Group), DoE. "The Effects of Acid Deposition on Buildings and Building Materials in the UK". HMSO, London. 1989.

Bhattacharya, S. and Mittal, K. L. *Surface Technology*. **7**: 413. 1978.

Biggins, B. D. E." Speciation and Environmental Chemistry of Automotive Emitted Inorganic Lead". PhD Thesis, University of Lancaster, 1979.

Black, F. and High, L. "Methodology for Determining Particulate and Gaseous Hydrocarbon Emissions". SAE 790422, 1979.

Bowling, R. A. "A Theoretical Review of Particle Adhesion". In *Particles on Surfaces 1: Detection, Adhesion and Removal* (Ed. Mittal, K. L.). Plenum Press, New York, NY. 1988.

Bray, E. E. and Evans, E. D. "Distribution of *n*-Paraffins as a Clue of Recognition of Source Beds" *Geochim. Cosmochim. Acta* **22**: 2-15. 1961.

Brimblecombe, P. "The Big Smoke: A History of Air Pollution in London". Methuen, UK. 1987.

Brimblecombe, P. "A Brief History of Grime: Accumulation and Removal of Soot Deposits on Buildings Since the 17th Century". In *Stone Cleaning and the Nature, Soiling and Decay Mechanisms of Stone Decay* (Ed. Webster, R. G. M). 1992.

Broddin, G. Cautreels, W. and Van Cauwenberghe, K. "On the Aliphatic and Polyaromatic Hydrocarbon Levels in Urban and Background Aerosols from Belgium and the Netherlands". *Atmospheric Environment*, **14**:895-910. 1980.

Brown, J. R., Field, R. A., Goldstone, M. E., Lester, J. N. and Perry, R. "Polycyclic Aromatic Hydrocarbons in Central London Air During 1991 and 1992". *The Science of the Total Environment*, **177**: 73-84. 1996.

BSI. "Reflectance Method". BS 1747, Part 11. BSI, London, 1993.

Busch, B., Ferron, G., Karg, E., Silberg, A and Heyder, J. "The Growth of Atmospheric Particles in Moist Air". *Journal of Aerosol Science*, **26**, Supplement 1: S435 - 436. 1995.

Butlin, R. N., Coote, A. T., Ross, K. D. and Yates, T. J. S. " Weathering and Conservation Studies at Wells Cathedral, England" in Science, Technology and European Cultural Heritage. Ed N. S. Baer, C. Sabbioni and A. I. Sors. Butterworth and Heinemann Ltd, UK. 1991.

Butlin, R. N., Coote, A. T., Devenish, M., Hughes, I. S. C., Hutchens, C. M., Irwin, J. G., Lloyd, G. O., Massey, S. W., Webb, A. H. and Yates, T. J. S. "Preliminary Results from the Analysis of Stone Tablets from the National Materials Exposure Programme (NMEP)". *Atmospheric Environment*, **26** Part B: 189-198. 1992.

Butlin, R. *et al* . *Water, Air and Soil Pollution*, **85**, No 4: 2655-2660. 1995.

Calder, K. L. "Atmospheric Diffusion of Particulate Material, Considered as a Boundary Value Problem". *Journal of Meteorology*, **18**: 413-416. 1961.

Camuffo, D., Del Monte, M., Sabbioni, C. and Vittori, O. "Wetting, Deterioration and Visual Features of Stone Surfaces in an Urban Area". *Atmospheric Environment*, Vol **16**, No 9: 2253-2259. 1982.

Carey, W. F. "Atmospheric Deposits in Britain: A Study in Dinginess". *International Journal of Air Pollution*, **2**: 1-26. 1959.

Carroll and Innes "Multielement and Sulphate in Particulate Surveys: Summary of the Eigth Year's Results 1983-84". WSL Report LR 655 (AP) M, Stevenage, UK. 1988.

Cartillieri, W. and Tritthart, P. "Particulate Analysis of Light Duty Diesel Engines (IDI and DI with Particular Reference to the Lube Oil Particulate Fraction". SAE 840418, 1984.

Caswell, R. London Scientific Services. Personal Communication. In Mansfield, T. "The Soiling of Materials in Urban Areas". PhD Thesis, Middlesex Polytechnic, London, 1989.

Cautreels, W. and Van Cauwenburghe, K. "Experiments on the Distribution of Organic Pollutants Between Airborne Particulate Matter and the Corresponding Gas Phase". *Atmospheric Environment*, **12**: 1133-1141. 1978.

CE Contract No STEP-CT90-0097. "Effects of Airborne Particulate Matter on Building Surfaces". Final Technical Report, Middlesex University, London. 1995.

Chamberlain, A. C. "Transport of Lycopodium Spores and Other Small Particles to Rough Surfaces". *Proceedings of the Royal Society London*, A296: 45-70. 1967.

Charlson, R. J., Schwartz, S. E., Hales, J. M., Cess, R. D., Coakley, J. A., Hansen, J. E. and Hofmann, D. J. *Science*, **9**, 225:422. 1992.

Cheng, R. J., Hwu, J. R., Kim, J. T. and Leu, S. M. "Deterioration of Marble Structures, The Role of Acid Rain". *Analytical Chemistry*, **59**: 104A-106A. 1987.

Cheng Kang Li and Kamens, R. M. "The Use of Polyaromatic Hydrocarbons as Source Signatures in Receptor Modelling". *Atmospheric Environment*, **27A**, No. 4:523-532. 1993.

Cheng, R. J., Mohnen, V. A., Shen, T. T., Current, M. and Hudson, J. B. "Characterization of Particulates from Power Plant". *Journal of the Air Pollution Control Association*, Vol. **26**, No. 8: 787-790. 1976.

Cheng, R. J. "Emissions from Electricity Power Plants and Their Impact on the Environment", *Atmospheric Environment*, 591-598. 1983.

Chow, J. C., Liu, C. S., Casmassi, J., Watson, J. G., Lu, Z. and Pritchetts, L. C. "A Neighbourhood-Scale Study of PM_{10} Source Contributions in Rubidoux, California".

Atmospheric Environment, **26A**: 693-706. 1992.

Christwell, C. D., Ogawa, I., Tschetter, M. J. and Markuszewski, R. "Effect of Hydrofluoric or Hydrochloric Acid Pretreatment on the Ultrasonic Extraction of Organic Materials from Fly Ash for Chromatographic Analysis". *Environmental Science and Technology*, **22**: 1506-1508. 1988.

Cieplak, M., Smith, E. D. and Robbins, M. O. "Molecular Origins of Friction: The Force of Adsorbed Layers". *Science*, **265** (5176): 1209-1214. 1994.

Clarke, A. G. "The Air". In *Understanding Our Environment,* Hester, R. (Ed.) Royal Society of Chemistry, Bristol, 1986.

Clarke, A. G., Willison, M. J. and Zeki, E. M. "A Comparison of Urban and Rural Aerosol Composition Using Dichotomous Samplers". *Atmospheric Environment*, **23**: 1767-1775. 1984.

Clarke, A. D. *Journal of Atmospheric Chemistry*, **14**: 479. 1993

Clarke, A. D. Personal communication. In Rickard and Ashmore, *Clean Air* Vol **26**, No 2: 37-42. 1996.

Clayton, P., Davis, B. J., Jones, K and Jones, P. "Toxic Organic Micropollutants in Urban Air". Report LR904 (AP). Warren Spring Laboratory, Stevenage, 1992.

Clough, W. S. "Transport of Particles to Surfaces". *Journal of Aerosol Science*, **4:** 227-234. 1973.

Cobourn,W. G., Gauri, K. L., Tamba, S., Li, S. and Saltik, E. "Laboratory Measurements of Sulphur Dioxide Deposition Velocity on Marble and Dolomite Stone Surfaces". *Atmospheric Environment*, **27**, Part B: 193-201. 1993.

Colbeck, I. and Harrison R. M. "Ozone-Secondary Aerosol-Visibility Relationships in North-West England". *The Science of the Total Environment*, **34:** 87-100. 1984.

Coleman, P. J. Personal Communication. AEA Technology, 11th December 1995.

Collins, G. and Harrison, R. M. Unpublished data, 1994.

Commins, B. T. and Hampton, I. "Changing Patterns in the Concentrations of PAH in the Air of Central London". *Atmospheric Environment*, **10**: 561-562. 1976.

Committee on the Medical Effects of Air Pollution (COMEAP). "Medical Effects of Non-Biological Particles". HMSO, London, 1995.

Coplin, N. "Monitoring of Personal Exposure to Respirable Particulates in Central London". Final Year Project, ENS3994, Middlesex University, London. 1995.

Corn, M. *Journal of Air Pollution Control Association,* **11**: 523-528. 1961.

Corn, M. and Stein, F. "Re-entrainment of Particles from a Plane Surface". *American Industrial Hygiene Association Journal*, **26**: 325-336. 1965.

Corn, M. "Adhesion of Particles". In *Aerosol Science*, (Ed. Davies, C. N.): 359-392. Academic Press, New York, NY. 1966.

Corn, M. and Stein, F. "Adhesion of Atmospheric Dustfall Particles to a Glass Slide". *Nature*, **211**, 60-61. 1966.

Coutant, R. W., Callahan, P. J. and Kuhlman, M. R. "Design and Performance of a High Volume Compound Annular Denuder". *Atmospheric Environment*, **23**: 2205-2211. 1988.

Creighton, P. J., Lioy, P. J., Haynie, F. H., Lemmons, T. J., Miller, J. L. and Gerhart, J. "Soiling by Atmospheric Aerosols in an Urban Industrial Area". *Journal of Air and Waste Management Association*, **40**, No. 9: 1285-1289. 1990.

Cuddihy, E. F. "Soiling Mechanisms and Performance of Anti-Soiling Surface Coatings". In Particles on Surfaces 1: Detection, Adhesion and Removal (Ed. Mittal, K. L.). Plenum Press, New York, NY. 1988.

Daisey, J. M. Cheney, J. L. and Lioy, P. J. "Profiles of Organic Particulate Emissions from Air Polluion Sources: Status and Needs for Receptor Source Apportionment Modelling". *Journal of Air Pollution Control Association*, **36**: 17-33. 1986.

Dahnecke, B. "The Influence of Flattening on the Adhesion of Particles". *Journal Colloid and Interface Science*, **40**, 1: 1-13. 1972.

Del Monte, M., Sabbioni, C. and Vittori, G. "Airborne Carbon Particles and Marble Deterioration". *Atmospheric Environment*, Vol **15**, No 5; 645-652. 1981.

Del Monte, M., Sabbioni, C. and Vittori, G. "Urban Stone Sulphation and Oil-Fired Carbonaceous Particles". *Science of the Total Environment*, **36**: 369-376. 1984.

Del Monte, M. and Sabbioni, C. "Chemical and Biological Weathering of an Historical Building: Reggio Emilia Cathedral". *Science of the Total Environment*, Vol **50**: 165-182. 1986.

Del Monte, M., Rattazzi, A., Romao, P. and Rossi, P. "The Role of Lichens in the Weathering of Granite". *Degradation and Conservation of Granitic Rocks in Monuments*, Protection and Conservation of European Cultural Heritage, Research Report No. 5: 301-306. 1996.

Delopoulo, P. and Sikiotis, D. "A Comparison of the Corrosive Action on Pentelic Marble of Nitrates and Sulphates with the action of Nitrogen oxides and Sulphur Dioxide". *Atmospheric Environment*, **26**, Part B: 183-188. 1992.

De Santis, F. and Allegrini, I. "Heterogeneous Reactions of SO_2 and NO_2 on Carbonaceous Surfaces", *Atmospheric Environment*, Vol **26A**, No 16: 3061-3064. 1992.

DoE. "Digest of Environmental Protection and Water Statistics". HMSO, London, 1989.

DoE, Government Statistical Service. "The UK Environment". HMSO, London, 1992.

DoE. "Digest of Environmental Protection and Water Statistics". HMSO, London, 1993.

DoE. "Digest of Environmental Protection and Water Statistics". HMSO, London, 1995.

Dockery, D. W., Pope, C. A., Xu, X., Spengler, J. D., Ware, J. H., Fay, M. E., Ferris, B. G. and Speizer, F. E. "An Association Between Air Pollution and Mortality in Six US Cities". *New England Journal of Medicine*, **329**: 1753-1759. 1993.

Draft, R. G., Mell, R. J. and Segers, E. "Investigation of soiling Characteristics of Polymeric Film". Report No LS-72-7451 for Jet Propulsion Laboratory. IIT Research Institute, Chicago, Illinois. 1982.

Duggan, M. and Hamilton, R. "PM_{10} and Other Particulate Material" UPRC Air Quality Factsheets. Middlesex University, London, 1994.

Eglington, G., Hamilton, R. H., Raphael, R. A. and Gonzalez, A. G. "Hydrocarbon constituents of wax Coatings of Plant Leaves: A Taxonomic Survey", *Nature*, **193**: 739-742. 1962.

Eichmann, R., Neuling, P., Ketseridis, G., Hahn, J. Jaenicke, R. and Junge, C. "N-alkane Studies in the Troposphere - I: Gas and Particulate Concentrations in North Atlantic Air". *Atmospheric Environment*, **13**: 587-599. 1979.

Eichmann, R., Ketseridis, G., Schebeske, G., Jaenicke, R., Hahn, J., Warneck, P. and Junge, C. "N-alkane Studies in the Troposphere - II: Gas and Particulate Concentrations in Indian Ocean Air". *Atmospheric Environment*, **13**: 587-599. 1979.

Esmen, N. A. "Adhesion and Aerodynamic Resuspension of Fibrous Particles". *Journal of Environmental Engineering*, May: 379-383. 1996.

Farago, M., Kavanagh, P., Blanks, R., Simpson, P., Kazantzis, G. and Thornton, I. "Platinum Group Metals in the Environment: Their Use in Vehicle Exhaust Catalysts and Implications for Human Health in the UK". IC Consultants Ltd, Imperial College, London. 1995.

Farmer, C. T. and Wade, T. L. "Relationship of Ambient Atmospheric Hydrocarbons (C_{12}-C_{32}) Concentrations to Deposition". *Water, Air and Soil Pollution,* **29**: 439-452. 1986.

Fassina, V., Lazzarini, L. and Biscontin, G. "Effects of Atmospheric Pollutants on the Composition of Black Crusts Deposited on Venetian Marbles and Stones". In the *Proceedings of the Second International Symposium on the Deterioration of Building Stones*, Athens, 27th September-1st October 1976. NTU, Athens. 1976.

Fassina, V. "New Findings on Past Treatments Carried out on Stone and Marble Monuments' Surfaces". *Science of the Total Environment*, **167**: 185-203. 1995.

Faude, F. and Goschnick, J. "Surface Analytical Investigations on the Water Uptake of Combustion Aerosol Particles Before and After Exposure to Fluoranthene and Toluene". *Journal of Aerosol Science*, Vol **24**, Suppl 1: S293-S294. 1993.

Figler, B., Sahle, W., Krantz, S. and Ulfrarson, U. "Diesel Exhaust Quantification by Scanning Electron Microscope With Special Emphasis on Particulate Size Distribution". *Science of the Total Environment*, **193**: 77-83. 1996.

Fisher, G. L., Chang, D. P. Y. and Brummer, M. "Fly Ash Collected from Electrostatic Precipitators: Microcrystalline Structures and the Mystery of the Spheres". *Science*, Vol ??: 553-555. 1976.

Fisher, G. L., Prentice, B. A., Siberman, D., Ondov, M., Biermann, A. H., Ragaini, R. C. and McFarland, A. "Physical Morphological Studies of Size-Classified Coal Fly Ash". *Environmental Science and Technology*, **12**: 447-512. 1978.

Fitzgerald, J. W. "Marine Aerosol: A Review". *Atmospheric Environment*, **25A**: 533-601. 1991.

Fobe, B. O., Vleugels, G. J., Roekens, E. J., Van Grieken, R. E., Hermosin, B., Ortega-Calva, J. J., Del Junco, A. S and Saiz-Jimenez, C. "Organic and Inorganic Compounds in Limestone Weathering Crusts from Cathedrals in Southern and Western Europe", *Environmental Science and Technology*, Vol **29**, No 6: 1691-1701. 1995.

Freeman, M. "Air and Water Pollution Control: A Benefit-Cost Assessment". Wiley and Sons, New York. 1982.

Garland, J. A. "Resuspension of Particulate Material from Grass and Soil". AERE-R9452, HMSO, London. 1982.

Ghosh, A. and Ryszytiwskyj, W. P. "Removal of Glass Particles: A Review". In *Particles on Surfaces: Detection, Adhesion and Removal* (Ed. Mittal, K. L.). Marcel Dekker, New York, 1995.

Gill, P. S., Graedel, T. E. and Weschler, C. J. *Rev. Geophys. Space Phys*, **21**;903-920. 1983.

Goodwin, J. "UK Emissions of PM_{10}". NSCA/Middlesex University Joint Training Seminar on Particulate Air Pollution, Birmingham NEC, 31 January 1996.

Government Statistical Service. "The UK Environment", HMSO, London, 1992.
Graedel, T. E. and Crutzen, P. J. "Atmospheric Change: An Earth System Perspective". W. H. Freeman, NY. 1993.

Griest, W. H. and Tomkins, B. A. *Science of the Total Environment*, **36**:209-214. 1984.

Grimalt, J. O., Rosell, A., Simo, R, Saiz-Jimenez, C. and Albaiges, J. In *Organic Geochemistry: Advances and Applications in the Natural Environment* (Ed. Manning, D. A. C.) pp513-515. Manchester University Press, Manchester, UK. 1991.

Grosjean, D, Fung, K. and Harrison, J. "Interactions of PAH with Atmospheric Pollutants". Environmental Science and Technology, **17**: 673-679. 1983.

Gundel, L. A., Dalsey, J. A., de Carvalho, L. R. F., Kado, N. Y. and Schuetzle, D. "Polar Organic Matter in Airborne Particles: Chemical Characterisation and Mutagenic Activity". *Environmental Science and Technology*, **27**: 2112-2119. 1993.

Haagenrud, S. E. and Henriksen, J. F. "Survey of Dose Response (DR) Functions for Corrosion Damage on Materials". UN/ECE Workshop, 1997.

Hadi, D. A., Crossley, A. and Cape, J. N. "Particulate and Dissolved Organic Carbon in Cloud Water in Southern Scotland". *Environmental Pollution*, **88**: 299-306. 1995.

Hahn, L.A., Stukel, J. J., Leong, K. H. and Hopke, P. K. "Turbulent Deposition of Submicron Particles on Rough Walls". *Journal of Aerosol Science*, **16**, 1: 81-86. 1985.

Hamilton, R. and Mansfield, T. "Airborne Particulate Elemental Carbon: It's Sources, Transport and Contribution to Dark Smoke and Soiling". Paper presentation to Aerosols and

Background Pollution Conference, Galway, June 1989.

Hamilton, R. and Mansfield, T. "Airborne Particulate Elemental Carbon: It's Sources, Transport and Contribution to Dark Smoke and Soiling". *Atmospheric Environment*, **25A**: 715-724. 1991.

Hamilton, R. and Mansfield, T. "The Soiling of Materials in the Ambient Atmosphere". *Atmospheric Environment*, Vol **26A**, No 18: 3291-3296. 1992.

Hancock, R. P., Esmen, N. A. and Furber, C. P. "Visual Response to Dustiness". *Journal of Air Pollution Control Association*, **26**: 54-57. 1976.

Haneef, S. J., Johnson, J. B. Thompson, G. E. and Wood, G. C. "Simulation of the Degradation Limestones and Dolomitic Sandstone Under Dry Deposition Conditions". In Proceedings of the 12th International Corrosion Control and Low-Cost Reliability Volume II. National Association of Corrosion Engineers, Houston, Texas. 1993.

Hanel, G. "Influence of the Relative Humidity on Aerosol Deposition by Sedimentation". *Atmospheric Environment*, **16**: 2703. 1982.

Harrison, R. M. and Allen, A. G. "Measurements of Atmospheric HNO_3, HCl and Associated Species on a Small Network in Eastern England". *Atmospheric Environment*, **24A**: 369-376. 1990.

Harrison, R. M. and Jones, M. "The Chemical Composition of Airborne Particles in the UK". *The Science of the Total Environment*, **168**: 195-214. 1995.

Harrison, R.M. and Pio, C.A. "Major Ion Chemical Composition and Chemical Associations in Inorganic Atmospheric Aerosols". *Environmental Science and Technology*, **17**: 1733-1738. 1983.

Harrison, R. M. and Williams, C. R. "Airborne Cadmium, Lead and Zinc at Urban and Rural Sites in North-West England". *Atmospheric Environment*, **16**: 2669-2681. 1982.

Hauser, T. R. and Pattison, J. N. "Analysis of Aliphatic Fraction of Air Particulate Fraction". *Environmental Science and Technology*, **6**: 549-555. 1972.

Haynie, F. H. "Size Distribution of Particles that may Contribute to Soiling of Material Surfaces". *Journal of the Air Pollution Control Association*, Vol **35**, No. 5: 552-554. 1985.

Haynie, F. H. "Theoretical Model of Soiling of Surfaces by Airborne Particles". In *Aerosols: Research, Risk Assessment and Control Strategies: Proceedings of the Second U. S.-Dutch International Symposium* May 1985, (Ed. Lee, S. D., Schneider, T. Grant, L. D., Verkerk, P. J.) Lewis Publishers, Williamsburg, VA. 1986.

Haynie, F. H. and Lemmons, T. J. "Particulate Matter Soiling of Exterior Paints at a Rural Site". *Aerosol Science and Technology*, **13**:941-944. 1990.

Head Stone Mason, St Paul's Cathedral. Personal Communication. 1997.

Helmers, E., Mergel, N. and Barchet, R. "Platin in Klarrschlammasche und an Grasen" Umweltwissenschaften und Schadstoff-Forschnung - *Zeit. Umweltchem. Okotox.*,**6**, 3: 130-134. 1994.

Henderson, T. R., Sun, J. D., Li, A. P., Hansen, R., Bechtold, W. E., Harvey, R. M., Shabanowitz, J. and Hunt, D. C. *Environmental Science and Technology*, **18**: 428 1984.

Hering, S. V., Miguel, A. H. and Dod, R. L. "Tunnel Measurements of the PAH, Carbon Thermogram and Elemental Source Signature for Vehicular Exhaust". *Science of the Total Environment*, **36**: 39-45. 1984.

Hidy, G. M. "Definition and Characterisation of Suspended Particles in Air". Aerosols: Research, Risk Assessment and Control Strategies. Proceedings of the Second U.S.-Dutch International Symposium, Virginia, US; May 19-25, 1985.

Hilden, D. L. and Mayer, W. J. " The contribution of Engine Oil to Particulate Exhaust Emissions from Light Duty Diesel Powered Vehicles". SAE 841395, 1984.

Ho, W., Hidy, G. M., Govan, R. M. "Micro-wave Measurements of the Liquid Water Content of Atmospheric Aerosols". *Journal of Applied Meteorology*, **13**: 871-879. 1974.

Hodge, V. F. and Stallard, M. O. "Platinum and Palladium in Roadside Dust". *Environmental Science and Technology*, **20**: 1058-1060. 1986.

Hinds, W. C. "Aerosol Technology". Wiley Interscience, New York, NY. 1986.

Hollander, W. and Pohlmann. "Measurement of the Influence of Direct Particle Motion on the Turbulent Particle Deposition Velocity By Means of Laser Doppler Anemometry". *Particles and Particle System Characterisation*, **8**: 12-15. 1991.

Hollander, W., Windt, H. and Bo, Y. "Reduced Sticking Upon Brownian Contact of Submicrometer Particles Coated with and Organic Liquid". *Journal of Colloid and Interface Science*, **173**; 478-485. 1995.

Honeyborne, D. B. and Price, C. A. "Air Pollution and the Decay of Limestone". BRE Note 177/77. 1977.

Horvath, H. "Atmospheric Light Absorption - A Review". *Atmospheric Environment*, Vol **27A**, No 3: 293-317. 1993.

Horvath, H. *et al* "Experimental Determination of the Deposition of Particulate Matter to Building Surfaces", in *Particulate and Stone Damage: Final Report*, EC Contract EV5V CT94 0519. 1997.

Hutchinson, A. J., Johnson, J. B., Thompson, G. E., Wood, G. C., Sage, P. W. and Cooke, M. J. "The Role of Fly-Ash Particulate Material and Oxide Catalysts in Stone Degradation", *Atmospheric Environment*, Vol **26A**, No 15; 2795-2803. 1992.

Inkpen, R. Personal Communication. Faculty of Environment, Portsmouth University. 1997.

Iwado, H., Naito, M. and Hayatsu, H. "Mutagenicity and Antimutagenicity of Airborne Particulates". *Mutation Research*, **246**: 93-102. 1991.

Jaenicke, R. "Properties of Atmospheric Aerosols". *Land-holt-Bornstein's Numerical Data and Functional Relationships in Science and Technology*, Vol **4b**. Springer, Berlin. 1988.

Jaynes, S. M. and Cooke, R. U. "Stone Weathering in Southeast England". *Atmospheric Environment*, Vol **21**, No 7: 1601-1622. 1987.

Jones, M. and Harrison, R. M. in COMEAP "Medical Effects of Non-Biological Particles". HMSO, London, 1995.

Junge, C. E. and Maclaren, E. "Relationship of Cloud Nuclei Spectra to Aerosol Size Distribution and Composition". *Journal of Atmospheric Science*, **28**:382-390. 1971.

Kamens, R. M., Guo, Z., Fulcher, J. N. and Bell, D. A. "Influence of Humidity, Sunlight, and Temperature on the Daytime Decay of Polyaromatic Hydrocarbons on Atmospheric Soot Particles". *Environmental Science and Technology*, **22**, 1: 103-108. 1988.

Kamens, R. M., Guo, J., Guo, Z. and McDow, S. R. "PAH Degradation by Heterogeneous Reactions with N_2O_5 on Atmospheric Particles". *Atmospheric Environment*, **24A**: 1161-1173. 1990.

Keeler, G. J. "Effect of Relative Humidity on Dichotomous Sampler Coarse/Fine Ratios". *Atmospheric Environment*, **22**: 1715-1720. 1988.

Kelly, G. W., Bartle, K. D., Clifford, A. A. and Scammells, D. "Identification and Quantitation of Polycyclic Aromatic Compounds in Air Particulate and Diesel Exhaust Particulate Extractsby LC-GC". *Journal of Chromatographic Science*, **31**: 73-76. 1993.

Kendall, M., Rickard, A. and Kendall, A. "Quantification and Toxicity of PM_{10}-Associated Organic Compounds in London". Poster presentation to the International Conference on the Health Effects of Particulate Matter, Prague, 23-25 April, 1997.

Kendall, K. "Adhesion: Molecules and Mechanics". *Science*, **263** (5154): 1720-1725. 1994.

Kendall, M., Hamilton, R. S., Williams, I. D. and Revitt, D. M. "Smoke Emissions from Petrol and Diesel Engined Vehicles in the UK". Proceedings for the Dedicated Conference on The Motor Vehicle and the Environment - Demands of the Nineties and Beyond, Aachen Germany, 1994.

Kitto, A. N. and Harrison, R. M. "Nitrous and Nitric Acid Measurements at Sites in South-East England". *Atmospheric Environment*, **26A**: 235-241. 1992.

Kleinman, L. I. and Daum, P. H. *Journal of Geophysical Research*, **96**: 991. 1991.

Kolattukudy, P. E. "Plant Waxes". *Lipids*, **5**: 259-275. 1970.

Konig, H. P., Hertel, R. F., Koch, W., Rosner, G. "Determination of Platinum Emissions from a Three-Way Catalyst Equipped Gasoline Engine". *Atmospheric Environment*, **26A**, 5: 741-745. 1992.

Kordecki, M. C., Gladden, J. K. and Orr, C. Jnr. "Adhesion Between Solid Particles and Solid Surfaces". Final Report B-148, National Institute of Health, September 30, 1959.

Koutrakis, P., Wolfson, J. M., Spengler, J. D., Stern, B. and Franklin, C. A. "Equilibrium Size of Atmospheric Aerosol Sulphates as a Function of the Relative Humidity". *Journal of Geophysics*, **94**: 6442-6448. 1994.

Lal Gauri, K. and Holdren Jr., G. C. "Pollutant Effects on Stone Monuments". *American Chemical Society*, **15**, 4: 386-390. 1981.

Lammel, G. and Novakov, T. "Water Nucleation Properties of Carbon Black and Diesel Soot Particles". *Atmospheric Environment*, Vol **29**, No 7: 813-823. 1995.

Lanting, R. W. "Black Smoke and Soiling". In Aerosols: Research, Risk Assessment and Control Strategies: Proceedings of the Second U. S.-Dutch International Symposium, May 1985 (Ed. Lee, S. D., Schneider, T. Grant, L. D., Verkerk, P. J. Lewis Publishers, Williamsburg, VA. 1986.

Leaitch, W. R. and Isaac, G. A. *Atmospheric Environment*, **25A**: 601. 1991.

Lee, D. S. and Nicholson, K. W. "The Measurement of Atmospheric Concentrations and Deposition of Semi-Volatile Organic Compounds". *Environmental Monitoring and*

Assessment, **32**: 59-91. 1994.

Lee, D. S., Garland, J. A. and Fox, A. A. "Atmospheric Concentrations of Trace Elements Urban Areas of the UK". *Atmospheric Environment*, **28**: 2691-2713. 1994.

Lewin, S. Z. and Charola, A. E. "Plant Life on Stone Surfaces and it's Relation to Conservation". *Scanning Electron Microscopy*, **1**: 563-568. 1981.

Leysen, L., Roekens, E. and Van Grieken, R. "Air Pollution Induced Chemical Decay of a Sandy-Limestone Cathedral in Belgium". *Science of the Total Environment*, Vol **78**: 263-287. 1989.

Li, C. K and Kamens, R. M. "The Use of Polyaromatic Hydrocarbons as Source Signatures in Receptor Modelling". *Atmospheric Environment*, Vol **27A**, No 4: 523-532. 1993.

Lindskog, A., Brormstrom-Lunden, E., Sjodin, A. *Environment International*, **11**: 125-130. 1985.

Lightowlers, P. J. and Cape, J. N. "Sources and Fate of HCl in the UK and Western Europe". *Atmospheric Environment*, **22**: 7-15. 1988.

Lipfert, F. W. "Atmospheric Damage to Calcareous Stones: Comparison and Reconciliation of Recent Experimental Findings". *Atmospheric Environment*, Vol **23**, No. 2; 415-429. 1989.

Little, P. and Wiffen, R. D. "Emission and Deposition of Petrol Engine Exhaust Pb - I. Deposition of Pb to Plant and Soil Surfaces". *Atmospheric Environment*, **11**: 437-447. 1977.

Lodge, J. P., Waggoner, A. P., Klodt, D. T. and Crain, C. N. "Non-Health Effects of Airborne Particulate Matter". *Atmospheric Environment*, Vol **15**: 431-482. 1981.

Long, X. Agnew, C. and Rose, N. "Monitoring and Characterisation of Airborne Particles in Urban Areas" PhD Workshop, Geography Department, UCL, London. 24th January 1996.

Loyalka, S. K. and Griffin, J. L. *Nucl. Sci. Eng.* **114**:135. 1993.

Mansfield, T. and Hamilton R. "The Soiling of Materials: Models and Measurements in a Road Tunnel". In *Man and his Ecosystem, Proceedings 8th World Clean Air Congress*, The Hague, September. Edited by Brasser, L. J. and Mulder, W. C. Vol **2**: 353-358. 1989.

Mansfield, T. "The Soiling of Materials in Urban Areas". PhD Thesis, Middlesex Polytechnic, London, 1989.

Mansfield, T., Hamilton, R. Ellis, B. and Newby, P. "Diesel Particulate Emissions and the Implications for the Soiling of Buildings". *The Environment*, **11**, No. 4: 243-254. 1991.

Martin, K. G. and Souprounovich, A. N. "Soiling of Building Materials About Melbourne - An Exposure Study". *Australian Clean Air*, Vol **20**, No 3: 95-100. 1986.

Mason, B. "Principles of Geochemistry". J. Wiley and Sons, New York, NY. 1966.

McFarland, A. R., Ortiz, C. A and Rodes, C. E. "Wind Tunnel Evaluation of the British Smoke Shade Sampler". *Atmospheric Environment*, **16**: 325-328. 1982.

Mcgee, E. S. and Mosotti, V. G. "Gypsum Accumulation on Carbonate Stone". *Atmospheric Environment*, **26**, Part B: 249-253. 1992.

McInnes, G. "Multi-Element Survey: Summary and Trend Analysis, 1976/77 - 1988/89". WSL Report LR771-(AP)M, Warren Spring Laboratory, Stevenage, UK. 1990.

Meetham, A. R. "Natural Removal of Atmospheric Pollution During Fog". *Quarterly Journal of the Royal Meteorological Society*, Vol **80**: 96-99. 1954.

Meyer, M. B., Rupprecht, E. and Patashnick, H. "Considerations for the Sampling and Measurement of Ambient Particulate Mass". Presented at "Particualte Matter: Health and Regulatory Issues", Pittsburgh, PA, 4-6 April, 1995.

Meyer, M. B., Lijek, J. and Ono, D. M. "Continuous PM_{10} Measurements in a Woodsmoke Environment". In **Transactions, PM_{10} Standards and Non-Traditional Particulate Source Controls** (Edited by Chow, J. C. and Ono, D. M.): 24-38. Air and Waste Management Association, Pittsburgh, P. A. 1992.

Monk, J. Personal communication. Westminster Council Air Pollution Department. 1995.

Monn, Ch., Brandli, O., Schappi, G., Ackermann, U., Leuenberger, Ph. and SAPALDIA Team. "Particulate Matter 10 (PM_{10}) and Total Suspended Particulate in Urban, Rural and Alpine Air in Switzerland". *Atmospheric Environment*, **29**; 2573. 1995.

Monn, Ch., Carabias, V., Junker, M., Waeber, R., Karrer, M. and Wanner, H. U. "Small Scale Spacial Variability of Particulate Matter (PM_{10}) and Nitrogen Dioxide". *Atmospheric Environment*, Vol **31**, No 15: 2243-47. 1997.

Mungur, A. S. "The Performance and Perception of Wetland Systems for the Treatment of Highway Runoff". PhD Thesis, Middlesex University, London. 1997.

Murray, M. and Massey, S. Personal communications from BRE. 1996 and 1999.

Murray, M. "Use of Colour Measurement to Characterise Stone Type and Rates of Soiling on Exposure" BRE Draft Report PD 74/98. April 1998.

Nagy, B., Nagy, L. A., Rigali, M. J., Krinsley, D. H. and Sinclair, N. A. "Rock Varnish in the Sonoran Desert; Micro-biologically Mediated Accumulation of Manganiferous Sediments". *Sedimentology*, **38**, 1153-1171. 1991.

Nazaroff, W. W. and Cass, G. R. "Protecting Museum Collections from Soiling due to the Deposition of Airborne Particles". *Atmospheric Environment*, **25A**, No. 5/6B: 841-852. 1991.

Needham, J. R., Doyle, D. M., Faulkner, S. A. and Freeman, H. D., *Technology for 1994.* SAE Paper 891949, 1989.

Newby, P. T., Mansfield, T. A. and Hamilton, R. S. "Sources and Economic Implications of Building Soiling in Urban Areas". *Science of the Total Environment*, **100**: 347-365. 1991.

Nicholson, K. W. "A Review of Particle Resuspension". *Atmospheric Environment*, **22**: 2639-2651. 1988.

Nord, A. G. and Ericsson, T. "Chemical Analysis of Thin Black Layers on Building Stone". *Studies in Conservation*, **38**; 25-35. 1993.

Nord, A. G., Svardh, A. and Tronner, K. "Air Pollution Levels Reflected in Deposits on Building Stone". *Atmospheric Environment*, Vol **28**, No 16: 2615-2622. 1994.

Novakov, T., Mueller P. K. , Alcocer, A. E. and Otvos, J. W. "Chemical Composition of Pasadena Aerosol by Particle Size and Time of Day". Aerosol and Atmospheric Chemistry (Ed. Hidy, G). Academic Press, New York. 1972.

Novakov, T., Chang, S. G. and Harker, A. B. "Sulfates as Pollution Particulates: Catalytic Formation on Carbon (Soot) Particles". *Science*, **184**; 259-261. 1974.

Ogren, J. A. and Charleson, R. S. "Wet Deposition of Elemental Carbon and Sulphate in Sweden". *Tellus*, **36b**: 262-271. 1984.

Ostro, B. "The Association of Air Pollution and Mortality: Examining the Case for Inference". *Archives of Environmental Health*, Vol. **48**, No. 5: 336-342. 1993.

Pandis, S. N., Wexler, A. S. and Seinfeld, J. H. "Dynamics of Tropospheric Aerosols". *Journal of Physical Chemistry*, **99**: 9646 - 9649. 1995.

Pedace, E. A. and Sansone, E. B. "The Relationship Between Soiling Index and Suspended Matter Concentrations". *Journal of Air Pollution Control Association*, Vol. **22**, No. 5: 348-351. 1972.

Penner, J. E., Charlson, R. J., Hales, J. M., Laulainen, N. S., Leifer, R., Novakov, T., Ogren, J. Radke, L. F., Schwartz, S. E., Travis, L. *Bulletin of the American Meteorological Society*, **75**: 375. 1994.

Pio, C. A., Harrison, R. M., Castro, M. and Smith, D. J. T. Unpublished data, 1994.

Pio, C. A. Personal Communication. 1997.

Porter, M. C. "Membrane Filtration". In Handbook of Separation: 2-3. McGraw-Hill, New York, New York. 1979.

Pratsinis, S., Novakov, T., Ellis, E. C. and Friedlander, S. K. "The Carbon Containing Component of the Los Angeles Aerosol: Source Apportionment and Contribution to the Visibility Budget". *Journal of Air Pollution Control Association*, **34**: 634-650. 1984.

Pye, K. and Schiavon, N. "Cause of Sulphate Attack on Concrete, Render and Stone Indicated by Sulphur Isotope Ratios". *Nature*, Vol **342**:663-664. 1989.

Quality of Urban Air Review Group (QUARG). "Urban Air Quality in the UK". First Report. HMSO, UK, 1993.

Quality of Urban Air Review Group (QUARG). "Urban Air Quality in the UK"; Third Report. HMSO, UK, 1996.

Radojevic, M. and Harrison, R. M. (Eds). "Atmospheric Acidity: Sources, Consequences and Abatement". Elsevier Applied Science, London, 1992.

Ramdahl, T. "Polycyclic Aromatic Ketones in Environmental Samples". *Environmental Science and Technology*, **17**: 666-670. 1983a.

Rickard, A. and Ashmore, M. R. "The Size Fractionation and Ionic Composition of Airborne Particulates in the London Borough of Greenwich". *Clean Air*, Vol **26**, No 2: 37-42. 1996.

Roberts, M. and D.C.M. Urquhart (1995). Stonecleaning and stone decay. Research Report to Historic Scotland. Robert Gordon University, Aberdeen.

Rocha, A. P. and Duarte, A. C. "Application of Chemometrics to the Application of Trends in Polynuclear Aromatic Hydrocarbons and Alkanes in Air Samples from Oporto". *Analyst*, Vol **122**: 1-7. 1997.

Rodriguez-Navarro, C. and Sebastian, E. "Role of Particulate Matter from Vehicle Exhaust on Porous Building Stones (Limestone) Sulfation (sic)". *Science of the Total Environment*, 187; 79-91. 1996.

Rogge, W. F., Mazurek, M. A., Hildemann, L. M., Cass, G. R. and Simoneit, B. R. T. "Quantification of Urban Organic Aerosols at a Molecular Level: Identification, Abundance and Seasonal Variation". *Atmospheric Environment*, Vol **27A**, No 8: 1309-1330. 1993.

Roth, E. P. and Anaya, A. J. "The Effect of Natural Cleaning On the Size Distribution of Particles Deposited on Silvered Glass Mirrors". Second Solar Reflective Materials Workshop, San Francisco, California, February 12-14, 1980.

Sabbioni, C. and Zappia, G. "Decay of Sandstone in Urban Areas Correlated with Atmospheric Aerosol". *Water, Air and Soil Pollution*, **63**: 305-316. 1992.

Sabbioni, C., Zappia, G. and Gobbi, G. "Carbonaceous Particles on Carbonate Building Stones in a Simulated System". *Journal of Aerosol Science*, **23**: S921-S924. 1992.

Sabbioni, C. and Zappia, G. "Characterization of Particles Emitted by Domestic Heating Units Fuelled by Distilled Oil". *Atmospheric Environment*, **27A**, No. 8: 1331-1338. 1993.

Sabbioni, C. "Contribution of Atmospheric Deposition to the Formation of Damage Layers". *Science of the Total Environment*, **167**; 49-55. 1995.

Saiz-Jimenez, C. and Bernier, F. "Gypsum Crusts on Building Stones: A SEM Study". Paper 81/10/5. In 6th Triennial Meeting ICOM, Committee for Conservation, Ottawa. 1981.

Saiz-Jimenez, C. "Analytical Approaches for the Study of Organic Compounds in Weathered Building Stones". In *Analytical Methodologies for The Investigation of Weathered Stones: Advanced Workshop*, Pavia, 1990.

Saiz-Jimenez, C. "Deposition of Airborne Organic Pollutants on Historic Buildings". *Atmospheric Environment*, Vol. **27B**, No. 1: 77-85. 1993.

Saiz-Jimenez, C. Hermosin, B. and Ortega-Calvo, J. J. "Pyrolysis/Methylation: A Microanalytical Method for Investigating Polar Organic Compounds in Cultural Properties". *International Journal of Environmental Chemistry*, Vol **56**: 63-71. 1994.

Salmon, L. G., Christoforou, C. S., Gerk, T. J., Cass, G. R., Casuccio, G. S., Cooke, G. A., Leger, M. and Olmez, I. "Source Contributions to Airborne Particle Deposition at the Yungang Grottoes, China". *Science of the Total Environment*, **167**; 33-47. 1995.

Savoie, D. L. and Prospero, J. M. *Nature*, **339**: 685. 1989.

Schaffer, R. J. "The Weathering of Natural Building Stones". DSIR Building Research Special Report, 18. 1932.

Schiavon, N., Chiavari, G., Schiavon, G. and Fabbri, D. "Nature and decay Effects of Urban Soiling on Granitic Building Stones". *Science of the Total Environment*, **167**; 87-101. 1995.

Schiavon, N. and Zhou, L. "Magnetic, Chemical and Microscopical Characterisation of Urban Soiling on Historic Monuments". *Environmental Science and Technology*, Vol **30**, No **12**: 3624-3629. 1996.

Schiavon, N. "Soiling of Urban Granite 1: Microfabrics and Mineralogical Aspects". *Degradation and Conservation of Granitic Rocks in Monuments*, Protection and Conservation of European Cultural Heritage, Research Report No. **5**: 301-306. 1996.

Schneider, H. "Mechanical Removal of Spacecraft Microbial Burden". Subtask I of Spacecraft Cleaning and Decontamination Techniques, Chapter 6 in Planetary Quarantine, Annual Review. Space Technology and Research, JPL TR-900-597, Jey Propulsion Laboratory, Pasadena, California. February 1973.

Schuster, P. F., Reddy, M. M. and Sherwood, S. I. "Effects of Acid Rain and Sulfur (sic) Dioxide on Marble Dissolution". *Material Performance*, **33**: 76-80. 1994.

Sehmel, G. A. "The Agglomeration of Solid Aerosol Particles" M. S. Thesis, University of Illinois. 1956.

Sehmel, G. A. "Dry Deposition: A Review". *Atmospheric Environment*, Vol **14**, 9: 983-1011.

Sehmel, G. A. "Particle Resuspension from an Asphalt Road Caused by Car and Truck Traffic". *Atmospheric Environment*, **7**: 291-301. 1973.

Sehmel, G. A. and Hodgeson, W. H. "A Model for Predicting Dry Deposition of Particles and Gases to Environmental Surfaces". PNL-SA-6721, Batelle, Pacific Northwest Laboratory, Richland, W. A. 1978.

Sengupta, M. and de Gast, A. A. "Environmental Deterioration and Evaluation for Dimension Stone". *CIM Bulletin*, **65**: 54-58. 1972.

Sharp, A. D. Trudgill, S. T., Cooke, R. U., Price, C. A., Crabtree, R. W., Pickles, A. M. and Smith, D. I. "Weathering of the Balustrade on St Paul's Cathedral". *Earth Surface Processes and Landforms*, **7**: 387-389. 1982.

Sheu, H.-L., Lee, W.-J., Su, C.-C., Chao, H.-R. and Fan, Y.-C. "Dry Deposition of Polycyclic Aromatic Hydrocarbons in Ambient Air". *Journal of Environmental Engineering*, Vol **122**, No 12: Decmber, 1101-1109. 1996.

Sicre, M. A., Marty, J. C., Saliot, A., paricio, X., Grimalt, J. and Albairges, J. "Aliphatic and Aromatic Hydrocarbons in Different Sized Aerosols Over the Mediterranean Sea: Occurrence and Origin". *Atmospheric Environment*, **21**: 2247. 1987.

Simoneit, B. R. T. "Air Pollution: The Organic Components". CRC Critical Reviews in Environmental Control. May 1981.

Simoneit, B. R. T. and Mazurek, M. A. "Organic Matter in the Troposphere - II: Natural Background of Biogenic Lipid Matter in Aerosols over the rural Western United States". *Atmospheric Environment*, **16**: 2139-2159. 1984.

Simoneit, B. R. T. "Organic Matter of the Troposphere - III: Characterisation and Sources of Petroleum and Pyrogenic Residues in Aerosols over the Western United States". *Atmospheric Environment*, **18**, 1: 51-67. 1983.

Simoneit, B. R. T. *The Science of the Total Environment*, **36**: 61-72. 1984.

Simoneit, B. R. T. "Application of Molecular Marker Analysis to Vehicular Exhaust for Source Reconciliations". *International Journal of Environmental and Analytical Chemistry*, **22**: 203-233. 1985.

Simpson, P. R., Robotham, H. and Hall, G. E. M. "Regional Geochemical Orientation Studies for Platinum". *Trans Instn. Mineralogy and Metallurgy* (Section B: Applied Earth Science), **99**: B183-B187. 1990.

Sitzmann, B., Kendall, M., Watt, J. and Williams, I. D. "Personal Exposure Study of Cyclists to Airborne Particulate Matter". Poster presentation at European Aerosol Conference, Delft, 9-12th September 1996.

Slinn, W. G. N. *Journal of Water, Air and Soil Pollution*, **7**: 513. 1977.

Slinn, W. G. N., Hasse, L., Hicks, B. B., Hogan, A. W., Lal, D., Liss, P. S., Munnich, K. O., Sehmel, G. A. and Vittorio, O. *Atmospheric Environment*, **12**: 2055. 1978.

Smith, R. A. "The Beginnings of a Chemical Climatology". Longman Publishing, London, UK. 1872.

Smith, D. J. T. and Harrison, R. M. Unpublished Data, Birmingham University. 1994.

Smith, D. J. T. and Harrison, R. M. "Concentrations, Trends and Vehicle Source Profile of Polynuclear Aromatic Hydrocarbons in the UK Atmosphere". *Atmospheric Environment*, Vol **30**, No 14: 2513-2525. 1996.

Stephanou, E. G. and Stratigakis, N. E. "Determination of Anthropogenic and Biogenic Organic Compounds in Airborne Particles: Flash Chromatographic Fractionation and Capillary Gas Chromatographic Analysis". *Journal of Chromatography*, **644**: 141-151. 1993.

Sturges, W. T., Harrison, R. M. and Barrie, L. A. "Semi-Quantitative X-Ray Diffraction Analysis of Size Fractionated Atmospheric Particles". *Atmospheric Environment*, **23**, No. 5: 1083-1098. 1989.

Taylor, G. J and Crowder, A. A. "Uptake and Accumulation of Copper, Nickel and Iron by *Typha latifolia* Grown in Solution Culture". *Canadian Journal of Botany*, **61**(7): 1825-1830. 1983.

Terrat, M.-N. and Joumard, R. "The Measurement of Soiling". *Science of the Total Environment*, **93**: 131-138. 1990.

Thurston, G. D. and Spengler, J. D. "A Quantitative Assessment of Source Contributions to Inhalable Particulate Matter Pollution in Metropolitan Boston". *Atmospheric Environment*, **19**:9-25.1985.

Tombach, I. "Conservation of Historic Stone Buildings and Monuments". In *Measurement of Local Climatogical and Air Pollution Factors Affecting Stone Decay*, National Research Council Report, 14: 197-207. 1982.

Trudgill, S. T., Viles, H. A., Cooke, R. U. and Inkpen, R. J. *Atmospheric Environment*, **24B,** No 2: 361-363. 1990.

Trudgill, S. T., Viles, H. A., Cooke, R. U., Inkpen, R. J., Heathwaite, A. L. and Houston, J. "Trends in Stone Weathering and Atmospheric Pollution at St Paul's Cathedral in London 1980-90". *Atmospheric Environment*, **25,** No 12: 2851-2853. 1991.

Trijonis, J. "Development and Applications for Estimating Inhalable and Fine Particle Concentrations from Routine Hi-Vol Data". *Atmospheric Environment*, **17**: 999-1008. 1983.

US EPA (United States Environmental Protection Agency). "Review of the National Ambient Air Standards for Particulate Matter: Assessment of Scientific and Technical Information". Staff Paper (Final), EPA-450/5-82-001. Environmental Protection Agency, Research Triangle Park, NY. 1982.

US EPA (United States Environmental Protection Agency). "Ambient Air Quality Standards for Particulate Matter". 40 CFR Parts 50-53 and 58, Federal Register 52: 24634-24750. Environmental Protection Agency, Research Triangle Park, NY. 1987.

US EPA (United States Environmental Protection Agency). "Air Quality Criteria for Particulate Matter". Vol II, Section 9: 1-54. Environmental Protection Agency, Research

Triangle Park, NY. 1996.

Urone, P., Lutsep, C. M., Noyes, C. M. and Parcher, J. " Statistic Studies of Sulphur Dioxide Reactions in Air". *Environmental Science and Technology*, **2**; 611-618. 1968

van Aalst, R. M. "Dry Deposition of Aerosol Particles". In Aerosols: Research, Risk Assessment and Control Strategies: Proceedings of the Second U. S.-Dutch International Symposium (May 1985), edited by Lee, S. D., Schneider, T. Grant, L. D., Verkerk, P. J. Lewis Publishers, Williamsburg, VA. 1986.

Van Borm, W. A., Adams, F. C. and Maenhaut, W. "Characterisation of Individual Particles in the Antwerp Aerosol". *Atmospheric Environment*, **23**: 1139-1151. 1989.

Van Cauwenberghe, K. A. "Atmospheric Reactions of PAH" In *Handbook of Polycyclic Aromatic Hydrocarbons* Vol. **2**: Emission Sources and Recent Progress in Analytical Chemistry (Ed. Bjorseth, A. and Ramdahl, T.). MArcel Dekker, New York. 1983.

Van Cauwenberghe, K. A. "Sampling, Size Distribution, Reactivity and Analysis of Organic Aerosol Constituents". Aerosols: Research, Risk Assessment and Control Strategies. Proceedings of the Second U.S.-Dutch International Symposium, Virginia, US; May 19-25, 1985.

Van Cauwenberghe, K. A. "Aerosols". Lewis Publishers, Michigan, 1986.

Viles, H. A. "The Early Stages of Building Stone Decay in an Urban Environment". *Atmospheric Environment*, Vol **24A**, No 1: 229-232. 1990.

Vicente, M. A., Delgado-Rodrigues, J. and Acevedo, J. (Ed.s) "Degradation and Conservation of Granitic Roacks in MOnuments". Proceedings of the EC Workshop held in santiago de Compostela, 28-30 November 1994. Protection and Conservation of European Cultural Heritage Research Report, No 5. EC, Brussels. 1996.

Vincent, K. J. "Atmospheric Particulate Matter and Historic Buildings". PhD Thesis, Middlesex University, London. 1993.

Visser, J. *Surface Colloid Science*, **8**: 3. 1975.

Waller, R. E. "Studies on the Nature of Urban Air Pollution". London Conference on Museum Climatology, International Institute for Renovation of Works of Art; 65-69. 1967.

Warneck, P. "Chemistry of the Natural Atmosphere". Academic Press, New York, NY. 1988.

Watt, J. and Kendall, M. "Particulate Pollution and Stone Damage". Final Report of EC

Contract: EV5V-CT94-0519. Middlesex University, January 1997.

Webster, R.G.M., C.A. Andrew, S. Baxter, J. MacDonald, M. Rocha, B.W. Thomson, K.H. Tonge, D.C.M. Urquhart and M.E. Young (1992). Stonecleaning in Scotland - Research Report, Volumes 1-3, Report to Historic Scotland and Scottish Enterprise by Masonry Conservation Research Group, Gilcomston Litho, Aberdeen. Vol 1: ISBN 0 7480 0449 1, Vol 2: ISBN 0 7480 0450 5, Vol 3: ISBN 0 7480 0451 3

Webb, A. H., Bawden, R. J., Busby, A. K. and Hopkins, J. N. "Studies on the Effects of Air Pollution on Limestone Degradation in Great Britain". *Atmospheric Environment*, 26, Part B:165-181. 1992.

Wells, A. C. and Chamberlain A. C. "Transport of Small Particles to Vertical Surfaces". *British Journal of Applied Physics*, **18**: 1793-1799. 1967.

Wei, C. and Morrison, G. M. "Platinum Analysis and Speciation in Urban Gullypots". *Anal. Chim. Acta.*, **284**: 587-592. 1994.

Weingartner, E., Baltensperger, U. and Burtscher, H. "Growth and Structural Change of Combustion Aerosols at High Relative Humidity". *Environmental Science and Technology*, **29**: 2982-2986. 1995.

Whalley, B., Smith, B. and Magee, R. "Effects of particulate Air Pollutants on Materials: Investigation of Surface Crust Formation". In *Stone Cleaning and the Nature, Soiling and Decay Mechanisms of Stone Decay* (Ed. Webster, R. G. M.). 1992.

Wild, S. R. and Jones, K. C. "PAH in the UK Environment: A Preliminary Source Inventory and Budget". *Environmental Pollution*, **88**: 91-108. 1995.

Williams, P. T., Andrews, G. E. and Bartle, K. D. "PAC in Diesel Fuels and Exhaust Particulates"". In *Polynuclear Aromatic Hydrocarbons: Chemistry, Characterisation and Carcinogenesis* (Ed. Cooke, M. and Dennis, A. J.), Battelle Press, Columbus Ohio. 1986.

Williams, P. T. "The Sampling and Analysis of Polycyclic Aromatic Compounds From Combustion Systems: A Review" Engine Emissions Measurement, 3-6 July, 1995. Leeds University.

Winkler, P. "The growth of Atmospheric Particles with Relative Humidity", *Physica Scripta*, **37**: 223-230. 1988.

Winkler, E. M. and Singer, P. C. "Crystallisation Pressures of Salts in Stone and Concrete". *Geol. Soc. Am. Bull.*, **83**; 3509-3514. 1972.

Yamasaki, H., Kuwata, K. and Miyamoto, H. "Effects of Ambient Temperature on Aspects of Airborne Polycyclic Aromatic Hydrocarbons", *Environmental Science and Technology*, 16: 189-194. 1982.

Yerrapragrada, S. S., Jaynes, J. H., Chirra, S. R. and Gauri, K. L. "Rate of Weathering of Marble due to Dry Deposition of Ambient Sulfur (sic) and Nitrogen Dioxides". *Analytical Chemistry*, **66**: 655-659. 1992.

Ying Xie and Hopke, P. K. "Airborne Particle Classification with a Combination of Chemical Composition and Shape Index Utilizing an Adaptive Resonance Artificial Neural Network". *Environmental Science and Technology*, **28**: 1921-1928. 1994.

Yocom, J. E. and Upham, J. B. "Effects on Economic Materials and Structures". In: *Air Pollution: Vol. 11, The Effects of Air Pollution*. 3rd Edition. Academic Press, Inc., New York, NY. 1977.

APPENDIX 1 Raw Soiling Measurement Data

Table A1 Reflectance Measurements of Samples Exposed in London (Expressed as %)
Blanks indicate missing data

	Protected Stone Samples				Unprotected Stone Samples				Protected Wood Samples				Unprotected Wood Samples			
Day No.	NW	NE	SE	SW	NW	NE	SE	SW	NW	NE	SE	SW	NW	NE	SE	SW
0	52	51	52	56	58	56	55	53	89	89	89	87	90	90	90	89
9	53	51	53	56	56	57	56	54	89	89	89	87	88	89	90	89
15	51	51	52	56	55	56	54	52	87	87	86	85	86	87	85	86
22	51	51	54	55	55	56	53	52	86	86	85	85	86	86	84	84
29	51	50	52	55	54	55	52	51	85	86	85	84	85	85	85	85
36	51	51	52	55	53	55	52	51	85	86	85	84	85	84	84	85
43	52	51	53	56	53	55	52	50	85	87	85	84	84	84	84	83
49	49	50	50	54	52	54	52	51	82	84	82	81	82	84	82	84
56	39	48	50	43	39	39	38	38	82	85	84	81	83	85	82	82
63																
70	49	50	49	54	53	53	53	52	82	84	83	81	81	85	81	83
78	48	50	49	53	51	53	52	51	83	83	83	80	82	84	80	82
85	49	51	49	54	52	54	53	52	83	84	83	81	82	84	80	82
92	49	50	49	53	51	53	52	52	83	84	82	80	81	84	80	82
99	49	51	49	54	52	54	53	52	82	84	82	80	81	84	80	81
105																
112	48	50	48	52	51	52	44	52	83	83	81	80	79	83	79	81
119	48	50	48	52	54	52	50	52	82	82	80	79	78	81	77	80
126	49	50	49	53	54	54	49	52	82	83	81	79	79	83	78	80
133	48	49	48	51	53	53	54	51	81	80	79	80	76	81	77	78
140	48	50	48	52	54	54	55	52	81	81	80	80	76	82	76	78
147	49	50	49	53	52	54	54	53	81	82	80	80	77	82	78	79
154	48	50	49	53	52	54	54	52	81	83	81	80	76	81	77	78
161	48	50	48	51	40	51	48	42	80	81	80	79	76	80	77	78
168	49	52	50	52	50	52	55	52	80	82	81	79	76	81	77	78
175	47	50	49	52	55	53	55	52	80	80	81	79	75	80	77	79
182	48	50	48	51	52	52	53	52	80	80	81	78	75	81	77	78
189																
196	48	50	48	51	52	52	54	52	80	80	81	79	74	80	77	78
203	47	49	48	52	52	52	55	52	79	79	79	80	75	81	77	75
211																

Reflectance Measurements of Samples Exposed in London (Expressed as %)
Blanks indicate missing data

218	48	49	48	50	52	52	55	52	80	79	80	78	74	80	77	77
225																
232																
242																
246																
253																
260																
267	46	48	46	49	53	54	55	52	77	76	78	77	71	78	75	76
274	46	48	45	49	51	53.5	55	51	76.5	76	78	76	70	77	74	74

Table A2 Reflectance Measurements of Samples Exposed in Vienna (Expressed as %)
Blanks indicate missing data

	Protected Stone Samples				Unprotected Stone Samples				Protected Wood Samples				Unprotected Wood Samples			
Day No.	N	S	E	W	N	S	E	W	N	S	E	W	N	S	E	W
0	87.0	93.0	95.8	86.4	93.0	90.7	92.7	92.2	102.0	105.4	106.1	101.0	102.7	101.0	104.1	101.9
61	86.9	90.4	94.6	80.9	81.8	79.0	81.6	80.3	94.4	93.8	96.8	93.2	93.4	92.9	94.9	93.4
73	86.3	89.6	94.0	80.1	80.6	76.4	81.6	77.8	93.4	92.7	96.1	92.3	91.8	90.6	93.6	91.2
82	85.7	89.4	93.8	79.7	81.0	76.2	80.9	76.9	93.5	92.9	95.9	92.1	91.6	91.3	93.3	91.3
90	86.0	89.5	93.0	79.4	80.7	75.9	81.0	76.2	93.3	92.5	95.6	91.9	91.3	90.6	92.8	91.1
97	85.8	89.2	93.1	79.1	81.2	79.1	81.3	77.6	92.9	92.0	95.5	91.7	92.5	90.5	93.8	90.6
104	85.6	88.9	93.1	79.2	81.0	77.8	80.5	77.3	92.9	92.2	95.5	91.5	91.9	89.4	93.4	90.4
110	85.2	88.5	92.3	78.7	80.4	77.1	80.1	76.7	92.1	91.9	95.1	91.3	91.3	88.7	93.0	89.8
119	85.3	88.7	92.8	78.9	81.1	76.3	80.1	76.9	92.1	91.9	95.1	91.1	91.9	88.7	93.2	90.0
125	84.8	87.8	91.7	78.4	80.1	75.8	79.0	76.8	91.3	91.5	94.2	90.6	90.8	86.9	92.1	89.0
131	84.8	88.0	91.7	78.2	80.1	75.8	79.0	76.5	90.9	91.0	94.0	90.2	90.3	86.6	91.7	88.5
139	85.0	88.1	92.1	78.8	80.7	75.7	78.8	77.1	90.8	91.6	93.9	90.1	90.3	87.0	91.7	86.6
146	84.5	87.7	91.7	77.9	80.5	75.2	78.7	77.4	89.8	91.1	93.5	89.5	89.8	86.8	91.1	88.5
152	85.1	88.0	91.5	78.5	80.8	76.6	79.0	79.2	89.9	91.1	93.4	89.7	90.3	86.6	91.0	88.3
160	84.6	87.4	91.4	77.8	80.4	76.2	78.7	78.7	89.4	91.2	93.5	88.8	90.6	86.6	91.0	87.4
166	83.7	87.3	91.2	77.2	81.4	76.8	78.6	81.5	89.0	91.6	93.2	89.3	89.7	86.0	90.8	87.5
175	84.2	85.4	91.3	80.2	80.5	81.0	78.5	83.0	90.2	92.3	93.1	90.0	89.9	86.1	90.5	86.9
181	85.4	85.7	91.7	80.3	81.3	80.9	78.8	83.4	90.4	93.0	92.5	90.0	90.0	86.4	90.6	86.8
195	84.5	84.8	91.0	79.6	82.0	81.2	81.0	83.3	89.2	91.4	92.2	88.9	89.5	85.6	90.6	85.9
202	83.1	83.1	91.8	79.2	82.4	81.5	80.6	83.2	89.5	91.4	92.0	89.0	89.3	85.7	90.7	85.7
210	83.7	83.2	90.8	79.8	82.2	82.2	80.4	83.8	88.7	90.8	90.6	88.6	89.2	85.5	90.4	85.4
216	83.3	82.8	90.7	79.6	81.9	81.2	80.5	82.9	88.0	89.6	89.5	87.6	88.9	85.0	90.2	85.3
225	83.1	82.6	90.4	79.2	81.5	81.1	80.4	82.7	87.8	89.6	89.6	87.5	88.4	84.9	89.8	84.9
233	82.9	81.7	90.6	79.4	84.4	82.7	81.8	83.3	88.3	89.7	89.7	87.6	89.1	84.7	89.8	84.4
239	81.8	81.1	90.6	78.2	84.6	82.2	84.6	83.0	87.9	90.1	89.7	87.9	88.4	84.5	89.5	84.0
246	82.2	81.4	90.6	78.5	84.3	82.6	84.5	83.5	88.2	90.2	89.8	87.7	88.1	84.2	89.1	83.6
252	82.3	81.2	90.5	78.6	84.1	82.0	84.4	82.8	88.3	90.4	89.9	87.7	87.9	84.1	88.8	83.9
261	82.4	81.4	90.4	78.4	83.7	82.0	84.1	82.9	88.2	90.4	89.8	87.7	87.4	84.0	88.9	83.6
267	82.2	81.0	90.6	78.2	83.4	81.7	83.5	83.3	88.2	90.3	90.2	87.5	87.9	83.9	89.1	83.7
275	81.5	80.5	89.7	78.0	83.6	81.8	85.4	83.5	87.5	89.7	89.3	87.2	87.9	83.8	88.4	83.3

Reflectance Measurements of Samples Exposed in Vienna (Expressed as %)
Blanks indicate missing data

	Protected Stone Samples				Unprotected Stone Samples				Protected Wood Samples				Unprotected Wood Samples			
Day No.	N	S	E	W	N	S	E	W	N	S	E	W	N	S	E	W
281	81.9	80.8	90.0	78.0	83.7	81.4	85.6	83.4	87.3	89.7	89.1	87.0	87.4	83.3	88.1	82.9
293	81.3	79.6	89.7	77.2	85.8	81.8	87.9	82.4	86.5	88.8	88.7	86.2	86.0	81.6	85.6	80.7
309	81.1	79.3	89.4	77.2	85.2	80.7	86.5	82.3	85.9	88.6	88.1	85.7	84.5	80.3	81.5	80.5
332	80.0	78.6	89.1	76.6	82.7	77.8	83.5	80.1	85.6	88.0	87.8	85.3	82.2	78.2	79.2	77.4
338	80.2	79.0	89.3	76.2	82.2	76.9	83.3	78.6	85.1	88.5	87.8	85.3	84.3	79.4	81.8	80.0
343	80.0	78.6	88.8	76.4	81.2	76.1	82.1	77.8	84.6	87.9	87.4	84.7	83.6	78.6	81.1	79.2
350	79.9	78.2	88.5	76.3	83.4	78.6	85.0	82.8	84.0	87.6	87.2	84.6	83.9	79.9	81.5	80.1
356	80.1	78.1	88.6	75.9	82.2	77.5	83.9	83.0	84.2	88.9	86.9	84.6	83.8	80.3	82.1	82.6
362	79.5	77.8	88.6	75.8	83.0	78.7	85.0	83.4	83.9	88.4	86.9	84.5	84.5	80.4	82.3	83.1
369	78.7	77.1	88.0	75.3	82.1	77.5	83.1	82.6	83.3	88.5	83.6	84.0	84.0	79.5	81.2	82.5
379	78.4	77.5	88.3	75.2	81.8	77.0	83.1	82.2	82.8	86.8	86.2	83.4	83.0	78.4	80.8	81.1
393	78.2	77.3	88.7	74.7	81.5	77.5	81.9	82.9	84.5	86.8	86.2	84.9	83.7	81.0	80.8	84.2

Table A3 Reflectance Measurements of Samples Exposed in Breitenfurt (Expressed as %)
Blanks indicate missing data

	Protected Stone Samples				Unprotected Stone Samples				Protected Wood Samples				Unprotected Wood Samples			
Day No.	N	S	E	W	N	S	E	W	N	S	E	W	N	S	E	W
0	94.7	79.1	89.0	87.8	92.6	86.8	87.1	86.7	100.5	94.4	99.6	101.9	100.3	98.0	101.5	100.0
3	94.6	79.7	90.9	89.1	94.0	86.8	87.2	87.5	94.0	86.8	87.2	87.5	99.7	97.6	101.2	99.8
43	94.6	80.2	90.8	87.9	84.7	87.1	88.0	83.2	100.6	94.4	99.2	102.4	98.9	96.5	101.0	98.4
54	95.1	81.0	91.9	87.7	85.5	86.9	89.2	83.7	101.4	95.3	100.3	103.8	99.1	97.8	102.4	98.5
107	97.8	83.8	92.2	86.2	87.3	88.0	92.7	86.0	96.5	90.6	94.2	97.7	93.1	92.7	98.5	93.0
118	98.5	85.2	93.5	87.1	87.1	89.3	92.1	87.0	97.3	91.9	95.4	98.6	93.7	93.7	99.4	93.8
127	99.7	86.0	93.8	87.3	86.3	89.3	92.1	86.4	100.0	92.1	95.7	98.9	93.0	93.7	99.5	93.2
135	98.6	84.7	92.7	86.8	87.1	90.2	95.0	86.0	99.3	91.4	94.9	98.2	93.0	93.5	99.0	93.4
142	99.0	85.1	93.1	86.8	88.3	90.8	95.8	87.2	99.1	91.3	94.6	98.3	92.3	92.9	98.5	92.7
149	98.6	84.9	92.9	86.7	88.4	90.5	95.8	87.5	99.0	91.2	94.8	98.1	92.0	92.4	98.0	92.5
156	99.1	85.0	93.2	86.7	88.2	91.2	97.0	87.9	98.7	90.6	94.4	97.4	91.3	92.6	97.8	92.0
163	98.7	85.0	92.8	86.7	85.5	90.1	96.2	78.6	98.0	90.0	93.6	96.8	90.5	91.6	96.8	91.0
169	98.5	85.1	92.9	86.4	88.6	91.5	97.2	88.2	97.6	89.8	93.5	96.5	90.3	91.3	96.3	90.7
175									98.1	90.4	93.8	97.3	90.1	92.4	96.9	91.0
184	99.6	85.6	93.9	87.3	89.0	91.1	97.8	89.9	97.6	90.2	93.6	96.9	89.6	91.8	96.7	90.4
191	99.0	85.3	93.3	86.7	89.2	91.2	97.5	89.6	97.3	89.8	93.1	96.4	89.5	91.5	95.9	89.8
219	99.4	85.6	93.6	87.5	89.7	91.4	97.8	90.1	96.9	89.6	93.0	96.1	88.8	92.0	95.6	88.8
225	99.4	85.4	93.4	87.0	89.6	90.5	97.6	90.0	97.1	89.6	93.1	96.2	88.2	91.6	95.8	88.2
233	99.6	85.4	93.6	86.9	88.9	91.4	97.9	89.5	97.2	89.7	93.2	96.4	88.2	91.3	96.1	88.1
240	99.1	84.9	92.9	86.2	88.9	91.6	97.9	88.9	96.7	89.0	92.5	95.7	87.8	91.1	95.4	87.4
247	99.1	84.9	93.0	86.5	89.0	90.6	97.2	89.3	96.2	88.8	92.4	95.5	87.3	90.8	95.0	87.0
253	99.0	85.2	92.9	86.6	89.1	90.7	97.6	89.4	96.2	88.9	92.3	95.5	87.4	91.4	95.0	87.4
297	99.2	84.1	92.9	86.1	89.6	90.2	97.2	90.6	96.0	88.3	92.2	95.5	86.3	91.9	95.5	87.6
304	99.8	85.3	93.4	86.8	88.8	90.8	97.7	89.8	96.4	88.9	92.5	96.1	87.2	92.3	95.6	87.8
310	99.8	85.3	93.2	86.0	88.6	90.5	96.8	89.0	96.2	88.4	92.3	95.8	86.8	91.1	94.2	86.3
317	100.2	86.2	94.0	87.3	89.3	90.8	96.5	90.1	96.0	88.5	92.3	95.6	85.9	91.1	95.0	87.2
324									95.8	88.5	92.5	95.5	84.7	90.9	93.9	86.1
331	99.9	86.0	93.7	86.7	87.8	90.8	97.2	87.4	95.2	87.8	91.7	95.0	83.1	89.9	92.9	83.9
373	100.2	85.9	94.2	86.7	85.5	87.7	95.7	84.9	95.5	88.3	92.2	95.4	81.8	88.4	91.5	83.1
379									95.5	87.7	91.6	95.0	81.4	88.4	90.9	83.1
414	99.8	85.2	93.6	85.9	86.6	88.8	97.0	87.2	94.7	87.5	91.3	94.6	81.5	87.9	91.2	82.9
422	99.6	84.3	93.3	85.1	86.3	88.3	96.8	86.7	95.4	87.9	91.1	94.9	83.8	88.0	89.4	82.3

Table A4 Reflectance Measurements of Samples Exposed in Oporto (Expressed as %)
Blanks indicate missing data

	Protected Stone Samples				Unprotected Stone Samples				Protected Wood Samples				Unprotected Wood Samples			
Day No.	N	S	E	W	N	S	E	W	N	S	E	W	N	S	E	W
0	52.2	44.6	49.6	47.7	45.3	42.4	41.6	40.4	72.8	73.1	72.3	70.9	73.1	71.8	74.6	76.5
7	51.7	44.6	50.0	47.9	45.4	42.3	42.0	40.5	72.9	72.7	72.4	71.0	73.2	71.6	74.5	76.2
14	52.1	44.7	49.7	47.6	45.5	42.3	41.7	40.4	72.9	73.3	72.2	71.0	73.2	71.7	74.8	76.5
21	49.8	46.0	47.4	47.7	31.1	32.0	29.3	27.6	70.8	75.7	73.6	74.0	74.2	75.5	75.6	73.0
35	47.1	42.2	45.4	46.1	37.9	44.9	45.8	40.3	70.4	75.0	69.1	75.1	71.8	74.2	75.5	71.1
42	49.8	42.3	47.6	47.2	28.7	31.4	34.2	31.7	70.8	72.8	72.4	74.0	71.3	72.0	74.2	70.0
49	53.1	44.0	46.1	48.3	45.6	44.2	44.8	51.8	72.6	71.8	72.7	68.9	71.6	71.5	71.9	67.2
56	42.0	38.7	48.8	47.2	35.6	29.8	44.0	31.7	71.8	70.8	73.3	71.1	68.1	70.5	71.0	68.5
63	44.0	40.4	44.5	46.3	46.0	45.2	46.6	45.0	73.3	71.4	68.8	68.9	68.1	70.1	73.7	68.9
70	41.6	41.9	42.5	47.2	46.8	44.6	47.2	44.9	71.1	72.7	70.8	71.5	70.6	69.8	73.5	68.1
76	32.2	40.4	45.9	38.6	27.3	29.2	29.9	29.7	72.5	74.9	68.1	71.0	68.6	69.6	69.4	65.6
90	44.8	37.4	40.6	41.6	41.5	43.4	41.9	41.5	71.7	73.9	70.0	68.3	67.8	68.0	71.2	65.8
96	44.3	41.7	42.3	44.6	29.9	33.6	36.6	29.3	69.9	74.2	69.9	68.4	69.4	65.7	71.7	63.9
103	40.3	28.7	41.8	33.8	30.8	30.8	31.1	29.7	73.0	72.4	69.8	71.2	68.5	66.2	68.9	60.6
110	42.1	38.9	42.3	44.9	43.3	42.7	43.3	41.9	69.8	70.6	68.2	67.2	67.7	65.5	70.8	65.1
117	48.0	37.5	43.1	41.6	42.5	42.2	42.0	41.3	70.0	71.0	69.2	67.9	66.4	66.9	70.9	65.2
124	48.0	37.5	43.1	41.6	42.5	42.2	42.0	41.3	70.0	71.0	69.2	67.9	66.4	66.9	70.9	65.2
131	46.4	39.9	42.5	43.6	42.1	42.4	41.7	41.1	67.7	68.9	67.0	67.7	64.6	64.1	67.4	60.2
138	42.8	40.1	45.4	42.9	39.4	45.6	43.1	41.4	66.2	68.8	64.8	64.7	66.0	64.9	64.6	63.2
146	44.2	41.7	43.8	43.6	39.6	42.4	39.4	39.2	67.2	64.5	68.2	64.3	60.8	64.6	67.4	62.3
151	41.3	37.7	44.3	42.8	39.4	41.0	43.7	39.0	62.4	64.2	65.6	64.6	61.1	61.9	64.7	60.7
159	42.6	40.0	43.4	42.7	40.5	41.9	42.6	39.3	66.3	70.1	66.7	66.2	63.8	63.6	64.0	61.6
166	43.6	39.9	42.0	43.0	39.4	43.4	42.4	41.2	65.4	67.1	67.9	64.9	65.0	64.4	67.9	62.1
173	44.7	39.8	42.5	42.2	27.3	32.7	34.7	30.0	65.8	69.6	68.8	66.3	63.4	61.0	65.9	62.0
180	42.5	37.5	41.8	41.6	39.1	42.8	43.7	42.3	65.0	68.6	69.0	65.7	63.0	62.8	67.4	62.1
187	43.0	39.5	40.5	42.4	42.0	43.8	44.0	42.4	62.9	69.1	69.1	66.8	63.0	63.2	64.1	59.6
195	41.4	39.9	40.6	42.0	30.9	33.4	36.8	31.5	66.7	68.3	69.4	67.5	65.3	64.5	67.0	63.0
201	44.8	40.2	43.3	40.5	43.6	44.3	45.5	43.5	67.8	68.7	66.5	67.9	64.1	64.7	67.7	62.5
208	42.0	38.2	41.1	39.4	30.1	31.5	32.9	31.7	67.9	68.3	64.9	65.4	63.3	61.4	64.9	59.8
215	44.9	37.1	40.2	40.3	43.0	43.0	45.8	47.0	68.4	70.2	64.2	65.3	64.5	64.4	66.5	61.6
221	43.8	38.7	40.9	41.5	43.5	44.2	44.6	45.4	66.8	69.4	64.2	66.4	63.1	63.4	65.5	61.0

Reflectance Measurements of Samples Exposed in Oporto (Expressed as %)
Blanks indicate missing data

	Protected Stone Samples				Unprotected Stone Samples				Protected Wood Samples				Unprotected Wood Samples			
Day No.	N	S	E	W	N	S	E	W	N	S	E	W	N	S	E	W
228	40.8	37.2	39.4	41.2	42.0	31.0	37.9	31.0	68.7	67.5	64.6	63.2	64.1	64.2	67.8	57.3
235	42.9	38.3	43.3	41.5	44.1	47.2	46.8	47.7	68.4	70.2	66.0	66.2	61.8	65.2	67.2	62.6
250	43.0	39.0	42.8	42.0	42.9	44.9	48.2	47.6	67.3	70.2	65.0	66.9	61.6	66.0	69.0	63.3
257	46.0	38.7	40.7	42.9	43.9	46.5	47.0	47.6	67.1	71.0	63.7	64.4	65.0	65.0	67.0	63.1
264	41.5	37.7	41.7	41.4	42.7	44.1	46.4	44.8	66.2	69.4	64.0	66.5	63.0	64.6	64.0	62.0
272	42.4	36.7	41.4	39.3	44.8	46.8	40.7	44.6	65.7	68.0	64.8	63.6	62.4	64.4	62.0	61.7
277	42.8	38.4	44.4	41.1	43.0	45.6	45.0	44.0	65.7	68.5	65.1	66.6	64.4	65.0	66.5	62.1
285	43.1	40.0	41.4	40.9	45.7	47.0	46.1	44.7	64.7	68.1	63.9	65.3	62.1	65.2	66.5	62.7
292	39.3	38.4	41.0	42.4	41.5	46.4	43.1	45.5	66.3	69.0	59.9	66.1	60.5	64.5	66.1	60.9
302	41.4	39.7	40.1	40.0	44.1	45.4	45.6	45.9	67.5	68.9	63.9	67.4	64.0	66.7	65.6	61.1
313	44.0	39.7	41.1	43.0	44.4	46.9	46.1	45.7	69.0	71.0	67.4	69.0	65.3	63.4	66.3	62.1
322	45.9	39.0	43.7	42.4	45.4	45.4	46.4	43.8	68.2	69.2	61.1	67.6	62.7	63.0	64.9	60.6
327	40.7	37.5	39.7	39.1	41.8	44.9	43.4	43.4	67.8	68.7	62.7	66.2	62.6	63.3	62.4	60.4
334	41.0	37.1	41.6	40.1	43.4	45.9	43.7	41.9	66.8	67.4	63.3	66.0	61.0	63.3	64.0	61.3
349	40.4	38.1	40.8	36.6	31.7	43.4	45.8	35.2	65.4	68.3	65.4	61.4	60.0	65.1	66.3	61.6

Table A5 Reflectance Measurements of Samples Exposed in Coimbra (Expressed as %)
Blanks indicate missing data

	Protected Stone Samples				Unprotected Stone Samples				Protected Wood Samples				Unprotected Wood Samples			
Day No.	N	S	E	W	N	S	E	W	N	S	E	W	N	S	E	W
0	41.0	40.0	40.0	45.0	44.3	40.1	46.7	45.1	75.0	73.0	74.0	74.0	75.9	74.9	74.0	75.2
7	41.5	41.8	41.5	44.5	47.2	40.6	47.3	48.1	76.1	78.6	72.7	75.7	74.7	76.8	77.2	75.5
14	39.6	45.6	41.8	44.0	31.4	26.6	28.7	32.0	75.5	77.0	75.8	74.3	74.0	71.8	70.9	74.3
21	42.3	44.1	42.6	47.9	46.2	42.8	49.3	47.3	74.1	74.0	75.4	74.2	77.0	74.5	74.9	75.3
28	42.2	42.0	42.6	47.9	46.4	40.6	44.5	46.4	72.4	72.0	74.3	74.6	72.4	75.1	66.6	74.3
35	44.1	46.0	41.4	47.3	32.8	36.4	35.6	36.5	76.1	77.2	73.4	73.9	76.3	75.1	70.5	70.1
42	39.7	44.4	42.7	47.4	45.6	40.2	47.0	44.1	71.8	77.3	74.1	73.9	67.4	69.9	71.0	74.3
49	39.1	44.5	39.8	39.4	30.4	29.7	33.0	31.7	71.2	71.2	72.2	73.5	74.2	69.0	69.1	64.2
56	41.1	43.0	43.6	47.5	45.7	44.1	46.8	47.4	74.6	74.8	70.6	74.4	74.9	74.2	68.9	73.0
62	41.5	44.7	47.5	47.5	47.2	41.5	48.4	47.3	74.9	74.2	72.5	74.8	71.5	69.5	73.8	73.1
68	38.5	45.5	38.4	46.1	48.3	44.2	46.8	45.9	73.7	70.3	73.9	68.7	71.1	73.0	72.1	69.6
76	43.2	46.1	43.1	47.3	44.5	41.3	47.1	47.6	73.9	75.6	74.9	74.9	74.0	74.4	71.8	71.3
82	42.6	44.6	43.5	47.3	44.2	44.1	46.8	47.1	73.8	74.2	72.2	75.4	74.2	73.8	71.6	72.8
89	44.3	46.4	46.7	52.3	47.3	40.9	48.5	48.7	71.9	76.9	71.8	74.9	74.7	73.6	74.2	71.1
96	41.5	45.4	49.1	48.7	46.9	41.9	50.9	48.0	75.2	77.5	69.0	73.9	75.4	75.0	70.5	71.9
103	42.1	48.9	45.5	47.8	50.4	41.7	49.9	48.1	75.9	75.1	71.1	73.4	70.5	69.5	72.0	72.9
110	42.3	46.9	52.3	49.0	47.8	46.4	47.7	49.8	74.9	77.6	72.9	70.8	71.4	74.9	73.3	73.6
117	41.7	47.4	49.4	47.4	46.9	42.1	47.4	46.6	72.5	73.6	69.4	71.6	70.3	71.0	68.0	69.2
124	40.9	45.8	41.1	42.6	45.7	45.0	45.0	43.4	70.2	71.1	66.1	68.0	67.7	68.4	65.5	64.4
131	41.4	44.1	46.3	46.4	47.4	41.0	47.2	48.5	70.7	72.5	69.6	70.4	70.2	69.4	66.2	65.4
139	41.7	44.5	43.5	44.4	47.4	42.0	47.4	46.0	71.7	72.7	67.0	71.0	70.3	67.7	69.0	68.0
145	41.7	44.6	43.3	46.9	47.1	44.0	46.5	46.4	70.2	67.6	67.0	70.6	69.4	68.4	67.4	67.4
152	40.4	44.1	46.3	46.5	49.1	43.8	47.9	50.1	70.8	72.5	68.0	70.3	72.5	70.3	69.1	68.7
159	42.6	45.0	44.0	46.5	46.4	43.5	46.7	46.4	69.2	71.7	70.6	69.9	69.7	69.3	67.3	68.6
166	42.8	45.1	44.1	46.5	44.9	43.3	46.1	47.7	69.3	72.4	70.9	68.7	70.0	69.4	67.3	68.2
181	42.5	44.4	42.5	46.8	35.0	30.8	35.9	35.1	71.4	70.2	69.3	69.3	68.4	71.2	68.0	69.5
187	42.9	43.5	43.3	49.1	49.7	44.4	49.8	50.0	70.7	68.6	68.6	69.7	70.8	70.2	69.4	68.5
194	41.5	40.5	44.2		47.3	42.6	47.3	47.5	72.3	70.3	65.3	68.8	68.4	68.6	66.8	66.6
201	41.1	45.2	46.8	46.6	48.0	44.7	46.6	48.2	70.0	71.7	65.0	67.7	69.0	69.4	68.4	67.3

Reflectance Measurements of Samples Exposed in Coimbra (Expressed as %)
Blanks indicate missing data

	Protected Stone Samples				Unprotected Stone Samples				Protected Wood Samples				Unprotected Wood Samples			
Day No.	N	S	E	W	N	S	E	W	N	S	E	W	N	S	E	W
209	41.8	46.6	42.2	42.8	47.4	42.9	49.6	47.4	67.1	68.8	69.1	67.9	68.4	68.9	63.8	68.5
216	41.0	44.0	39.8	44.2	47.0	41.6	47.7	46.7	67.8	71.0	69.0	68.4	68.5	65.7	64.3	67.6
229	41.5	46.1	41.2	44.6	47.1	44.0	47.3	47.1	65.2	68.0	67.9	67.9	68.6	69.1	66.6	67.0
236	39.7	45.1	40.0	45.1	47.7	45.4	49.5	47.9	66.0	68.5	66.2	66.1	69.6	68.1	67.4	67.0
243	39.6	44.3	42.3	47.5	47.1	42.7	47.0	47.7	65.5	69.4	68.4	67.9	68.1	69.0	67.1	67.9
250	41.3	44.5	43.1	46.7	47.2	41.7	47.4	46.7	69.9	71.7	66.3	68.8	69.6	68.2	67.6	67.7
258	40.4	43.0	45.6	46.1	47.0	44.6	46.6	48.6	70.4	71.9	67.6	70.6	70.4	70.1	70.3	68.7
266	42.1	44.0	42.6	46.9	49.0	41.7	47.3	49.2	69.6	72.7	67.4	70.1	69.8	69.0	68.4	67.7
274	42.3	47.1	42.6	46.0	49.7	45.1	44.9	48.8	68.1	71.2	69.3	67.8	69.8	68.8	67.4	65.9
281	40.7	46.1	48.0	47.0	48.2	44.3	46.7	49.1	70.1	72.1	68.6	70.6	69.8	70.1	67.1	68.0
287	43.1	45.2	44.0	45.0	48.5	42.7	47.4	48.1	68.7	73.0	68.8	69.8	69.5	69.6	69.0	65.1
299	43.1	42.9	43.7	47.2	48.9	44.3	48.7	46.4	71.1	69.5	69.0	66.5	67.7	67.6	67.5	65.7
313	43.7	45.2	42.4	45.4	48.1	42.1	45.4	47.7	69.7	72.1	69.5	68.6	68.5	68.7	66.9	65.5
320	44.0	47.2	46.0	47.1	50.0	46.4	47.9	49.7	69.9	72.1	65.8	70.0	68.9	69.2	68.4	66.2

APPENDIX 2 Graphs Showing Models 1 and 2 Fitted To the Reflectance Measurements

Brief Description of the Two Models Tested

Model 1 (described in pages 73-76 and pages 81-82) predicts that the reflectance of an exposed surface reduces exponentially with time, producing the soiling constant k_1.

$$R = R_o e^{k_1 t}$$

Model 2 (described in pages 74-75 and pages 81-82) assumes reflectance loss is related to the square root of time, producing the soiling constant k_2.

$$R = R_o - k_2 \sqrt{t}$$

Table 6 overleaf provides the page numbers for the raw data for each site presented in Appendix 1 and the corresponding graphical data presented for each sample type and model fit in Appendix 2.

Table A6 Location of Raw and Graphical Data for Each Sample Type and Model Fit

Site	Sample	Raw Data		Model Fit	Graphs	
		Table No.	Page No.		Figure No.	Page No.
London	Protected Stone	A1	212	Model 1	A1	223
				Model 2	A2	224
	Unprotected Stone	A1	212	Model 1	A3	225
				Model 2	A4	226
	Protected Wood	A1	212	Model 1	A5	227
				Model 2	A6	228
	Unprotected Wood	A1	212	Model 1	A7	229
				Model 2	A8	230
Vienna	Protected Stone	A2	214	Model 1	A9	231
				Model 2	A10	232
	Unprotected Stone	A2	214	Model 1	A11	233
				Model 2	A12	234
	Protected Wood	A2	214	Model 1	A13	235
				Model 2	A14	236
	Unprotected Wood	A2	214	Model 1	A15	237
				Model 2	A16	238
Breitenfurt	Protected Stone	A3	216	Model 1		
				Model 2		
	Unprotected Stone	A3	216	Model 1		
				Model 2		
	Protected Wood	A3	216	Model 1		
				Model 2		
	Unprotected Wood	A3	216	Model 1		
				Model 2		
Oporto	Protected Stone	A4	217	Model 1	A17	239
				Model 2	A18	240
	Unprotected Stone	A4	217	Model 1	A19	241
				Model 2	A20	242
	Protected Wood	A4	217	Model 1	A21	243
				Model 2	A22	244
	Unprotected Wood	A4	217	Model 1	A23	245
				Model 2	A24	246
Coimbra	Protected Stone	A5	219	Model 1	A25	247
				Model 2	A26	248
	Unprotected Stone	A5	219	Model 1	A27	249
				Model 2	A28	250
	Protected Wood	A5	219	Model 1	A29	251
				Model 2	A30	252
	Unprotected Wood	A5	219	Model 1	A31	253
				Model 2	A32	254

Figure A1 Graphs of Model 1 Fitted to the London - Protected Stone - Reflectance Measurements

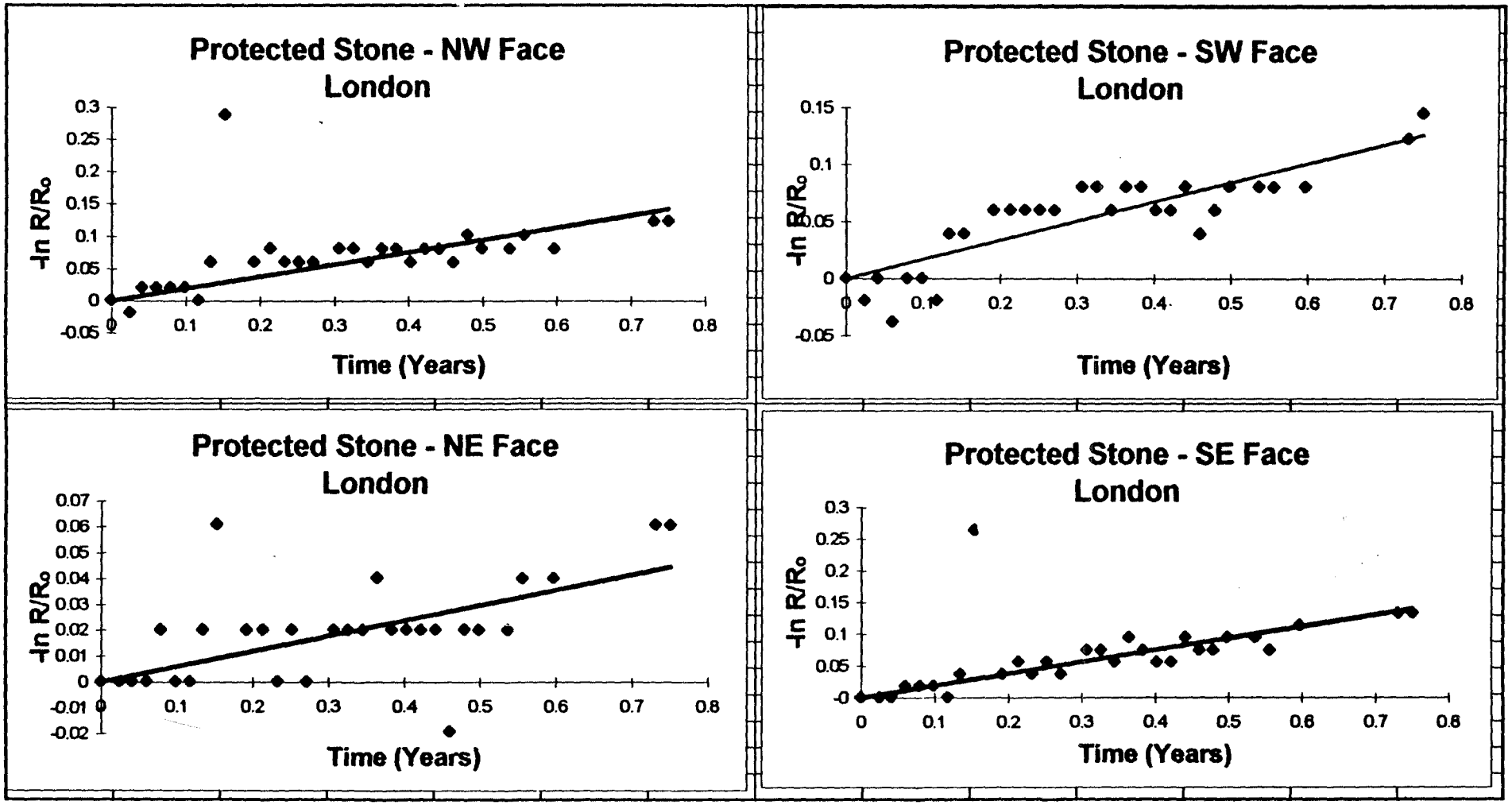

Figure A2 Graphs of Model 2 Fitted to the London - Protected Stone - Reflectance Measurements

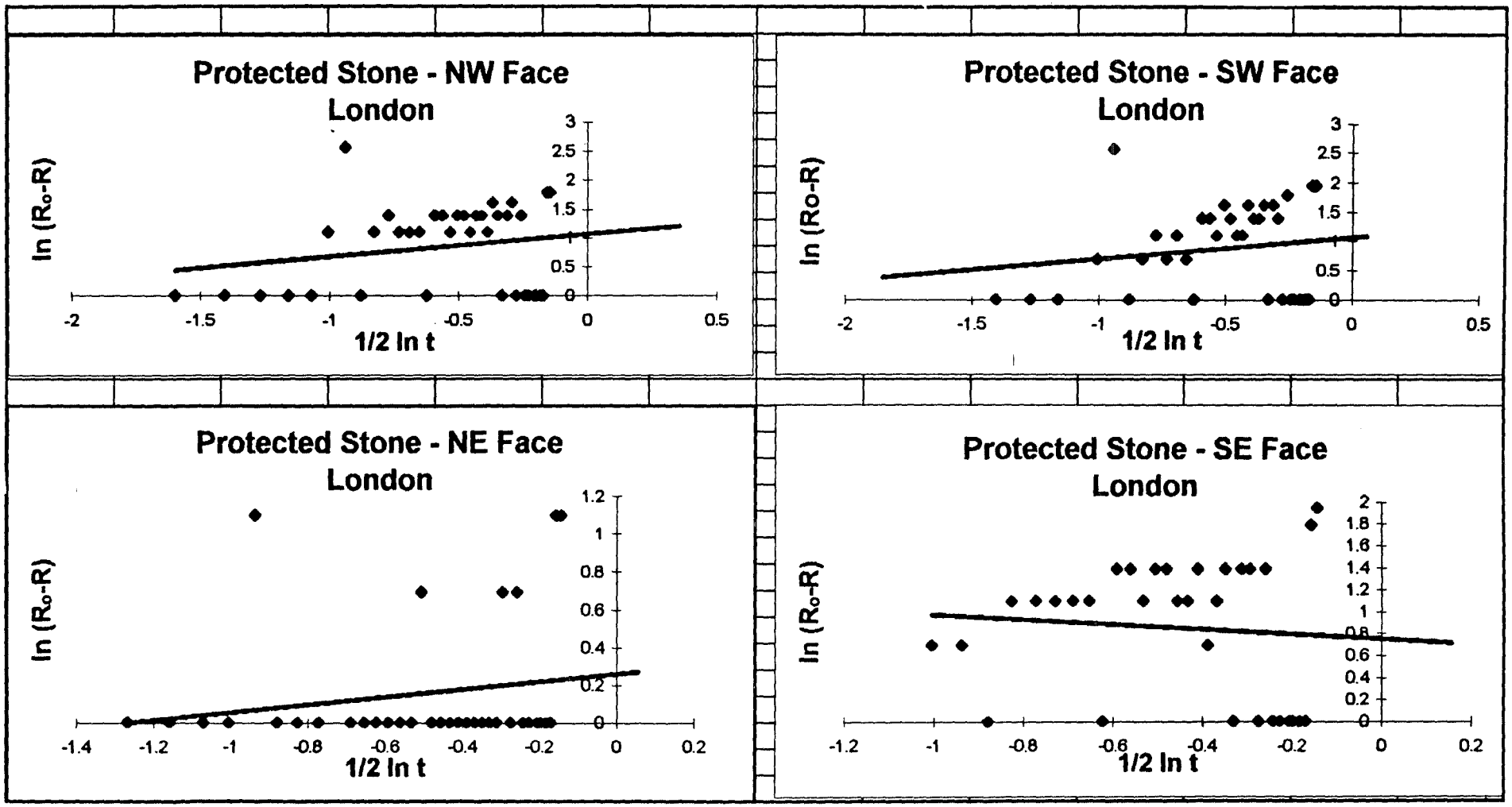

Figure A3 Graphs of Model 1 Fitted to the London - Unprotected Stone - Reflectance Measurements

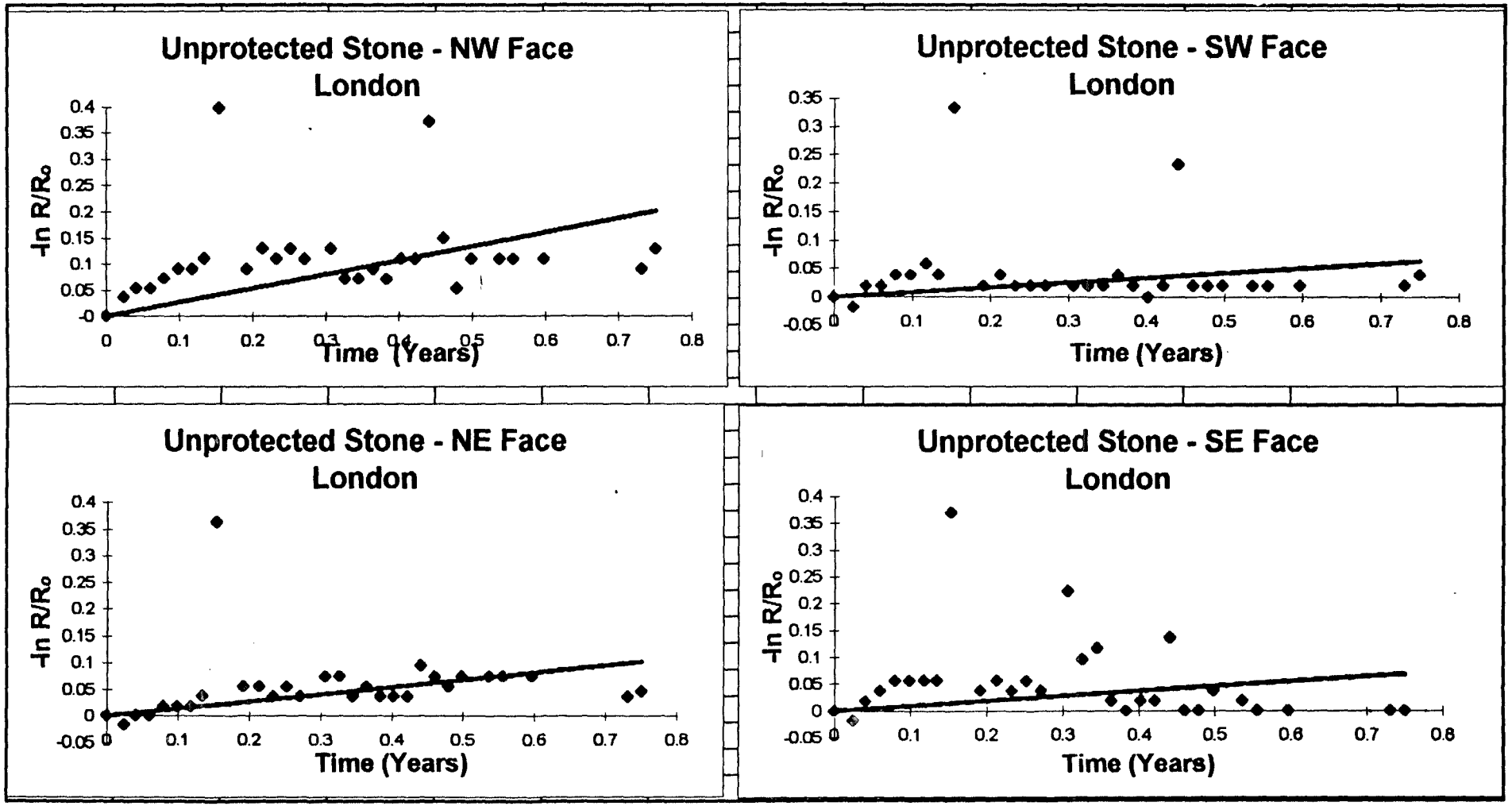

Figure A4 Graphs of Model 2 Fitted to the London - Unprotected Stone - Reflectance Measurements

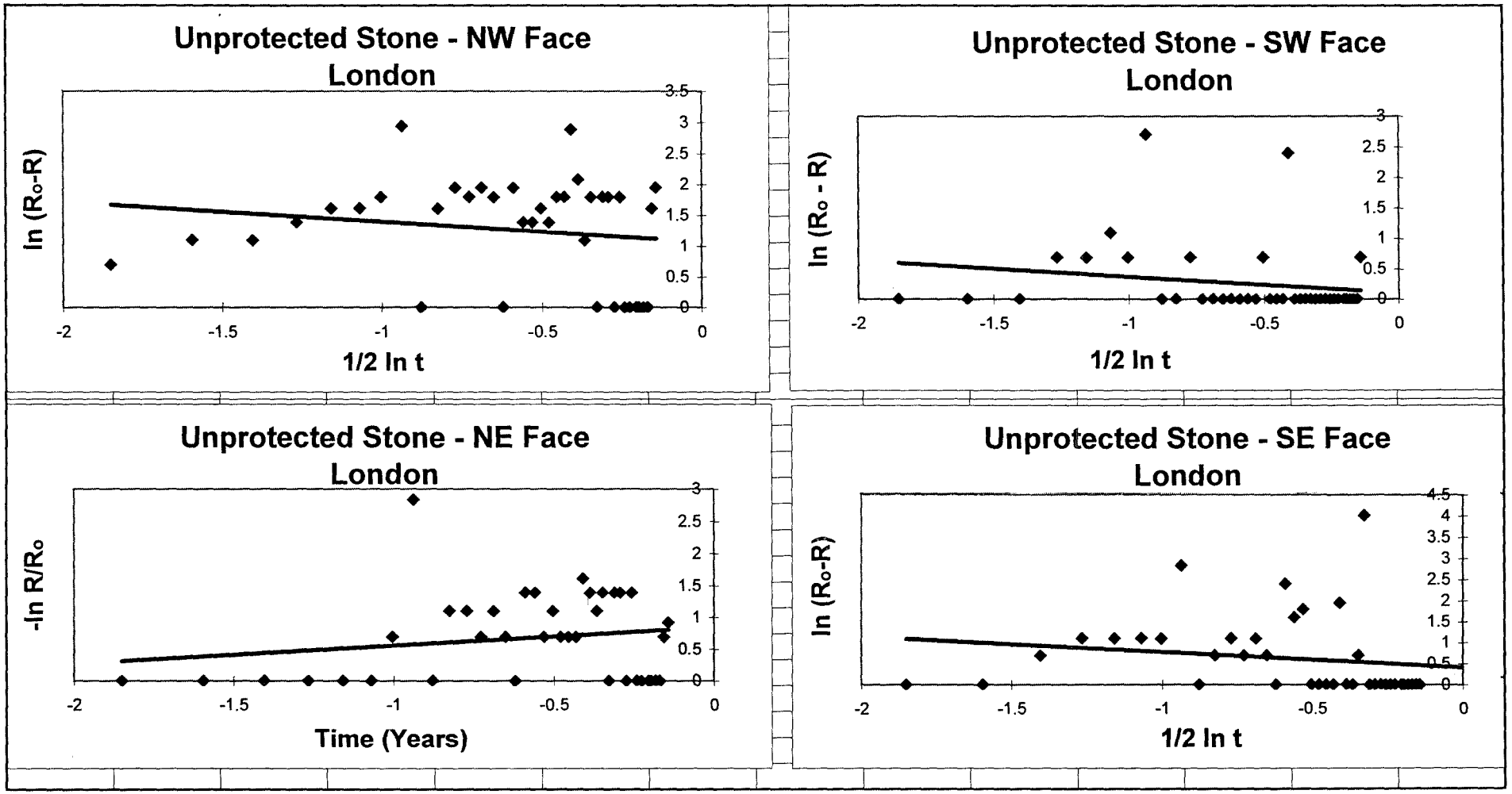

Figure A5 Graphs of Model 1 Fitted to the London - Protected Wood - Reflectance Measurements

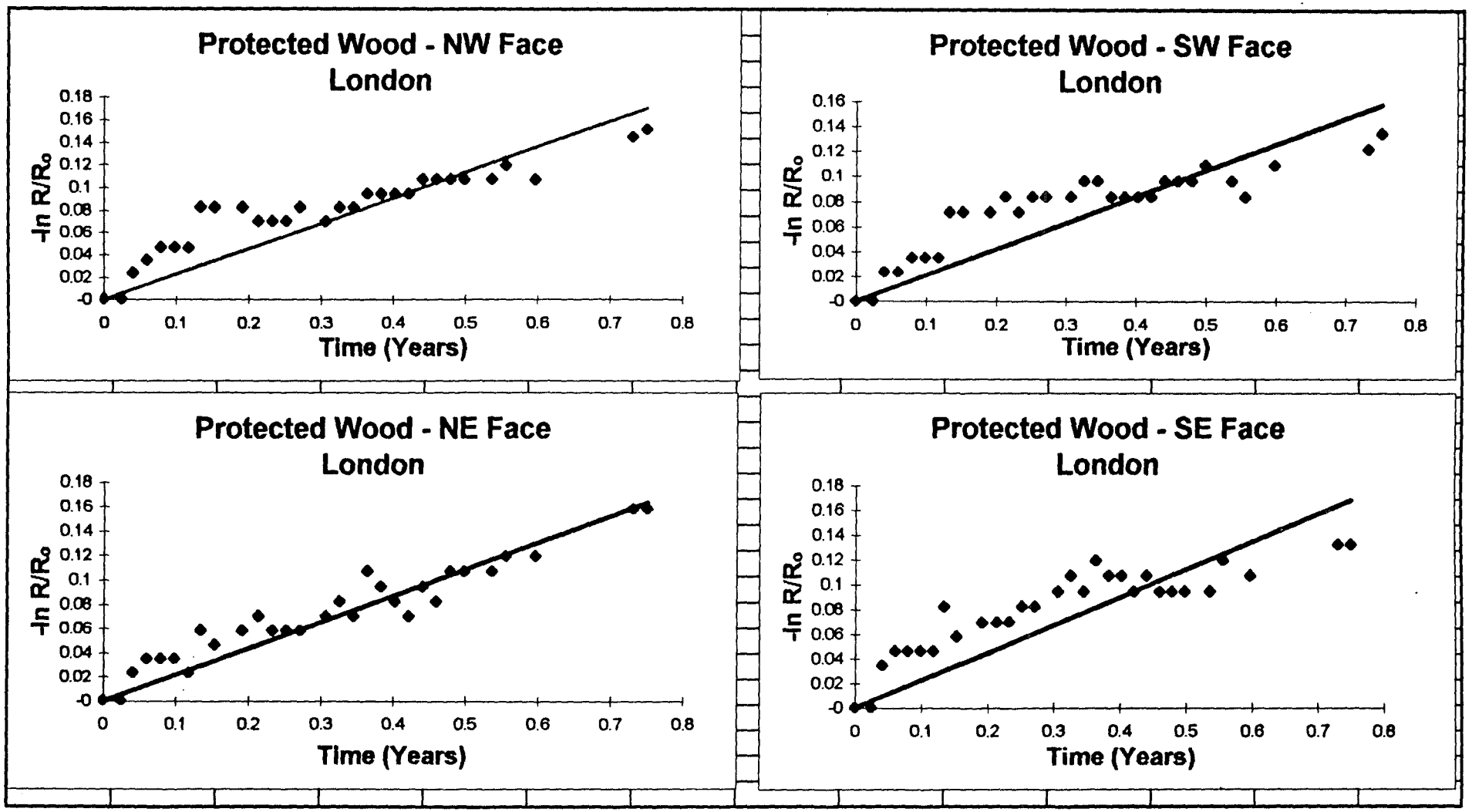

Figure A6 Graphs of Model 2 Fitted to the London - Protected Wood - Reflectance Measurements

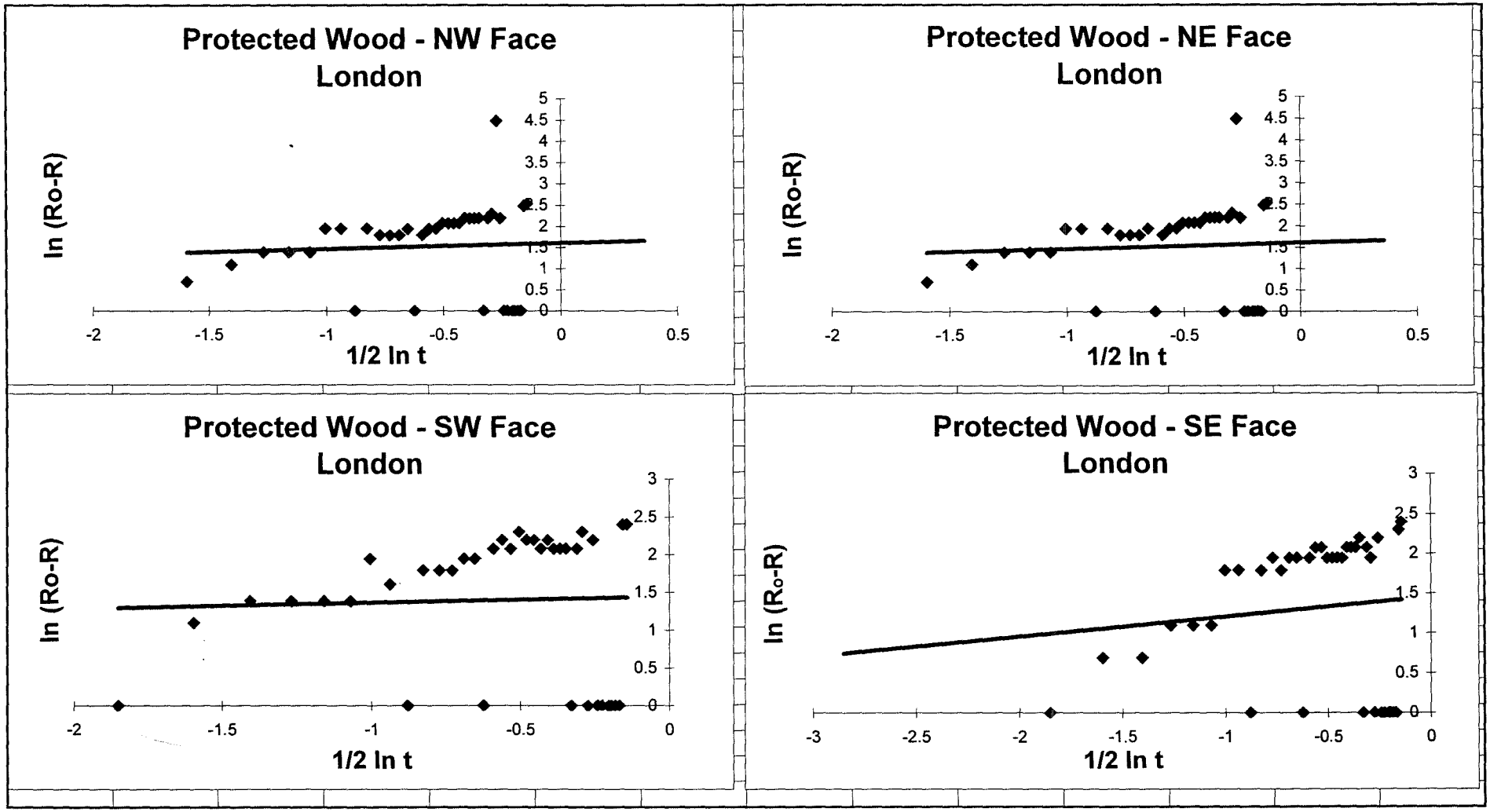

Figure A7 Graphs of Model 1 Fitted to the London - Unprotected Wood - Reflectance Measurements

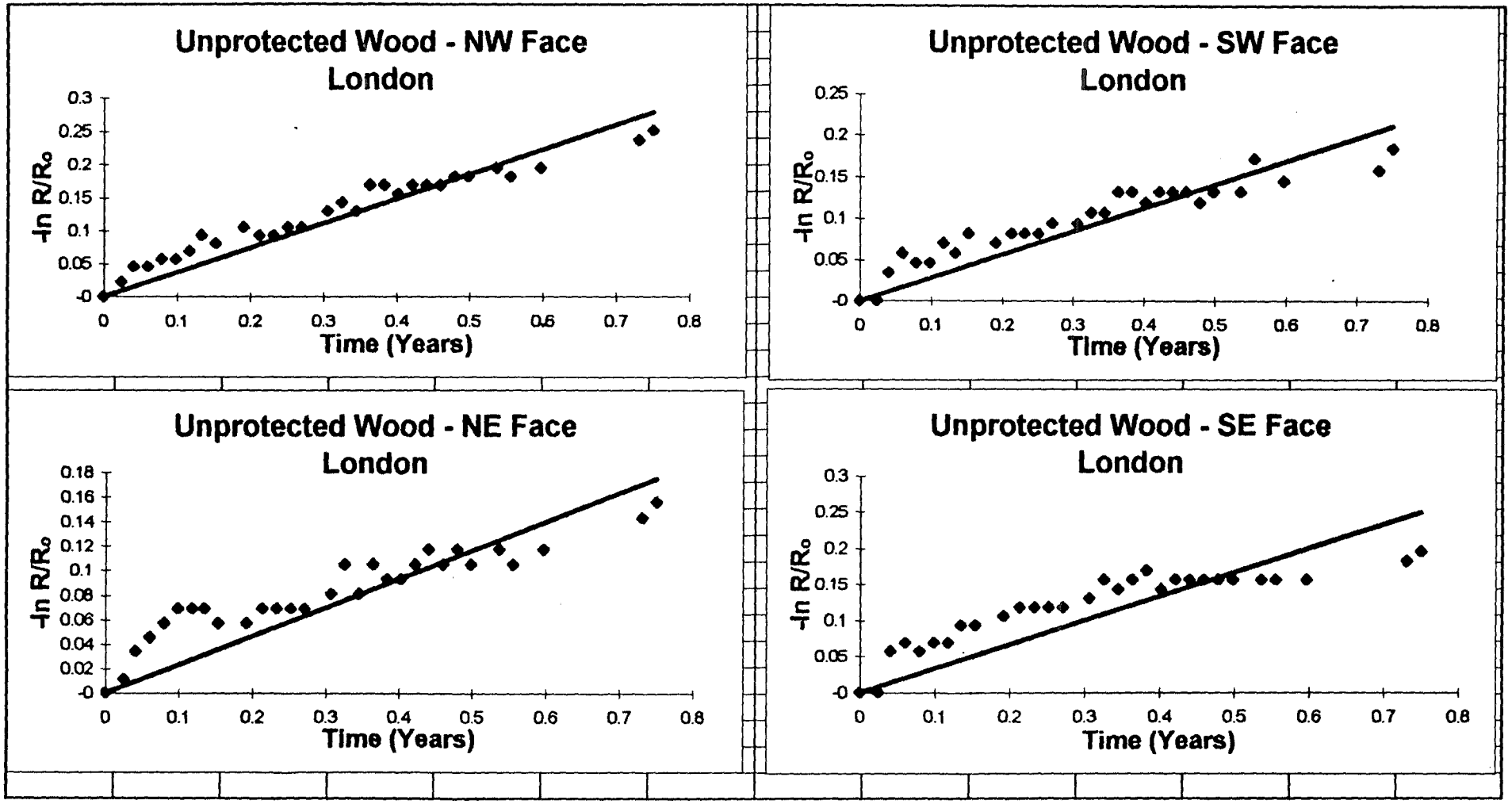

Figure A8 Graphs of Model 2 Fitted to the London - Unprotected Wood - Reflectance Measurements

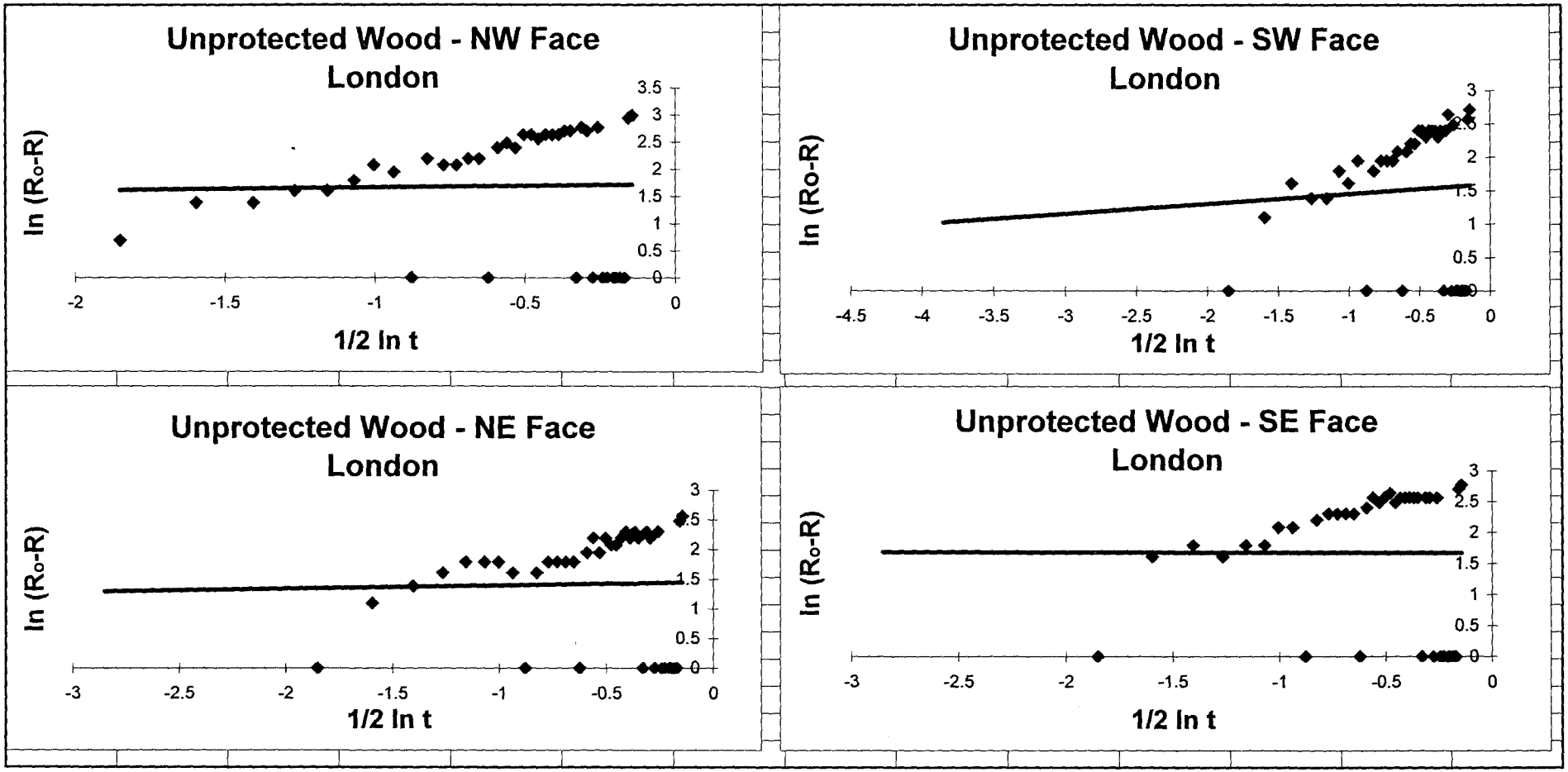

Figure A9 Graphs of Model 1 Fitted to the Vienna - Protected Stone - Reflectance Measurements

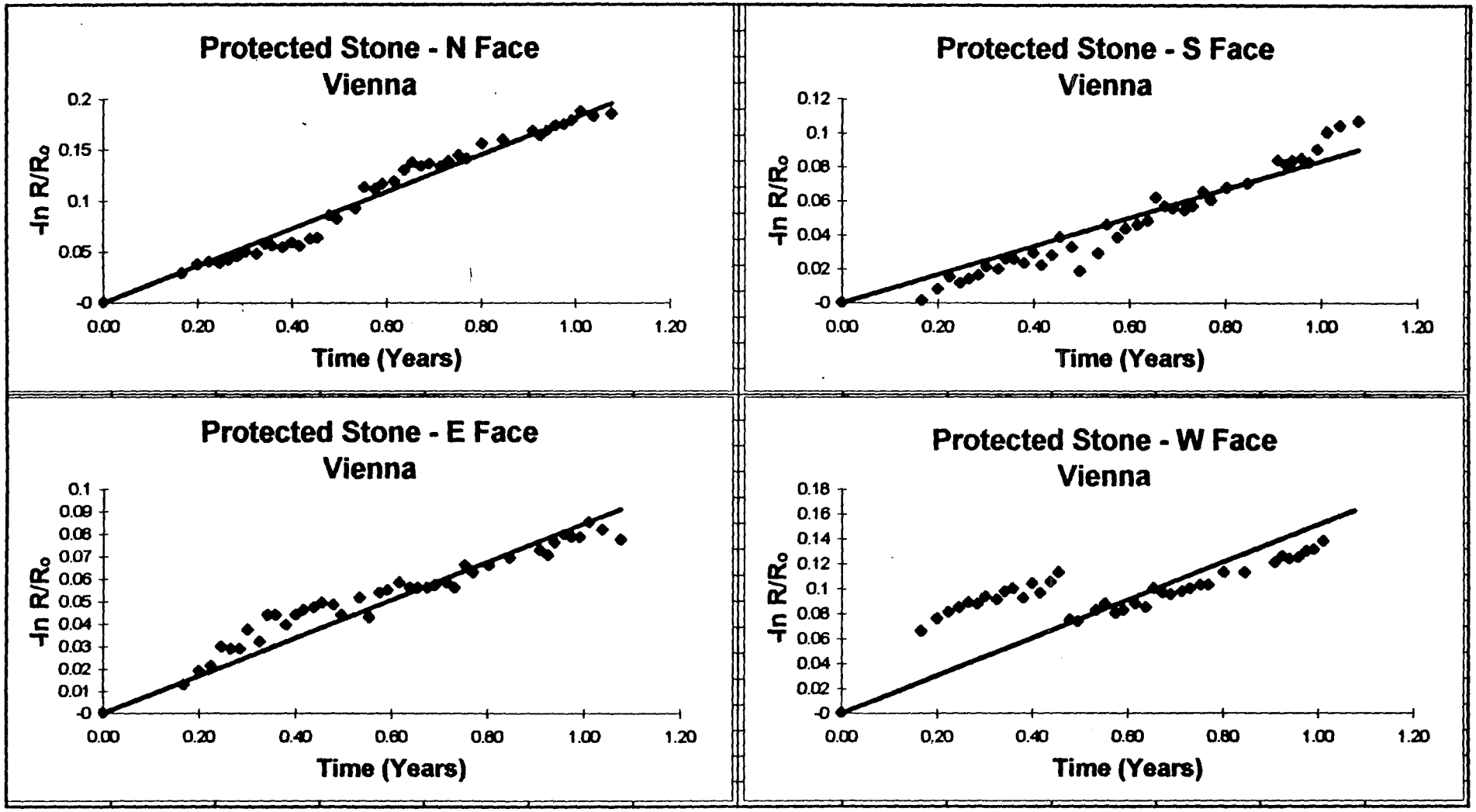

Figure A10 Graphs of Model 2 Fitted to the Vienna - Protected Stone - Reflectance Measurements

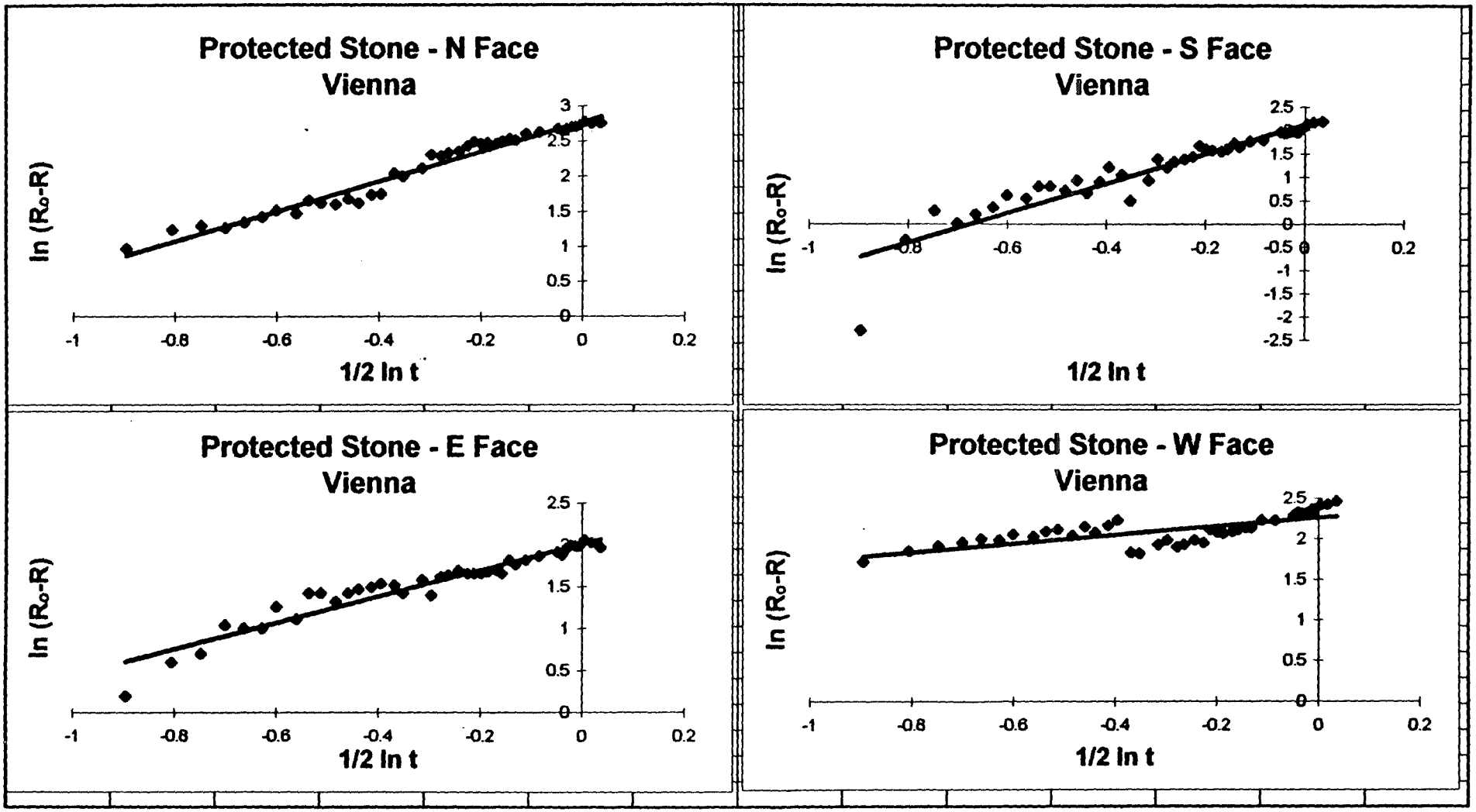

Figure A11 Graphs of Model 1 Fitted to the Vienna - Unprotected Stone - Reflectance Measurements

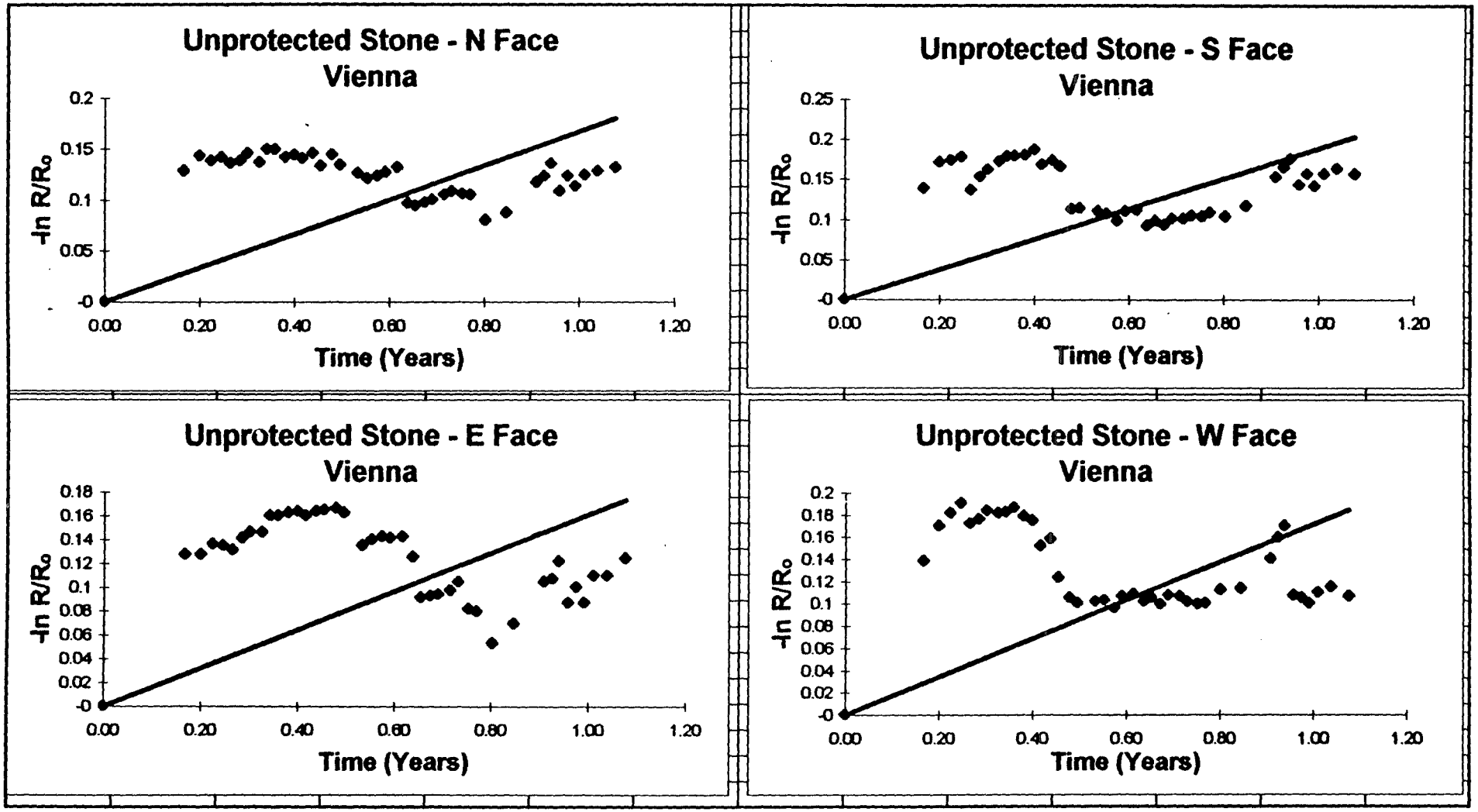

Figure A12 Graphs of Model 2 Fitted to the Vienna - Unprotected Stone - Reflectance Measurements

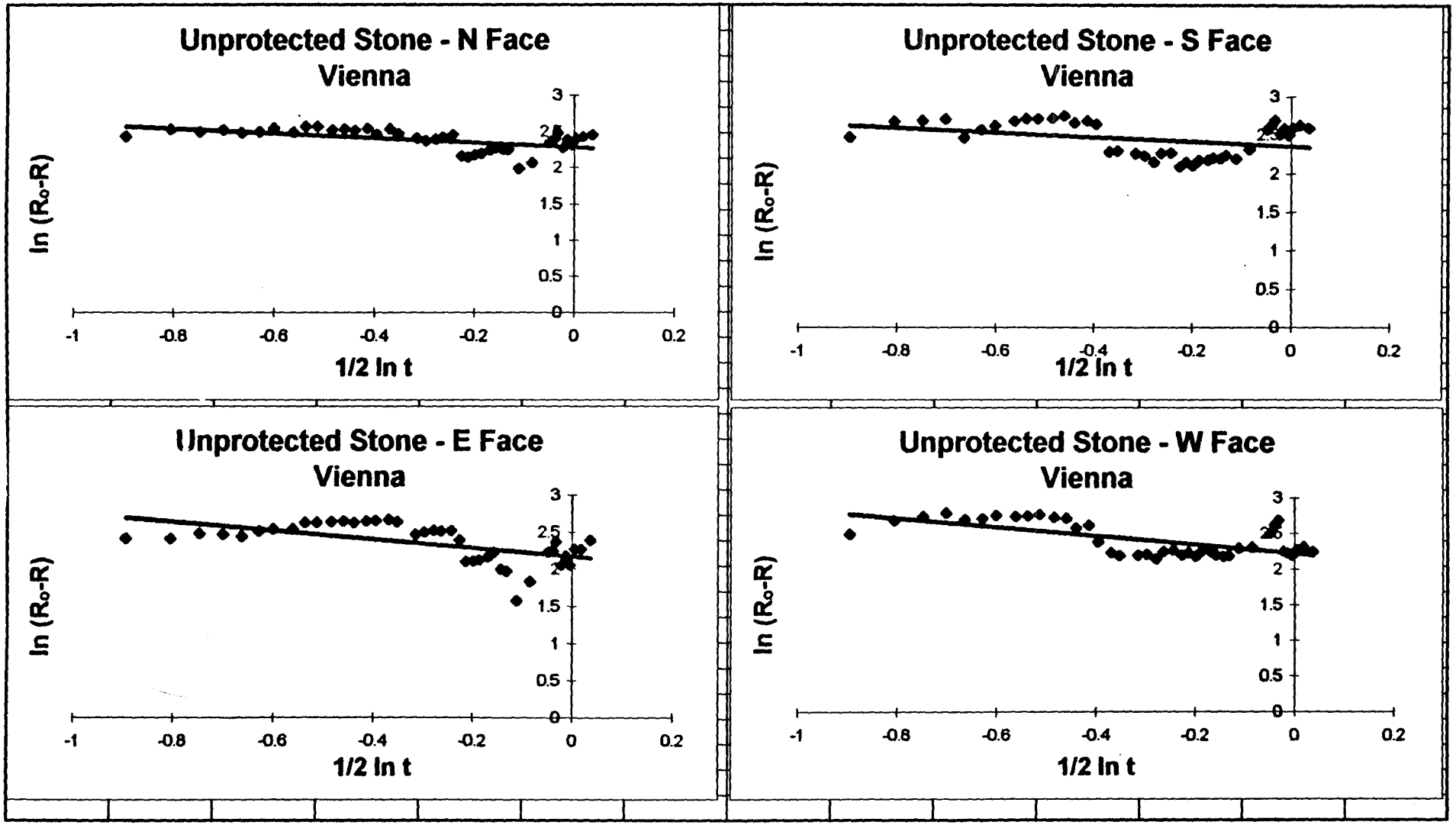

Figure A13 Graphs of Model 1 Fitted to the Vienna - Protected Wood - Reflectance Measurements

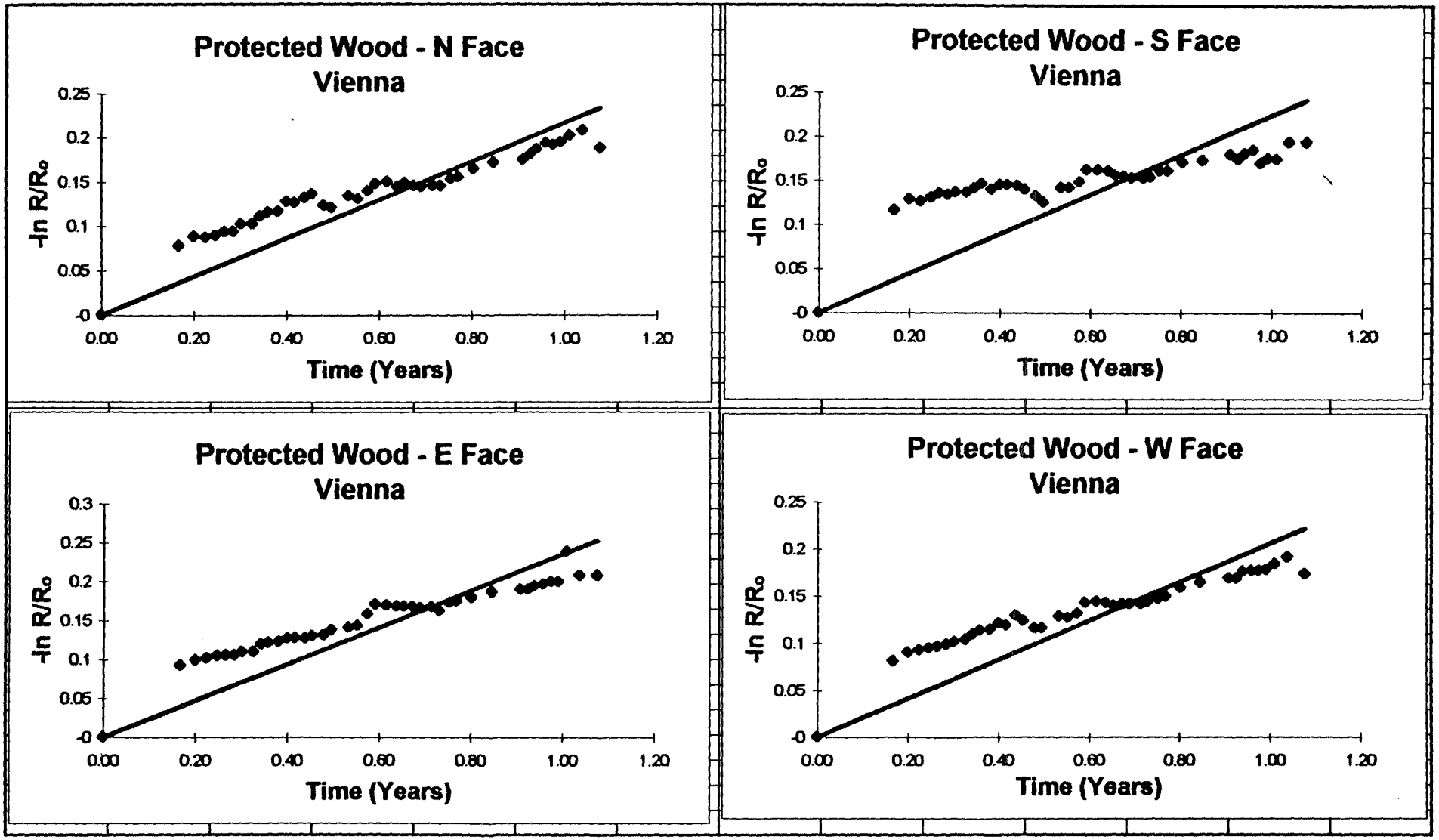

Figure A14 Graphs of Model 2 Fitted to the Vienna - Protected Wood - Reflectance Measurements

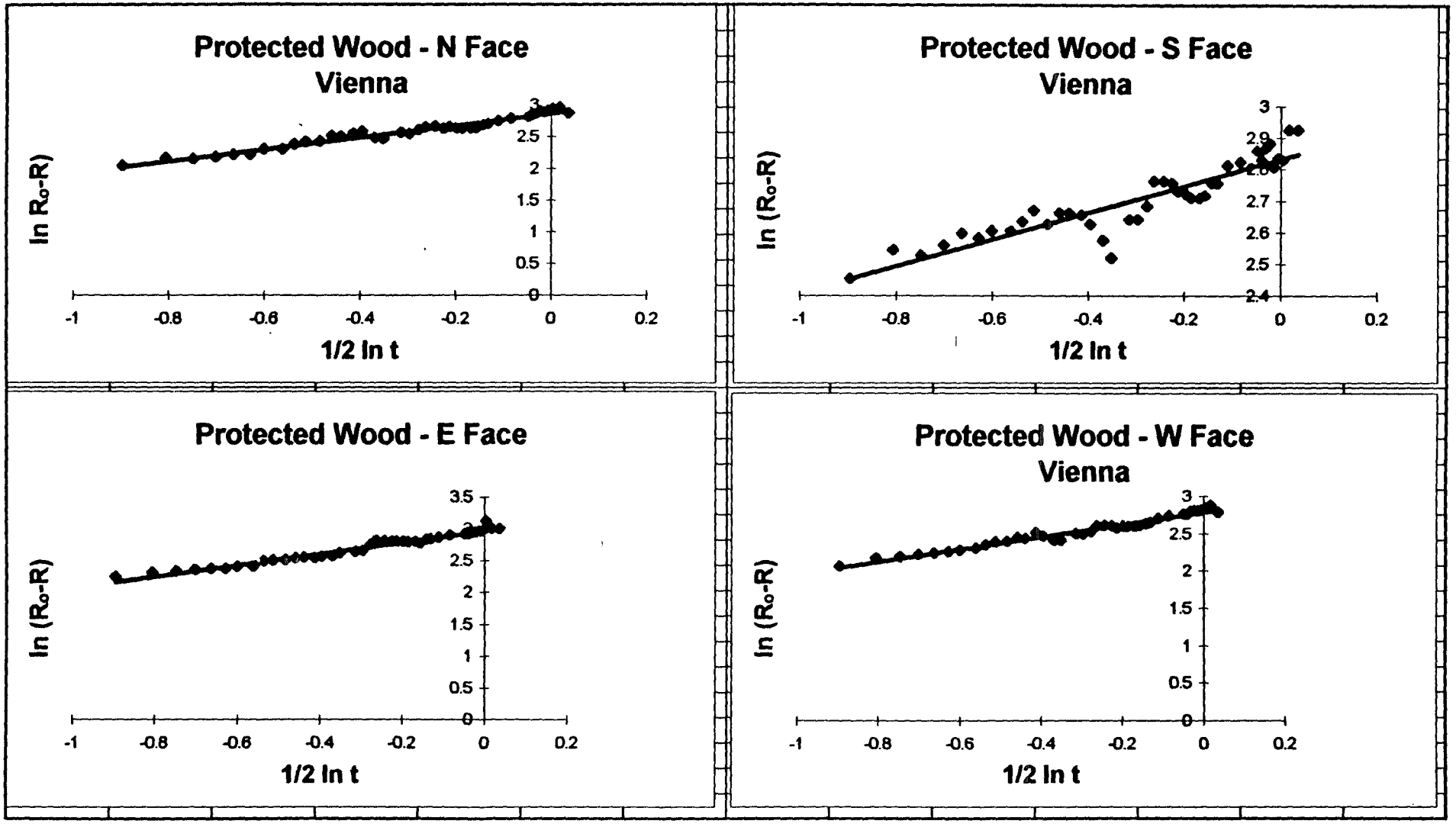

Figure A15 Graphs of Model 1 Fitted to the Vienna - Unprotected Wood - Reflectance Measurements

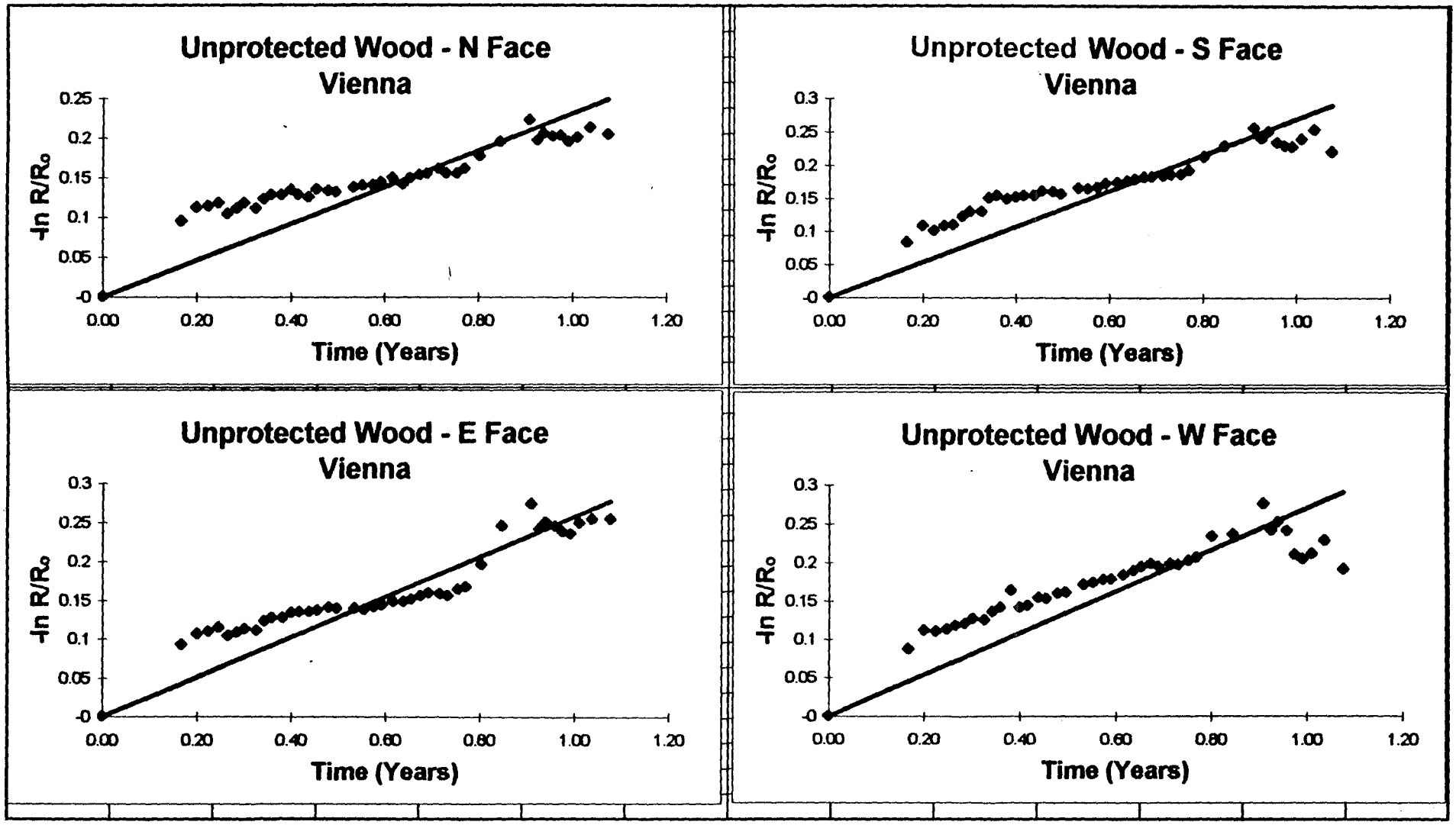

Figure A16 Graphs of Model 2 Fitted to the Vienna - Unprotected Wood - Reflectance Measurements

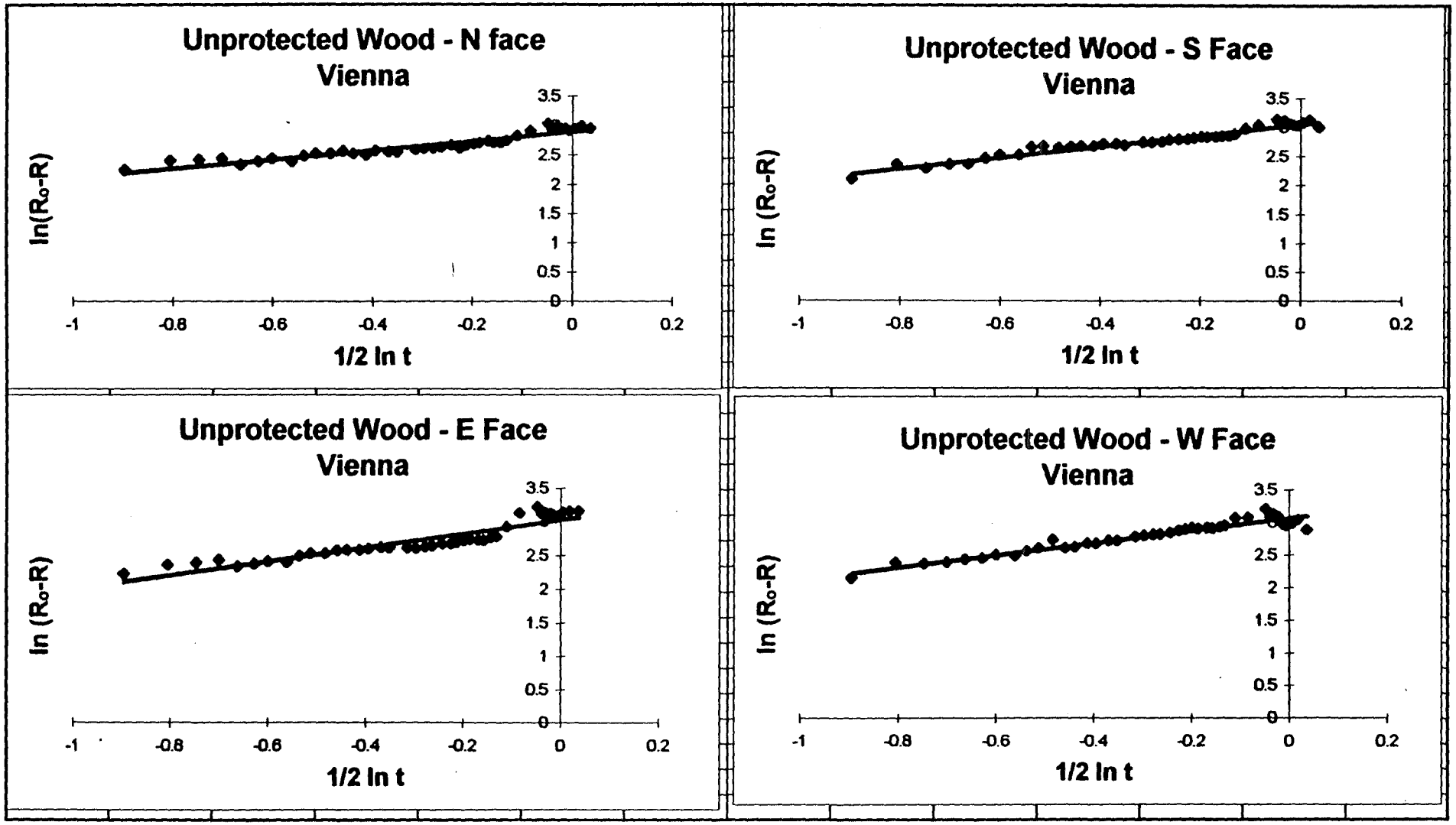

Figure A17 Graphs of Model 1 Fitted to the Oporto - Protected Stone - Reflectance Measurements

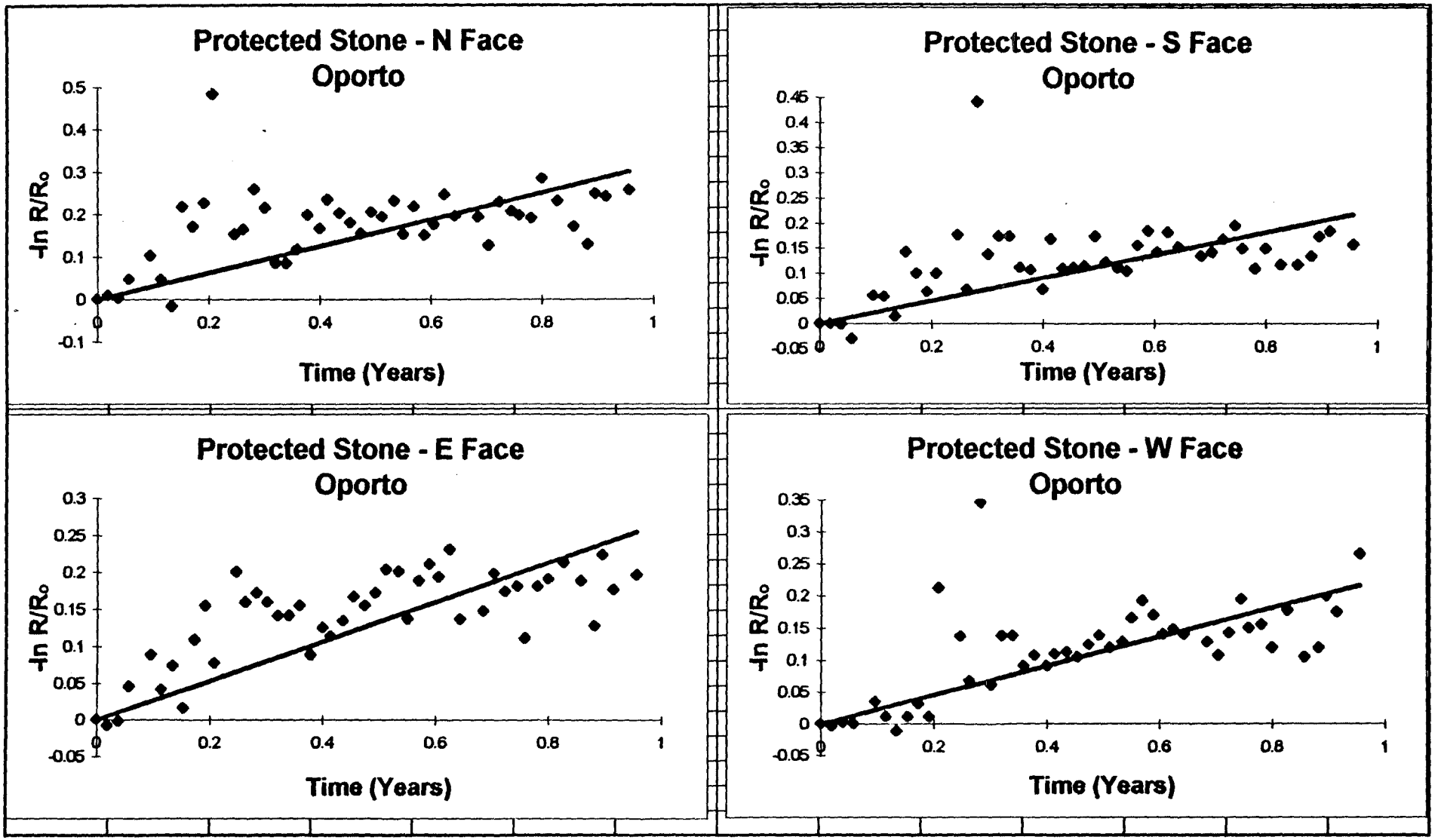

Figure A18 Graphs of Model 2 Fitted to the Oporto - Protected Stone - Reflectance Measurements

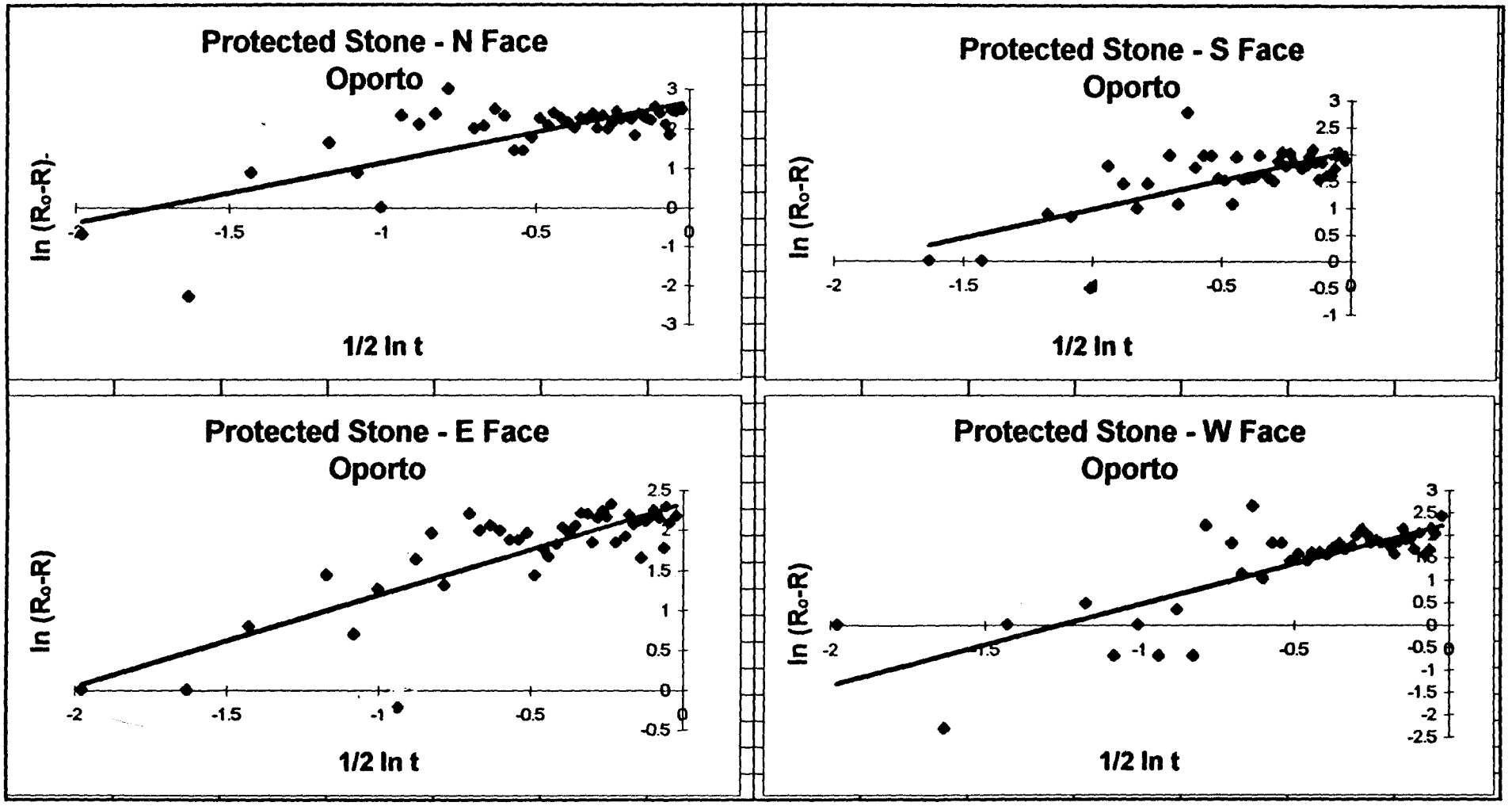

Figure A19 Graphs of Model 1 Fitted to the Oporto - Unprotected Stone - Reflectance Measurements

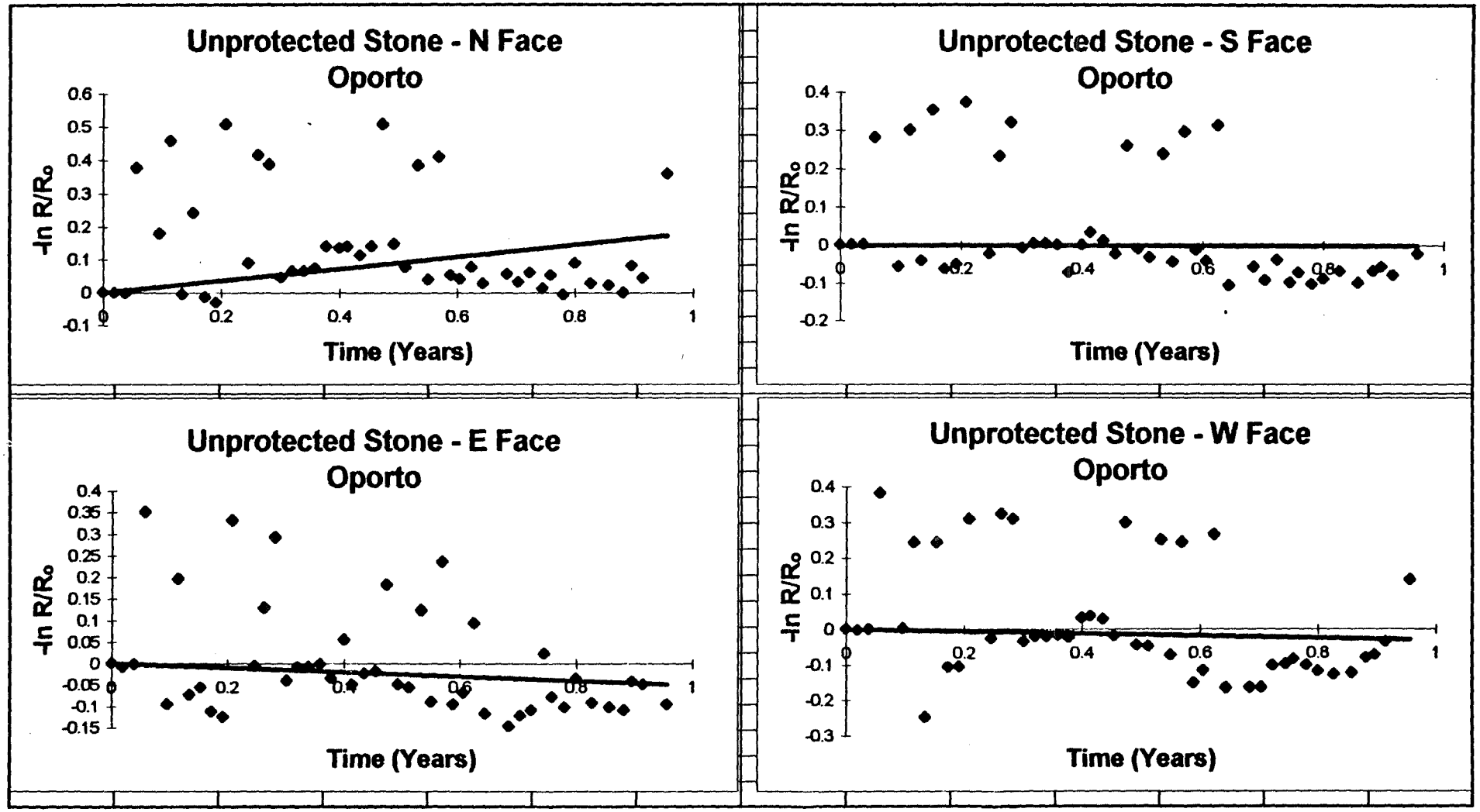

Figure A20 Graphs of Model 2 Fitted to the Oporto - Unprotected Stone - Reflectance Measurements

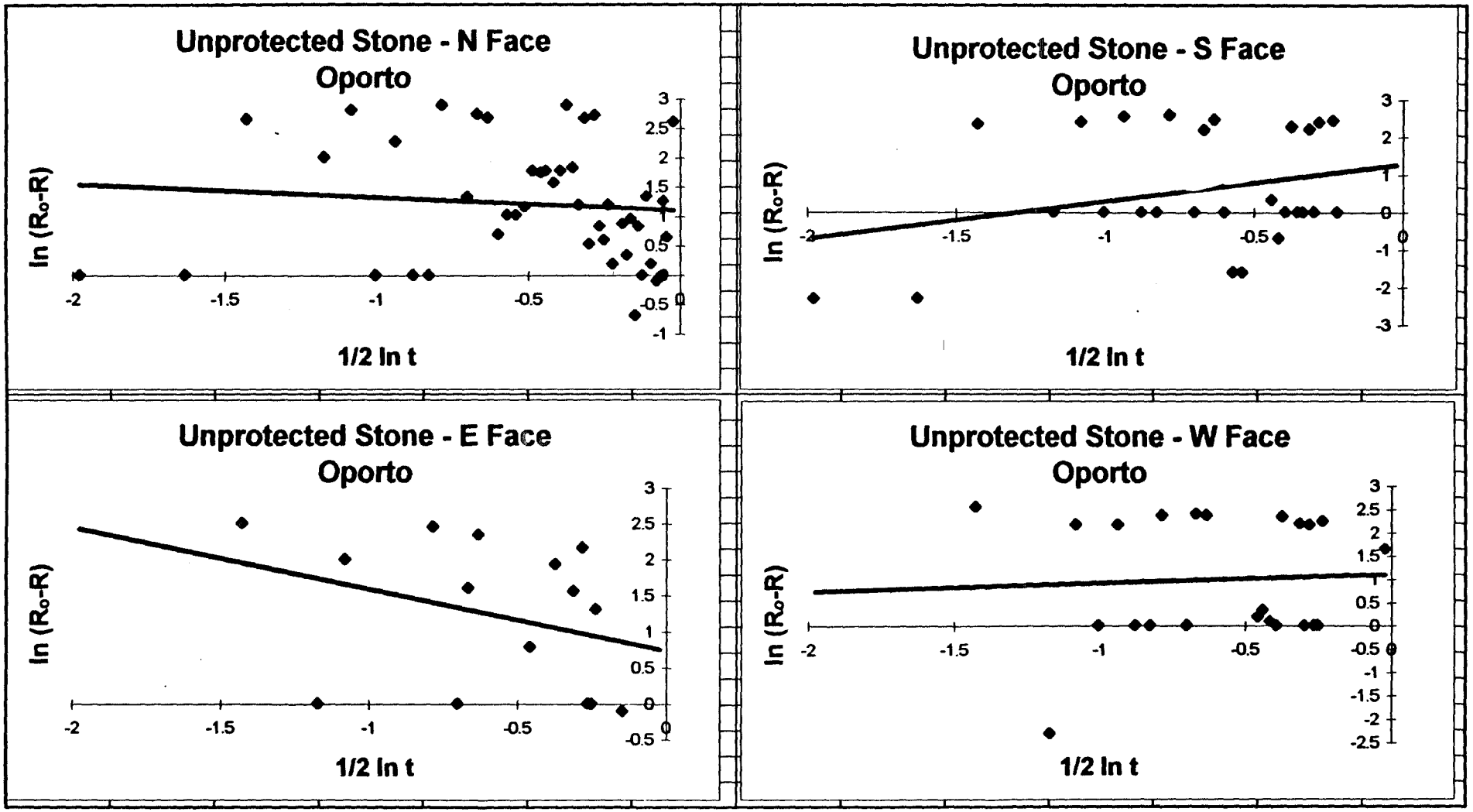

Figure A21 Graphs of Model 1 Fitted to the Oporto - Protected Wood - Reflectance Measurements

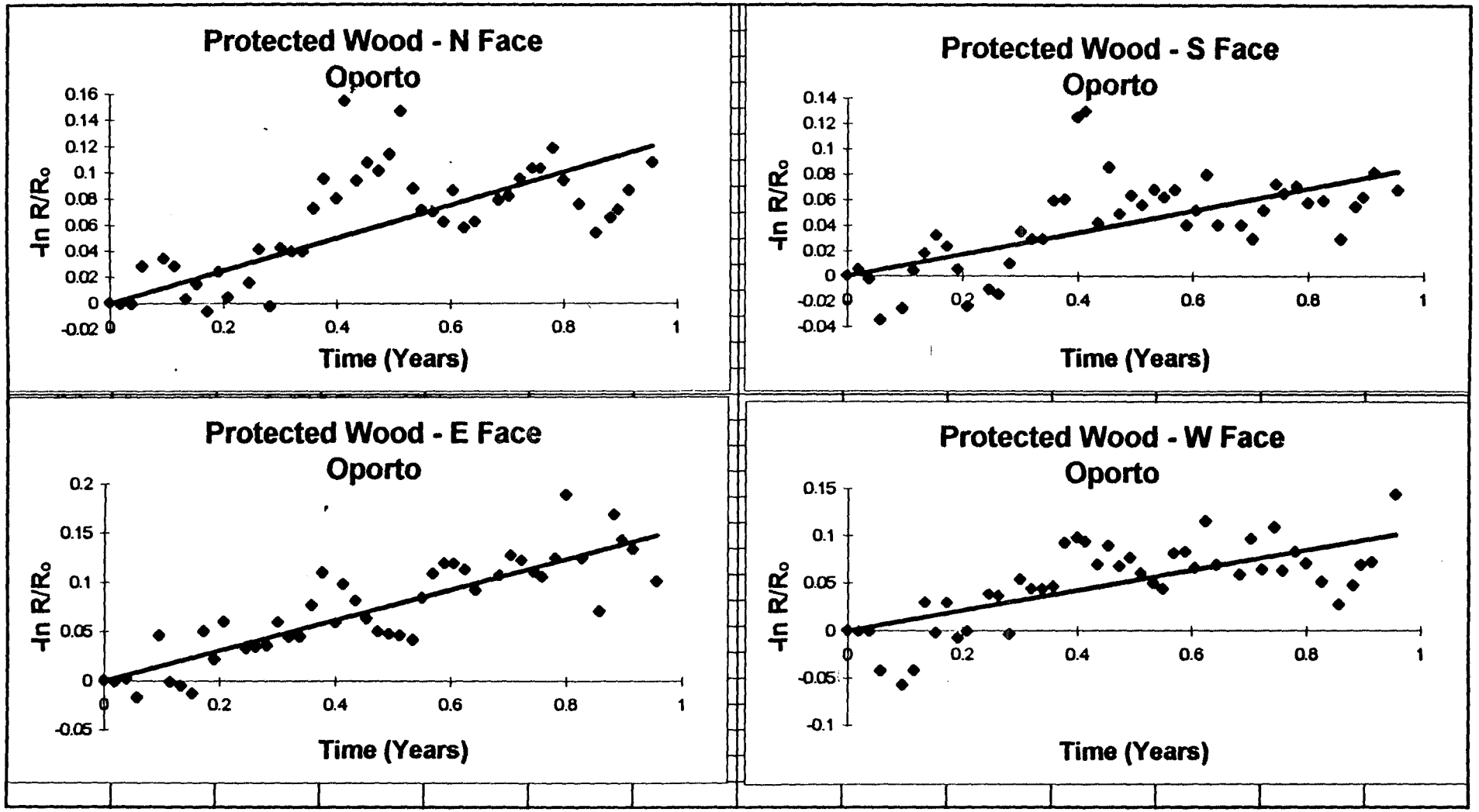

Figure A22 Graphs of Model 2 Fitted to the Oporto - Protected Wood - Reflectance Measurements

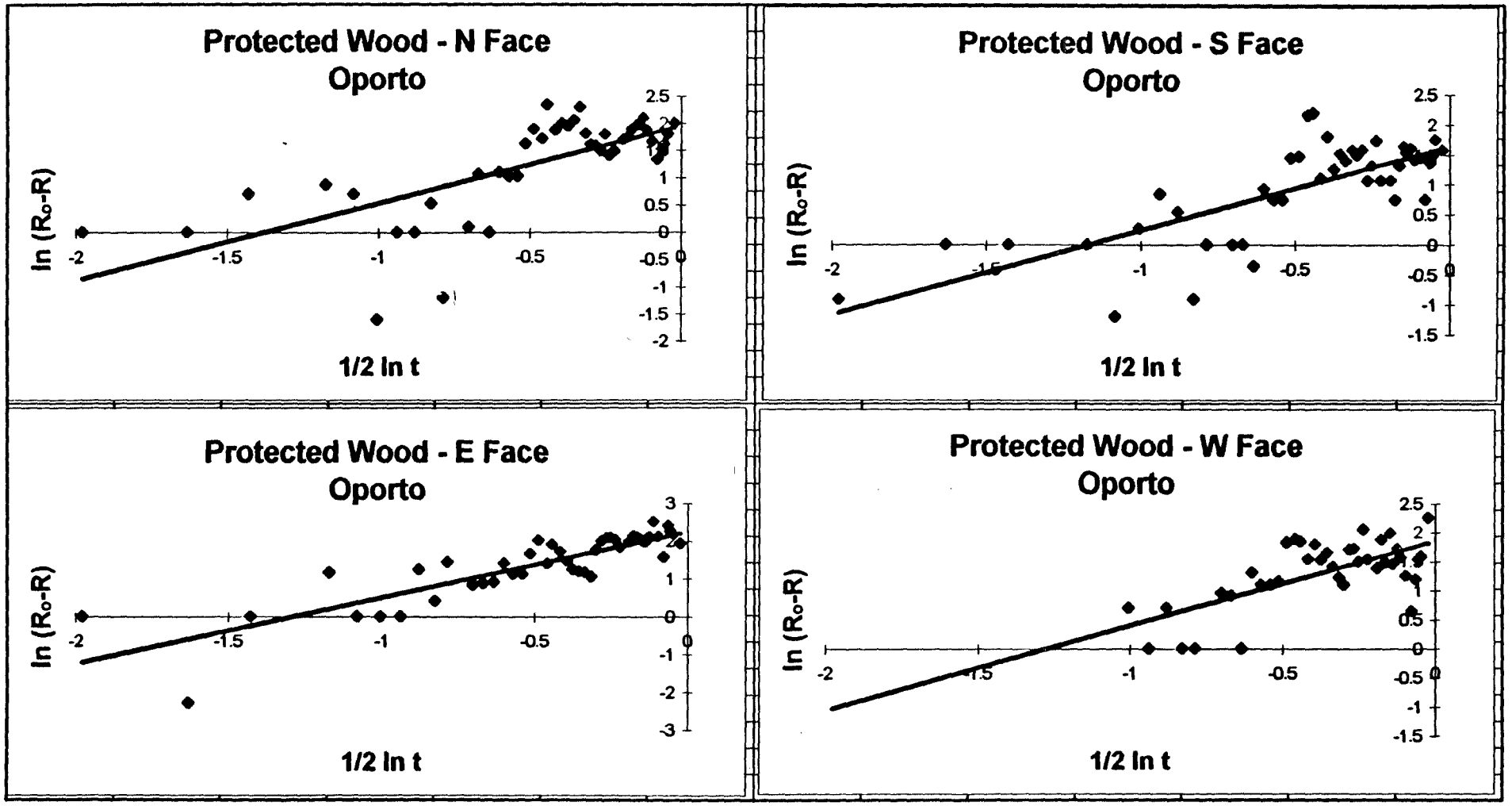

Figure A23 Graphs of Model 1 Fitted to the Oporto - Unprotected Wood - Reflectance Measurements

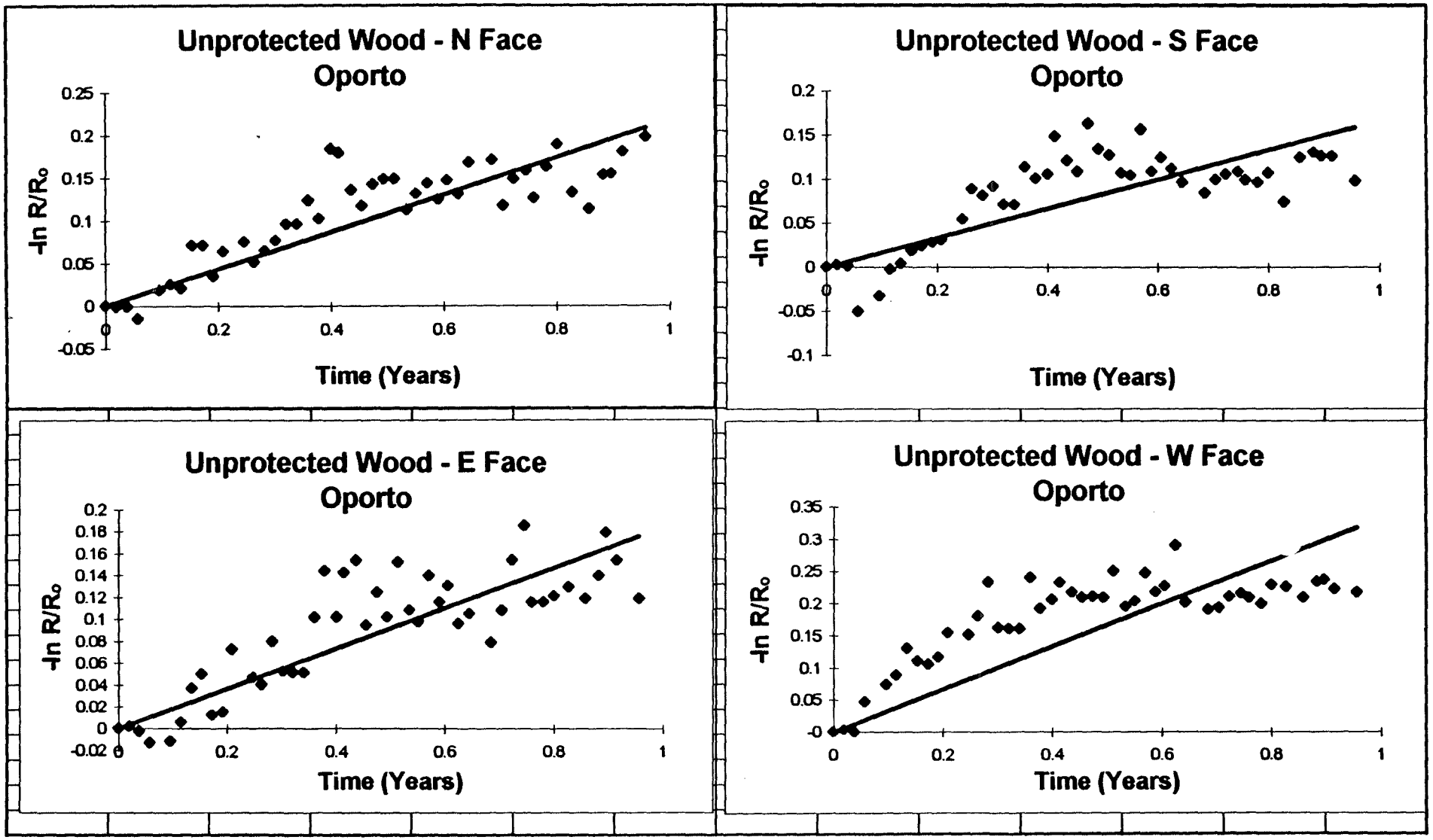

Figure A24 Graphs of Model 2 Fitted to the Oporto - Unprotected Wood - Reflectance Measurements

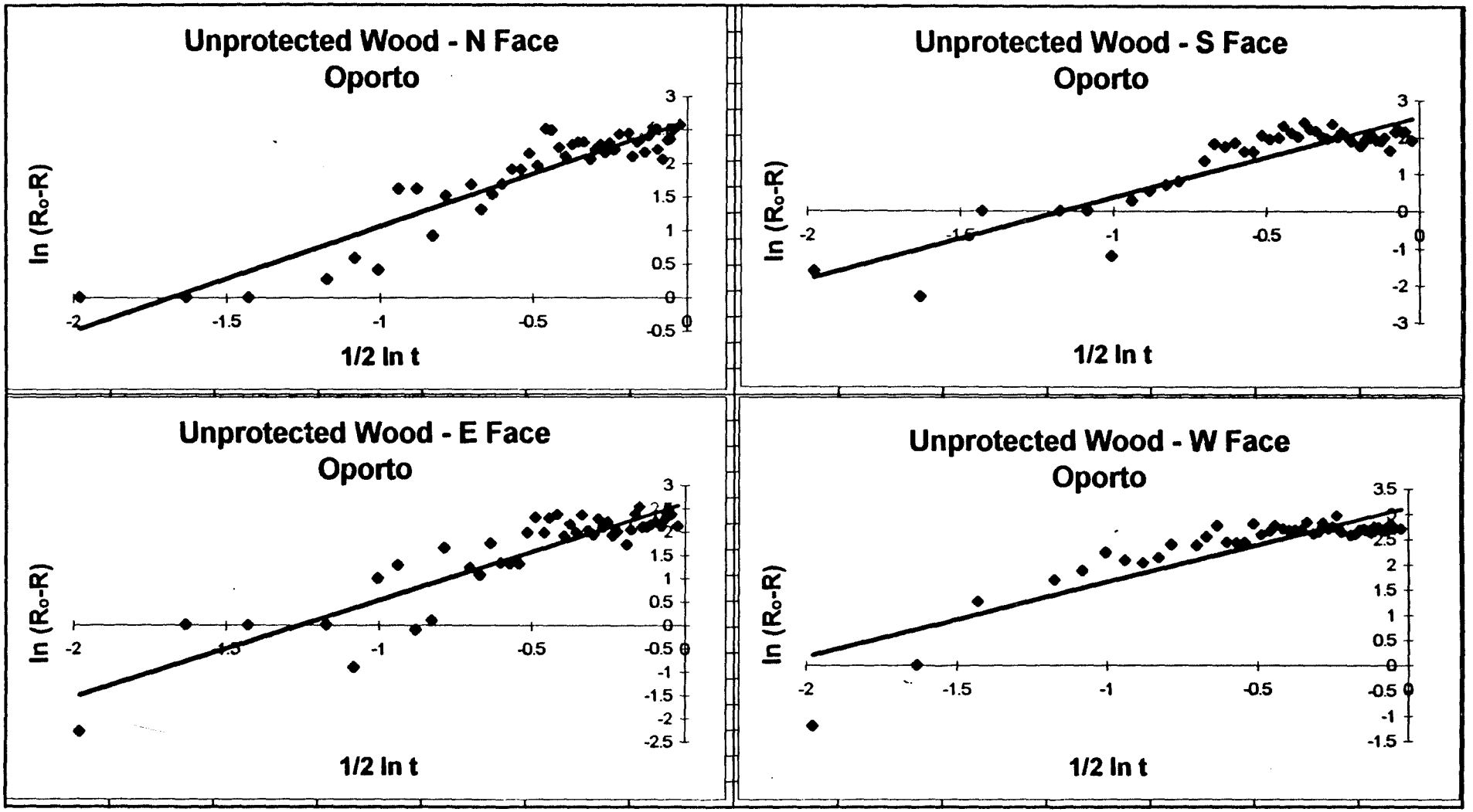

Figure A25 Graphs of Model 1 Fitted to the Coimbra - Protected Stone - Reflectance Measurements

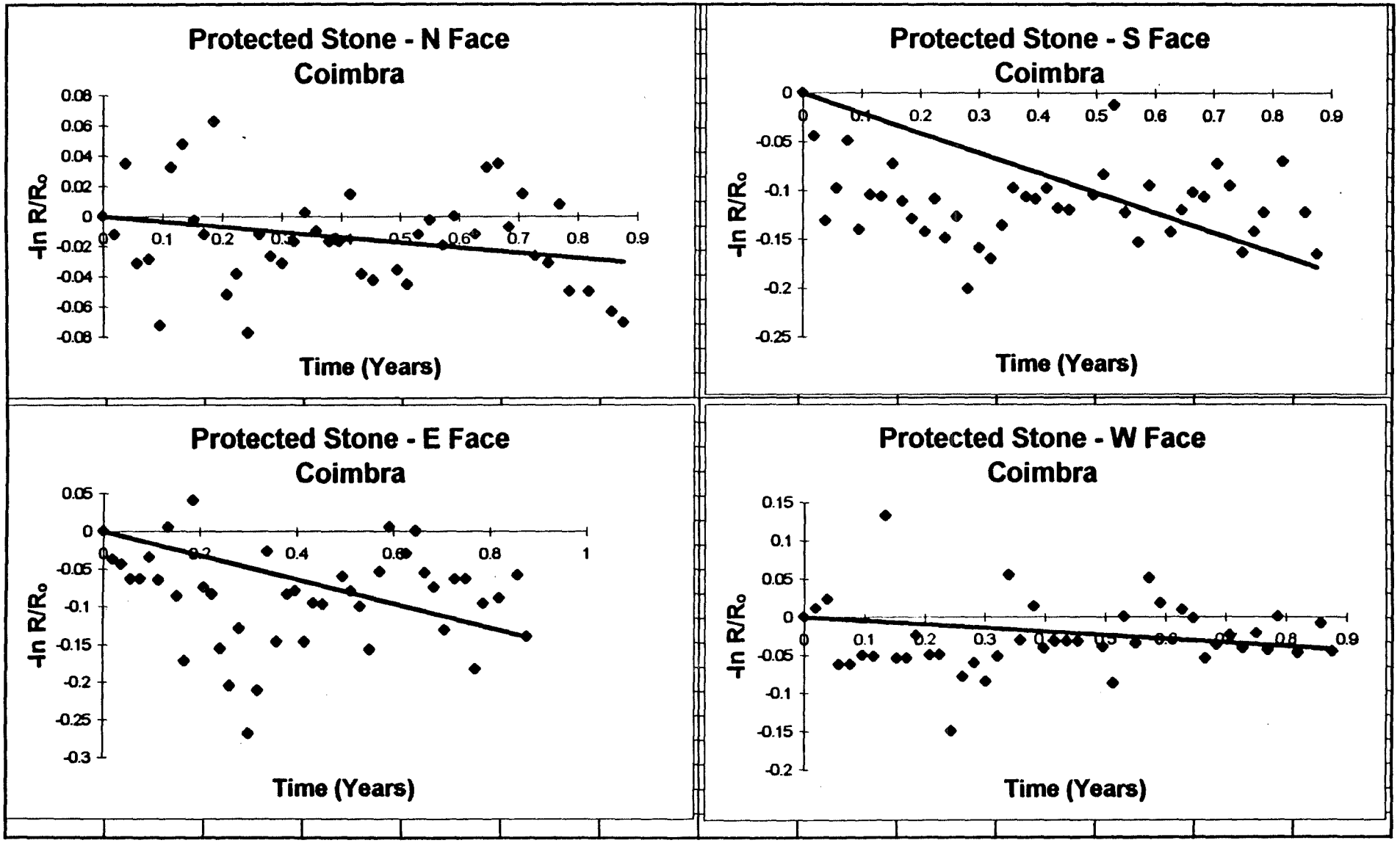

Figure A26 Graphs of Model 2 Fitted to the Coimbra - Protected Stone - Reflectance Measurements

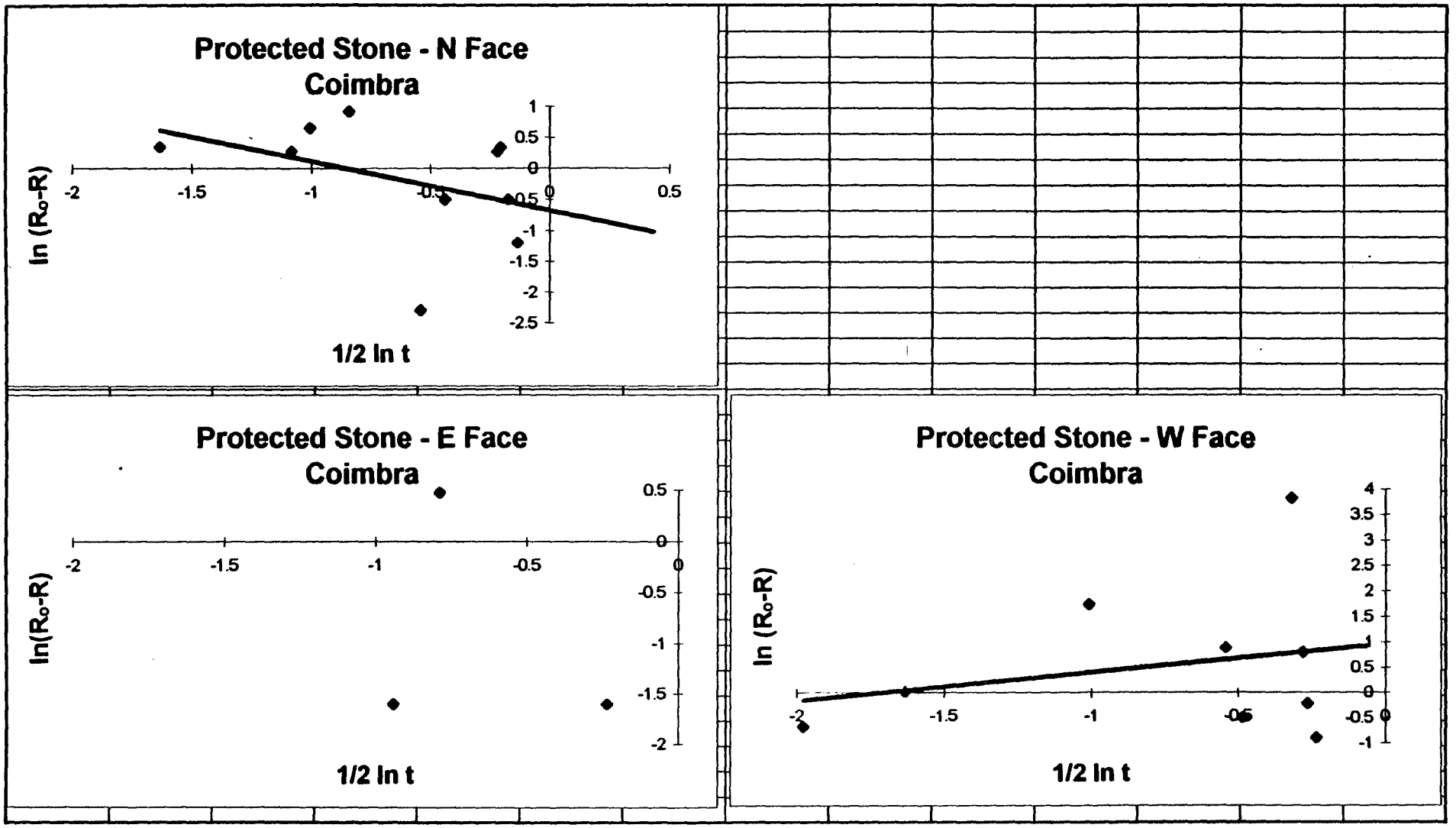

Figure A27 Graphs of Model 1 Fitted to the Coimbra - Unprotected Stone - Reflectance Measurements

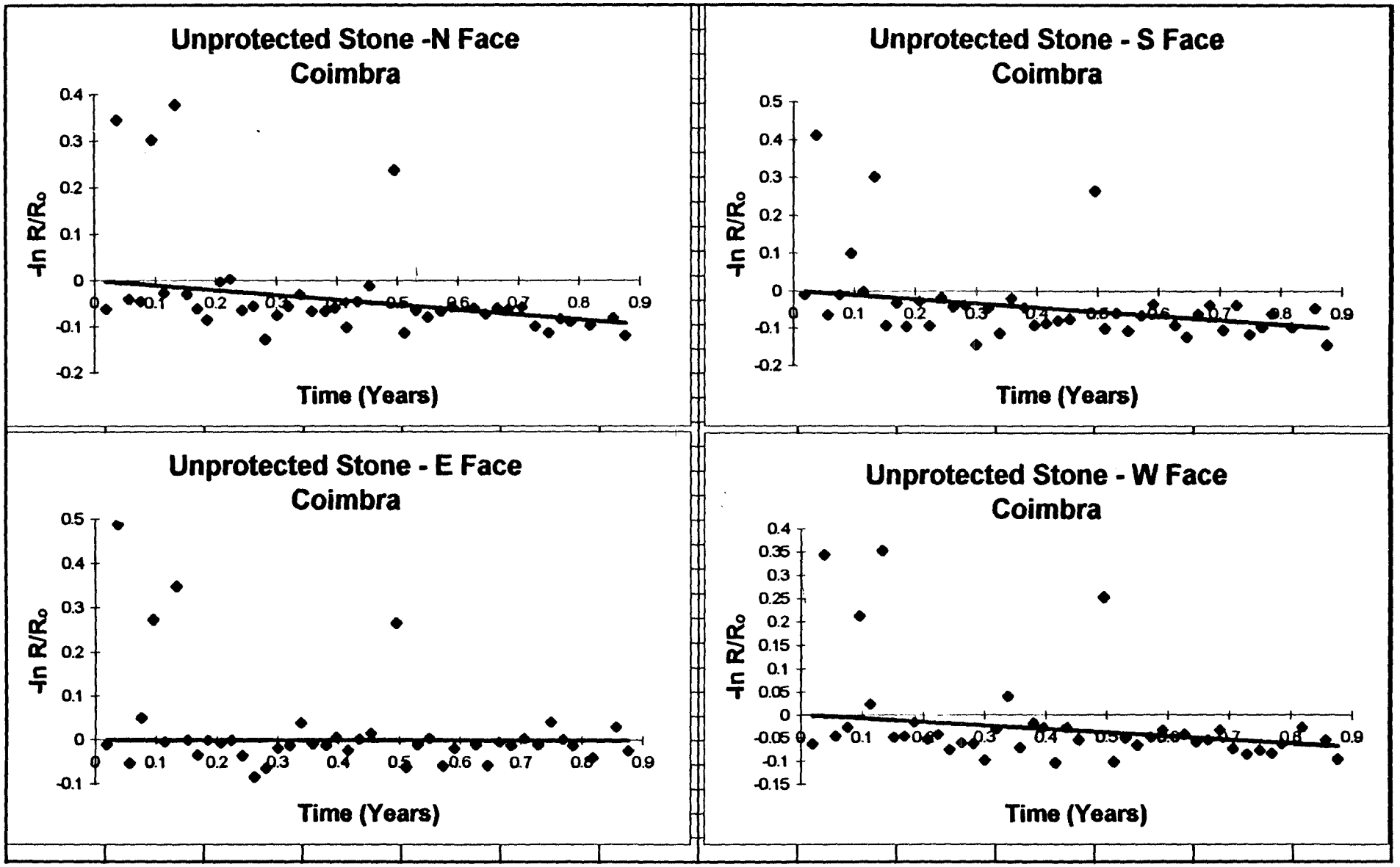

Figure A28 Graphs of Model 2 Fitted to the Coimbra - Unprotected Stone - Reflectance Measurements

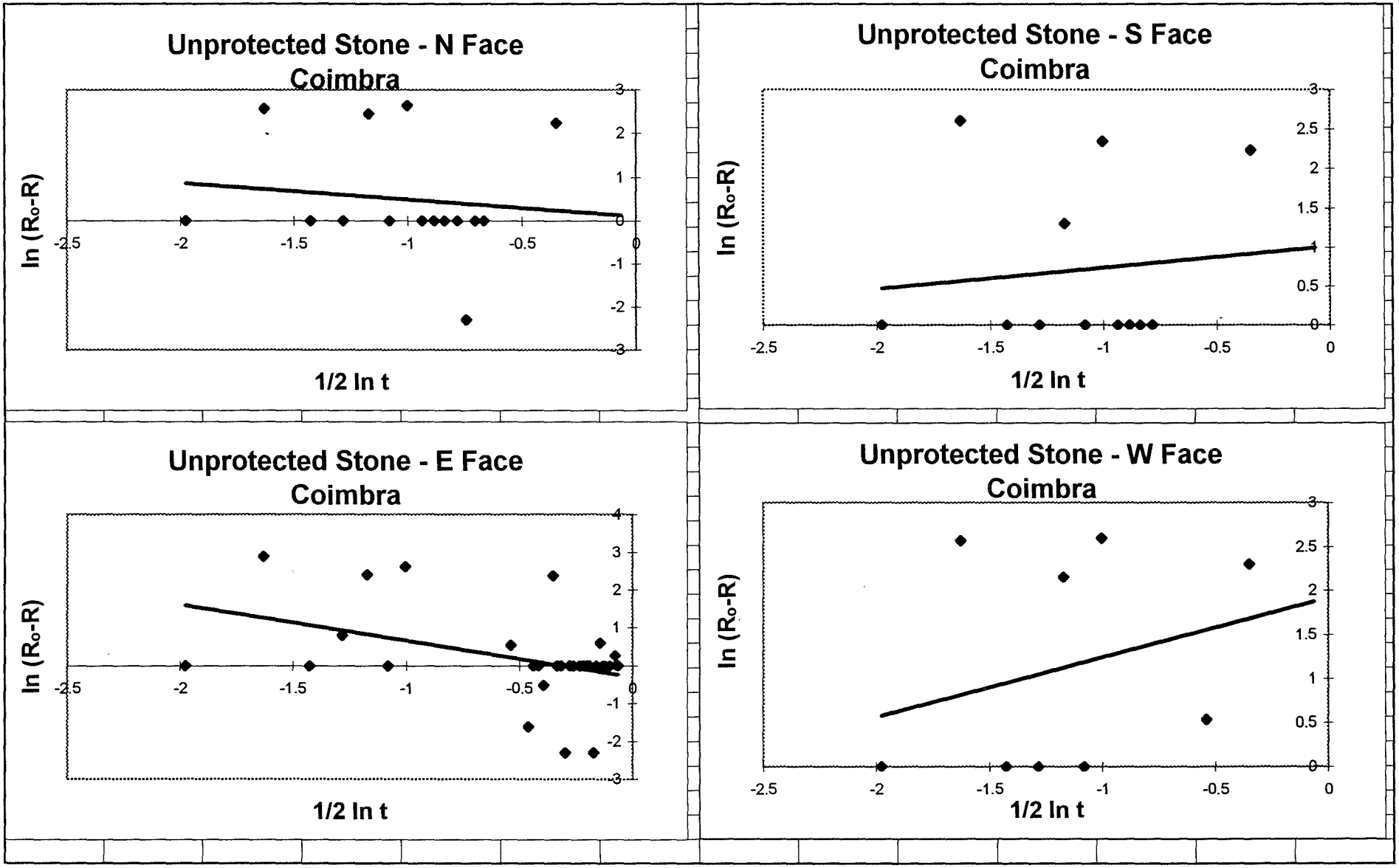

Figure A29 Graphs of Model 1 Fitted to the Coimbra - Protected Wood - Reflectance Measurements

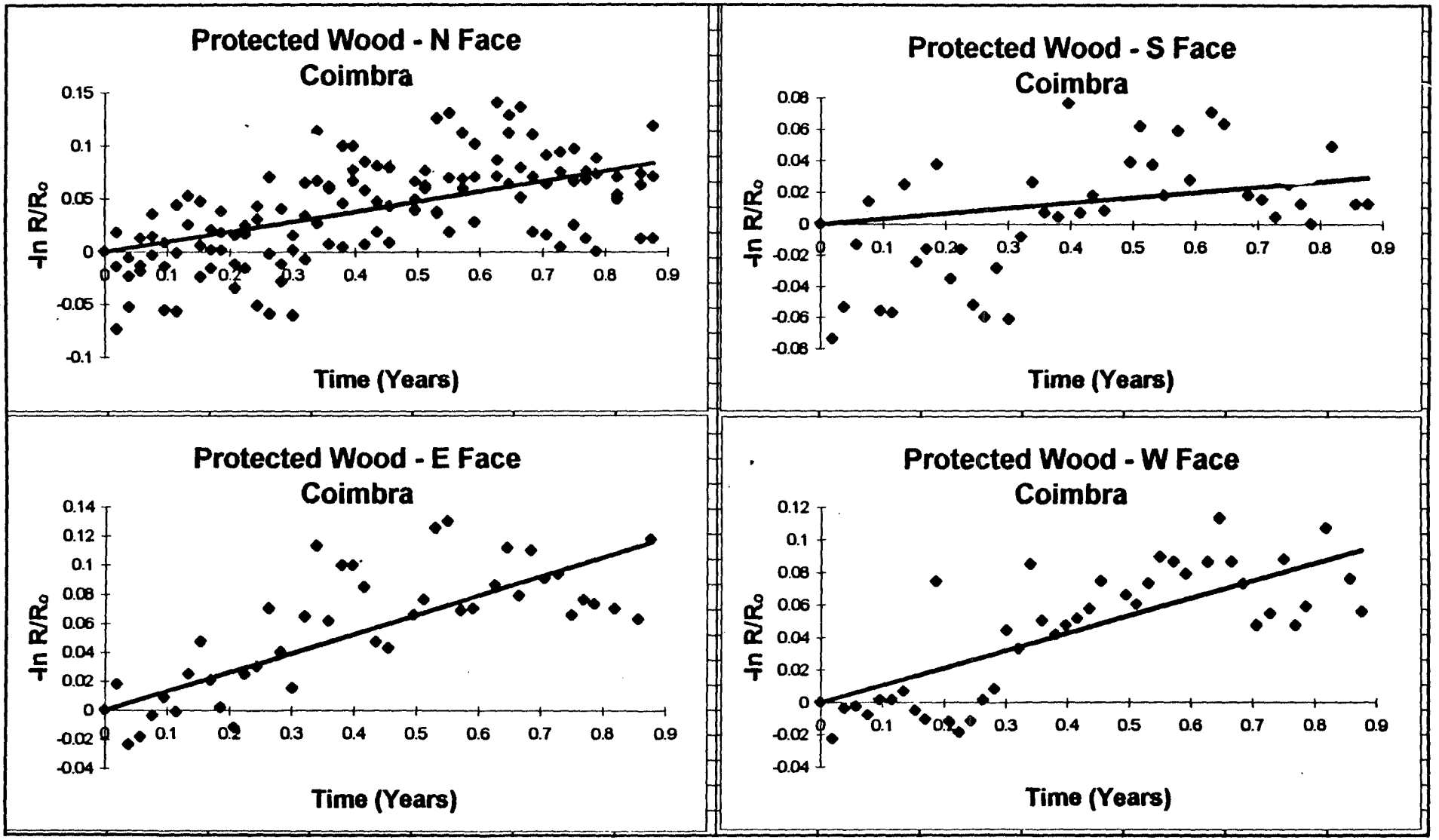

Figure A30 Graphs of Model 2 Fitted to the Coimbra - Protected Wood - Reflectance Measurements

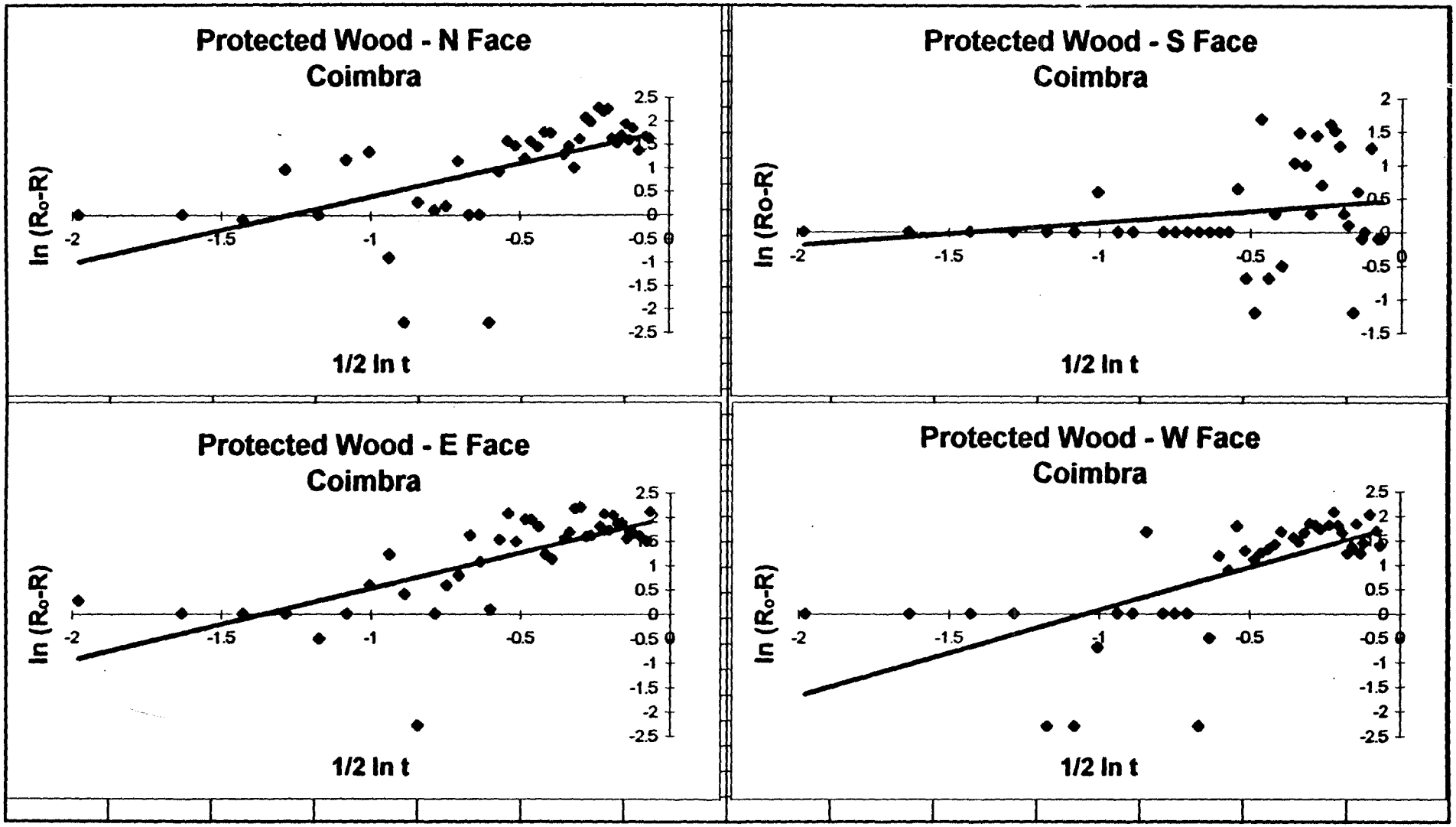

Figure A31 Graphs of Model 1 Fitted to the Coimbra - Unprotected Wood - Reflectance Measurements

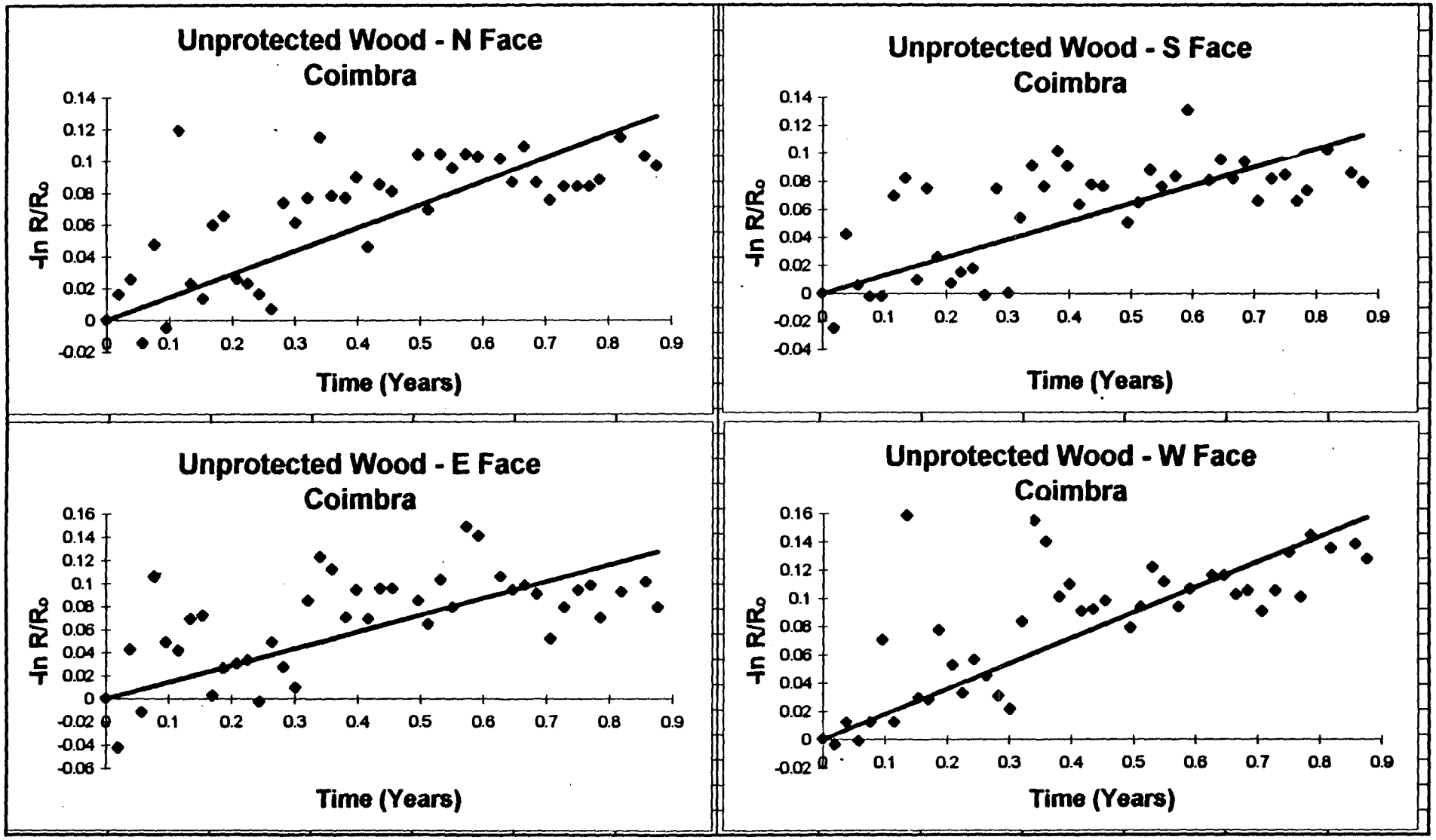

Figure A32 Graphs of Model 2 Fitted to the Coimbra - Unprotected Wood - Reflectance Measurements

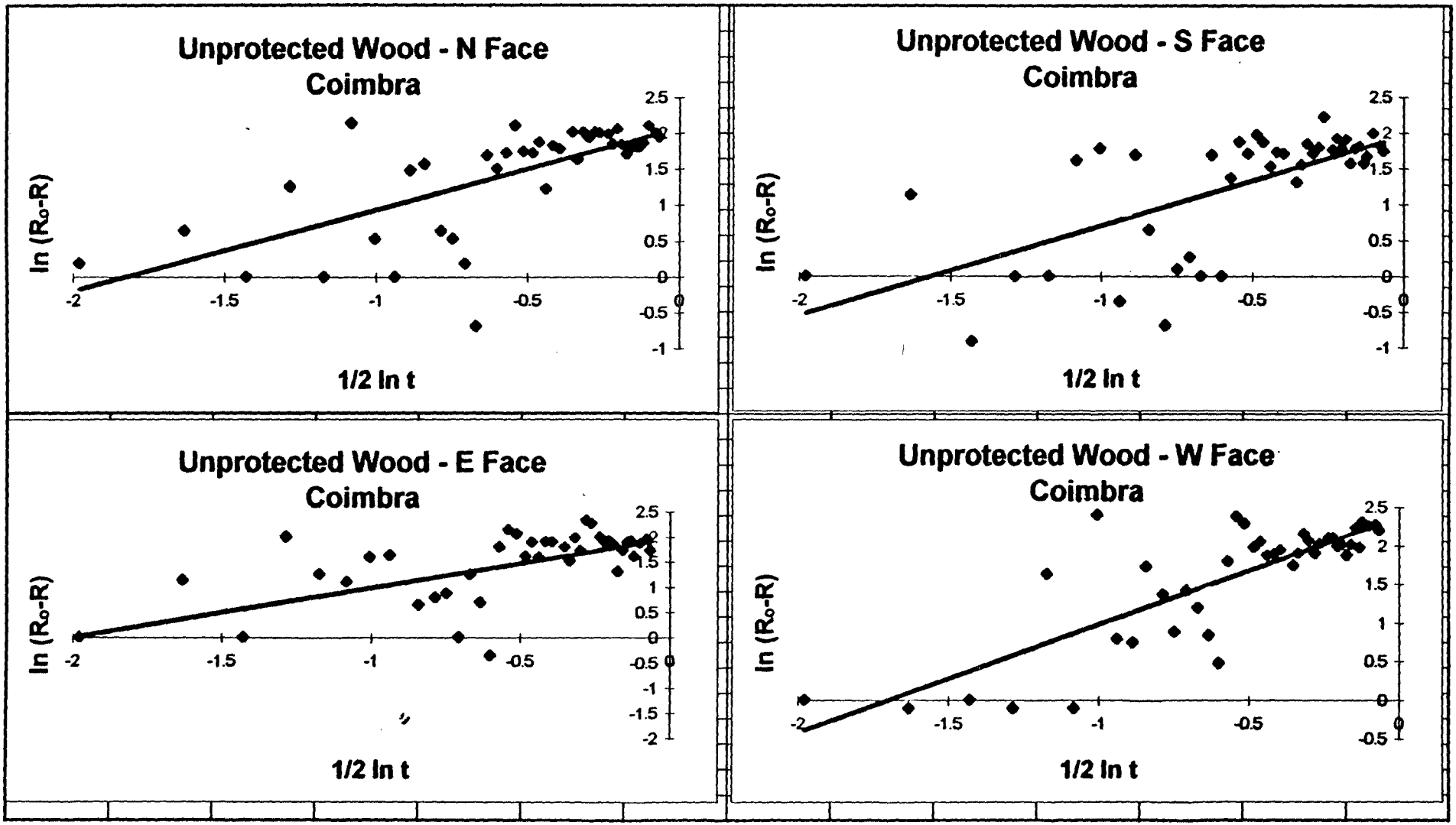

Table A7 Tabulated k_1 and k_2 Values for Each Sample Face

SPSS												
				k_1 Values	r^2 Values	Average k_1	Average r^2	Unpro/Pro Ratio	k_2 Values	r^2 Values	Average k_2	Average r^2
London	Stone	Unprotected	NW	0.27	0.54	0.18	0.66	1.17	7.58	0.19	5.08	0.11
			SW	0.16	0.83				1.2	0.03		
			NE	0.13	0.37				4.07	0.13		
			SE	0.14	0.91				7.46	0.08		
		Protected	NW	0.19	0.67	0.15	0.74		6.75	0.52	5.38	0.42
			SW	0.19	0.71				7.55	0.53		
			NE	0.06	0.66				1.68	0.11		
			SE	0.17	0.9				5.55	0.52		
	Wood	Unprotected	NW	0.37	0.98	0.30	0.95	1.38	22.93	0.97	17.79	0.92
			SW	0.28	0.96				16.14	0.93		
			NE	0.23	0.94				13.99	0.84		
			SE	0.33	0.93				18.1	0.94		
		Protected	NW	0.22	0.98	0.22	0.95		16.16	0.55	13.63	0.80
			SW	0.21	0.93				12.74	0.87		
			NE	0.23	0.95				13.33	0.88		
			SE	0.22	0.92				12.28	0.89		
Vienna	Stone	Unprotected	N	0.17	0.77	0.17	0.73	1.39	9.75	0.31	9.55	0.30
			S	0.19	0.76				10.51	0.12		
			E	0.16	0.69				8.73	0.34		
			W	0.17	0.69				9.19	0.44		
		Protected	N	0.18	0.99	0.12	0.97		15.94	0.97	10.32	0.83
			S	0.08	0.98				8.32	0.87		
			E	0.08	0.99				7.45	0.92		
			W	0.15	0.92				9.56	0.55		
	Wood	Unprotected	N	0.23	0.96	0.26	0.97	1.16	17.92	0.9	20.22	0.91
			S	0.27	0.97				21.15	0.95		
			E	0.26	0.97				20.5	0.85		
			W	0.27	0.96				21.3	0.92		
		Protected	N	0.22	0.97	0.22	0.95		17.4	0.96	17.44	0.93
			S	0.22	0.91				16.98	0.83		
			E	0.24	0.97				19.3	0.97		
			W	0.21	0.96				16.09	0.97		

				k_1 Values	r^2 Values	Average k_1	Average r^2	Unpro/Pro Ratio	k_2 Values	r^2 Values	Average k_2	Average r^2
Coimbra	Stone	Unprotected	N	-0.01	0.03	-0.02	0.03	1.17	1.09	0.11	2.98	0.15
			S	-0.06	0.06				7.43	0.01		
			E	0	0				0.37	0.41		
			W	VOID	VOID				3.04	0.06		
		Protected	N	-0.03	0.22	-0.11	0.24		0.62	0.1	1.14	0.06
			S	-0.2	0				-	VOID		
			E	-0.16	0.52				0.21	0.09		
			W	-0.05	0.2				2.6	0.06		
	Wood	Unprotected	N	0.15	0.86	0.15	0.84	1.53	7.67	0.39	8.25	0.38
			S	0.13	0.83				7.47	0.36		
			E	0.15	0.8				6.9	0.17		
			W	0.18	0.87				10.98	0.58		
		Protected	N	0.12	0.83	0.10	0.67		7.33	0.34	6.87	0.34
			S	0.03	0.18				1.66	0		
			E	0.13	0.84				7.58	0.4		
			W	0.12	0.82				10.93	0.6		
Oporto	Stone	Unprotected	N	0.18	0.24	0.03	0.08	1.39	2.18	0.3	4.81	0.21
			S	0	0				8.56	0.16		
			E	-0.05	0.05				2.65	0.37		
			W	-0.03	0.01				5.85	0.01		
		Protected	N	0.31	0.77	0.26	0.80		14.44	0.53	10.66	0.49
			S	0.23	0.74				7.3	0.29		
			E	0.27	0.88				9.82	0.49		
			W	0.23	0.81				11.07	0.64		
	Wood	Unprotected	N	0.22	0.93	0.23	0.90	1.88	14.22	0.77	16.00	0.77
			S	0.17	0.86				13.21	0.78		
			E	0.18	0.91				14.52	0.79		
			W	0.33	0.89				22.05	0.73		
		Protected	N	0.13	0.83	0.12	0.82		8.01	0.46	7.48	0.49
			S	0.09	0.74				5.49	0.53		
			E	0.15	0.92				10.79	0.71		
			W	0.11	0.78				5.63	0.26		

Breitenfurt	Stone	Unprotected	N	0.07	0.71	-0.04	0.63	1.39	3.91	0.17	2.54	0.10
			S	-0.05	0.74				-	-		
			E	-0.14	0.9				-	-		
			W	-0.02	0.17				1.16	0.03		
		Protected	N	-0.07	0.92	-0.06	0.87		-	-	VOID	#DIV/0!
			S	-0.1	0.87				-	-		
			E	-0.07	0.87				-	-		
			W	0.02	0.82				-	-		
	Wood	Unprotected	N	0.19	0.99	0.14	0.98	1.60	16.62	0.88	10.55	0.78
			S	0.1	0.96				8.81	0.69		
			E	0.09	0.98				7.97	0.87		
			W	0.18	0.99				8.81	0.69		
		Protected	N	0.09	0.81	0.09	0.83		3.36	0.01	5.00	0.03
			S	0.08	0.9				4.9	0.02		
			E	0.1	0.84				6.49	0.05		
			W	0.08	0.76				5.25	0.05		

Figure A33 Example of a GCMS Calibration Graph - Heptadecane

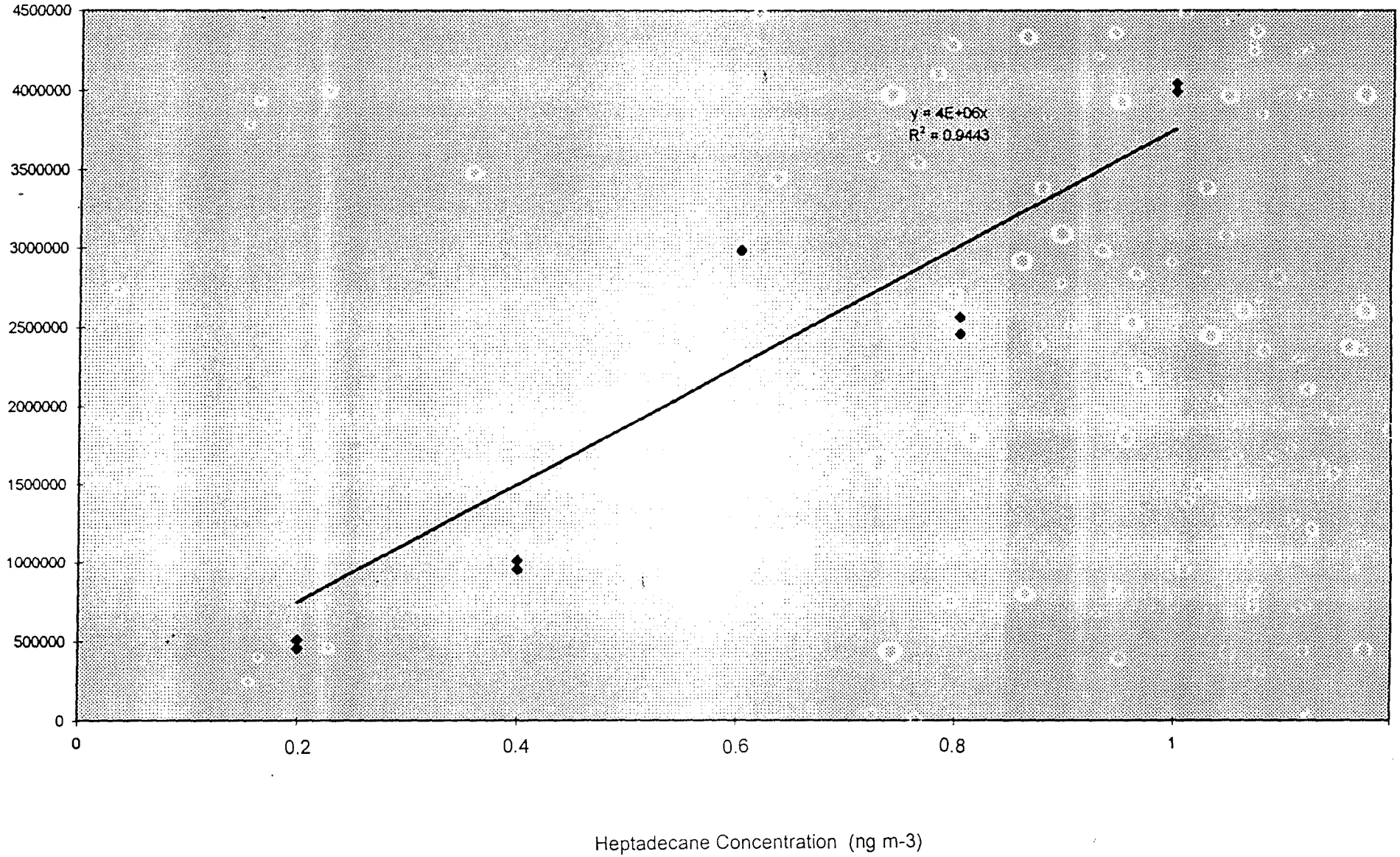

APPENDIX 5 The 16 PAHs Species Detected

Table A8 Nomenclature, Structure, Melting Point and Boiling Points of the 16 PAHs Detected

Nomenclature	Structure	MP (°C)	BP (°C)
Naphthalene		80	218
Acenaphthylene		92	270
Fluorene	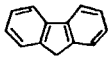	116	294
Acenaphthene		96	279
Phenanthrene	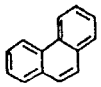	100	340
Anthracene	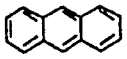	218	340
Fluoranthene	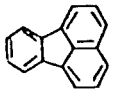	110	375
Pyrene	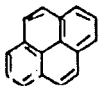	156	399
Benz(a)anthracene	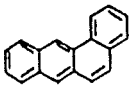	158	400
Chrysene	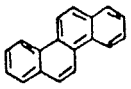	255	448
Benzo(b)fluoranthene	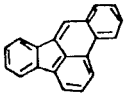	168	481
Benzo(k)fluoranthene	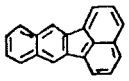	217	480
Benzo(a)pyrene	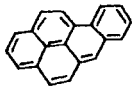	177	495
Dibenz(a,h)anthracene		262	524
Benzo(ghi)perylene		273	542
Indeno[1,2,3,c,d]pyrene		163	534

APPENDIX 6 Discussion of the Derivation of *k* Values

MODEL 1: Forcing the Line of Best Fit Through the Origin

Model 1 uses an exponential relationship, a function which is applicable to many scientific systems. The conventional approach to fitting experimental data to an exponential relationship is to plot (ln Y) against (X) and this is the approach which has been used in this thesis, with Y = reflectance and X = time. The soiling constant has been calculated from the gradient of the best-fit straight line.

The question remains as to whether the line should be forced through the origin, or the origin should be treated as a data point with equal weighting to all other data points in the set. It was decided to adopt the former approach in this thesis because the initial value warrants additional weighting – soiling at time zero has been taken to be zero, whereas measurement variation may be associated with the other points. Subsequent values can be influenced by a range of microclimatic variables which are responsible for the scatter in the data; these variables do not exert an influence on the initial value and it is for this reason that the best-fit line was forced through the origin.

MODEL 2: Using Log Plots of Soiling Data for the Derivation of k_2

In the absence of a consensus on data presentation, log plots were used for the derivation of k_2 values. The main advantage of this method was an improved visual comparison with the log plots used for the derivation of k_1 values which aided interpretation. This method did not affect the measure of best-fit used in this analysis (the r^2 values) which were generated during the regression analysis, nor did they significantly affect the k_2 values.

This may be demonstrated with the data from a randomly selected sample. Figures A34 and A35 show plots of the reflectance data measured at the south facing sample of the protected wood material in Vienna. Figure A1 shows the plot of data as used in the derivation of k_2 for all samples in Chapter 4. (Although the first data point R_o is not included on this figure, it was included in the analysis). Figure A35 shows the same data as an alternative plot of R versus square root t.

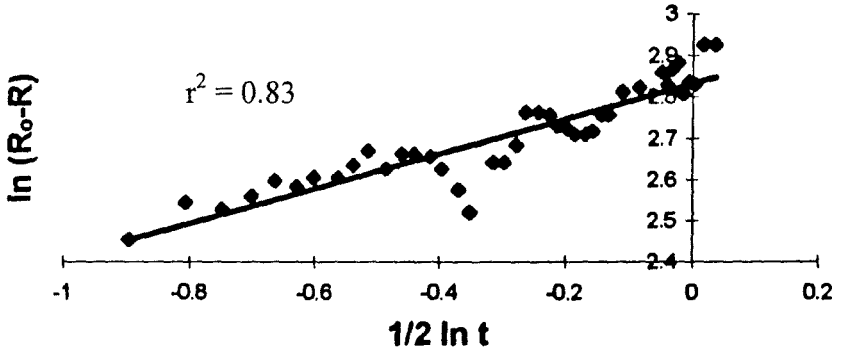

Figure A34 Graphical representation of the derivation of the k_2 value for the south face of the protected wood sample in Vienna.

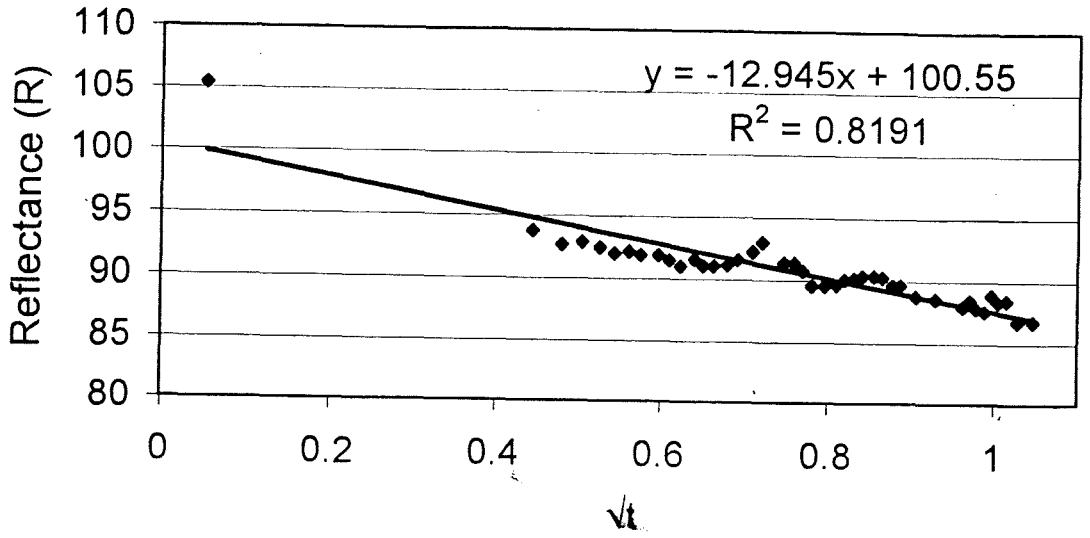

Figure A35 Graphical representation of an alternative derivation of the k_2 value for the south face of the protected wood sample in Vienna.

Comparison of the r^2 values shows almost identical values $r^2 = 0.83$ for the plot in Figure A34 and $r^2 = 0.82$ for the plot in Figure A35. This very small difference may be accounted for by the different computer packages used to compute these values; SPSS was used in the original analysis and Microsoft Excel was used for Figure A35. Clearly the method of plotting these values does not cause any change in the r^2 value where the variation of reflectance values is large. Therefore the derivation of k_2 values using either method is valid.

Where weekly soiling change (or reflectance variation) is small, the line of best fit may not be an appropriate measure of the relationship between the soiling process, nor does it represent the soiling rate accurately. When the value of $ln(R_o - R) = 0$, R_o minus R is equal to 1; i.e. the smallest measurable change in reflectance of 1% has occurred. In cases where the measured reflectance changes by only a few percent over the one year measurement period, the log plot method of k_2 value derivation is subject to difficulties due to the low data variation throughout the year. The data appear to produce a set of horizontal lines in the log plots, as can be seen in Figures A36 and A37. This is due to the fact that the weekly measurements are distributed between a limited number of values. For example, in the case of the north west face of the London stone sample (Figure A36), reflectance values of between 39-52% were recorded over the year. Consequently, only six values of $ln(R_o - R)$ are plotted against $0.5\ (ln\ t)$, producing a "banded" appearance. In such cases, and irrespective of the manner in which the graph is plotted (see Figure A38), the r^2 values are low due to the limited distribution of reflectance values and it should be concluded that the model is a poor fit of the data.

In order to demonstrate this, two samples with low and moderate variation in reflectance values were selected. Figures A36 and A37 show the plots of two faces of protected stone at the London site - north west and north east faces, respectively. Reference to the original reflectance data in Appendix 1 shows that the variation in recorded soiling values was moderate and low in these cases, relative to variation in other sample types. The plots presented graphically represent the regression analysis used in the analysis in Chapter 4 to infer the r^2 and k_2 values presented. The appropriateness of the model is reflected in the r^2 value, together with the p values (see page 84).

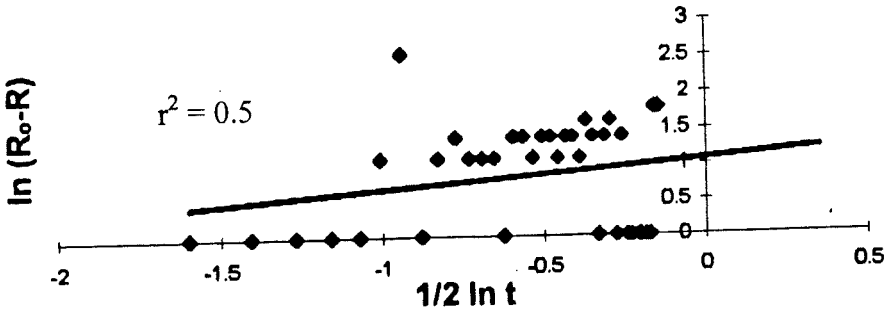

Figure A36 Graphical representation of the derivation of the k_2 value for the north west face of the protected stone sample in London.

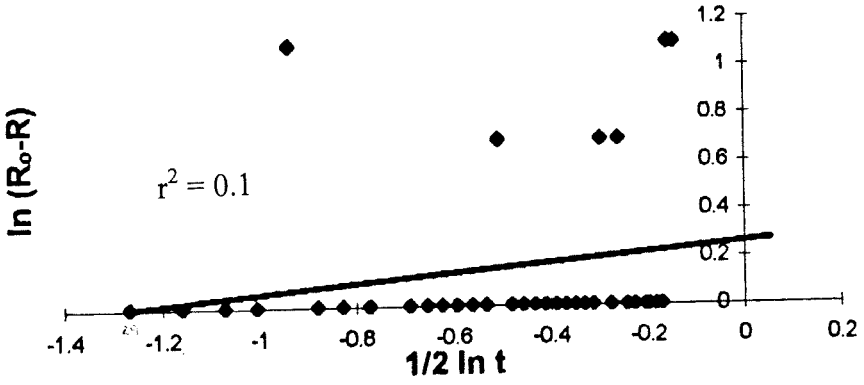

Figure A37 Graphical representation of the derivation of the k_2 value for the north east face of the protected stone sample in London.

Figures A38 and A39 show plots of the alternative method of regression by which k_2 values may also be derived.

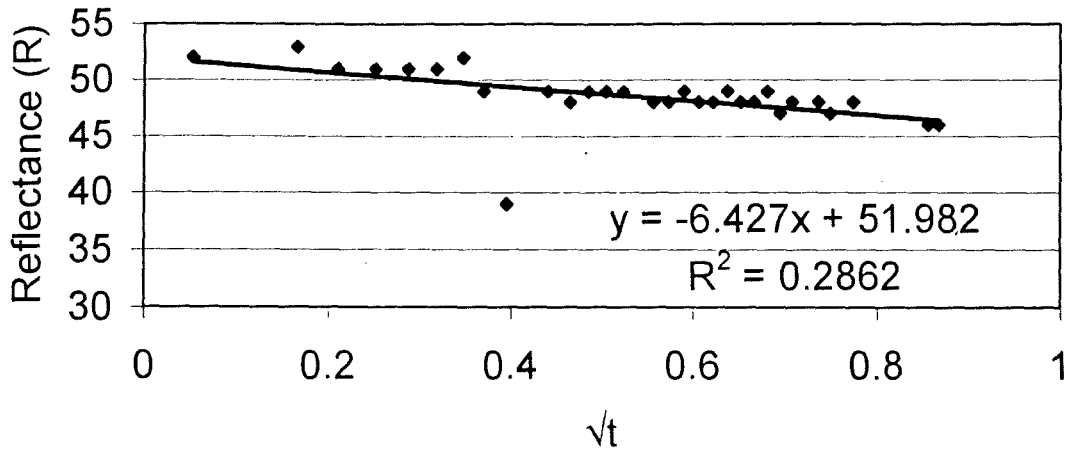

Figure A38 Graphical representation of an alternative derivation of the k_2 value for the north west face of the protected stone sample in London.

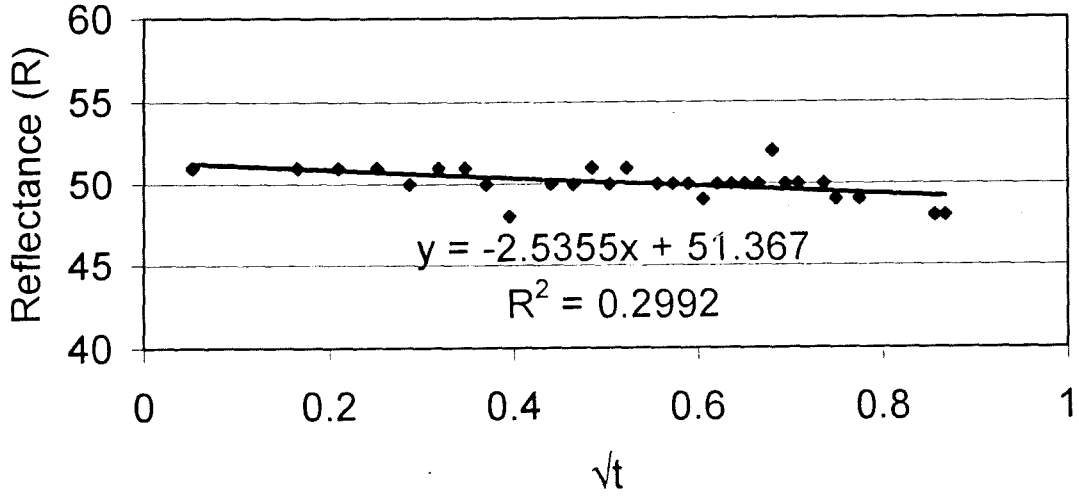

Figure A39 Graphical representation of an alternative derivation of the k_2 value for the north east face of the protected stone sample in London.

Comparison of Figures A36 with A38 and Figures A37 with A39 show that r^2 values do vary slightly with the method of regression used. In the case of moderate data variation (where there are several values of $R_o - R = 1$) such as the north west face, when $ln(R_o - R)$ is used $r^2 = 0.5$ compared to $r^2 = 0.3$ for R versus square root t. In other words, the log plot provides a better model fit r^2 value. In the case of extremely low data variation (where there are many values of $R_o - R = 1$) such as the north east face, when $ln(R_o - R)$ is used $r^2 = 0.1$ compared to $r^2 = 0.3$ for R versus square root t. In this second case, the R versus square root t approach provides a better model fit value. Different derivations of k_2 therefore produce different values. However, these values are very low r^2 values and are still lower than the r^2 values derived for Model 1 (see Table 4.3 on page 84).

In conclusion, where the r^2 value is high, the k value may be taken as a good representative of the soiling rate of the sample. Where the r^2 value is low, the associated k value determined is of limited importance since the data are not well represented by the line of best fit from which the k value is calculated. It is therefore only appropriate to use the k value in conjunction with the associated r^2 value, which in turn should be considered in conjunction with the p value.